Hachinohe Institute of Technology

Service Life Prediction and Economic Evaluation of Concrete Treated by a Compound Impregnating Agent in Marine and Severe Cold Environment

A Thesis Submitted to Graduate Department of Civil Engineering and Architecture

Requirements for Degree of Doctor of Engineering

Yanhua Kuang

D 19301

Under Supervision of Associate Professor Yuki Sakoi (chief referee), Professor Minoro Aba (co-referee) and Professor Yoichi Tsukinaga(co-referee), February 2022.

ABSTRACT

At present, many infrastructures face the phenomenon of ageing year by year, and more and more infrastructures need to be maintained and updated. How to effectively and economically prolong the service life of concrete in harsh service environments is a significant issue facing our engineers today. It is also the obligatory social responsibility of our professionals. This thesis studies the maintenance effect of a group of composite penetrants applied to the concrete surface. First, through indoor experiments, the influence of impregnants on the performance of concrete was studied. Secondly, through the follow-up study of the actual project, Tomakomai Dam, for nearly 20 years, the dynamic evaluation of the application of this group of composite impregnants in the cold ocean environment was carried out. Moreover, its life span and economy are estimated.

This set of composite impregnation is composed of two impregnants: a sodium silicate solution applied on the surface of the concrete as the bottom layer and a silane solution applied on the sodium silicate solution as the upper layer.

① Concrete surface water absorption, air permeability, pH, surface micro-pore size distributions, and the anti-salt freezing-thawing properties of concrete after applying the impregnating agents were conducted indoor experiments. The results show that: Compared with the untreated groups after applied the impregnants, the concrete surface: The surface water absorption is significantly reduced by 60.97%;

② The air permeability is almost unaffected. When the concrete surface water content decreases slightly, there is even a slight tendency to increase;

③ pH increases at the time of testing (390 days after the test block is formed, about 330 days after the impregnant is applied) ;

④ The distribution of the pores in size range of 400-1000nm in the surface layer (0-10mm) is significantly reduced in the 12th year;

The composite impregnants can make the concrete surface denser and form a hydrophobic film on the surface of the concrete. The hydrophobic film has water-blocking and air-permeable properties. The dosage of composite impregnant was studied, and a reasonable dosage of penetrant was proposed according to the quality conditions of concrete: the water absorption of concrete is low before treatment (surface water coefficient is ≤ 0.12 (ml/m^2/s)), and when the quality is good, the dosage can be 50% of the recommended dosage.

In the 3rd, 12th and 20th years after the construction of Tomakomai, core samples from the part of Tomakomai project treated with impregnant and the comparison part where the impregnant is not applied were taken. The samples were delivered to the laboratory for the following experiments: carbonization depth determination, chloride ion diffusion, pH measurement, concrete surface micropore size measurement (MIP), freeze-thaw and freeze-thaw experiments after retreated. Based on the data from the above tests, the life expectancy of Tomakomai was calculated, the selection and economic of maintenance plans and was analyzed.

Through deterministic calculation method, probability and reliability method and Monte Carlo method, the life of Tomakomai dike under carbonization, chloride erosion and freeze-thaw cycles was calculated, respectively. The results show that:

① In the marine environment, applying this set of impregnants on the concrete surface will shorten its life by about 70% under carbonization erosion. However, the progress of concrete carbonization is slow. When the concrete cover thickness reaches 50mm, the carbonization life of the treatment concrete can reach up to 170 years which is generally longer than the concrete designed target life.

② The impregnants can effectively reduce the corrosion of chloride ions and extend the life of concrete in this situation to 1.1-3.5 times the group without treatment.

③ In the 20th year, the alkalinity of the treated concrete surface is lower than that of the untreated group, and It is consistent with the conclusion that the concrete life is shortened by applying penetrants under the carbonization environment.

④ In the cold ocean environment, concrete life is determined by the deterioration of the salt-freezing-thawing. Therefore, although the application of the impregnating agents on the concrete surface will lose part of the carbonization life, it is helpful to extend the concrete life in the salt-freezing-thawing

erosion environment and finally extend the actual concrete service life.

⑤ The calculation also shows that the construction quality related to the thickness of the concrete protective layer has a significant impact on the life of the concrete. If the construction quality improves, the probability of the concrete cover construction deviation of 10mm is reduced from 15% to 5%; the guaranteed rate is increased from 85% to 95%. The life under chloride ion attack can be extended by 10%, and the concrete carbonization life will be significantly improved. When the concrete cover is more than 20mm (30mm in the treatment groups), when the guaranteed rate is increased by 10%, the total carbonization life of the concrete can be prolonged by an average of 37 years. The untreated groups are slightly longer than the treatment groups.

⑥ Different impregnating agents should be used for concrete under different service environments. As far as the conclusions of this article are concerned: Impregnant used in this study significantly improve the resistance of concrete to chloride corrosion and freeze-thaw deterioration, but it is not conducive to the resistance to carbonization. Therefore, they are not suitable for the dry and warm environment easily corroded by carbon dioxide.

⑦ The pore size larger than 1000 nm distribution of the concrete surface layer is small at the 12th year. However, It increased a lot in the 20th year with the passage of service years, indicating that the effect of the impregnants is gradually weaker by year.

⑧ The re-application of the compound impregnants can delay the appearance time of concrete rapid scaling for about 20 to 65 cycles under salt-freezing-thawing (ASTM-C 672) erosion in indoor experiments.

⑨ The use of composite penetrant maintenance before the scaling depth reaches 2.5 mm can effectively reduce the life cycle cost by at least 50%. Fortheinfrastructures treated with composite penetrant in the construction year, and the secondary maintenance time should be ≤33 years. For the infrastructures without maintenance in the construction year, the maintenance interval should be ≤17 years. The impregnant can make the concrete "freeze age" for 17 years.

⑩ The calculation also shows that the construction quality related to the thickness of the concrete protective layer has a significant impact on the life of the concrete. If the construction quality improves, the probability of the concrete cover construction deviation of 10mm is reduced from 15%

to 5%; the guaranteed rate is increased from 85% to 95%. At this time, the concrete carbonization life will be significantly improved. When the concrete cover is more than 20mm (30mm in the treatment groups), when the guaranteed rate is increased by 10%, the total carbonization life of the concrete can be prolonged by an average of 37 years. The untreated groups are slightly longer than the treatment groups.

Among the three concrete life calculation methods, the Monte Carlo method is recommended. This method not only considers the random distribution characteristics of the calculated parameters and the failure probability of the material but also has a high degree of computerization, and the calculation speed and calculation accuracy are also more excellent than the other two methods.

ACKNOWLEDGEMENTS

When the stars move, time flies, in the twinkling of an eye, my three-year PhD study in Japan will come to an end. This has been an extraordinary three years in my life. The past three years have been tense and fulfilling. Although there are some regrets, it is more about harvest and growth. I would like to express my gratitude to all the teachers, classmates, friends, and family who cared about and helped me.

First of all, In particular, I would like to express my high respect and heartfelt thanks to my respected tutor, Associate Professor Yuki Sakoi, who has given me care, help and guidance in my study and life for many years! The topic selection, research plan, experimental design, theoretical analysis, conference papers, journal papers and the final thesis are all condensed with the hard work and sweat of the tutor. Throughout my PhD study, Associate Professor Sakoi has always inspired me and carefully guided me with his profound professional knowledge, keen thoughts, and passionate care to make continuous progress in my studies. The rigorous and serious academic spirit of Associate Professor Sakoi inspired me forever. I especially want to thank the tutor for giving me enough trust and a relaxed and autonomous learning environment to relieve the enormous mental pressure before starting the PhD study. It was an honour of my life to meet such an open-minded mentor and friend mentor during my PhD. Apart from busy work, Associate Professor Sakoi also cared about my life, worrying about getting a vaccine for me, etc. which always makes me feel the warmth of the spring sun. Thank you, dear Associate Professor Sakoi!

At the same time, I would also like to thank my other two mentors, Professor Minoro Aba and Professor Yoichi Tsukinaga, for your review and guidance of my thesis. Thank you, Professor Aba, In every dinner, you not only let us taste delicious Japanese food but also inspired my idea of the paper in the free chat, which always gave me a sudden sense of enlightenment. Thanks to Professor Tsukinaga for presenting your precious conference proceedings to me, which allowed me to learn much knowledge.

I would like to thank Mr Sasada, Mr Mitsuo Natsusaka, Mrs Mikami, Mr Nakamura Kazusato and Mr Shimada of the Student Affairs Division. Especially Mr Natsusaka, I have got countless help from him in school life, from handling the medical insurance card, bus ride tickets, reservations for Covid-19 vaccine, etc. I was very touched by everything that he helped me. Thank you, Mr Natsusaka. Thanks to staffers in the Finance Department, Mr Kota Kimura, Ms Masuya, Ms Joumae, Mr Ebina and his wife Ms Eriko, thank you for your help. Thank you, Ms Megumi Nishimura, of the Academic Affairs Section. Thank Ms Kazuko of Oku of general affairs, who handled the procedures for studying abroad for me 3 years ago. Although some staffers I have never met, they are silently helping me. Thank you.

Thanks to Japanese language teachers Prof. Watanabe and Associate Prof. Yamamoto. Prof. Watanabe could have enjoyed a comfortable retirement life. Still, he sacrificed part of his time to teach us Japanese for free. His selfless dedication moved me. I think his dedication and spirit of international friendship are a model for me to learn from. I also hope I will never stop learning the language and be able to help foreigners who want to learn Chinese in the future. This is the spirit that Prof. Watanabe gave me, more important than language. Thank you, Prof. Watanabe. When I first came to Japan, Associate Prof. Yamamoto's fluent Chinese translation relieved my anxiety of not knowing Japanese at all. The bus transfer information printed by Associate Prof. Yamamoto was detailed and comprehensive, which left a deep impression on me; thank you, Associate Prof. Yamamoto.

Thanks also to the laboratory instrument maintenance staff Mr Yamamoto for your help in maintaining the equipment and providing us with good experimental conditions. Thank you.

Thank you to all the members of our research team: Master Naoto Takashima Kun, Master Kohei Shimomukai Kun, Master Seiji Zyutani Kun, 2020th undergraduates: Kanata Kikuchi Kun, Taku Nakamura Kun, Junpei Morita Kun; 2021st undergraduates: Tatsuya Shimada Kun; Masaki Furukawa Kun, Riko Mizuguchi Kun, Kyoka Chiba Kun, Ryo Takahashi Kun and Keiichi Onishi Kun; 2022nd undergraduates Ren Michigami Kun, Yuto Suzuki Kun, Shogo Muramatsu Kun and Kazuto Yanagihara Kun; graduation Dr Mr Meng Zhang and studying Dr Mr Shinya Sukegawa: Thank all of you for spending a good time in school with me, and thank you for your help in experiments. In particular, I would like to thank Master Takashima Kun for the organization and implementation process of the experiments of our research team. You have devoted a lot of hard work and time. It is your detailed and thoughtful plan and organization that made our experiment go smoothly. Thank you for your three years of cooperation, help and hard work. In my thesis, I used many data tested by my supervisors and seniors many years ago. Thank you here, although I don't know exactly who you are.

Thanks to the experts and teachers who have worked hard to defend and review this paper! Finally, many teachers, school office staffers, and classmates have helped, cared about, and supported me. Forgive me for failing to mention them here. I would like to express my heartfelt thanks to you!

I would like to thank Mr Toshimichi Yanagiya, Chairperson, Board of Directors, Educational Corporation, the former principal Prof.Hasegawa, and the principal Prof. Sakamoto of Hachinohe Institute of Technology for providing me with such a rare opportunity to study in Japan. Without this inter-university international cooperation project, there would be no chance for me to learn here. Thank you for your great love, thank you for your support to Xinjiang University and me. I also thank Xinjiang University for its support.

I would also like to extend my sincere gratitude to my beloved husband, Chuansheng Ren, my parents, and two lovely sons. Your understanding, support, and encouragement have motivated me to successfully complete the three-year PhD study. I especially want to thank my husband. In the past three years, he has been giving the children more love than I thought so that the children can grow up healthily and happily. He is undoubtedly a loving and good father. I also thanked my brothers and sisters for caring for our small family when I was far away. Your presence has made me feel more solid in studying here.

This work was supported by the Japan Society for the Promotion of Science (JSPS) KAKENHI [Grant Number 20K04647]. Thanks!

CONTENTS

LIST OF FIGURES

LIST OF TABLES

CHAPTER 1. INTRODUCTION

1.1 Background

For a long time, reinforced concrete has become one of the most commonly used materials in various buildings and infrastructures because of its good mechanical properties, reasonable cost, easy material selection, and convenient construction. It is widely used to construct houses, factories, railways, highways, bridges, canals, ports, wharves, drainage, dikes, power plants, pipelines, and sidewalks. It provides an essential guarantee for people's clothing, food, shelter, use, transportation, and medical care, protects people's lives and property, and ensures that floods do not erode the land. Concrete is a material with enormous consumption after water. It occupies a dominant position in civil engineering worldwide, about 80% to 90% (2018). Various essential infrastructure projects are mostly reinforced concrete structures—twice the sum of the other building materials. As an indispensable engineering material for infrastructure construction, the world's annual output of concrete is nearly 7 billion cubic meters (2014), and China accounts for more than 60% of the world's total. Every person in the world uses about 3 tons per year[1, 2]. It is one of the vital material foundations of infrastructure and the backbone of industrialization. Furthermore, there is no doubt that concrete will continue to be widely used as a building material in the future.

Different buildings and infrastructures have different design goals and service life span depending on the nature of use. As infrastructure and other livelihood projects, it is of great importance, it is not easy to replace, and the replacement cost is enormous. Therefore, under normal circumstances, it should be guaranteed that it can be used continuously for 50 to 100 years, and some even require more than 100 years， commonly known as hundred-year projects. However, in the case of improper design, construction, use, and maintenance, and poor service environment, some projects are forced to retire or have to repairs even if they have been in service for less than 20 years. Many infrastructures were built in the past 50 years, which means that many infrastructures require extensive maintenance to continue to operate[3].

Meanwhile, although some of the infrastructures has reached its designed service life, it can still run relatively well. It can be regenerated through proper maintenance and repair and continue to serve. Compared with demolition and new construction, the repair and upgrade of infrastructure have many advantages, such as fewer building materials, less environmental impact, rapid restoration of use, fewer traffic obstacles, and more economical. The budget for infrastructure in Western countries also illustrates the importance of formulating concrete structure repair and restoration strategies. We have now reached a point where the annual maintenance budget of most countries is higher than the budget for new structures [3]. According to the 2016 infrastructure report of the US ASCE, 56,007 of the 614387 existing bridges have suffered structural failure due to severe steel corrosion. The recent bridge repair costs have reached US$123 billion [4].

In Japan, according to Summary Of The White Paper On Land Infrastructure Transport And Tourism In Japan 2020, the ageing infrastructure is gradually increasing. There is a historical peak period for construction, about 1970-1980. However, although the annual increase of ageing bridges and port facilities have a peak (Fig. 1-1, Fig. 1-2), the existing ageing facilities do not have a peak. They will accumulate year by year (Fig. 1-3), although some infrastructure will be demolished and newly built. The older the infrastructure, the more and the more serious problems they will face. The percentage of bridges that are at least 50 years old is up to be 52% as of 2029. Local governments, which manage more than 90% of the approximately 720,000 bridges, will manage large amounts of ageing infrastructure in the future. The percentage of port facilities that are at least 50 years old is expected to be 32% as of 2023. [5]

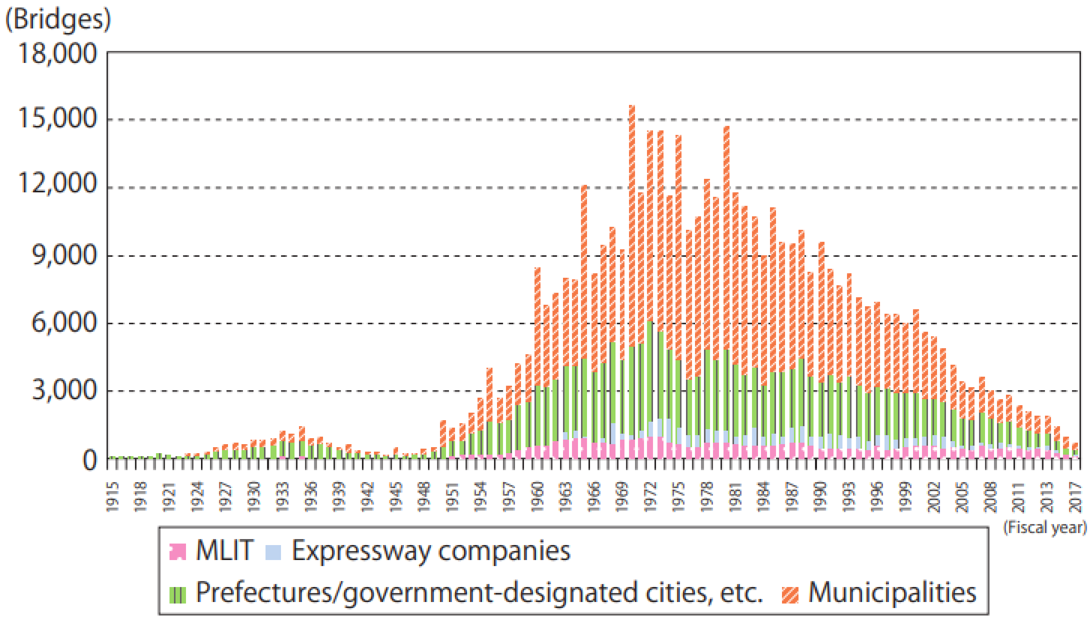

Fig. 1-1 Number of Bridges by Construction Year (in Japan, Source from MLIT, p11/33)

https://www.mlit.go.jp/hakusyo/mlit/r01/hakusho/r02/pdf/English%20Summary.pdf

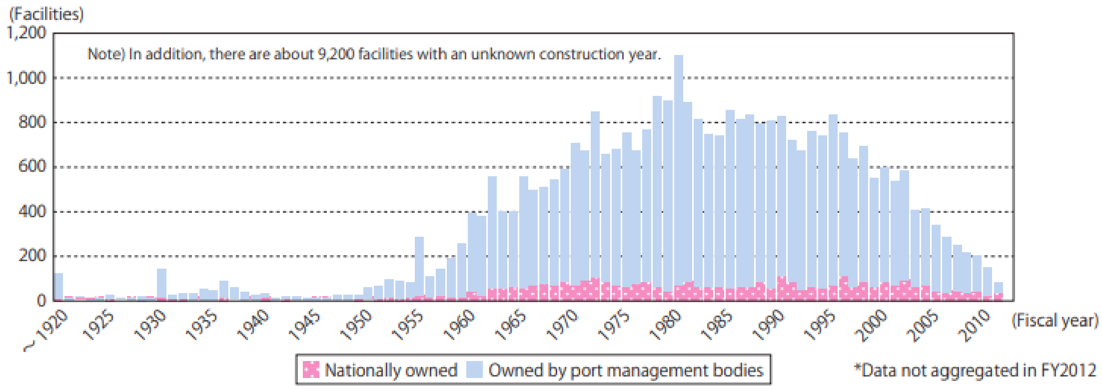

Fig. 1-2 Number of Port Facilities by Construction Year (in Japan, Source from MLIT, p11/33)

https://www.mlit.go.jp/hakusyo/mlit/r01/hakusho/r02/pdf/English%20Summary.pdf

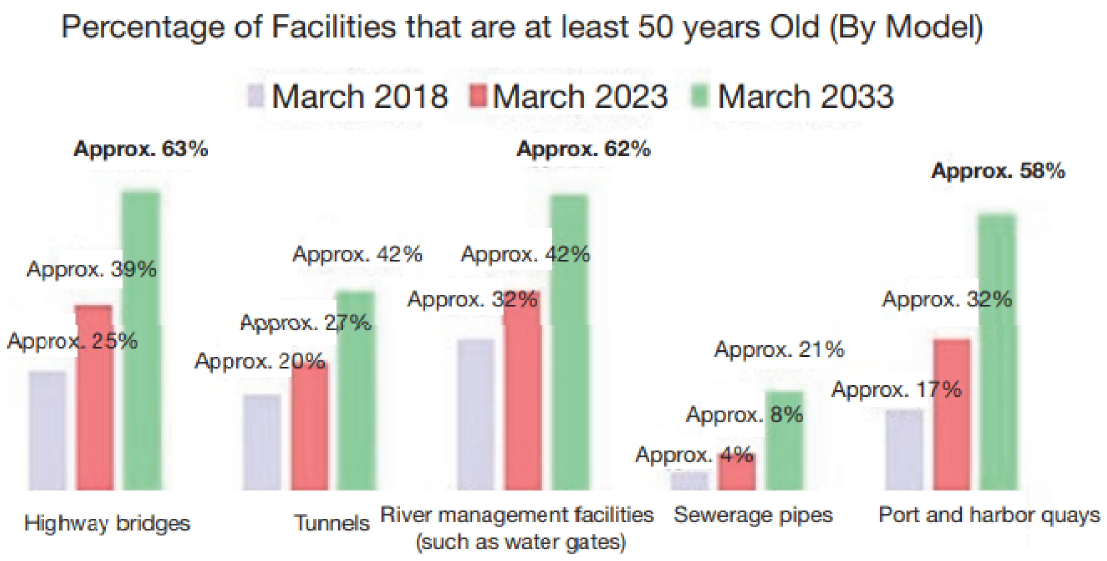

Fig. 1-3 The percentage of facilities that are at least 50 years old is on the rise. (Source from MLIT, p14/33)

https://www.mlit.go.jp/hakusyo/mlit/r01/hakusho/r02/pdf/English%20Summary.pdf

The ageing infrastructure that is increasing year by year means that more and more engineers and technicians are required to participate in maintenance, renewal or even new construction. However, with the ageing of infrastructure, population ageing in various developed and even developing countries is also becoming increasingly severe, and labour is gradually lacking. As a result, the number of employees in civil engineering has decreased year by year, from 105,187 in 2005 to 90,788 in 2018, a drop of 14% (Fig. 1-4). Although the population birth incentive policy is constantly exploring and improving, regardless of its effect, the growth rate of the population and labour regeneration cycle lasts as long as the 20th anniversary is obviously far less than the speed of the ageing of infrastructure. Therefore, we are currently facing the contradictory status quo of increasing labour demand and decreasing labour supply. In order to alleviate this contradiction, we must formulate reasonable infrastructure maintenance and repair strategies and adopt a proactive approach to prevention. Try to delay the arrival of updated infrastructure with high-density human, material and financial requirements.

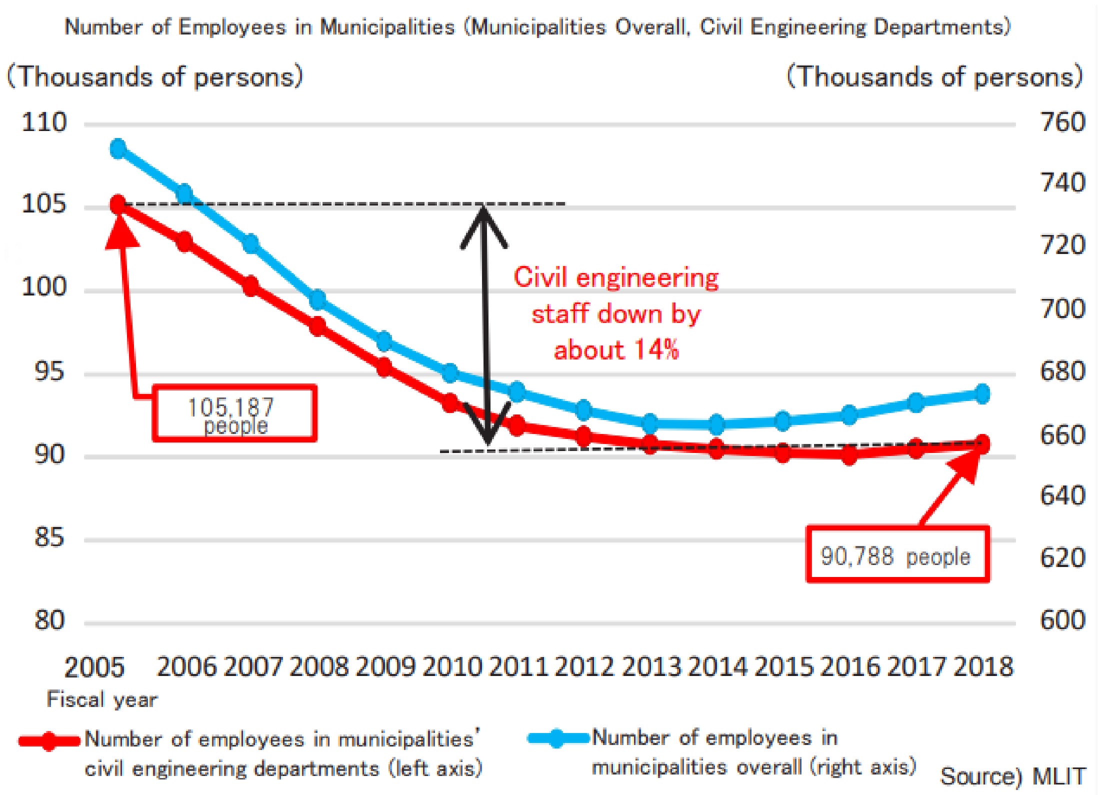

Fig. 1-4 Decreasing Number of Engineers The number of civil engineering and construction staff in municipalities is decreasing (Source from MLIT, p14/33)

https://www.mlit.go.jp/hakusyo/mlit/r01/hakusho/r02/pdf/English%20Summary.pdf

In response to this contradiction, MLIT pointed out three points for the direction of future initiatives[5][14], which is the guideline for our engineering practitioners.

(i) Switch to"Preventive Maintenance."

• Switch from the"corrective maintenance" in which measures are taken after problems occur in a facility to the"preventive maintenance" in which measures are taken before problems occur in a facility to reduce maintenance and replacement costs, which are expected to increase in the future.

[Examples of Concrete Measures]

• Implement intensive infrastructure measures that need work at an early stage, as revealed by previous inspections and assessments.

(ii) Make Use of New Technologies

• Make use of new technologies such as AI, robots, drones, and 5G, and develop and utilize data to improve the sophistication and efficiency of infrastructure maintenance and management.

[Examples of Concrete Measures]

• Enhance river monitoring through overflow detection, etc., using AI cameras.

• Digitize and accumulate maintenance information for each manager and support the development of an environment that enables its use and application to improve the sophistication and efficiency of infrastructure maintenance by local governments.

(iii) Cooperation among local governments and national government support for local governments

• Cooperation among local governments and national government support for local governments is essential for sustainable and efficient infrastructure maintenance. However, it is also necessary to deepen discussions, including on how to share costs.

The development of infrastructure in various countries and regions is not balanced. In developed countries, it has basically been completed and has gradually entered the maintenance and upgrade stage. However, for developing countries and underdeveloped countries, it still needs to be further improved. Although infrastructure construction has passed the stage of leaping growth, it is expected that global infrastructure demand will continue to grow steadily at a rate of 1-3% per year in the future and will expand to US$4.6 trillion in 2040 (Fig. 1-5). Looking at infrastructure demand by region, Asia is expected to account for more than half of global infrastructure demand by 2040, and China's infrastructure demand will account for about 60% of Asia. Judging from the comparison of infrastructure demand in 2007 and 2040, China has a tremendous demand at 31.3%, Asia (including Japan) at 23.5%, Europe at 15%, and Africa at 6.8%. It can be seen from the growth rate of infrastructure demand. It is expected to grow substantially in the future, with 232.7% in China, 138% in Asia, 64.6% in Europe, and 330.6% in Africa. Therefore, it can be said that from a global perspective, the demand for infrastructure construction is still very great, and the demand for concrete is still strong.

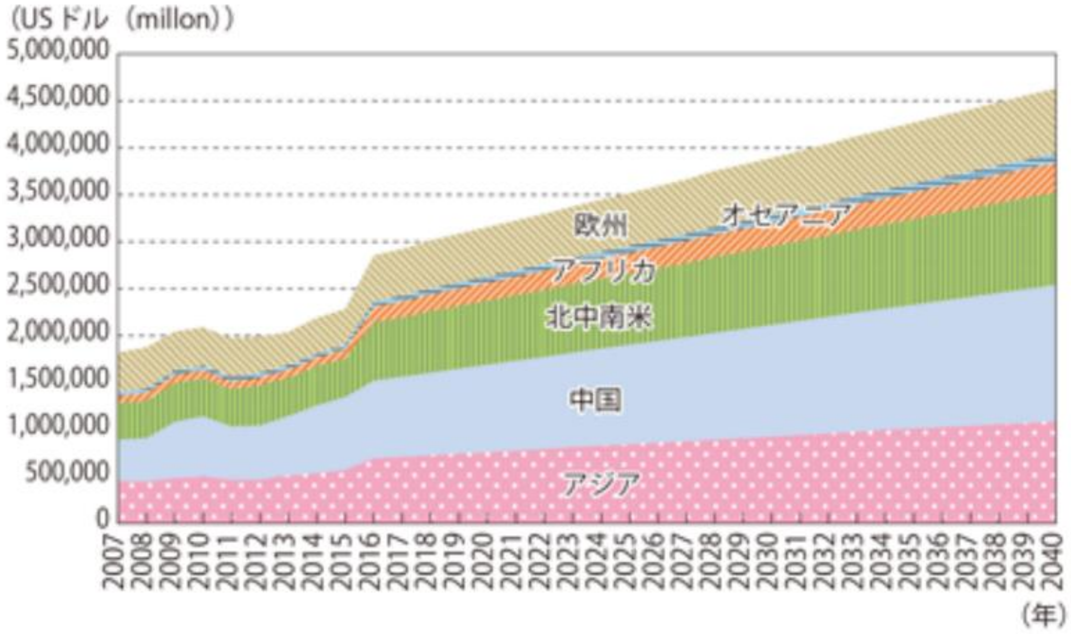

Fig. 1-5 Future forecast of infrastructure demand [5][131]

However, concrete, which is bulk consumption, is not sustainable. The greenhouse gases emitted from the concrete (cement) production process account for 8% of the world's total emissions. According to statistics, the global average atmospheric carbon dioxide concentration in 2019 is about 409.8 ppm (referred to as ppm), which are higher than at any time in the past 800,000 years (Fig. 1-6). The increase in the concentration of carbon dioxide in the air will, in turn, act on the concrete structure, neutralize the concrete structure, reduce the alkalinity of the concrete environment, and even cause further damages such as corrosion of steel bars for a long time. Carbon dioxide will also dissolve into the ocean like soda in a soda can. It reacts with water molecules to produce carbonic acid and lower the pH of the ocean. Since the beginning of the industrial revolution, the pH value of ocean surface water has dropped from 8.21 to 8.10. This drop-in pH is called ocean acidification. A decrease of 0.1 may not seem like much, but the pH is logarithmic; a decrease of 1 unit in pH means a 10-fold increase in acidity. Increased acidity will destroy the typical growth environment of marine organisms [6] and cause acid corrosion on marine environmental infrastructures.

Another well-known environmental impact of the greenhouse effect is that the annual average temperature rises year by year. The annual rainfall increases [5][12]. As a result, glaciers melt, sea levels rise, and organisms in the glacial zone lose their homes for survival. The living space of coastal residents is threatened. The area of arable land is reduced, and the port facilities are eroded by seawater and rivers in a larger area, which further aggravates the ageing of infrastructures.

In addition, the transportation of concrete raw materials will inevitably increase air pollution. The demolished buildings and infrastructure have generated a large amount of construction waste, causing environmental pollution and land occupation. Although more and more scholars are committed to recycling construction waste, the usable part is limited.

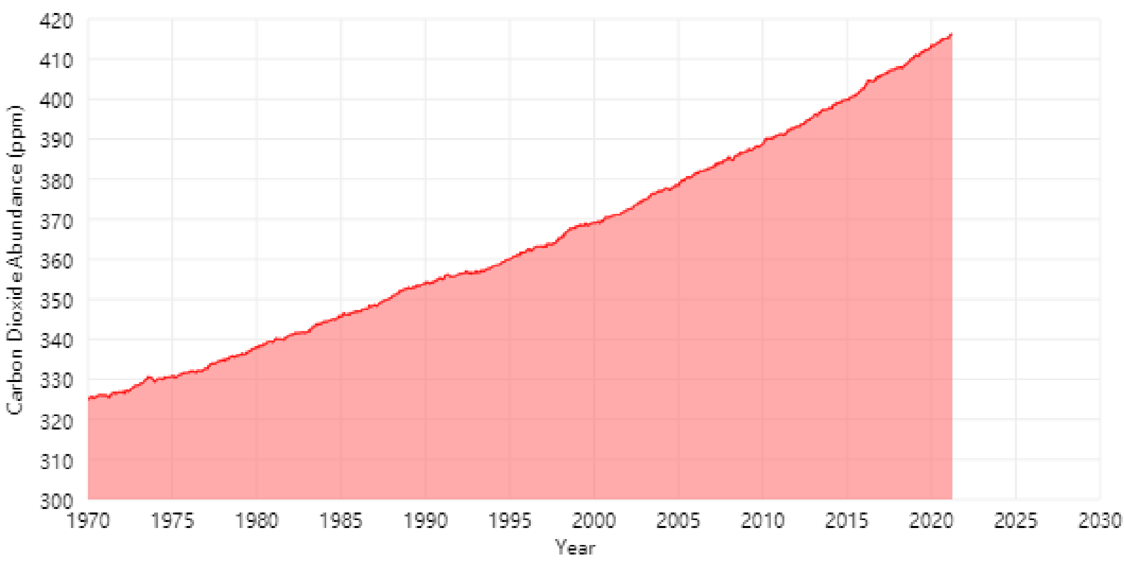

Fig. 1-6 Increasing carbon dioxide concentration year by year[6]

We live on the same earth, and climate warming concerns the people of all countries and the destiny of humanity. The "Paris Agreement" was formally signed at the United Nations Climate Summit on

December 12, 2015. On April 22, 2016, 171 countries signed the "Paris Climate Agreement" at the United Nations Headquarters on Earth Day. Regarding security threats in non-traditional areas, global cooperation is used to advance the governance process and curb global warming jointly. On September 22, 2020, at the General Debate of the Seventy-fifth United Nations General Assembly, China had committed to increasing its independent national contribution, adopt more effective policies and measures, strive to reach the peak of carbon dioxide emissions by 2030, and strive to achieve carbon neutrality by 2060. Achieve the promise of carbon neutrality by 2060. Following China, Japan and South Korea also announced a "net-zero declaration" to achieve almost zero greenhouse gas emissions. After years of cooperation with the government, these three Asian economies have officially stated to reduce greenhouse gas emissions to almost zero by 2060 (China) or 2050 (Japan, South Korea) [7]. On January 20, 2021, US President Joe Biden signed an executive order to return to the Paris Agreement [8]. On February 19, 2021, the United States officially returned to the Paris Agreement (W. Zhao, 2021). All countries are planning and working hard to create a low-carbon environment.

In order to gradually achieve the goal of carbon neutrality and zero emissions, all walks of life need to make necessary and fruitful efforts. As a sizeable energy-consuming industry with a high proportion of carbon dioxide emissions, the construction industry is vital to make necessary efforts and improvements in building materials' green and sustainable development.

Because of the different functions of concrete infrastructure, the service environments are also different. For example, buildings such as flood control dikes, reservoirs, etc., are under the erosion of seawater chloride salt(or river water) all year round. In severe cold areas, the winter also experiences freezing and swelling damage. In spring and autumn, they may experience a freeze-thaw cycle. The part above the water surface has experienced carbonization, erosion by wind, rain and snow, and the effects of dry and wet cycles for a long time. The durability of concrete materials is the guarantee of the life of concrete structures in the service environment. The vast maintenance costs caused by insufficient durability are alarming worldwide[9, 10]. Among the many factors that degrade the durability of concrete, freeze-thaw cycles, chloride erosion and carbonization are the most common and main factors[11, 12]. The durability problems accounted for more than 80% [13].

After learning from the historical lessons of the collapse and destruction of many infrastructures, which even caused severe casualties and the economy, countries are paying more and more attention to infrastructure durability. Corresponding industry standards have been formulated from durability design and construction to maintenance management and life prediction. Such as Asian Concrete Molde Code (2014), fib Model Codes 2010 and its upgraded edition Model Code 2020 -<Durability Design and Through Life Management of New and Existing Structures> which is to be taken forward by TG10.1[14], and ISO 13823 (2008) < General principles on the design of structures for durability> and the latest ISO 16311< Maintenance and Repair of Concrete Structures>. In addition, in terms of maintenance management, various departments have also formulated corresponding dynamic management bills. Japan revised its river law in 2013, for example, stipulating that river management facilities such as dikes should be inspected at least once a year. Dams under the jurisdiction of the Ministry of Land, Infrastructure, Transport and Tourism are required to undergo regular inspections and comprehensive inspections to assess their soundness. At the same time, to let the public understand the importance of managing the soundness of the dam and the importance of maintenance, the evaluation results are announced [15]. In 2017, China drafted the "Guiding Opinions of the Central Committee of the Communist Party of China and the State Council on Carrying out Quality Improvement Actions" (Zhongfa [2017] No. 24)[16]. The guidance requires that the construction quality of significant projects be ensured and the construction of century-old projects, including bridges, tunnels, ports, waterways, subgrade and pavement projects, high slope projects, ship locks, etc. It is necessary to establish a high-quality evaluation index system for highway and water transportation projects. Other developed countries have also carried out long-term durability research and implementation in the field of infrastructure. The United States has launched a long-term performance plan for bridges. The Longevity Bridge Project has been launched in Europe. South Korea has proposed the Super Bridge 200 project to reduce the working life of major structural components. The default is 200 years. Various countries have shifted their work orientation from the initial focus on meeting the mechanical safety requirements to the later introduction of durability design, and then to the recent focus on the durability and life prediction design of new buildings and quality monitoring of materials and construction processes, but also the maintenance and repair of ageing buildings, and the remaining life prediction assessment.

In the standard design, construction and use, material durability is the first line of defence to achieve a long life cycle of structures. There are various measures to improve the durability of concrete. Among them, improving the surface quality of concrete has the advantages of convenient construction and little impact on the environment and life during maintenance. The surface layer of concrete is to the inner structure, what the skin is to the human body. An ideal surface layer of concrete can effectively resist various adverse factors in the external environment.

In this paper, the surface quality of existing buildings (damaged surfaces) and new buildings (non-damaged surfaces) are improved by treated with a compound impregnant. The improvement of performance, remaining service life, and material reliability indicators under different improvement schemes are studied. In addition, a series of studies have been carried out on failure probability, life cycle cost, etc. It is expected to provide a reference value for maintaining and modifying new buildings and existing buildings in the future.

In short, protect people's lives and property from the perspective of infrastructure safety and reliability, create a safe, comfortable, and environmentally friendly living environment, attach importance to the design, construction, operation and maintenance of new infrastructure. Studying the maintenance of existing ageing infrastructure and buildings, from the perspective of the entire life cycle, with moderate economic investment, to maximize the service life of existing infrastructures is an urgent mission for our engineering construction practitioners.

1.2 Research Scope And Objectives

1.2.1 Research Scopes

1. Indoor simulation experiments:

The effect of penetrants and its dosage on the surface properties of concrete, such as air permeability, water absorption, pore structure, pH value, salt freezing resistance, etc.;

2. Experiments about specimens from nature cold marine environment:

The influence of impregnants on the carbonization of concrete and the calculation of the anti-carbonization life of the concrete;

The development of salt freeze degradation under the action of impregnant and calculate the estimated salt-freezing-thawing resistance life;

3. The influence of the impregnants on the anti- salt-freezing-thawing performance of the concrete after re-applied the penetrants.

4. Life cycle economic analysis

1.2.2 Objectives

1. Based on the impregnant instructions, to further grasp its applicable environment and adjust the dosage of impregnant according to the quality of the concrete needing repair, so that the application effect is much better and the cost-effectiveness is much higher;
2. To provide a basis for concrete maintenance and decision-making by the relationship of the concrete life span and surface impregnants;
3. Research for a calculation method that can reflect the actual condition of concrete as realistically as possible, and with a high degree of computerization and a high probability of accurately predicting the life of concrete;
4. Propose an economical and reasonable maintenance plan.

1.3 Organization Of Thesis

This thesis consists of seven chapters.

Chapter 1. Introduction: Introduced the current status of various infrastructures, the pressure of the ecological environment, which explained the necessity of maintenance and management of the infrastructures concrete in their life cycle cost. It outlined the research content and objectives of the research.

Chapter 2. Literature Review: Summarized and reviewed the theoretical basis required for experimental analysis and life calculation in the subsequent chapters. Focus on the following aspects: the common corrosion and corrosion mechanisms of concrete; concrete surface quality maintenance and repair measures and principles; concrete service life prediction theory and the concrete life-cycle-cost analysis theory.

Chapter 3. Influence of concrete impregnant on the durability of concrete surface in the laboratory environment: It shows the effects of different dosages impregnants on concrete surface air permeability, water absorption, micro-pore structure, pH values, and its influence on scaling amount of concrete surface in the salt freeze-thaw environment (ASTM-C672) in the lab.

Chapter 4. The Effect Of Concrete Impregnant On The Durability Of Concrete Surface In Marine Environment——Tomakomai Project: A follow-up survey was conducted on the Tomakomai Breakwater after serviced for 3, 12 and 20 years, separately. The changes of chloride ion diffusion, carbonization depth, concrete surface microscopic pore structure, and pH of the concrete surface (with penetrants and without penetrants) were researched, and the anti-salt-freezing-thawing performance after re-application of penetrants was tested. Here, not all the test items were the same every time.

Chapter 5. Lifetime Distributions Prediction Of Tomakomai Dam Project: Concrete life prediction was conducted based on chloride ion attack, carbonization erosion, and salt-freeze-thaw damage. The calculation methods included the deterministic, reliability, and Monte Carlo methods.

Chapter 6. Evaluation Of The Economic Effect Of The Maintenance Plan: it discusses the calculation method of maintenance and repair cost of Tomakomai dam based on chloride ion diffusion factors and freeze-thaw scaling depth. It provides a theoretical basis for maintenance and repair, determining the time nodes for maintenance and repair and selecting maintenance measures.

Chapter 7. Conclusions And Outlook. It is a summary of the full-text work and prospects for the future.

The roadmap of the thesis is shown in Fig. 1-7.

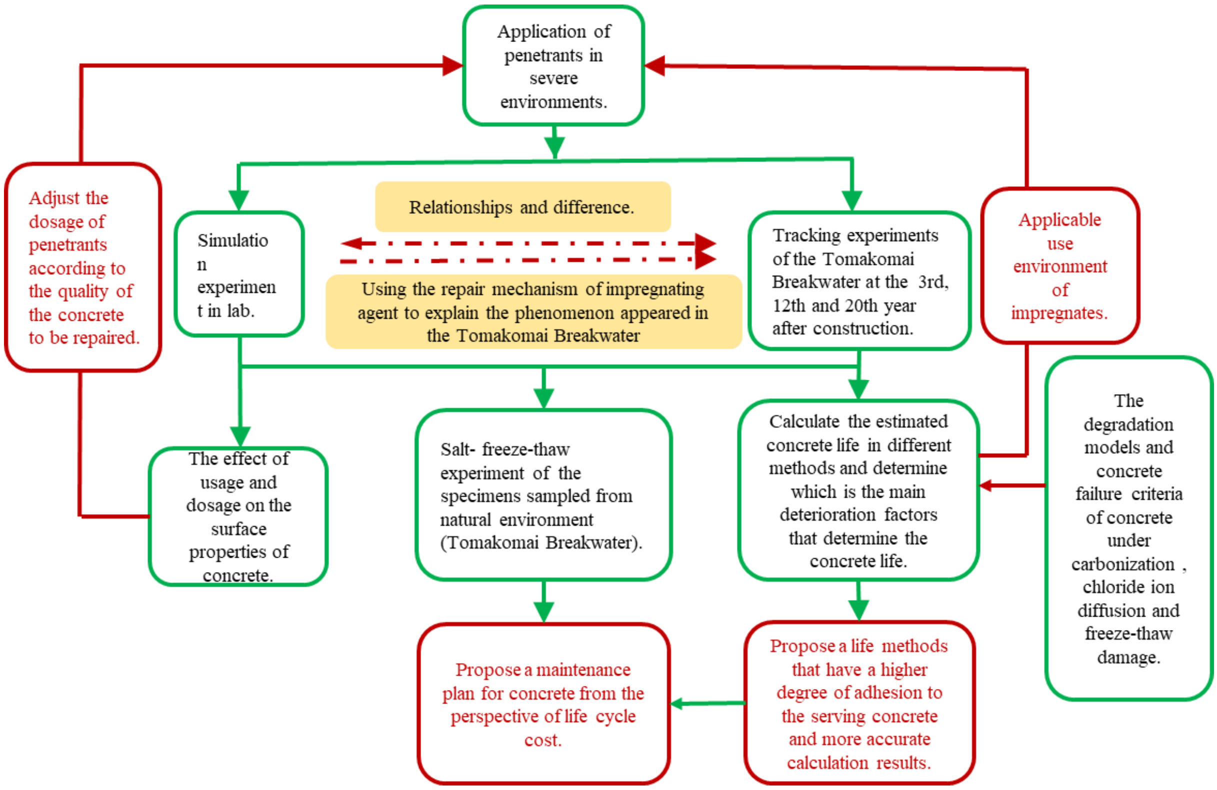

Fig. 1-7 Thesis road map

CHAPTER 2. LITERATURE REVIEW

2.1 Common Corrosion And Corrosion Mechanisms Of Concrete

2.1.1 Common corrosion factors of concrete in cold (in winter) ocean environment

In Showa 54 [17], Saeki and others conducted various investigations and studies on the harbour concrete (built-in Showa 53) that had gone through winter after the construction was completed, and a total of 194 survey sites, including wave-elimination projects 65, 80 breakwaters/quay walls (including 25 on the chest wall), 49 retaining wall/shed. The frost damage and spalling survey statistics show that the probability of scaling off the concrete surface after winter after construction is that there are 134 scaling damages, and the total scaling rate is about 69%, of which 88% are wave-elimination projects, and 69% of breakwaters/quay walls. 45% of the retaining wall/shed. Frost damage and spalling occur all along the coast of Hokkaido. The main types of damage are surface scaling damage. In some places, the surface scaling damage is mixed with the pop-up scaling caused by the coarse internal aggregate with high water absorption.

The Taizhou area in Zhejiang Province, China, belongs to the offshore environment. Scholars Guo Dongmei and Xiang Yiqiang [18][p7] conducted a quality survey of more than 300 bridges in the area. The specific damages were steel corrosion 11.3% and concrete spalling 10.1 %. Among the rusted parts, the proportion of pier and abutment foundations easily eroded by river water (seawater) is as high as 19%-34%.

In 1963 and 1965, the relevant units of the Ministry of Communications of my country conducted surveys on the concrete structures of 27 seaports in South China and East China. They found that the structural damage caused by the corrosion of steel bars accounted for 74%. In 1981, a survey of 18 reinforced concrete wharves in South China used for 7-25 years showed that 89% of the steel bars were corrupted or not durable. The corrosion damage occurred only for 5 to 10 years. The service life of these structures fails to meet the design base period requirements [19].

Coastal infrastructures are easily affected by the cycles of dry and wet caused by tidal fluctuations, hydraulic erosion caused by tsunamis induced by earthquakes, carbonisation, frequent occurrence of intense storms, erosion of chloride salts in seawater and sea air, sun ageing, and microorganisms in the water corrosion and the effect of greenhouses has led to rising sea levels. When located in cold regions, they are also subject to freeze-thaw cycles. It can be said that the environment in which coastal facilities are located is harsh. The primary consideration for concrete in offshore or marine environments in cold areas is the Influence of chloride on the corrosion of concrete steel bars and the scaling caused by sal – freezing-thawing.

These erosion factors will lead to the deterioration of reinforced concrete, which seriously affects the safety and durability of concrete structures. For concrete served in severe cold marine environments, the main corrosive factors are the erosion of chloride salts in seawater and sea fog, the destruction of freeze-thaw cycles in winter, and the constant carbon neutralisation in the atmosphere. This thesis focuses on the three major corrosion factors.

The harsh operating environment also determines the inconvenience of its construction and maintenance. Therefore, we hope coastal infrastructures can have the most extended service life and reduce maintenance with a reasonable economic cost. Thus, in the various construction and use processes of concrete， strictly controlling the construction quality, concrete surface protective measures should also be taken to reduce the corrosion from outside.

2.1.2 Chloride ion erosion

2.1.2.1 Ingress of chloride ions in concrete

There are usually two ways for chloride ions to invade concrete [19]: One is "incorporation", that is, during the formation of concrete, it is brought in by the raw material itself or added with other admixtures during the construction process. For example, in construction projects, the abuse of sea sand and seawater that have not been desalinated or the desalination treatment does not meet the standards, the use of admixtures containing chloride ions, the invasion of seawater during the construction of the marine environment, or the maintenance of seawater after construction, etc. The other is "infiltration". Hardened concrete is a heterogeneous porous material with multiple phases and multiple scales. Chloride ions in the service environment pass through defects such as cracks, pits and pores on the surface of the concrete and undergo capillary action (the saltwater moves to the dry part of the concrete) and penetrate. (Under the action of water pressure, the saltwater moves in the direction of lower pressure), diffusion (when the concentration difference exists, the chloride ion moves from the place where the concentration is high to the place where the concentration is low) and electrochemical migration (the chloride ion moves to a higher potential Move in a high direction), etc., enter the interior of the concrete in one or more combinations, and undergo various physical and chemical changes with the concrete, resulting in deterioration of the concrete [13]. In addition, it is also affected by the chemical bonding, physical bonding, and adsorption between chloride ions and concrete materials. Corresponding to specific conditions, one of the erosion methods is the main one. For example, the de-icing salt used on roads in winter, the chloride salt in the marine environment such as seawater and sea fog, and the chloride ions in the salt lake and saline soil infiltrate the concrete in the service environment. "Infiltration" is mainly caused by man-made reasons. It can be controlled and restricted by improving construction management and formulating relevant normative measures to reduce chlorine content. At the same time, "infiltration" is a comprehensive technical problem. It is related to the characteristics of concrete materials such as material quality, construction quality, concrete surface protection measures, chloride ion environment and other factors. "Penetration" is the primary way for chloride ions to enter concrete.

2.1.2.2 The mechanism of corrosion of steel bars caused by chloride ions[19, 20]

1) Destruction of the passive film: The concrete that has not been carbonised and corroded by chloride ions is highly alkaline, and there is a dense passive film on the surface of the steel bars. When chloride ions enter the concrete, they continue to migrate internally and accumulate on the surface of the steel. When the concentration of chloride ions on the surface of the steel exceeds the critical value of steel corrosion, it will destroy the passivation film on the surface of the steel and activate the iron atoms on the surface of the steel. Rust gradually occurs.

2) The formation of "corrosion battery": Chloride ion destroys the passivation film so that these parts (points) on the surface of the steel bar expose the iron matrix and form a potential difference between the area of the passivation film that is still intact. (As an electrolyte, there is generally water or moisture in the concrete). Corrosion often starts locally and gradually spreads on the surface of the steel bar.

3) Anodic depolarisation of chloride ions: accelerating the anodic process is called anodic depolarisation. In the corrosion process of steel bars, chloride ions only participate in the reactive approach. As an intermediate product that promotes corrosion, it does not change the composition of the corrosion products. The content of chloride ions in the concrete will not decrease due to the corrosion reaction. That is to say, wherever it enters, The free chloride ions in the concrete will destructively over and over again.

The chemical reaction formulas are:

$$Fe^{2+} + 2Cl^{-} + 4H_2O \rightarrow FeCl_2 \bullet 4H_2O \tag{2.1}$$

$$FeCl_2 \bullet 4H_2O \rightarrow Fe(OH)_2 \downarrow + 2Cl^{-} + 2H^{+} + 2H_2O \tag{2.2}$$

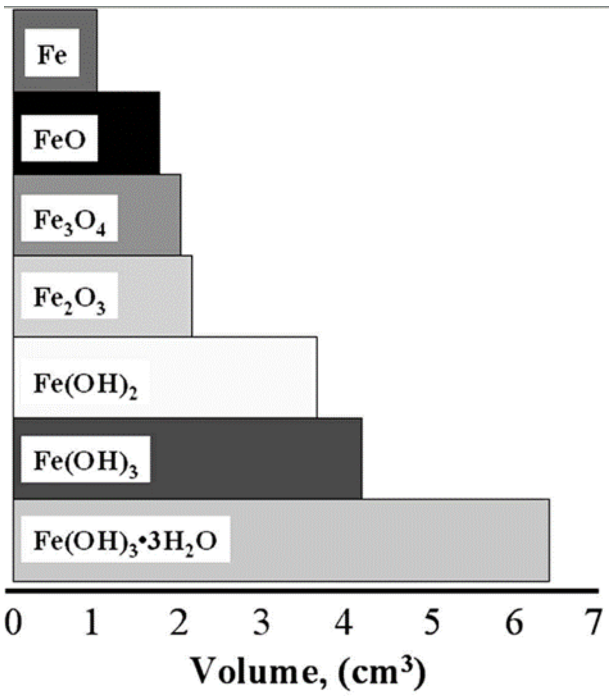

Fig. 2-1 The relative volumes of iron and its reaction product [21, 22]

The volume of corrosion reaction products can be increased by at least 3 times (see Fig. 2-1), forming a large expansion force in the concrete.

4) The conductive effect of chloride ions: the presence of chloride ions in the concrete strengthens the ion pathway, reduces the ohmic resistance between the anode and the anode, improves the efficiency of the corrosion battery, and accelerates the electrochemical corrosion process.
5) The role of chloride ions with cement and its effect on steel corrosion: Tricalcium aluminate in cement can react with chloride salts to form insoluble "double salts" under certain conditions, reducing the number of free chloride ions in concrete. From this perspective, cement varieties with high tricalcium aluminate are beneficial to resist the attack of chloride ions. However, the "double salt" can only be generated and kept stable in a strongly alkaline environment, and when the alkalinity of the concrete decreases, the "double salt" will decompose and re-release chloride ions; it may also be transformed under certain conditions. In this regard, "double salt" has a potentially dangerous side.

2.1.3 Carbonation-induced corrosion

Fresh concrete just after pouring is strongly alkaline (pH 12-13) due to the presence of potassium hydroxide and calcium hydroxide produced by cement hydration. Still, it changes into calcium carbonate over the years under the Influence of carbon dioxide in the air. This reaction is called neutralisation or carbonation.

The carbonisation of concrete by carbon dioxide in the atmosphere mainly includes two chemical reaction processes, Hydration and Carbonation:

Hydration reactions:

$$3CaO \cdot SiO_2 + 3CO_2 + nH_2O \xrightarrow{rH,C_3S} SiO_2 \cdot nH_2O + 3CaCO_3 \quad 2.3$$

$$2(2CaO \cdot SiO_2) + 4H_2O \xrightarrow{rH,C_2S} 3CaO \cdot 2SiO_2 \cdot 3H_2O + Ca(OH)_2 \quad 2.4$$

$$3CaO \cdot Al_2O_3 + 3\left(CaSO_4 \cdot 2H_2O\right) + 26H_2O \xrightarrow{r_{H,C_3A}} 3CaO \cdot Al_2O_3 \cdot 3CaSO_4 \cdot 32H_2O \tag{2.5}$$

$$4CaO \cdot Al_2O_3 \cdot Fe_2O_3 + 2Ca(OH)_2 + 2\left(CaSO_4 \cdot 2H_2O\right) + 18H_2O \xrightarrow{r_{H,CAAF}} 6CaO \cdot Al_2O_3 \cdot Fe_2O_3 \cdot 2CaSO_4 \cdot 24H_2O \tag{2.6}$$

Carbonation reactions

$$3CaO \cdot SiO_2 + 3CO_2 + nH_2O \xrightarrow{r_{C,C_3S}} SiO_2 \cdot nH_2O + 3CaCO_3 \tag{2.7}$$

$$2CaO \cdot SiO_2 + 2CO_2 + nH_2O \xrightarrow{r_{C,C_2S}} SiO_2 \cdot nH_2O + 2CaCO_3 \tag{2.8}$$

$$3CaO \cdot 2SiO_2 \cdot 3H_2O + 3CO_2 \xrightarrow{r_{C,CH}} 3CaCO_3 \cdot 2SiO_2 \cdot 3H_2O \tag{2.9}$$

$$Ca\left(OH\right)_2 + CO_2 \xrightarrow{r_{C,CH}} CaCO_3 + H_2O \tag{2.10}$$

This series of complex chemical reaction processes can be briefly and vividly expressed in Fig. 2-2 and Fig. 2-3.

The carbonisation process of concrete consumes the OH- inside the concrete and reduces the alkalinity of the concrete. When the depth of carbonisation reaches the thickness of the concrete cover, the pH near the steel bar gradually decreases. When the pH drops to a certain level (usually considered to be less than 11), the loss of the passive film's protective effect on the steel bar's surface will trigger the corrosion of the steel bar. The corrosion of the steel bars will cause cracks, stress reduction, etc. However, the dense product of the carbonisation reaction reduces the porosity of the concrete to a certain extent and improves the concrete density. At the same time, the diffusion of harmful gases into its interior is inhibited, and the carbonisation process is slowed down. The carbonisation process is affected by the humidity and temperature of the environment in which the concrete is served.

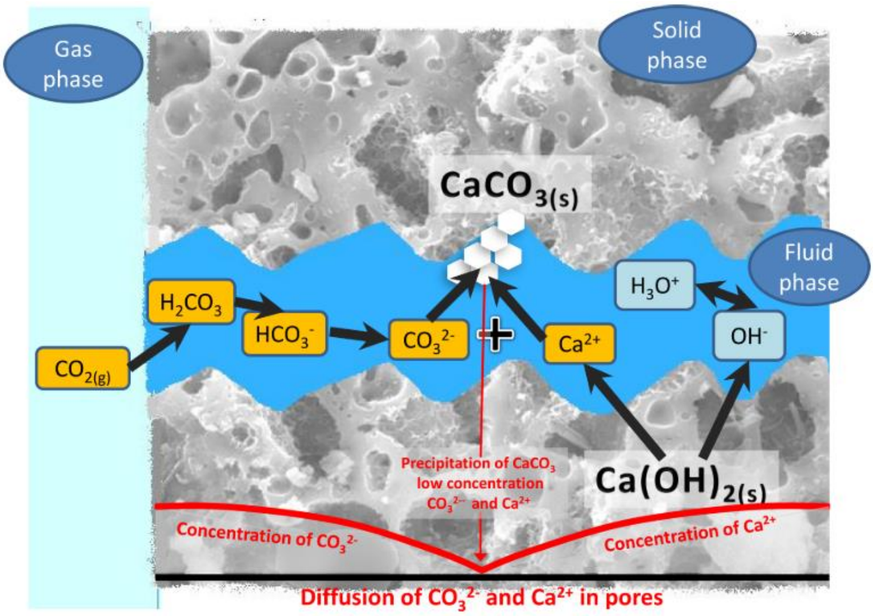

Fig. 2-2 Mechanism of carbonation [23]

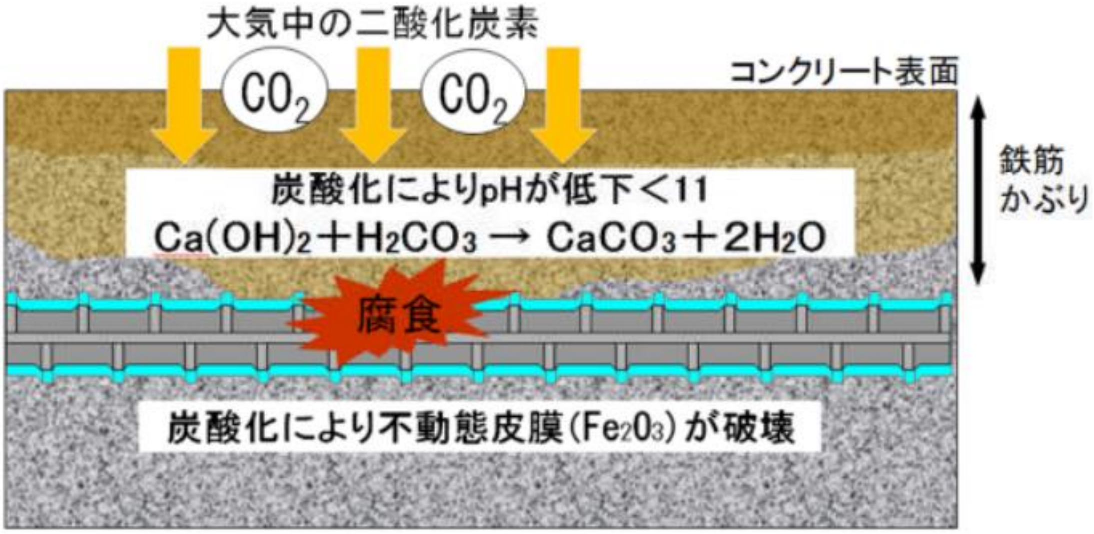

Fig. 2-3 Mechanism of carbonation [24] P1-8

2.1.4 Freeze-thaw damage and salt-freeze-thaw combined damage

The classic supported theories as the primary mechanism of frost damage are the "hydraulic pressure theory" a) published by Powers in 1945[25] and the "osmotic pressure theory[26]" with subsequent modifications. The hydraulic pressure theory is that the moving pressure (water pressure) of water is generated by the volume expansion when the water is existing in the pores changes to ice. This pressure causes the tissue to expand and destroy. Explains that. This theory explains the importance of entrained air to absorb the moving pressure of water and mitigate frost damage.

Furthermore, the moving pressure of water is affected by the moving distance of water. When the distance between bubbles is 250 μm or less, the bubbles efficiently absorb the moving pressure of water. Explain that it reduces the expansion of the tissue. That is the importance of air entrainment to ensure frost damage resistance is not in the amount (air volume) but in the distance between air bubbles (air bubble interval factor). In the case of smouldering, air volume measurement during freshness is performed as a countermeasure for intermittent evaluation because there is no easy way to measure the distance between bubbles[27].

However, it is known that the amount of air during freshening does not always match the amount of air after curing, and in the field of vibration compaction, too much emphasis is placed on surface aesthetics. However, there are problems such as the disappearance of the entrained air and the uneven distribution of bubbles. In the future, it is desired to develop a technique for securing the required distance between bubbles and a simple test method for confirming the distance. According to the water pressure theory, deterioration progresses as the freezing temperature decreases.

The contraction phenomenon that occurs when the AE concrete freezes cannot be explained. For this reason, this theory was modified, and a new osmotic pressure theory was developed.

The osmotic pressure theory explains that when water in large pores freezes, unfrozen water in small pores is attracted toward the large pores, causing water movement pressure. The alkaline component is dissolved in the water in the pores. When this alkaline solution is cooled, ice crystals are formed, and the alkaline components contained in the solution before it turns into ice crystals are precipitated in the unfrozen alkaline solution, and the concentration of the unfrozen solution becomes high. .. Therefore, osmotic pressure is generated and water moves between the concentrated residual solution in the large pores and the unfrozen low-concentration solution in the smaller pores. This theory explains that as the freezing temperature decreases, the solution concentrates, smaller pores are frozen in sequence, and the smaller pores shrink due to the attraction of the solution. In addition, it will be explained that chlorides such as anti-freezing agents increase the concentration of the solution in the pores existing on the surface layer of the concretion, and a larger osmotic pressure is generated to cause scaling[27].

Valenza et al. [28] proposed a glue-spall theory to explain the damage mechanism of concrete salt frost erosion. According to this theory, the salt frost erosion of concrete originates from the cracking of the salt-containing icing layer. The thermal expansion coefficient between ice and concrete does not match, and stress will be generated. As the temperature decreases, the stress causes the ice to crack under tension. The cracks on the ice layer will penetrate and propagate to the concrete base layer and then drive the concrete surface to peel off. However, scholars (Yang, 2012) analysed from the perspective of finite element and fracture mechanics theory and the spalling shape of the concrete surface caused by a force that this theory is still unreasonable. It is believed that assuming this theory is true, there should be a certain distance between cracks on the ice layer, and the spalled concrete should have a larger size instead of the fragmented shape shown in the actual experiment.

It is generally believed that salt will bring both beneficial and unfavourable effects on the freezing damage of concrete. Salt can reduce the freezing point of the aqueous solution and is considered to be a positive effect that is beneficial to reducing the frozen damage of concrete. Salt can also bring four adverse effects. ① The hygroscopicity of salt improves the water retention inside the concrete; ② The super-cooled water produced by the double salt will make more destructive power once it freezes; ③ The salt concentration gradient in the concrete will cause delamination and icing, which will produce different stresses; ④ Salt supersaturation in the concrete pores will destroy salt crystals. The combined effect of these positive and negative effects of salt leads to the most severe salt freeze damage of concrete caused by the salt concentration.

2.2 Concrete Surface Quality Maintenance And Repair Measures And Principles

There are many ways to improve the durability of concrete, from design, construction, curing[29], operation, and maintenance. There are mainly the following methods to maintain and improve the surface quality of concrete during operation:[24] p1-12

1) Water treatment, including water stop and drainage treatment, can cut off the carrier of harmful substances such as salt or other acids, alkalis into the concrete and also cut off the leading causes of freeze-thaw damage;
2) Surface coating, impregnation packing method. The surface coating method often uses resin or PCM series to smear the surface of the concrete to form a protective layer. The impregnation packing method can penetrate the surface of the concrete and chemically react with the concrete to form a hydrophobic film or dense layer by applying silane or silicate on the concrete surface to prevent the intrusion of external moisture salt damage and so on.
3) The section repair method repairs the structure's durability by cutting away the concrete cover with rusted swelling cracks and treating the corroded steel bars with high-strength mortar. However, the intervention time of the physical repair method is relatively late, and the cost is relatively high. The electrochemical incompatibility of new and old concrete is likely to cause steel corrosion and concrete shrinkage cracks nearby. The application range is limited, and it is far from meeting actual engineering needs[30]. In actual engineering, it can be combined with other protection methods. Its specific construction methods include the Plastering method, Wet spray method, Dry spray method, and Grout injection method.
4) Electrochemical anti-corrosion construction method. Including the Electrocorrosion protection method, Desalting method, and Realkalization method. Electrochemical salt discharge can play a role in reducing the total amount of chloride ions in concrete. The principle of electrochemical salt discharge is to form an electric field between the steel bars and the external electrolyte solution of the concrete so that the Cl^- near the steel bars moves in the direction of the outer electrolyte, enters the solution, and at the same time reacts to generate OH^-, which improves the alkalinity around the steel bar, which is beneficial to the steel bars. Keep it passivated. The main reaction process is as follows[31]

Anode reaction:

$$2H_2O \rightarrow O_2 + 4H^+ + 4e \quad 2.11$$

$$4OH^- \rightarrow 2H_2O + O_2 + 4e \quad 2.12$$

$$2Cl^- \rightarrow Cl_2 + 2e \quad 2.13$$

Cathodic reaction:

$$2H_2O + 2e \rightarrow 2OH^- + H_2 \quad 2.14$$

$$O_2 + 2H_2O + 4e \rightarrow 4OH^- \quad 2.15$$

The salt discharge effect (salt discharge rate) of the electrochemical salt discharge method is usually affected by the duration of electrification[32], current density, electrolyte[33], the form of steel bars, cross-sectional shape [34], rebar placement[35] and concrete cover[36] and so on.

2.3 Concrete Service Life Prediction Theory

2.3.1 Basic terms and definitions of service life[37]p3

Service life is the period after manufacture during which the performance requirements are fulfilled. As with performance, service life can be treated at different levels. The necessary actions taken at the end of service life depend on the grade applied. At the building level, the end of service life would normally entail complete renovation, reconstruction, or rejection. It would mean replacing or repairing those components or materials at the structural member or material level.

- Durability limit states

Corresponding to the state in which the deterioration of the structure or structural member from the environmental impact reaches a certain specified limit or mark of durability.

- Degree of reliability, reliability

The probability that the structure will complete the predetermined function under the specified conditions within the specified time.

- probability of failure: p_f

The probability that the structure cannot perform its intended function.

- Reliability index β

A numerical index to measure the reliability of the structure, the reliability index β is the inverse function of the standard normal distribution function with negative failure probability pf.

- Probability distribution

The statistical law of random variable value is generally expressed by probability density function or probability distribution function.

- Statistical parameter

In the probability distribution, it is used to represent the average level and discrete degree of the numerical characteristics of random variables.

2.3.2 Life prediction methods and models

i. Method for estimating durability of structural members can divide into four aspects in usual: [37][p36][38][P6-7]:

1) The empirical method. Based on many laboratory and field test results and the accumulation of experience, a semi-quantitative prediction of the service life is made, including empirical knowledge and reasoning. Some current concrete standards also estimate the life span in this way. It is believed that if the principles and methods proposed by the standards can be followed, the concrete will have the required life span. If the design life is relatively long, the use environment is terrible, or a new situation is encountered without experience, this prediction method is unreliable.
2) The method of verifying or calibrating the existing degradation model based on the actual

degradation situation. The current life prediction models commonly used in the durability evaluation of concrete structures include: the carbonisation degradation model, chloride ion diffusion model, freeze-thaw damage degradation model, rust expansion cracking model, crack width and steel corrosion limit model and bearing capacity degradation model, etc. . The use of mathematical models to predict service life is currently the most commonly used method. The prediction reliability is related to the rationality of the model and the accuracy of the selection of materials and environmental parameters.

When using deterioration models for life prediction, the key is to clarify the life evaluation criteria corresponding to each prediction model. Before life prediction, we must first clarify the intended function of concrete and which technical index is used to determine the functional failure of concrete. The corrosion development of steel bars can be roughly divided into three stages, as shown in Fig. 2-4[39], Early age cracking stage→Corrosion initiation stage→Propagation stage→Failure. There are many life evaluation criteria based on the development stage of steel corrosion, which mainly include three categories [40-42]: the life criterion of steel bar bluntness, the life criterion of rust expansion cracking, and the life criterion of crack width and the amount of steel corrosion. They take "rebars begin to corrode" [43-45], "rust-expanded cracks of extension bars appear on the surface of the concrete"[46-48], and "the width of rust-expanded cracks or the amount of corrosion of steel bar reaches a certain limit value" [49]—these three progressive indicators as signs of their end of life. Chloride ion diffusion models mostly use steel depassivation as their life criterion. In the bearing capacity model, there are two criteria: ① Bearing capacity life criterion: the bearing capacity is reduced to a certain limit value as the end of life symbol-bearing capacity life criterion [50, 51]; and ② fatigue damage life criterion: the limit value of the index that can characterise the degree of fatigue damage is used as the end of life sign. In the study of concrete life prediction based on freeze-thaw damage, six leading indicators can be used as the end of life of the criterion[52]: ① mass loss rate; ② Strength loss rate; ③ Ultrasonic or resonance frequency; ④ Fracture energy or fracture toughness reduction rate; ⑤ Relative dynamic elastic modulus or dynamic elastic modulus loss rate; ⑥ Strain (Du, Yao, Wang, & Cao, 2014); ⑦ Spalling depth, Which index is selected as the basis for judgment depends on the standard (ASTM-C

672, ASTM-C 666, RILEM CDF and JIS A 1148 etc.) that the freeze-thaw experiments are based on, and it is closely related to the indoor freeze-thaw experiment or the on-site freeze-thaw experiment.

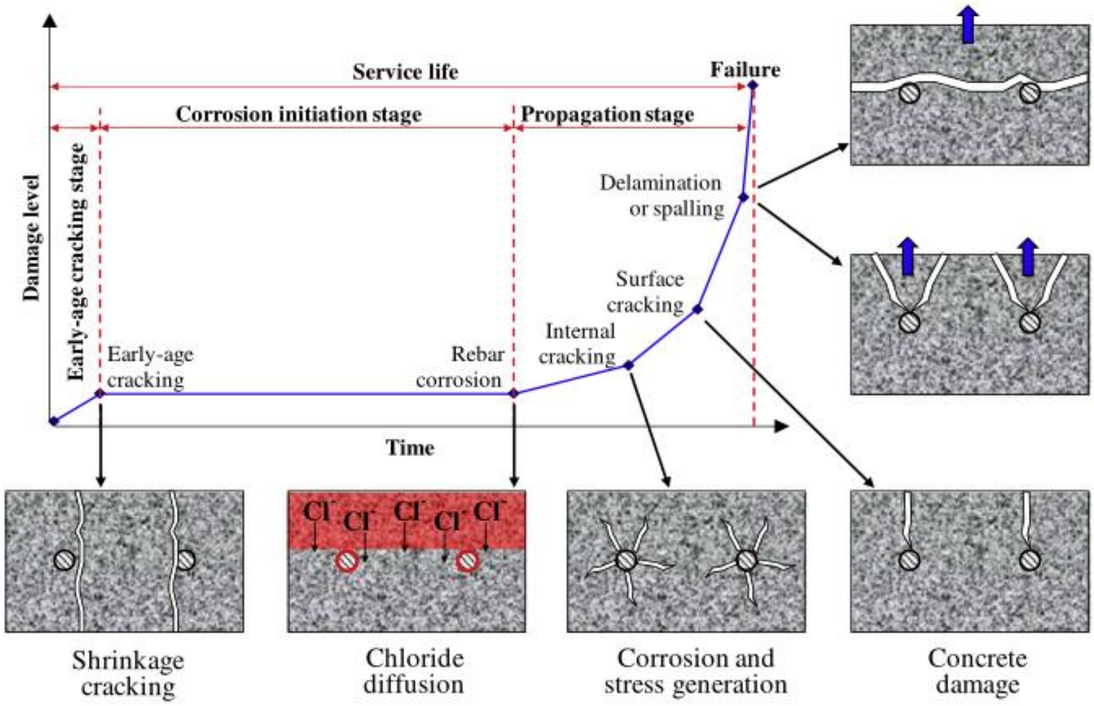

Fig. 2-4 Schematic description of service life model based on Chloride ion erosion [39]

3) Methods based on rapid testing, such as indoor rapid freezing and thawing, and rapid carbonisation experiments to derive the estimated life;
4) Other applicable methods.

ii. From the perspective of the reliability of life prediction, it can be divided into random methods and deterministic methods

Since many factors affecting the service life of concrete are variables that change with time or space, such as the thickness of the concrete protective layer, environmental temperature, humidity, the concentration of harmful media, etc., it can be said that many random variables determine the generalised load and resistance. Therefore, it is very reasonable to predict the remaining service life of the structure based on the method of probability or reliability index. However, this method has the disadvantage of requiring a lot of statistical data to obtain the distribution probability function of each variable. It is difficult to operate for actual projects, especially when destructive testing is required to obtain data. Usually, the data obtained by the predecessors in similar engineering research or the statistical data of universal laws can be used. To a certain extent, it may conceal the unique personality differences of specific projects. Deterministic calculation method, data is easy to obtain, but the calculation structure has a certain degree of contingency, and it is of little reference for similar projects.

The state of the structure or material is represented by the following three functions

$Z = R - S > 0$ Indicates that the structure or material (such as concrete) is in a reliable state;

$Z = R - S = 0$ Indicates that the structure or material (such as concrete) has failed or destroyed;

$Z = R - S < 0$ Indicates that the structure or material (such as concrete) is in a critical state.

Where:

Z : Is the limit state equation;

R : Generalised resistance of structure or material, Such as the concrete cover, the threshold of chloride ions, allowable scaling depth and allowable scaling amount etc.

S : Generalised load on the structure or material, For example, the corrosion concentration of chloride salt on the concrete (reinforced steel surface), the depth of neutralisation, the depth of freeze-thaw or the amount of freeze-thaw spalling, etc.

The deterministic calculation method is the concrete life calculated when Z=0. The calculation process does not consider the probability distribution of R and S.

The random methods consider the probability distribution of R and S and the failure probability P_f Pf (or reliability index β), the concrete life calculated when Z is satisfied $P_f = P\{Z \leqslant 0\} \leqslant P_t$, where P_t Pt is the limit of the allowable failure probability.

2.3.3 Based on the chloride attack

2.3.3.1 Chloride diffusion model

i. Deterministic calculation model

Salt prediction: The diffusion process of chloride ions in concrete complies with Fick's second law:

$$C(x,t) - C_i = C_{0s}\left\{1 - \mathrm{erf}\left(\frac{x}{2\sqrt{D_{aps} \cdot t}}\right)\right\} \tag{2.16}$$

Where

C(x,t): the total chloride ion concentration at the distance x from the concrete surface, kg/m^3;

x: The distance between the test point of the total chloride ion concentration from the concrete surface, mm;

t: exposure time, years;

C_{0s}: surface total chloride ion concentration, kg/m^3;

C_i: the initial total chloride ion concentration in the concrete, kg/m^3;

D_{aps}: the apparent diffusion coefficient of perchloride ions, mm^2/year

erf: error function (Formula

2.17).

$$\operatorname{erf}(s)=\frac{2}{\sqrt{\pi}}\int_0^s e^{-\eta^2}\,d\eta \tag{2.17}$$

The durability limit state of concrete structures in marine environments is generally defined as the time when the corrosion begins, that is, the time when the chloride ion concentration on the surface of the steel bars reaches the chloride threshold [53]. Once the corrosion of the steel bar begins, the subsequent development speed is relatively fast. Generally, the subsequent corrosion of the steel bar, the development of cracks, and the reduction of the load-bearing capacity are used as a safety reserve.

Therefore, the above formula C(x,t) is replaced by the critical value of chloride ion concentration on the surface of the steel bar, C_{cr}. After the Deformation of the formula

2.16, the concrete life calculation formula

2.18 can be obtained

$$t=\frac{x_c^2}{4D_{aps}\left[erf^{-1}\left(1-\frac{c_{cr}-c_i}{c_{0s}}\right)\right]^2} \tag{2.18}$$

C_{cr}: Critical value of chloride ion concentration on the surface of steel bars (threshold value).

ii. Probabilistic model

Based on the chloride ion lifetime estimation criteria, the expression of the Probabilistic model can be different when the calculation ideas are different.

- One calculation idea is to use the critical state when the chloride ion concentration on the surface of the steel bar reaches the threshold. The expression is shown in

$$Z(t)=C_{cr}-X(c,t)=0 \tag{2.19}$$

Where:

$Z(t)$: The limit state equation based on chloride concentration; C_{cr} : Chloride threshold; $Z(c,t)$: The concentration of chloride ions on the surface of the steel bars.

$$P_f = \{Z \leqslant 0\} = P\{C_{cr} - X(c,t)\} \leqslant P_t = \Phi(-\beta) \qquad 2.20$$

Where P_f : Failure probability; P_t : Allowable failure probability; β: Reliability index.

- Another calculation idea is setting the depth of the chloride ion threshold frontier developing to the concrete cover as the critical state Fig. 2-5, and the expression is:

$$Z(t) = X_{cr} - C(t) = 0 \qquad 2.21$$

Where:

$Z(t)$: The limit state equation based on the concrete cover; X_{cr} : concrete cover; $C(t)$: depth of ingress of the chloride threshold in concrete.

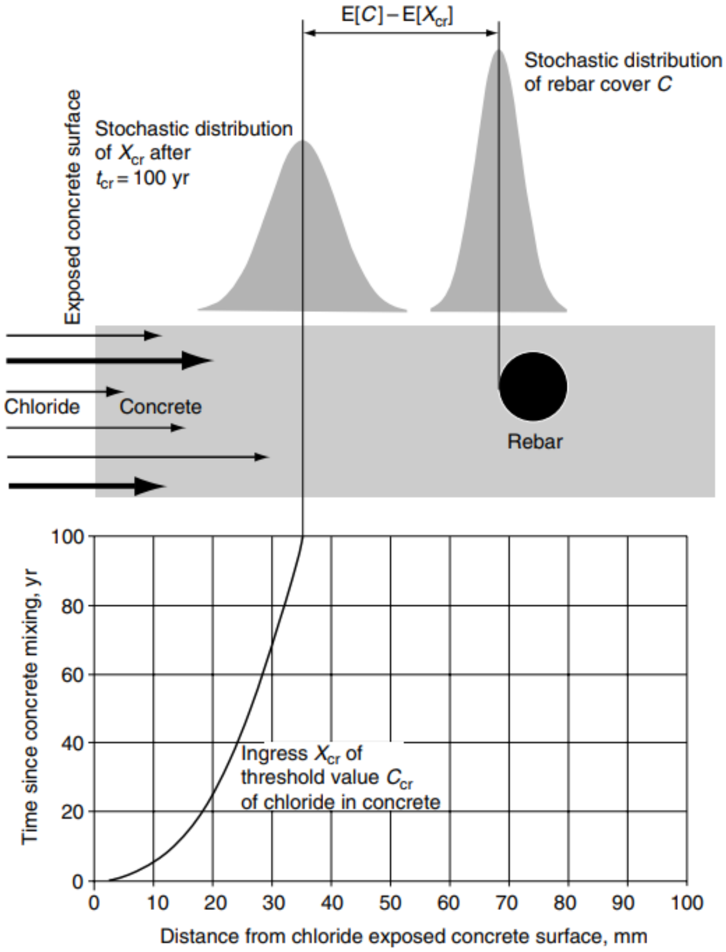

Fig. 2-5 Failure model diagram of concrete under chloride ion erosion based on probability distribution [54]

When the statistical distribution characteristic parameters of $C(t)$ and X_{cr} are known, and their distributions are independent of each other, the reliability index can be expressed as:

$$\beta = \frac{E[C] - E[X_{cr}]}{\sqrt{S^2[C] + S^2[X_{cr}]}} \quad 2.22$$

Where,

$E[C]$ and $E[X_{cr}]$ are the expectation values of C and X_{cr};

$S[C]$ and $S[X_{cr}]$ are the standard deviation of C and X_{cr}.

Then there is the failure probability formula:

$$P_f = \{Z \leqslant 0\} = P\{C_{cr} - X(c,t)\} = \Phi(-\beta) = \Phi\left(-\frac{E[C]-E[X_{cr}]}{\sqrt{S^2[C]+S^2[X_{cr}]}}\right) \leq \Phi(-[\beta]) \quad 2.23$$

2.3.3.2 The value of C_{0s}: the surface total chloride ion concentration

In evaluating the corrosion progress of reinforcing bars, first, the surface chloride ion concentration C0 (surface salt content) according to the distance from the coast is obtained. The surface chloride ion concentration is related to the distance from the coast, and the Japan Society of Civil Engineers uses the following relationship

Table 2-1 Chloride ion concentration on concrete surface（kg/m^3）

Splash zone	Distance from the coast (km)				
	Near the shoreline	0.1	0.25	0.5	1
13	9	4.5	3	2	1.5

2.3.3.3 Chloride threshold C_{cr} and [Cl-]/[OH-]

When the chloride ion concentration on the surface of the steel bar exceeds a specific concentration, it will induce the corrosion of the steel bar. However, this value is not a fixed value. It is related to many factors: such as whether there is anti-corrosion treatment on the surface of the steel bars; the of cement types; whether the concrete participates in rust inhibitors; the proportion of chloride ions and OH^- in the concrete [55][p166]. Regarding this value, different countries, specifications, and scenarios have different requirements for this value in concrete.

The Japanese Society of Civil Engineering recommends that C_{cr} is $1.2kg/m^3$.

In <Draft recommendation for repair strategies for concrete structures damaged by reinforcement corrosion >[56], as a recommendation, a chloride content in the range 0.3-0.5% and below by the weight of cement can be considered to lead to a low corrosion risk in most cases. Or 0.05% by the weight of concrete. The critical chloride ion concentration of concrete can be increased by 4 to 5 times when the alkalinity of concrete increases or the rust inhibitors are added, or anticorrosive steel bars are used [55, 57]. Therefore, it has become common in European countries and North America to limit the chloride content threshold to about 0.4% by weight of cement.

Scholar Kenichi Horiguchi [58] concluded that the threshold is related to cementitious materials and concrete mixing ratio. The chloride threshold value for corrosion initiation of concrete using ordinary cement was 1.6, 2.5, 3.0, and 3.0 kg/m^3, respectively, when the unit binding material was 254, 291, 362, 446 kg/m3. It was approximately 0.8 % binding material by weight. It was a reasonable result within the range of 0.3 to 1.8 % of cement shown in the past research. It is about 2.2 kg/m^2 in this study, calculated from his experimental conclusion.

Takuro Matsumura(松村　卓郎) [59] had also shown that the chloride ion threshold for steel corrosion might be as high as 4-6 kg/m^3 in the marine dry-wet cycle environment.

According to a 5-10 year follow-up survey of existing buildings coated with silane in Hokkaido by scholar Endoh and others, the application of silane can effectively inhibit the spread of salt and the development of corrosion of steel bars. It can increase the corrosion threshold of reinforced concrete surfaces by 3.5 kg/m^3[60].

Scholar Glass summarised the different research results in Table 1. On this basis, Masao Kitago made a further summary in Tables 2 and 3.

Table 2-2 Summary of chloride threshold C_{cr} and [Cl$^-$]/[OH$^-$] by g [61]

Total Chloride wt% cem.	Free Chloride Mole/l	[Cl$^-$]:[OH$^-$]	Exposure	Sample	Reference
0.17–1.4			Outdoors	structure	Stratful *et al.*[18]
0.2–1.5			Outdoors	structure	Vassie[19]
0.5–0.7			Outdoors	concrete	M. Thomas[22]
0.25–0.5			Laboratory	mortar	Elsener and Böhni[26]
0.3–0.7			Outdoors	structure	Henriksen[20]
0.32–1.9			Outdoors	concrete	Treadaway *et al.*[23]
0.4			Outdoors	concrete	Bamforth and Chapman-Andrews[24]
0.4	0.11	0.22	Laboratory	paste	Page *et al.*[27]
0.4–1.6			Laboratory	mortar	Hansson and Sorensen[28]
0.5–2			Laboratory	concrete	Schiessl and Raupach[1]
0.5			Outdoors	concrete	Thomas *et al.*[25]
0.5–1.4			Laboratory	concrete	Tuutti[29]
0.6			Laboratory	concrete	Locke and Siman[30]
1.6–2.5		3–20	Laboratory	concrete	Lambert *et al.*[31]
1.8–2.2			Outdoors	structure	Lukas[21]
	0.14–1.8	2.5–6	Laboratory	paste/mortar	Pettersson[13]
		0.26–0.8	Laboratory	solution	Goni and Andrade[32]
		0.3	Laboratory	paste/solution	Diamond[33]
		0.6	Laboratory	solution	Hausmann[10]
		1–40	Laboratory	mortar/solution	Yonezawa *et al.*[14]

Table 2-3 Chloride ion thresholds of in concrete and mortar [62]

	鋼材腐食に関する全塩化物イオン量の閾値　(Cl$^-$ wt% Cem)	
コンクリート構造物	0.17～2.2	(4)
コンクリート供試体（屋外曝露）	0.32～1.9	(4)
コンクリート供試体（実験室）	0.5 ～2.5	(4)
モルタル供試体（実験室）	0.25～1.5	(2)

( )は，もととなる文献数

Table 2-4 Thresholds of [Cl-]/[OH-] [62]

	pH	Cl^-/OH^-	実験条件
Hausmann	11.6 ～ 12.4	0.6	アルカリ水溶液中の鋼材
Gouda & Diamond	11.8 12.1 12.6 13.0 13.3	0.57 0.48 0.29 0.27 0.30	アルカリ水溶液中の鋼材
Page	13.91	0.54	セメントペースト中の鋼材
Page & Havdahl		62	シリカフューム30%を含むセメントペースト中の鋼材
米澤 (Yonezawa)		5	セメントモルタル中の鋼材
Syed , Ehtesham & Hussain	13.3 以下 13.3 以上	1.7～2.0 1.28～1.86	セメントモルタル中の鋼材

It can be seen that many factors affect the chloride ion threshold, and the threshold range for reference is relatively wide. Choosing a reasonable threshold is the key to correct life calculation under chloride erosion. When selecting the threshold value, the experimental background of the threshold value should be the same as or similar to the target project.

2.3.4 Based on carbonation-induced corrosion

- Carbonisation degradation model

The carbonation of concrete in the part of the atmospheric environment is also one of the main reasons for the corrosion of steel bars, deterioration of material performance and reduced durability.

At present, the generally accepted carbonisation model can express [63]p66:

$$x = k\sqrt{t} \tag{2.24}$$

Where x is the carbonisation depth， mm；

t: carbonisation time, year;

k: Carbonisation coefficient, indicating the speed of carbonisation.

$$t = \frac{x^2}{k} \tag{2.25}$$

- Carbonisation life criterion

Concrete carbonisation depth develops to the surface of the steel bars is usually regarded as a sign of the end of the carbonisation life of the structure.

The carbonisation life model based on probability distribution and reliability indicators is very close to the chloride model: "setting the depth of the chloride ion threshold frontier developing to the concrete cover as the critical state".So the details do not go into here, and it will be list in the later calculation chapter.

2.3.5 Based on freeze-thaw damage

2.3.5.1 Rapid freeze-thaw experiment methods and evaluation indexes

The freeze-thaw deterioration of concrete in the actual environment develops slowly. To quickly obtain the deterioration state of the performance of concrete with the freeze-thaw development, indoor fast freeze-thaw cycle experiments are usually carried out. The indoor rapid freeze-thaw cycle is divided into surface freeze-thaw and internal freeze-thaw (the whole is immersed in freeze-thaw solution) according to different test purposes. The surface freeze-thaw is divided into upper saltwater and lower saltwater (or water) freeze-thaw according to the freezing and thawing liquid supply method. Respectively simulate concrete in different service states in real life. Under different experimental procedures, the judgment standards of freeze-thaw deterioration are different. Common freeze-thaw experiment procedures and corresponding freeze-thaw damage evaluation standards are listed in Table 2-5.

Table 2-5 Commonly used rapid freeze-thaw experiment standards and evaluation methods[64]

Items	Test solution supply method	Evaluation method
ASTM C672	above	Visually
RILEM CDF	below	Scaling amount
JSCE-K 572	below	——
JIS A1148 A	all sides	Relative dynamic elasticity coefficient, the mass change rate

The visual evaluation standard of ASTM C672 is shown in Table 2 6. The specification does not have a clear numerical limit for it.

Table 2-6 ASTM C672 Freeze-thaw scaling visual evaluation standard [65]

Rating	Condition of Surface
0	no scaling
1	very slight scaling (3 mm [1⁄8 in.] depth, max, no coarse aggregate visible)
2	slight to moderate scaling
3	moderate scaling (some coarse aggregate visible)
4	moderate to severe scaling

5	severe scaling (coarse aggregate visible over the entire surface)

There is no maximum allowable spalling limit in the standards of JSCE-K 572. However, it has almost the same freezing and thawing experimental procedure as RILEM-CDF[66]. Therefore, the maximum allowable scaling amount of 1500g/m^2 at 28cycles[67] in RILEM-CDF is used in this study for comparison calculation.

For JIS A1148 A, the endurance limit state is based on the relative elastic modulus becoming 60% or the number of cycles of 300 cycles, whichever is less.

It isn't easy to obtain the actual amount of scaling in the existing project, except for the visual rating. The literature [68][資 1-10] defines the scaling degree (see formula 2.26,图), which describes the actual project's frost damage and flaking conditions further data quantify the development of frost damage.

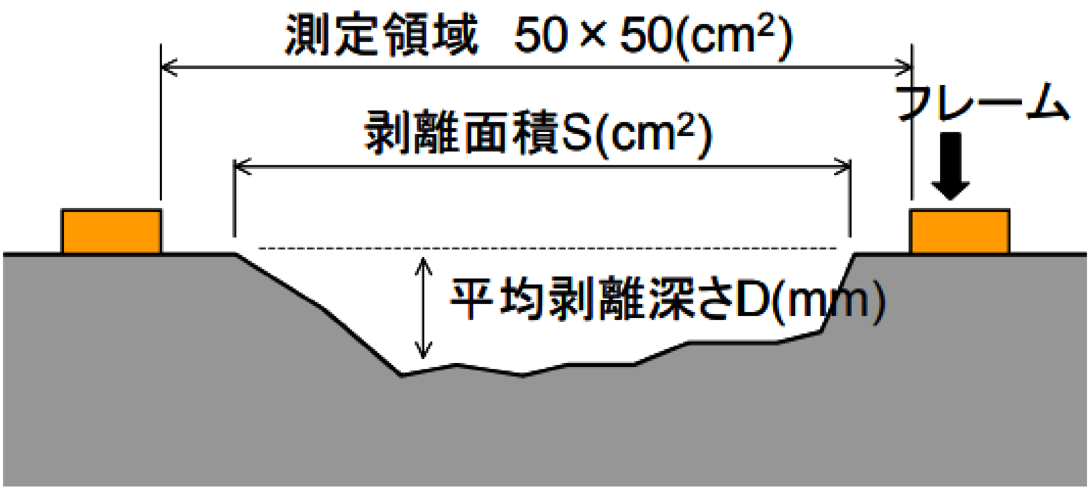

Fig. 2-6 Schematic diagram of scaling degree measurement method[69]

$$D_m = D \times A_s = D \times \frac{S}{50 \times 50} \qquad 2.26$$

Where

D_m: Scaling degree， mm

D: Average scaling depth, mm

A_s: The percentage of scaling area in the range of 50*50cm, %

S: Scaling area, cm^2.

The average scaling depth equals the scaling degree when scaling occurs on the entire area(As=100%).

The allowable scaling degree of the concrete surface and the corresponding deterioration degree are shown in Table 2-7.

Table 2-7 The allowable scaling depth value[69]

Deterioration of allowable scaling degree	Allowable scaling degree	Literature source
Within 2.5mm	2.5	[70]
Slight	5	[71]
Moderate	10	[71]
Sever	20	[71]

When the allowable upper limit of the scaling depth is 2.5mm, the literature [72][52] calculated that the acceptable spalling amount is approximately $0.09g/cm^2$ for ordinary concrete pouring surface, and $0.03g/cm^2$ for formwork surface and bottom surfaces.

For on-site engineering, with the year-by-year scaling, it is difficult to determine and fix the test reference surface of the scaling depth. Some externally leaked aggregates are used as the reference surface in common. The scaling depth measured in the subsequent test years is less than the previous year sometimes. These situations need to be corrected. It can be said that it is more difficult to obtain the precise spalling depth of the immovable on-site concrete.

The relationship between the maximum scaling depth and the average scaling depth is shown in Fig.

2-7[73].

RILEM's Concrete Durability Committee defines a maximum scaling depth of 5 mm as "mild" [71]. From Fig. 2-7， it can be said that the average scaling depth of 2 mm is the upper limit of "mild".

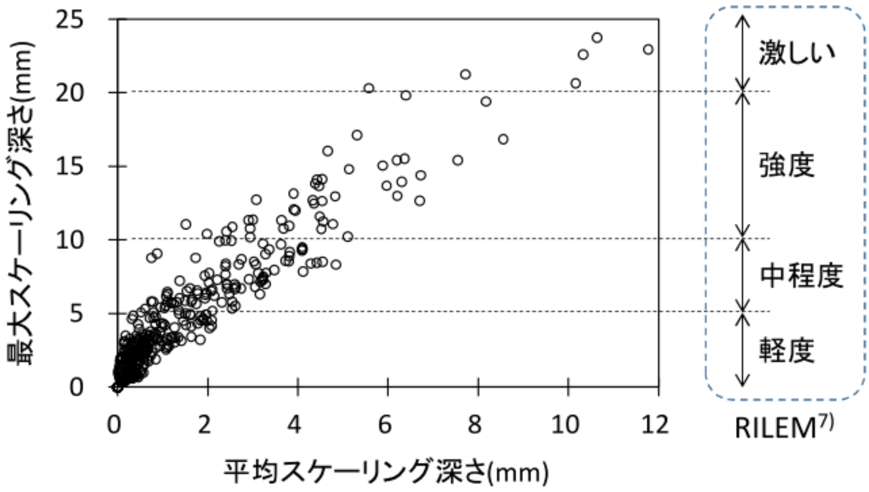

Fig. 2-7 Average scaling depth vs maximum scaling depth [71, 73]Fig.10

2.3.5.2 Scaling progress prediction formula

The revised material of the Japan Society of Civil Engineers Concrete Standard Specification [Maintenance] [74]published in 2018 shows the following scaling progress prediction formula.

$$D_m = ae^{b\log\frac{t}{A}} \tag{2.27}$$

Where,

Dm: an index that quantitatively expresses the degree of scaling (scaling amount： dmsc, scaling depth DMdep, etc.).

T: the freeze-thaw history (years of service, etc.).

A and b: coefficients and A is for making t non-dimensional. Coefficient (unit is the same as t).

The role of coefficient A is only to make t dimensionless. A and b are defined to be consistent with Dm depending on the value of A. For this reason, A is assigned a value of 1/2 of the longest elapsed years in the revised material [74], but basically, any value can be assigned as long as it is a positive value[73].

Through many field experiments, investigations, and indoor simulation experiments and analyses, the scholar Endo team has gradually established the relationship between the scaling degree, the scaling amount, and the water-cement ratio. And recently (June 2020) developed and announced its latest research results: based on the 2.27 formula to further refine the concrete scaling prediction model formulas (see Fig. 2-8). Furthermore, they shared its EXCEL version of the calculation program Fig. 2-9.

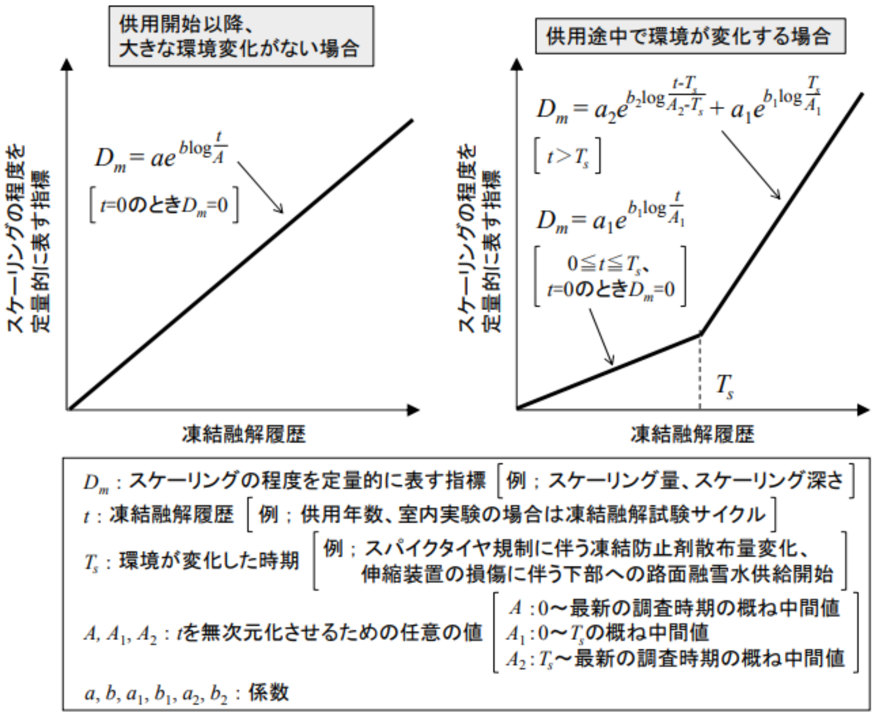

Fig. 2-8 Prediction formula of concrete spalling progress

https://zairyo.ceri.go.jp/ceri_zairyo/topics5/scalingpr-dr.html

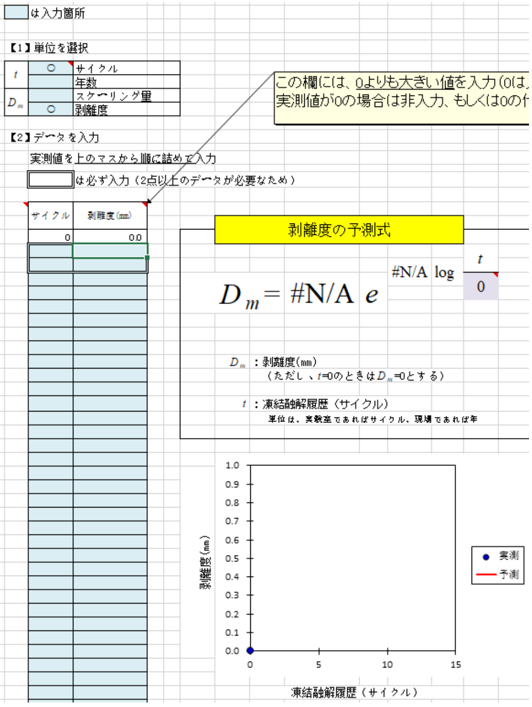

Fig. 2-9 The interface of the prediction program for concrete spalling progress

https://zairyo.ceri.go.jp/ceri_zairyo/topics5/scalingpr-dr.html

This formula is suitable for predicting the development of frost damage to concrete without concrete surface treatment.

2.4 Life Cycle Cost Analysis Theory

2.4.1 Cost composition

The life cycle cost involves each link of the building from the blueprint planning to the end of service dismantling. According to the different division angles, various scholars have proposed different elements Table 2-8.

Table 2-8 Life cycle cost composition classification

Proposer	Life cycle cost composition	Point

Frangopol[75]	Design cost, construction cost, inspection cost, preventive or complete maintenance cost, renovation cost, failure cost, earthquake disaster action cost, etc.	The composition of each cost is further divided to clarify the meaning of user cost and environmental cost
NCHRP	Institutional costs, user costs and third-party costs	
Singh	Institutional costs, user costs, accidents and other additional costs	A user cost model was proposed
Asko Sarja	Environment and ecology, concrete materials, structural durability design	Full life design

Generally,, then the expected life-cycle cost up to time T, LCC(T), may be represented as ：

The composition of life cycle costs:

$$LCC = C_i + \sum C_m + C_r + R \quad [76]^{P31} \qquad 2.28$$

Ci : Initial construction costs

$\sum C_m$: The total cost of functional preservation, including investigation, design, maintenance and management, maintenance, repair and renewal, residual value, etc

Cr : Renewal, removal, reconstruction costs

R : Loss during disasters and other periods

$$R = \sum P \times C \qquad 2.29$$

R : Risk, Expected Loss

P : Probability of P Accident Occurrence

C : Loss of C Facility_

This thesis focuses on the maintenance and repair costs of the functional preservation cost and considers the social discount rate, which is expressed by $\sum C_{PV}$.

$$\sum C_{PV} = \sum_{1}^{t} \frac{C_i}{(1+r)^t} \tag{2.30}$$

C_{PV} : present value of management

C_i : Maintenance cost at the end of the year i,

r : The discount rate of the i-th year

t : Number of investment periods: Cost at the end of each maintenance period

According to the technical guidelines (common edition) on cost-benefit analysis of public works evaluation [77]published by the Ministry of Land, Infrastructure, Transport and Tourism in June 2008, "social discount rate will be applied to 4% for the time being". ing. This paper uses a single social discount rate of 4% for calculation.

2.4.2 LCC considering the residual value

When comparing functional maintenance costs, if there is residual value in the facility as of the final year of the calculation period, this will be deducted for comparison[78][p8]2.

$$C_{rest-pv} = C_{last} \times (1 - \tfrac{T_P}{T_D}) \times r \tag{2.31}$$

$C_{rest-pv}$: Survival value (current price)

C_{last} : Last maintenance or update cost

T_P :: The number of years from the last update to the target lifespan or the service life from the last update to the year of calculation

T_D :: Durable years corresponding to the last update

r : The discount rate at the final annual point of the functional maintenance cost calculation period

Then, the LCC calculation expression for deducting residual value can be obtained:

$$LCC = \sum C_{PV} - C_{rest-pv} \tag{2.32}$$

LCC Life cycle cost.

CHAPTER 3. INFLUENCE OF CONCRETE IMPREGNANT ON THE DURABILITY OF CONCRETE SURFACE IN THE LABORATORY ENVIRONMENT

3.1 Overview

The non-destructive Torrent and SWAT (surface water absorption test) experiments were carried out on normal cement-based concrete before and after applying a combined use of concrete surface penetrants in different dosages. Penetrants included the sodium silicate solution (A) of the lower layer and the silane series solution (B) of the upper layer. The salt-freezing-thawing, MIP (Mercury intrusion porosimetry) and pH tests were also conducted after surface treatment. The results showed that the impregnants almost did not affect the surface air permeability. However, it can reduce the surface's water absorption rate and significantly improve salt-freezing spalling resistance. The salt-freezing-thawing resistance had a good correlation with the surface water absorption rate. Therefore, it is recommended to use the SWAT rather than the Torrent to estimate concrete surface quality changes after treatment. 50% of the recommended dosage was proposed. The relationship between the non-destructive test (SWAT) and the destructive test (salt-freezing-thawing) was established. The pH value gradually increases with the dosage increase, which is beneficial to protect the steel bars from corrosion.

Concrete serving in severe cold areas in winter will inevitably undergo a freeze-thaw cycle at the turn of autumn and winter and winter and spring. Concrete in roads and marine environments, due to the use of de-icing salt and the existence of sea salt, may also be subjected to the chemical erosion of salt compounds. The coupling effect of salt and freezing is greater than that of a single physical or chemical deterioration on the concrete's surface [79]; its durability has withstood a great test. The concrete's surface is the first barrier to prevent harmful external media from entering the concrete's interior. It plays a vital role in the durability of the concrete. Therefore, it is of great significance to improve the quality of the concrete surface. Concrete durability is affected by many aspects of its life cycle[80, 81]. Many kinds of maintenance materials and repair techniques improve concrete surface quality [82-85]. The concrete surface treatment is mainly including surface coating, hydrophobic impregnation, and pore-blocking surface treatments. Surface coatings can be subdivided into traditional polymer coatings, cementitious coatings, and polymer nanocomposite coatings[86]. The conventional polymer coatings often out of work due to the following failure patterns: blistering, cracking, holes and peeling [87-91]. Cementitious coatings may change the appearance of the concrete. It is not suitable for the maintenance of historical buildings that require the care of the original appearance. A composite of two impregnants (sodium silicate solution and silane solution) was applied to the concrete surface in this study. This treatment had the advantage of not changing the original appearance.

Although various impregnants' application on the concrete surface has been studied for a long time, the researchers rarely involve the treated surface's curing method after construction. The dosage varies among different scholars[92-95], and there will inevitably be excessive design [86]dosage in actual construction. Based on this, this article has carried out a variety of design for the dosage of penetrants. In addition to the construction according to the impregnant product's instructions, the treated concrete surfaces also took an action of additional curing of water spraying for 14 days from the perspective of the chemical reaction principle between the penetrants and concrete.

The main objective is to confirm the rational dosage of this kind of composite penetrants and their influence on the internal pore structure, pH and sail-freeze-thaw resistance of concrete. Furthermore, to establish the internal connection between the salt and freeze resistance of concrete (destructive test) and Torrent or SWAT (non-destructive test) data after surface treatment to predict the salt-freeze-thaw resistance performance through non-destructive testing in the future.

3.2 Experimental Program

3.2.1 Materials and mixture

Normal cement was used. The fine aggregate was blended by natural sand (density: 2.60 g/cm^3, water absorption: 2.47 %, fineness modulus: 2.03) and crushed-lime sand (density: 2.67 g/cm^3, water absorption: 1.08 %, fineness modulus: 2.03), and crushed-limestone (density: 2.68 g/cm^3, water absorption: 0.82 %) was used as coarse aggregate. Admixtures included water reduction agent (WR) and air-entraining agent (AEA). For fresh concrete, the target slump is 12±1 cm, and the air content is 5±1%，and the concrete mixture list in Table 3-1.

Table 3-1 Mixture of concrete.

s/a [%]	W/C [%]	Unit weight [kg/m^3]						Admixtures (g/m^3)		[MPa]
		W	C	Sand		Gravel		AEA [A] [C×A*]	WR* [C×%]	At 28 days
				Crashed sand	Natural sand	1005	2010			
45	60	161	268	252	570	522	524	5.0~6.0	0.2~0.3	28.53

* 1A = 0.001%.

Penetrants and dosages: Sodium silicate solution (A) was brushed on the test faces as the undercoat; 48 hours later, the silicone solution (B) was applied as the topcoat. Then shower treated faces with water once a day for 14 days in the air room. Coating amounts adopt 0% (blank group), 50%, 100%, and 200% of the recommended dosage (200 g/m^2) for both type-A and type-B. For physical properties of materials, see Table 3-2.

Table 3-2 Physical properties

Material name	Undercoat material-A silicate system	Topcoat material-B silane series
Main component	Modified sodium silicate	silicone
Appearance	colourless and transparent	colourless and transparent
Properties	Aqueous liquid solvent-based	(alcoholic) liquid
specific gravity	1.10-1.20	0.80-0.90
Viscosity	9.0 seconds (ford cup)	9.5second (ford cup)

pH	12	6

3.2.2 Maintenance mechanism

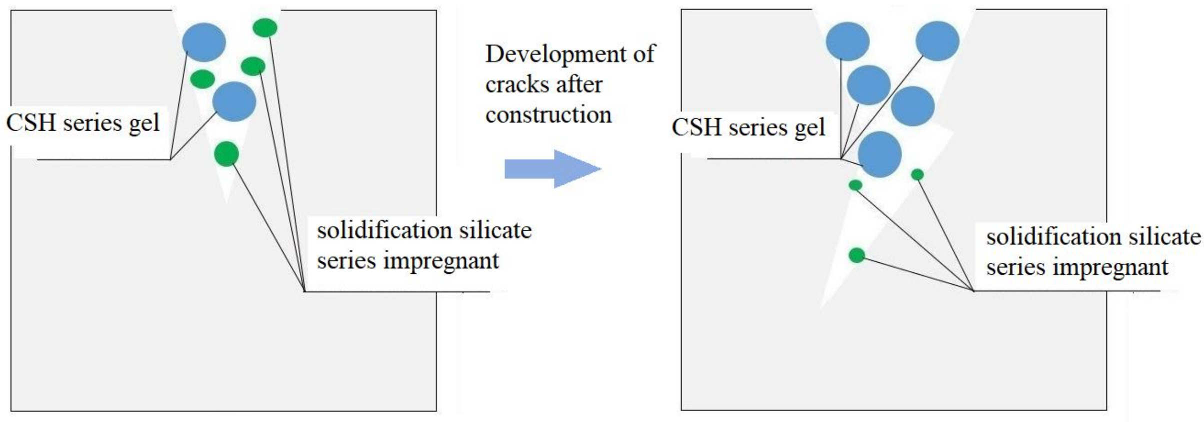

Fig. 3-1 The mechanism of silicate impregnant repair [96]

Sodium silicate reacts with the $Ca(OH)_2$ dissolved in the concrete to form dense calcium silicate hydrate (CSH) (**formula** 3.1), filling the nearby pores and cracks in the early stage. Unreacted parts of sodium silicate become soluble solid materials and fill the pores as it dries. When new cracks occur on the surface of the concrete or the original cracks continue to develop and encounter water (such as rainwater, etc.), the unreacted part of the solid sodium silicate continue to react with $Ca(OH)_2$ and form CSH.

$$Na_2O.SiO_2 + xCa(OH)_2 + yH_2O \rightarrow xCaO.SiO_2.zH_2O + 2NaOH + (x+y+z-1)H_2O \qquad 3.1$$

This process can be repeated until the sodium silicate is wholly consumed to achieve a long-term repair.

The silane's primary reaction to siloxane species includes two steps [97, 98].In the first steps (**formula** 3.2), "hydrolysis", the alkoxy groups are replaced with hydroxy groups forming silanols releasing alcohol under alkaline conditions. In the second step (**formula** 3.3), "condensation", silanol species react to siloxane, forming Si-O-Si-bonds. It was shown that the formation of siloxane species starts with monomeric silanol compounds in an aqueous environment followed by condensation steps.Hydrolysis under ethanol:

$$\mathrm{R}-\mathrm{Si}(OC_2H_5)_3 + xH_2O \rightarrow R-Si(OC_2H_5)_x + xC_2H_5OH \qquad 3.2$$

with x,y=1,2,3 and x+y=3

Condensation:

$$R\text{-}Si\text{-}OH + HO\text{-}Si\text{-}R \rightarrow R\text{-}Si\text{-}O\text{-}Si\text{-}R + H_2O$$

3.3It can be seen from formula 3.2 and 3.3 that water is one of the necessary conditions for the chemical reaction between the bottom layer of sodium silicate and the upper layer of silicone. Therefore, 14-days of additional curing by water spraying was taken from the reaction conditions' perspective after penetrants applied; the details are mentioned in the section **3.2.1**.

3.2.3 Specimens and test method

Specimen for Torrent method and SWAT was the same specimen used. Its size was 220 * 220 * 80mm. Moreover, the scaling test was 100 * 100 * 100mm, taken from 100 * 100 * 400mm prismatic specimen. The test face was the side face.

Torren and SWAT experiments were carried out on the concrete's surface (220 * 220mm) before and after coating penetrants in this study. The MIP, pH and salt-freeze-thaw cycles experiments were also conducted after treatment.

After casting, the specimens were cured with mould in the standard environment (Temp.: 20 ± 2 °C: R.H.:60 ± 5 %). Two days later, they will be demolded and placed in water for curing until the 28th day. Then, they will be moved to a constant room (Temp.: 20 ± 2 °C: R.H.:60 ± 5 %) for further curing for 28 days. The moisture on the concrete's surface evaporated to reach a state of equilibrium with the atmosphere. Then Torrent and SWAT data were collected on the faces (not end faces) that were side face for casting directions. Subsequent penetrants were applied to the test faces and then cured according to the method described in the last paragraph of the section **3.2.1** following Torrent and SWAT data's recollection. The rapid salt-freeze-thaw experiment was carried according to JSCE-K 572[99] in the following Temp.-time control program Fig. 3-2.

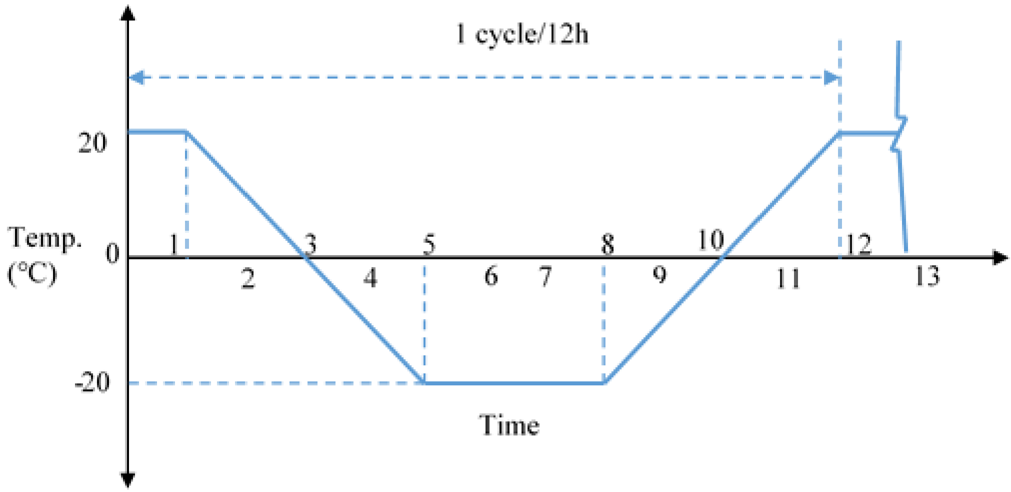

Fig. 3-2 Freeze-thaw cycle temperature control program

The evaluation of the air permeability and water absorption of concrete surfaces is according to Table 3-3 and

Table 3-4, respectively. Table 3-3 is a classification of concrete surface air permeability, based on kT (air permeability coefficient, m^2). It was proposed by Torrent and E. Denarié [100].

Table 3-3 Classification of concrete permeability as a function of kT

Permeability Grade	PK1	PK2	PK3	PK4	PK5
Description	Very Low	Low	Moderate	High	Very High
kT($\times 10^{-16} m^2$)	0.001～0.01	0.01～0.1	0.1～1.0	1.0～10	10～100

Table 3-4 Evaluation criteria for surface water absorption

Water absorption resistance	Good	Fair	Bad
p_{600} (ml/m^2/s)	≤0.25	0.25＜p600≤0.5	＞0.5

The MIP specimens were sampled 390 days after casting and about 310 days interval the application of penetrants. The MIP samples from surface to inner at 10mm interval.

pH test method: Taking mortar from the concrete surface layer (0-10mm), mashing them into powder, passing them through a 0.15μm sieve, taking 1g of powder, 99 g of water, and stirring them by a magnetic stirrer at room temperature at least 20min, then reading the pH value with an acid-base tester.

3.3 Results and Discussion

3.3.1 Torrent

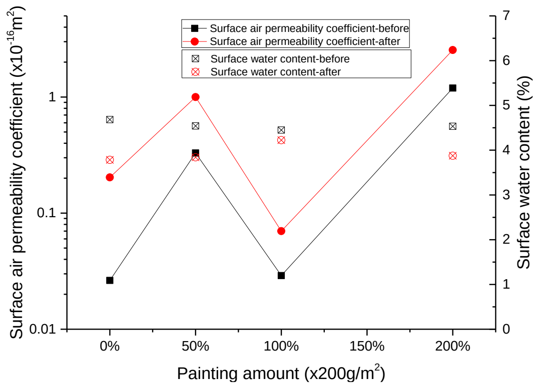

Fig. 3-3 kT vs painting amount

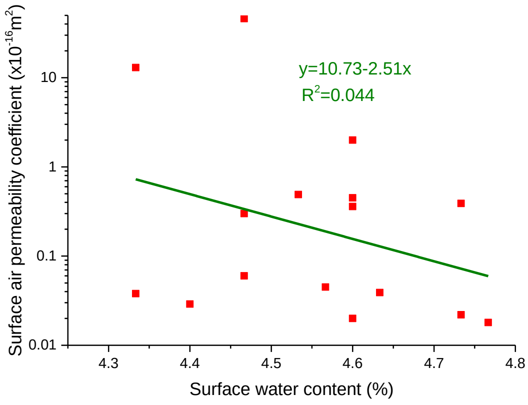

Fig. 3-4 kT vs surface water content

Fig. 3-3 shows that after coating penetrants, surface air permeability change law is consistent with uncoating, and the values are even slightly increased. According to Table 3-3, we can see the air permeability coefficients are between PK2 (low) and PK3 (Moderate); even though they are at the PK3 level before treating, they did not decrease by applying penetrants.

Fig. 3-4 indicates that surface air permeability somewhat reduced with the increase of surface water content. However, the correlation between them is very low (R^2 = 0.044) in the condition of a small range change of surface water content. Combined with Fig. 3-3 and

Fig. 3-4 due to the slight decrease in the surface water content because of the specimens placed in the air condition during the passing time of more than 14 days between the two Torrent test, the concrete surface air permeability became a little higher after coating. It can conclude that concrete the combined-penetrants in this study had little impact on surface air permeability. It is consistent with many scholars' conclusions that silicon-based treatments, particularly silanes, have the same breathability as untreated concrete; they are not as good as surface film-forming treatments to reduce surface air permeability[101]。

3.3.2 SWAT

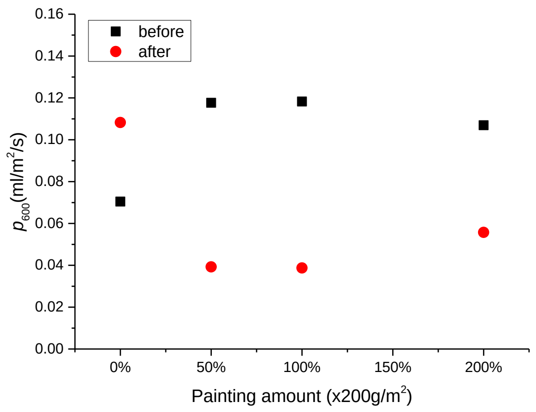

Fig. 3-5 Surface water absorption VS painting amount

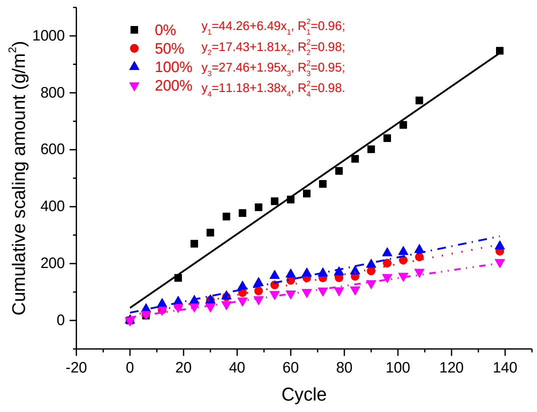

Fig. 3-6 cumulative scaling amount VS cycles

Fig. 3-5 shows that after the application of penetrants, the water absorption rate at the end of 10min (p_{600}) on the concrete surface shows a downward trend with the increase of dosage. The surface water absorption resistance of these test blocks was in a "good" state (according to

Table 3-4) before treatment. However, its drop space was small; a significant reduction trend of P_{600} can still be seen in the treatment group. In contrast, the control group increased somewhat may due to the drop in surface water content. The reason is that type- A impregnation agent in the concrete surface formed a material filled with concrete pores, making its texture denser. Secondly, type-B makes the contact angle of concrete and water increased and improves the concrete surface's hydrophobicity.

PK2 and PK3 were equivalent to the class of "good" in this study. However, the Torrent method does not help detect the effect of impregnation agents coating. The composite impregnants have the unique characteristics of not affecting concrete surface air permeability. In this situation, the SWAT method can better reflect the changes in the concrete surface quality.

3.3.3 Scaling

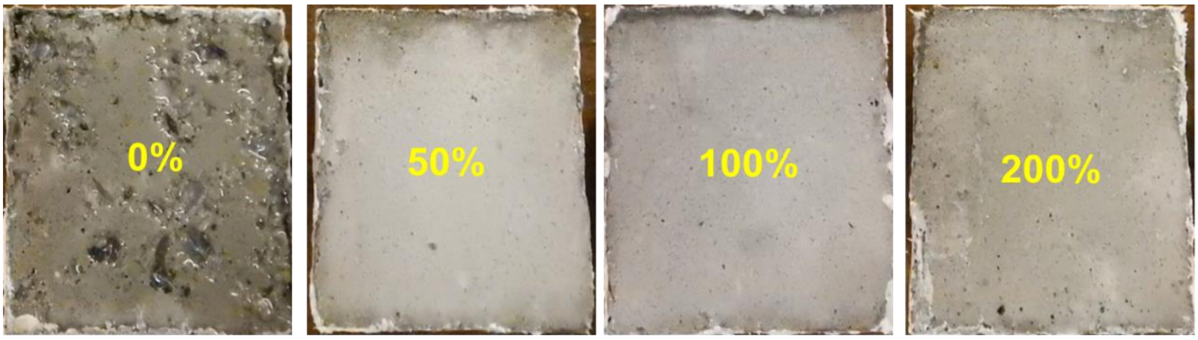

Fig. 3-7 Concrete surface morphology after freeze-thaw damage

Fig. 3-7 shows the spalling form of the concrete surface after 108 freeze-thaw cycles. They exhibit the excellent performance of anti-salt freezing-thawing spalling after treated with type - A+B impregnant. Even if the dosage is only 50% of the recommended amount, they can still maintain an entire concrete surface. It can be seen from Fig. 3-6 that the intercept and slope of the control group are both greater than the treated ones. The intercept reflects the outermost layer concrete quality (approximately equal to the spalling amount at the end of the six freeze-thaw cycles). The slope reflects the development of internal resistance; the smaller the slope, the better the anti-salt-spalling ability. After coating, both the intercept and the slope were significantly reduced, indicating that the type - A+B impregnant had improved concrete quality at a certain depth. It also showed that the uncoating group's scaling rate (6.49) was much larger than those of the treated groups (1.81-1.95). There were no significant differences in the treated groups. Combined with Fig. 3-7, from the perspective of economic consumption, 50% of the recommended dosage is efficient enough. Under this dosage, the scaling amount decreased by 74.30%

compared to the blanked group.

There is no maximum allowable spalling limit in the standards of JSCE-K 572. However, it has almost the same freezing and thawing experimental procedure with RILEM-CDF[66]. Therefore, the maximum allowable peeling amount of 1500g/m^2 in RILEM-CDF is used in this study for comparison calculation.

The maximum number of freeze-thaw cycles that each treatment can withstand can be calculated using 1500 g/m^2 as the Y value in the formulas in Figure 6. It can be obtained that after 224.25 cycles of untreated concrete, the scaling amount is up to the maximum allowable value. Simultaneously, the group coated with 50% could withstand 819.10 cycles. Suppose the number of freeze-thaw cycles that can withstand is simply equivalent to its service life. In that case, it can be considered that the service life of the concrete surface can be extended to 3.65 times the original one after treated with 50% of the recommended dosage of type -A+B impregnant. It dramatically increased the service life of the concrete.

3.3.4 The relationships between Torrent, Swat and scaling

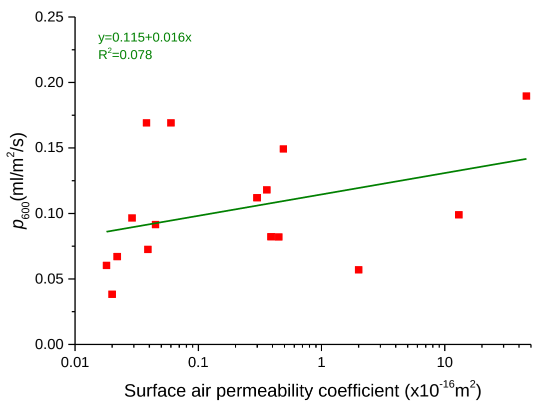

Fig. 3-8 p_{600} vs surface air permeability coefficient

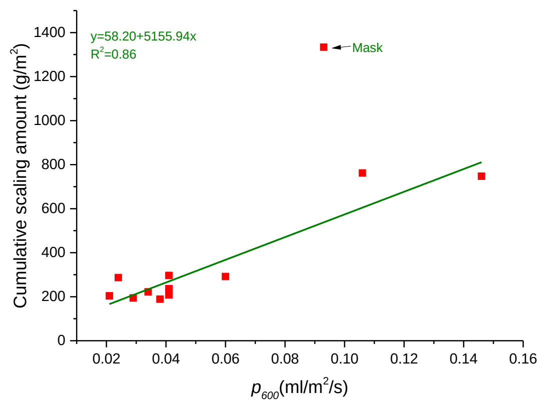

Fig. 3-9 Cumulative scaling amount VS p_{600}

When performing the surface quality appraisal of actual projects, the speed-freeze-thaw (in laboratory) experiment is a destructive method. It needs to take a core sampling from onsite engineering and transport it back to the laboratory. The experiment period is relatively much more prolonged than SWAT and Torrent. The latter two are non-destructive and can be conducted efficiently and easily to inspect surface quality onsite or in the laboratory when meeting simple conditions. The speed-salt-freezing-thawing experiment has the advantage of simulating the concrete's service environment in the lab. Its results are highly recognizable by the naked eyes. Suppose the relationships between these non-destructive testing and destructive testing are established. In that case, it is possible to speculate on the salt-freezing resistance of the concrete surface through non-destructive methods.

Fig. 3-8 shows the relationship between concrete surface air permeability and water absorption. The air permeability has a high scatter[102, 103]. Outliers are likely to occur (probability greater than 50%) and can make the mean, even the geometric value, a misleading parameter[104]. To avoid the above and reflect better the relationship between P_{600} and KT, Fig. 3-8 adopted each test point's original data, that is, the non- mean value. It ensured that each point's X and Y values came from the same measuring point to reduce the impact of differences from points. Fig. 3-9 used a similar data processing process. Despite this, the correlation between the surface air permeability coefficient and the two is very low (R^2=0.078) (Fig. 3-8). There were two main reasons: Firstly, the impregnant material has good "breathability". Secondly, there are not enough test points limited by the specimens' size. The Torrent data has great discreteness. Moreover, Torrent test results are easily affected by the concrete thickness around the test chamber. It may be easier to establish the relationship between P_{600} and kT when Torrent is applied to measure a concrete surface with a large enough size, for example, onsite constructions.

In comparison, the concrete surface's water absorption rate is hardly affected by specimens' size due to the different test mechanism. It has a good correlation with the cumulative scaling amount, and they are in line with the linear fitting formula 3.4 (R^2=0.86) (Fig. 3-9). The scaling amount increases linearly with the water absorption rate increase. Simultaneously, it can be concluded that SWAT can more genuinely reflect the concrete surface's quality than Torrent on the specimens with limited size in the lab. The surface water absorption is much more sensitive to the treatment materials due to the characteristics of penetrants.

$$y = 58.20 + 5155.94 x_{P_{600}} \qquad 3.4$$

Let $y = y_2$, where $y_2 = 17.43 + 1.81x_2$ ($R^2 = 0.98$)(Fig. 3-6), the functional relationship between the concrete surface water absorption P_{600} and the number of freeze-thaw cycles can establish as formula 3.5 at the proposed dosage:

$$58.20 + 5155.94x_{p_{600}} = 17.43 + 1.81x_2 \quad 3.5$$

Further, simplify and use the commonly used function relational expression as follows formula 3.6**:**

$$y_{cycle} = 22.52 + 2848.59x_{p_{600}} \quad 3.6$$

In the future, the improved performance of scaling resistance after treatment by type - A+B penetrants can be evaluated by formula 3.6.

3.3.5 MIP

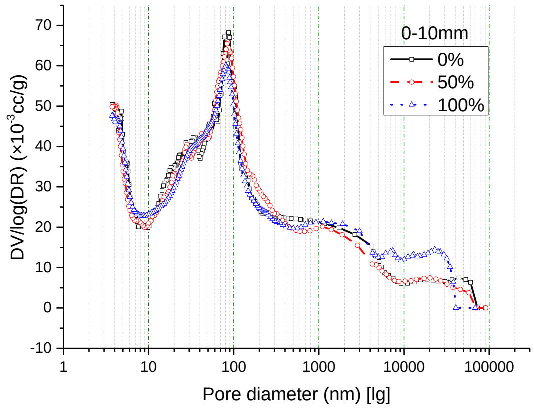

(a) 0-10 mm

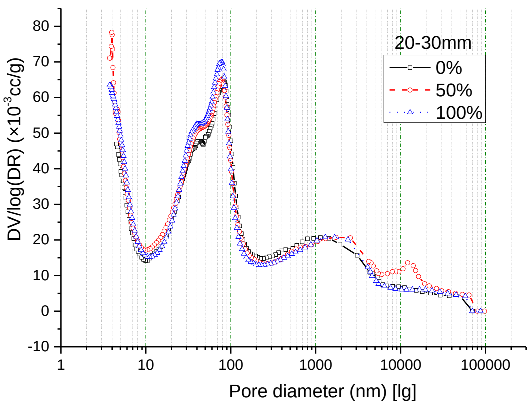

(b) 20-30 mm

Fig. 3-10 DV/log（DR）VS pore diameter

Fig. 3-10 shows the differential distribution of pore volume with pore diameter under different application dosages. Although the first layer's total pore volume (0-10mm) (Table 3-5) hardly changed when the dosage was 50% of the recommended amount until 100% (Fig. 3-10-a), their pore size distributions were quite different from the untreated group. In the range of pore size greater than 300nm, the pore size distribution of the treated group is smaller than that of the untreated group; it is contrary in the field of 100-200nm. After the impregnant is applied, the macropores' pore volume decreases and the small pores increase. When the dosage reaches 100%, the total pore volume is significantly reduced. The distribution of super-large pores (greater than 40,000 nm) is also reduced considerably.

Table 3-5 Total pore volume (mm^3/g)

Painting amount (×200g/m^2)	0-10mm	10-20mm	20-30mm	30-40mm	40-50mm
0%	68.46	64.68	53.07	62.22	–
50%	67.74	60.7	62.49	60.76	65.9
100%	61.8	–	–	–	–

Fig. 3-10- (b) shows that each group's differential pore size distributions tend to overlap in the 20-30mm layer. It can be inferred from this; the depth of penetration action should be less than 20mm. The pore size distribution of the 10-20mm layer was between these two layers, so it is omitted here.

The law of pore volume changes from the surface to the inner:

Through the salt-freeze-thaw cycle experiment, it can be known that 50% of the recommended amount is enough to anti- salt-freeze-thaw efficiently. Therefore, in the following part, only the 50% group and the control one is discussed.

Fig. 3-11 shows that when the pore size ranges from 20nm to 1000nm, from the surface to the inner, the untreated group (a) and the treated group (b) have the same pore distribution change law. The deeper the depth, the less distribution of the larger pores (100-1000nm), and the more distribution of the smaller pores (20-100nm). Fig. 3-12 is the distribution of the relative volume changes of each layer compared to the first layer. The changes of relative volumes are calculated by the formula 3.7. The graphics manifestation of Fig. 3-11 were reflected in the macropore range (100-1000nm) with lower troughs (corresponding to the 400-200nm range in Fig. 3-12) and the small pore range (10-100nm) with higherpeaks (corresponding to the 40-60nm range in Fig. 3-12). Here, the gel pores [105]（<10nm） have little effect on the concrete's durability, so no analysis was done. In short, the larger pores were reduced, and the smaller pores were increased. The total pore volumes of inner layers were also smaller than those of the first layers for both treated and untreated groups in the range of 10-1000nm. It means that the law has nothing to do with the application of impregnants. The quality of the concrete surface layer is poorer than the inner layer. The possible reason is that during placing, especially the pouring and vibrating process, the air bubbles in fresh concrete are lighter and present a state of upward escape. So, there are more large bubbles on the surface and fewer in the inner, while the smaller bubbles are contrary. After using the impregnant, the pore size greater than 1000nm in the first layer has been dramatically decreased. In the range of ＞1000nm, it can be found that the control group (Fig. 3-11-(a)) still had the law of being the deeper the depth and the lower the distribution of pores. However, after treatment (Fig. 3-11-(b)), it was changed to the first layer (0-10mm), being of the lowest pore distribution. However, the other layers still follow the rules same as the untreated ones. It can be concluded that the use of impregnant has a pronounced filling effect for pores larger than 1000nm (corresponding to the range of ≥800nm in Fig. 3-12). It can be further determined that the depth of penetration was mainly reflected in the first layer (0-10mm). It is close to the penetration depth (5mm) measured by Caijun Shi et al.[106] through thermal analysis of free $Ca(OH)_2$ in hardened concrete.

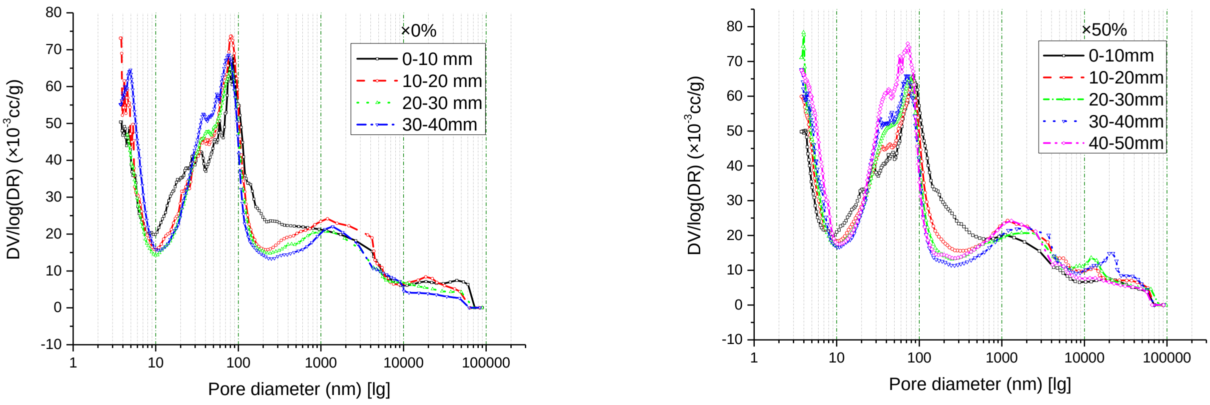

(a) Untreated group (b) Treated group

Fig. 3-11 Differential distribution of pore size of each layer

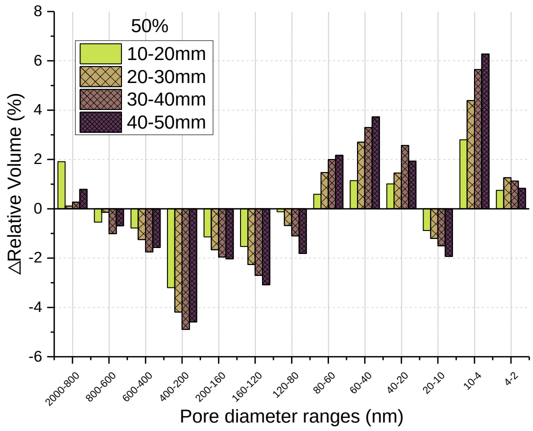

Fig. 3-12 Relative volume changes of each layer compared with their first layer

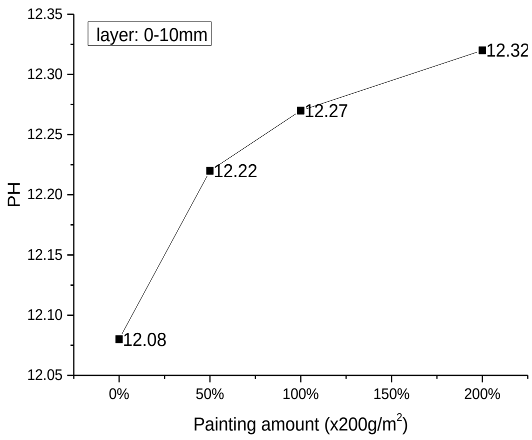

Fig. 3-13 pH VS painting amount

$$\Delta Relative\ Volume = Relative\ volume\ of\ \ inner\ layer - Relative\ volume\ \ of\ \ the\ first\ layer \quad 3.7$$

3.3.6 pH

According to the definition of pH($pH = -lg[H^+], p(OH) = 14 - pH$), the pH scale is logarithmic. So we can deduce that a pH value above 7 is ten times more alkaline than the next lower value. For example, pH 13 is ten times more alkaline than pH 12 and 100 times (10 times 10) more alkaline than pH 10. The same holds for pH values between them. Therefore, although the pH increase is slight after treatment (Fig. 3-13), the OH^- ion concentration inside the concrete has changed significantly. It can be calculated that the OH^- ion concentration of treated groups are 1.39, 1.56, and 1.75 (Corresponding to 50%, 100%, 200%, separately) times of the control group. The ion concentration increased by 39%, 56%, and 75%, respectively.

There are two main reasons. Firstly, the sodium silicate is not entirely consumed by the reaction within the range of its penetration depth, with the dosage increasing at the sampling time (about 390d). According to Fig. 3-1, the sodium silicate unparticipated in the reaction is filled in the pores in a solid form. When the pH test is conducted, it will be dissolved in water. Because sodium silicate is a strong alkali and weak acid salt, it can generate strong alkali sodium hydroxide when hydrolyzed. So it shows that the more the dosage, the stronger the alkalinity. It is well known that the stronger the alkalinity of concrete, the more beneficial to protect the steel bars in the concrete from corrosion. Secondly, it can be seen from formula 3.1 that the $Ca(OH)_2$ with low water solubility can be replaced by $NaOH$ with higher water solubility by reacting after treated with sodium silicate solution.It can be considered the un-reaction sodium silicate as a safety reserve. When cracks appear on the concrete surface, they can further penetrate the concrete with rainwater or seawater， and continue to react with the calcium hydroxide in the internal concrete and generate CHS to fill the cracks and surrounding pores. It continues to play a role in improving the quality of concrete. However, how deep it will eventually penetrate as far as time goes and how much can the quality be improved in quantity(for example, how many years to ensure that the protective layer continues to be highly alkaline) are unknown. The economics between the dosage and the effect needs to be further studied. If only according to the salt-freezing-thawing experiment, 50% of the recommended dosage has been well able to protect the concrete surface from damage. It can also play a good role in protecting the steel reinforcement.

3.4 Summary

The economical and reasonable applied amount is 50% of the recommended dosage.

Experiments show that 14 days of water spray curing after constructing the impregnant on the concrete surface can improve the protective performance, especially the scaling resistance. The limitation of this article is that there is no comparison group without additional curing.

It hardly affects the concrete surface air permeability.

Concrete surface water absorption (non-destructive testing) is proposed to identify and evaluate the surface quality improvement after such treatment. And the expected freeze-thaw resistance can be calculated by formula 3.6 ($y_{cycle} = 22.52 + 2848.59x_{p_{600}}$) with non-destructive testing data.

It can fill the large pores (especially >1000nm) in the surface layer (0-10mm), reduce the surface water absorption rate, and improve the concrete's salt and freeze resistance significantly.

After treatment, when the actual amount is 50% of the recommended dosage, the concrete's surface pH increases by 0.14, equivalent to a rise of 39% OH^- ion concentration in the concrete. It is effective in improving the re-neutralization of the concrete and preventing the corrosion of steel bars.

CHAPTER 4. THE EFFECT OF CONCRETE IMPREGNANT ON THE DURABILITY OF CONCRETE SURFACE IN MARINE ENVIRONMENT—— TOMAKOMAI PROJECT

4.1 Project Overview

Various materials have been developed for improving the surface quality of concrete. Many laboratory experiments have shown [107-109]that sodium silicate and silane can significantly improve the salt-freezing-thawing resistance of concrete surfaces than many other materials. However, there is not much data about its protective effect on concrete in a severe natural environment. The scholars of the Japanese Cold Land Institute of Civil Engineering and some universities scholars have conducted follow-up investigations in this area for many years: the exposure time after applying the penetrants was from 4 years [110], 5-10 years to more than 10 years [111]. These studies confirmed that the impregnants still has good salt-freezing-thawing resistance for concrete after serving for more than 10 years in bridges and ports located in a cold environment with salt erosion. This section is a continuation of the previous research, which studies the concrete surface state after being treated with impregnants for 12 and 20 years of service in the cold marine environment. The objective of this study is to dynamically follow up the changes in the protective effect of impregnation on the concrete surface, revealing the influence of impregnant protection on the concrete surface.

4.1.1 Introduction to the project

The target structure is the chest wall of the F part of the Tomakomai Port breakwater. The main construction period is from May 11, 2000, to November 20, 2000; T&C (Treated with compound penetrants) construction time for anti-corrosion in October of the same year.

The concrete mix ratio sees Table 4-1.

Table 4-1 Concrete mix ratio of F part of the Tomakomai Port breakwater

粗骨材最大寸法	スランプ	水セメント比	空気量	細骨材率
[mm]	[cm]	[%]	[%]	[%]
40	5	51.9	4.5	39.9

単位量 [kg/m^3]

水	セメント	細骨材	粗骨材		混和剤
W	C	S	5mm ~ 20mm	20mm ~ 40mm	
144	277	775	588	585	0.069

4.1.2 Introduction of the experiments

In the 3rd, 12th, and 20th years after the completion of the construction, several core samples were taken on Tomakoma's chest wall where T&C impregnants was applied (left part of Fig. 4-1 and Fig. 4-2) and unpainted parts (right part of Fig. 4-1 and Fig. 4-2). The sampling size is Φ150×about 200mm, and they were brought back to the laboratory for various performance tests. The test items are different each year. The test year, test items and the concrete surface morphology of the 12th and 20th years are shown in Fig. 4-3.

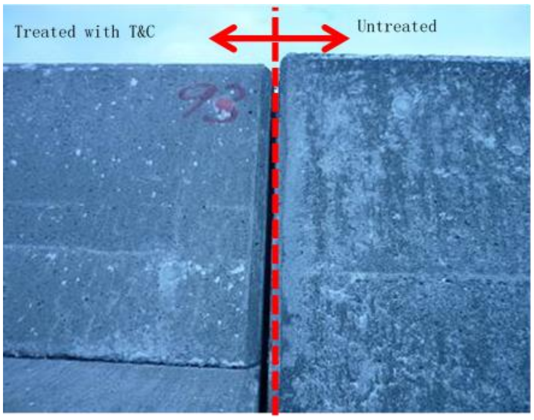

Fig. 4-1 On-site situation of the target structure

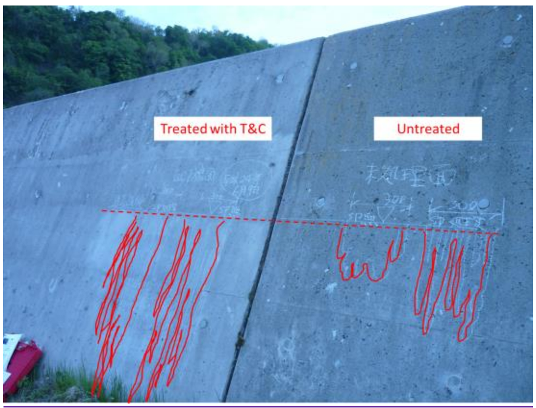

Fig. 4-2 On-site situation —The effect durability of surface water repellency (watering test)(12th)

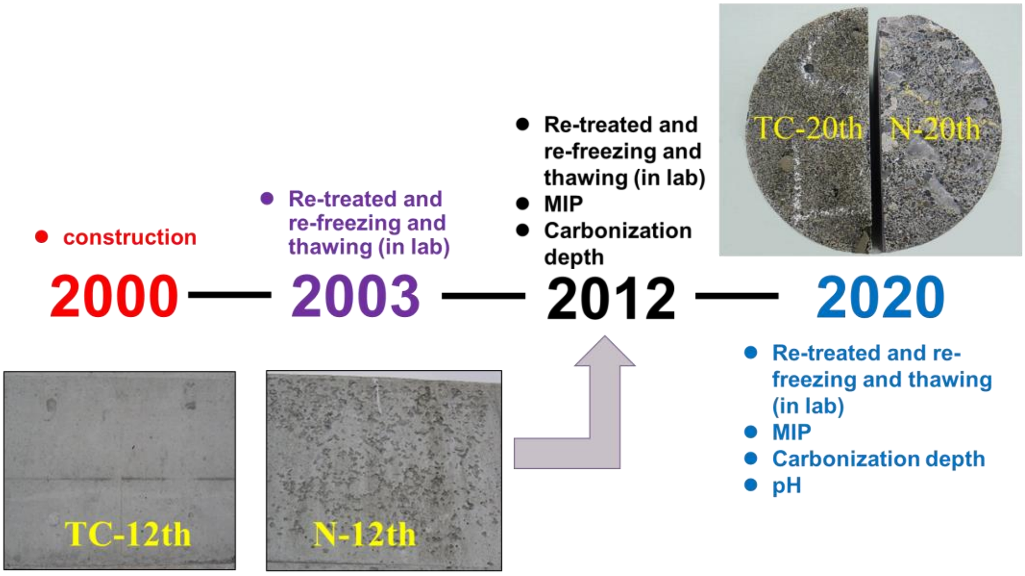

Fig. 4-3 timelines, test items and concrete surface morphology

The test items are briefly described as follows:

① Total chloride ion concentration distribution test;

Take 10mm as one layer from the concrete surface to the inner and sample layer by layer. The test depth range was 0-60mm.

The experiment was conducted following the standard test method (precision analysis) of the Civil Engineering Research Institute-JCI-SC5 Simple analysis method for total salt in hardened concrete.

② Measurement of neutralization depth

The concrete core columns sampled from Tomakomai Port breakwater were split into two along the diameter direction. Then the measurement neutralization depths were performed in accordance with JIS A 1152 by spraying a 1% solution of phenol phthalene onto the split surface.

③ Pore structure characteristics

In the 12th year, samples were taken from the concrete surface (0-10mm) and inside (60-70mm) and measured by the mercury intrusion method (MIP) (Pascal140/240).

The 20th year took 10mm as intervals from the surface to 70mm, and the test method is the same as in the 12th year. A total of 7 layers are sampled.

④ pH test

The test method is the same as Chapter 3. The test depth ranges from 0 to 60mm, and samples were taken every 10mm as a layer.

⑤ Scaling experiments

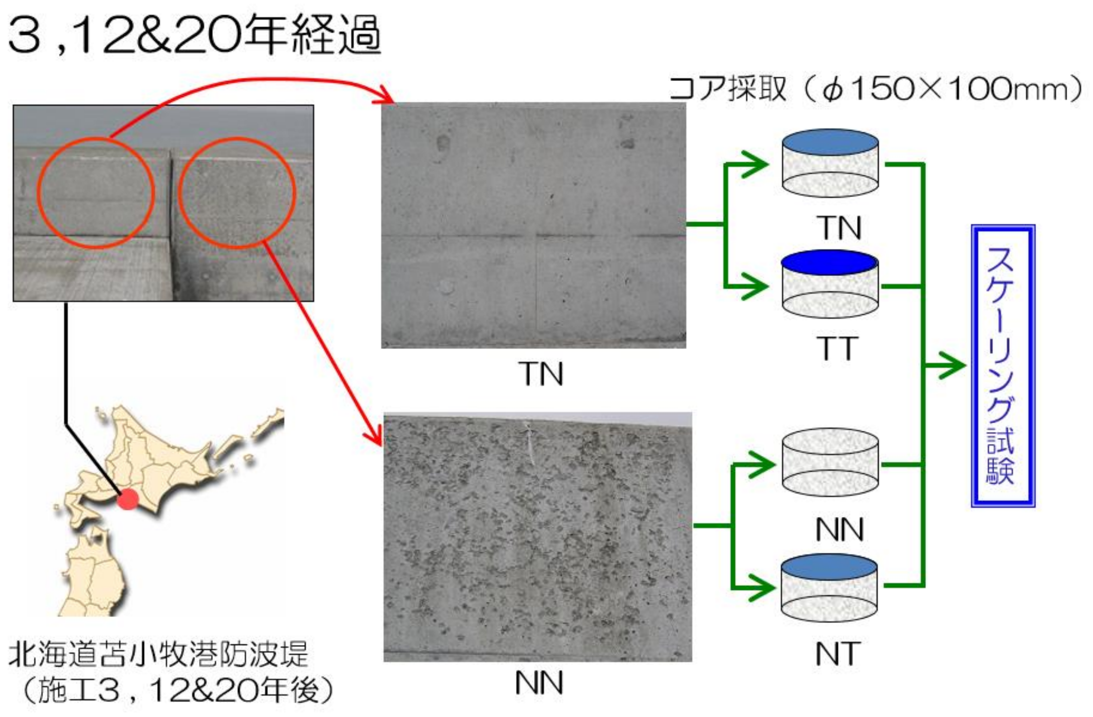

Fig. 4-4 Scaling schematic picture from Sakoi teacher

Notes:

① TN: Treatment in construction year + No re-treatment in the test year;

② TT: Treatment in construction year + Re-treatment in the test year;

③ NN: No treatment in construction year+ No treatment in the test year;

④ NT: No treatment in construction year+ treatment in the test year;

Cut the sampled specimens with a thickness of 100mm on the surface, seal them with waterproof aluminium tape around the cylinder of the specimens, and make them about 10mm higher than the concrete surface to ensure no water leakage (Fig. 4-5). Designed the specimens into four comparison groups (Fig. 4-4 for details), then applied or re-applied the impregnants on the surface of part of the specimens. The brushing dosages of A and B were both 200g/m^2. Furthermore, proper maintenances of impregnant materials were carried out. The maintenance method for the 12th year is the same as Chapter 3 (after the application of B liquid, 14 days of watering shower maintenance). The 20th year after the B liquid was brushed, one group used 14 days of the watering shower, one group without watering maintenance. There were three specimens under the same condition.

Moved the cured specimens to the weather room as shown in Fig. 4-4 and conducted a fast salt-freeze-thaw experiment according to ASTM C 672 [65]. The freezing and thawing solution was 3% NaCl. Pour the NaCl solution onto the upper surface of the concrete surrounded by waterproof aluminium tape. The height of the liquid level was controlled to be about 6mm. The freeze-thaw temperature control program is shown inFig. 4-7. The data was collected (Fig. 4-6) every five cycles of freezing and thawing. Fifty freeze-thaw cycles were carried out in the third year, 80 cycles in the 12th year, and 110 cycles in the 20th year. For the convenience of comparison, in the 20th year, the data of the first 80 cycles were used, while for the visual rating of the concrete surface, photos of the 110th cycles were taken because their quality was higher than that of the 80th cycles.

Fig. 4-5 Freeze-thaw state of the specimens in the freeze-thaw weather room (20th year)

Fig. 4-6 Freeze-thaw scaling amount collection

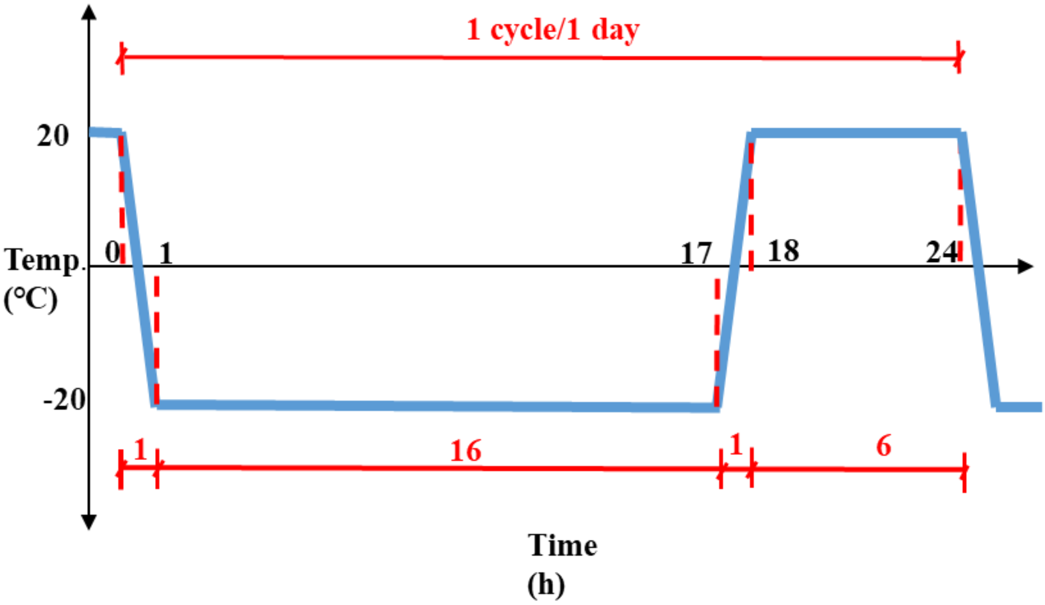

Fig. 4-7 Temperature control procedure of ASTM C 672 method

4.2 Experimental Results And Discuss

4.2.1 Diffusion of chloride ions

Multiply the chloride ion content percentage (%) of the experimental data by the concrete unit volume mass of 2300kg/m^3 to obtain each layer's total chloride ion content (kg/m^3), as shown in Fig. 4-8.

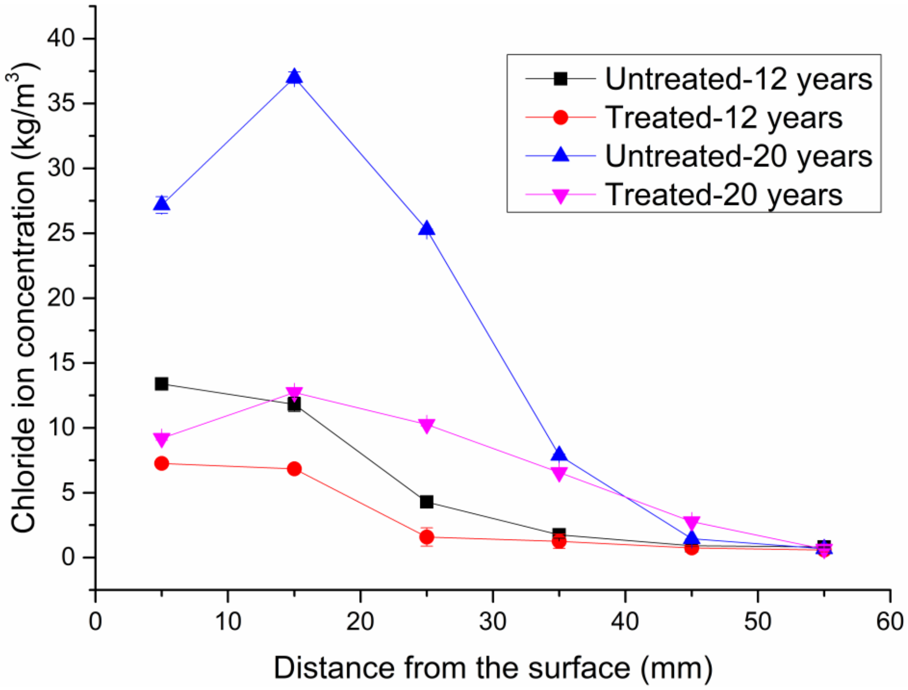

Fig. 4-8 Chlorine distribution (kg/m^3)

Fig. 4-8 shows that at the same test depth: (a) In the same year, the chloride ion concentration of the treated groups was lower than the untreated groups. The reason is that the sodium silicate solution (A liquid) can fill concrete pores to make it dense. In addition, silane (B liquid) can form a hydrophobic layer. They can effectively resist the water and corrosive substances into the concrete. (b) For the same groups, the concentration of the 12th year is lower than the 20th year; this is well understood. It is because chloride ions cumulated over time. Along the depth direction: (a) In the 12th year, the chloride ion concentration decreases gradually from the surface to the inside. The chloride ion development frontier is roughly 35mm. (b) In the 20th year, the first layer chloride ion concentration is lower than the second layer; from the second layer, there is a gradual downward trend from the surface to the inside.

The chloride ion front reaches a depth of 45mm. The reason is that the concentration of chloride ions on the concrete surface is affected by rain and tidal erosion, and there is a convective zone[112, 113]. After the surface chloride ions increase to a specific value, it is not easy to continue to grow. In this convective zone, the surface chloride ions The concentration tends to deviate from Fick's second law [114], so the subsequent calculation should select the surface chloride ion concentration obtained by curve fitting regression. The interior of the concrete is dominated by diffusion, which conforms to Fick's second law.

4.2.2 The development of carbonization

Fig. 4-9 shows the carbonization status of the treated groups and untreated groups at the 20th year. The carbonization depth measured in the 12th and 20th years is shown in Fig. 4-10.

Fig. 4-9 Carbonization depth 20th after construction (N: Untreated groups; TC: treated groups)

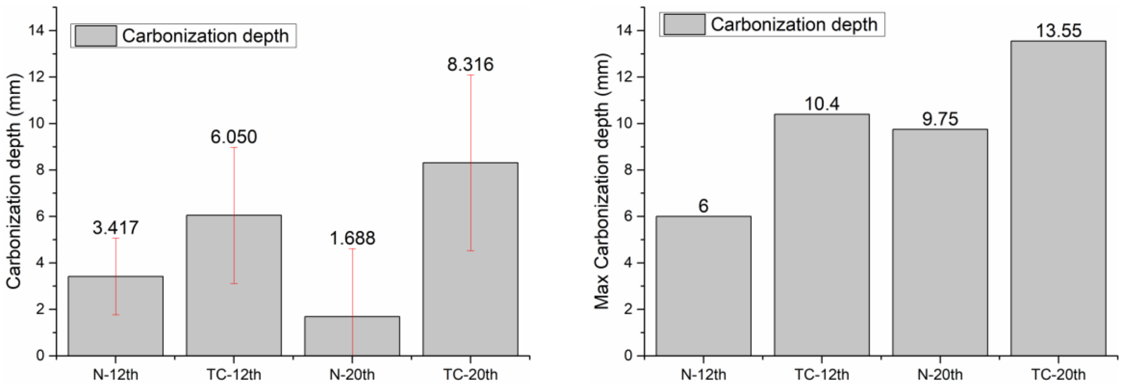

(a) Mean value (b) Max. value

Fig. 4-10 Carbonization depth

Fig. 4-10 shows that whether it is in the 12th year or the 20th year, the carbonization depths of the treated groups are smaller than that of the untreated groups. Even the 20th year neutralization depth of the untreated groups was less than the 12th year of itself, and it is tiny, only 1.688mm. Obviously, this is not the actual carbonization depth of the untreated groups concrete in the 20th year. As shown in Fig. 4 3, the concrete surface was severely peeled off to expose the coarse aggregate in the 20th year. Some of the carbonized concrete on the surface had also peeled off together. Therefore, it is necessary to correct the carbonation depth of the untreated groups concrete in the 20th year.

$$\text{From} \quad x = k\sqrt{t} \qquad 4.1$$

Where x is the carbonization depth， mm； t: carbonization time, year;

k: Carbonization coefficient, indicating the speed of carbonization.

So，

$$k = x / \sqrt{t} \qquad 4.2$$

According to formula 4.1(That is, formula 2.19), the carbonization coefficient calculation formula is derived, and the carbonization coefficient in each detection year is calculated as Table 4-2.

Table 4-2 Carbonization coefficient (mm/year$^{0.5}$)

Group	x_{mean}	x_{max}	t	$\sqrt{t}$	k_{mean}	k_{max}
N-12th	3.417	6	12	3.464	0.986	1.732
TC-12th	6.050	10.4	12	3.464	1.746	3.002
N-20th	1.688	9.75	20	4.472	0.377	2.180
TC-20th	8.316	13.55	20	4.472	1.859	3.030

Correction method one:

It is assumed that after the 12th year, the untreated groups maintained the carbonization rate of the 12th year. In the 20th year, it can be calculated from the formula 4.2, The theoretical depth of carbonization in the 20th year is :

For average: $x_{U20} = k_{12-U-Mean} \bullet \sqrt{20} = 0.986 \times \sqrt{20} \approx 4.41mm$ 4.3

For maximum: $x_{U20} = k_{12-U-Max} \bullet \sqrt{20} = 1.732 \times \sqrt{20} \approx 7.746mm \leq 9.75\text{mm}$

Taking it as $\overline{x_{U20}} = \dfrac{7.746 + 9.75}{2} = 8.748\text{mm}$ 4.5At the same time, it is also explained here that the scaling depth of the untreated groups from the 12th year to the 20th year is

For average: $4.41 - 1.688 = 2.722\ mm$

For maximum: $8.748 - 1.688 = 7.06\ mm$ Correction method two:

Assuming that the carbonization depth of the treated groups and the untreated groups always maintain a linear proportional relationship, then:

$$\frac{x_{U12}}{x_{T12}} = \frac{x_{U20}}{x_{T20}}$$

For average: $x_{U20} = \dfrac{x_{U12}}{x_{T12}} x_{T20} = \dfrac{3.417}{6.050} \times 8.316 = 4.697mm$

For maximum: $x_{U20} = \dfrac{x_{U12}}{x_{T12}} x_{T20} = \dfrac{6}{10.4} \times 13.55 = 7.817mm \leq 9.75\text{mm}$

Taking it as $\overline{x_{U20}} = \dfrac{7.817 + 9.75}{2} = 8.784\text{mm}$ where, U is the untreated group, and T is the treated group.

By this method, the spalling depth of the untreated groups from the 12th year to the 20th year is about

For average: $4.693 - 1.688 = 3.005\ mm$

For maximum: $8.784 - 1.688 = 7.096\ mm$ To be conservative, take the average and maximum values of 20th-year carbonization depth of untreated groups 5mm and 9mm here, and re-enter the formula 4.2. The carbonization coefficient after the correction for the untreated groups are 1.118mm/year$^{0.5}$ ($k_{20\text{-}u\text{-}mean}$) and 2.012 ($k_{20\text{-}u\text{-}max}$) mm/year$^{0.5}$. The life prediction are based on these corrected datas.

The spalling depth of the untreated groups from the 12th year to the 20th year ranges from 2.722 to

7.096 mm. From a safe and conservative perspective, it is taken as 7.096 mm. The total spalling depth of the 20th year should be added to that of the previous 12 years. It will be further calculated in Chapter 5.

It can be seen that the carbonization depth of the untreated groups at the 20th year after correction is still smaller than that of the treated groups. Why does this happen? Generally speaking, the solubility of the gas in water is lower. The higher the humidity of concrete, the less likely it is for carbon dioxide to invade. Under the infiltration of salt spray, tide and rainwater in the marine environment, the concrete surface of the untreated groups have high humidity and small carbon dioxide intrusion. So the carbonization speed is slow, and the carbonization depth is shallow. As for the treated groups, the concrete surface is relatively dry because the impregnant has good hydrophobic(Fig. 4-2); and it does not affect the gas in and out due to excellent air permeability (see the experiment and conclusion in Chapter 3). Hence, the carbonization effect is significant than that of the untreated groups.

4.2.3 Changes in pH

Many studies have shown that the corrosion of steel bars in concrete is related to the content of chloride ions and the ratio of [Cl-]/[OH-]. Table 4-3 simply calculates and summarizes the pH value and corresponding [Cl-]/[OH-] of each layer of the treated and untreated groups at the 20th year.

Table 4-3 pH value and corresponding $[Cl^-]/[OH^-]$

Specimens			$[OH^-]$	$[Cl^-]$		
	pH	pOH	mol/L	kg/m^3	mol/L	$[Cl^-]/[OH^-]$
TC-10	11.277	2.723	0.002	9.200	0.259	137.049
TC-20	11.497	2.503	0.003	12.722	0.358	114.194
TC-30	11.660	2.340	0.005	10.258	0.289	63.216
TC-40	11.770	2.230	0.006	6.562	0.185	31.392

TC-50	11.977	2.023	0.009	2.764	0.078	8.215
TC-60	11.997	2.003	0.010	0.648	0.018	1.838
N-10	11.910	2.090	0.008	27.180	0.766	94.195
N-20	12.227	1.773	0.017	37.004	1.042	61.852
N-30	12.333	1.667	0.022	25.277	0.712	33.050
N-40	12.183	1.817	0.015	7.873	0.222	14.540
N-50	12.017	1.983	0.010	1.445	0.041	3.917
N-60	12.013	1.987	0.010	0.679	0.019	1.855

Table 4-3 indicates that the most significant differences between the treatment and the untreated groups are: The pH of the concrete in the treatment groups is less than 12 within the range of 0-60mm, and it is very close to 12 in range of 40-60mm; While for the untreated groups, except the pH of the first layer is slightly lower than 12, and the inner layers are all greater than 12; which is consistent with the carbonization results in section 4.2.2.

Syed, Ehtesham and Hussain [62, 115]et al. found that when the pH is below 13.30, the [Cl-]/[OH-] threshold for corrosion of the steel bars is 1.7 ~ 2.0; When the pH value is higher than 13.30, it is in the range of 1.28 ~ 1.86. Judging by it, in the 20th year, the depth in which steel bar corrosion will happen has been developed to at least 60mm for treated and untreated groups. The treated groups are slightly smaller than the untreated groups at a depth of 60mm. However, some researchers have found that the [Cl-]/[OH-] threshold is between 2.5-20 [116, 117]. Based on the results of this study, the depth of the corroded area of the steel bar will not exceed 50mm. The two sets of threshold data used above are the test results obtained from the experimental samples with steel bars built-in mortar or concrete (there are many studies where steel bars are placed in a simulated solution). However, due to the different experimental conditions, the thresholds are also very different. It can be seen that there is a certain deviation in the evaluation by the ratio of [Cl-]/[OH-], and the [Cl-]/[OH-] threshold is not easy to control and use in practical applications [19].

Because at the sampling location of the Tomakomai flood dike, no steel bars were sampled. The concrete cover was greater than 60mm, so there was no direct evidence of whether the steel bars were corroded. However, through this experiment, it can be roughly determined that in the 20th year, the depth of the front edge that will corrode the steel bars in the concrete has reached about 50mm.

4.2.4 Impact on microscopic pore structure

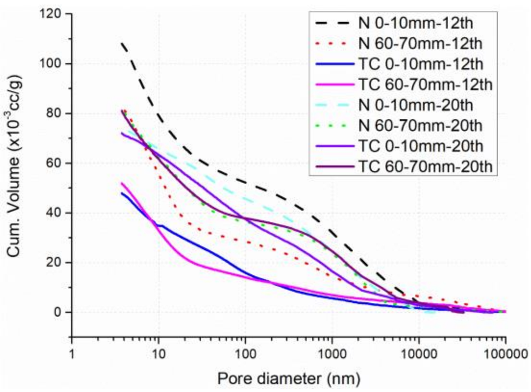

Fig. 4-11 Cumulative pore volume

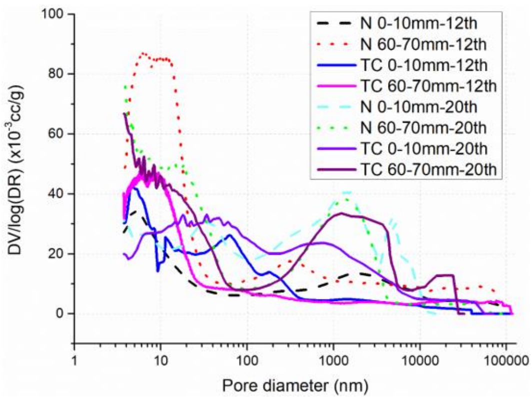

Fig. 4-12 Differential distribution pore volum

Fig. 4-11 shows that the cumulative volume of pores in the first layer (0-10mm) of the untreated groups is more significant than that in the inner layer (60-70mm), Whether it is the 12th or 20th year. The reasons are as follows: First, in the process of pouring and vibrating concrete, air bubbles are easy to overflow to the surface, so there are more pores on the surface than inside; second, in years of use, freeze-thaw spalling develops from the surface to the inside, and there are freeze-thaw cracks, pit corrosion, crisp looseness, etc. on the surface. So the cumulative pore size is larger than the inside.

The cumulative pore volume of the first layer and the inner layer of the treatment groups are not much different. In the 12th year, the final cumulative pore size of the first layer is even slightly smaller than that of the inner layer. In terms of pore size distribution, the cumulative pore volume of the first layer is smaller than that in the pore size range greater than about 200nm. The inner layer shows that the treatment groups have fewer large pores and more small pores. In the 20th year, under the slow development of freezing and thawing, although the total cumulative pore volume of the surface layer was slightly larger than that of the inner layer, the pore size distribution was very similar to that of the

12th year. In the large pore size range greater than about 100nm, the cumulative pore size of the first layer is significantly smaller than the inner layer.

Regardless of whether it was the 12th year or the 20th year, the cumulative pore volume of the surface layer of the treated groups was smaller than that of the untreated groups. From the 12th year to the 20th year, the cumulative pore volume of the surface layer of the treated group increased. In contrast, that of the untreated groups decreased. The increasing phenomenon is easier to understand because the surface layer of the treated groups have gone from almost intact to scaling off by freezing and thawing, and the deterioration gradually develops. While for the untreated groups, it can be seen from Fig. 4-3 that the pit corrosion of the first layer appeared evident in the 12th year. At this time, the pores are naturally very large, and by the 20th year, the coarse aggregate has been exposed. The 5mm weak layer of the concrete surface that is easy to peel and damage has almost fallen off. The "first layer" we measured in the 20th year is not the "first layer" in the 12th year but the newly exposed "first layer". The interior of the concrete is denser than the surface layer, so the cumulative volume of the "first layer" in the 20th year is smaller than the "first layer"—the situation in 12 years. In the 20th year, the inner layer cumulative volume curves of the treated and untreated groups almost overlap. Of course, the actual depth of the inner layer of the untreated groups is greater than that of the treated groups. Overlap indicates that the concrete impregnant cannot reach this depth. The pore structure of the two groups of concrete in this depth range is similar.

It can be further seen from the differential pore size distribution of Fig. 4 12 that at the 12th year, the pore size distribution of the concrete surface layer of the treatment groups greater than 400nm is smaller than that of the other groups (except for the inner layer that year), indicating that the impregnants have an excellent filling effect on the pores larger than 400nm size. Observing the distribution peaks of the large apertures (greater than 100nm) in each group at the 12th year: the order of the aperture sizes at the peaks is TC-60-70mm < TC-0-10mm < N-60-70mm < N-0-10mm, the impregnants make the large pore size distribution move to the small pore size direction (left shift). In the 20th year, each group's large pores (greater than 1000nm) increased sharply due to the deterioration of freezing and thawing. The rule is no longer evident, but the first layer large pores of the treated groups moving to the left compared with other groups are still apparent.

It is worth noting that in Fig. 4-11, in the 20th year, the cumulative pore volumes of the inner layer of the treated groups and that of the untreated groups are almost equal. The pore size distribution also has many similarities in Fig. 4-12. The pore size distribution larger than 1000nm of the inner layer is more than the first layers. It means that maybe the deterioration of the internal pore structure of the treatment groups is more severe than that of the first layer. It may be why some literature studies ([118])showed that after a certain depth of the scaling of the concrete surface coated with silane, there will be a sharp increase in freeze-thaw scaling. The reason may be that sodium silicate and silane can improve the pore structure of the concrete surface and form a hydrophobic seal to reduce water penetration significantly. However, it cannot completely prevent the entry of water. Water penetrates slowly over the years, and due to the hydrophobicity of silane in the surface layer, water is difficult to exist in this thin layer. The water passes through this layer and is stored in the inner concrete where the impregnants cannot reach. In severe cold winter, When the freezing depth reaches this range, there will be frost cracks inside the concrete, and internal damage will be formed. When the impregnants penetrated layer is ultimately scaling off and the freezing and thawing progress to the inner, there will be a sharp scaling increase.

4.2.5 Salt-Freezing-Thawing performance after re-treatment

4.2.5.1 Evaluation of freeze-thaw state of concrete surface

The visual rating of the surface after Freeze-thaw cycles by the following scale The visual evaluation standard of ASTM C672 is shown in Table 2 6. The specification does not have a clear numerical limit for it.

Table 2-6The scaling state can refer to the example for details, see Fig. 4-13.

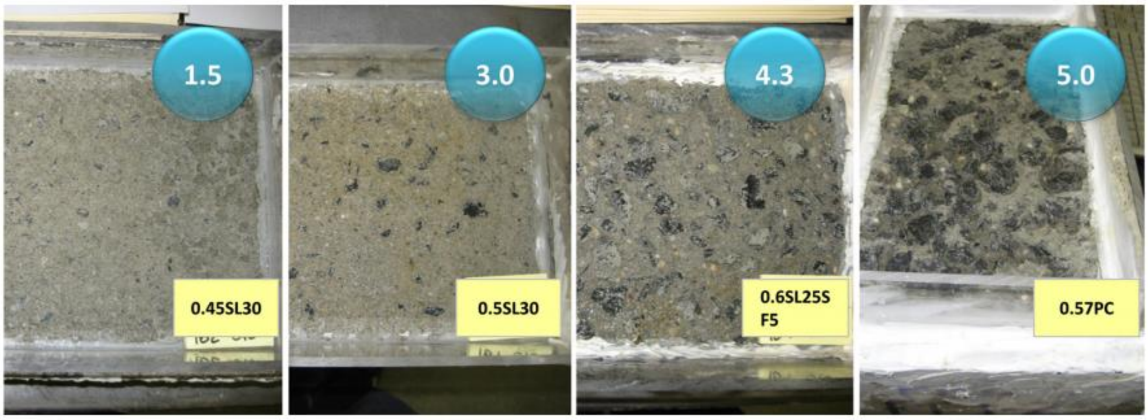

Fig. 4-13 Reference sample for evaluation of concrete surface spalling [119]

Table 2-6 and Fig. 4-13show the visual evaluation of the concrete surface after rapid salt freezing and thawing (for 110 cycles) in the laboratory in the 20th year is shown in Fig. 4-14.

Fig. 4-14 Visual evaluation of concrete surface- in the 20th year (110cycles)

NO Treatment in the first year			Treated in the first year		
NO.	Rating	Morphology	Morphology	Rating	NO.
N1	3			3	T1

N2	3.5			4.5	T2
N3	3.5			3	T3
N4	4			2.5	T4
N5	4			3	T5

N6	4.5			3	T6
N7	3.5			3.5	T7
N8	3.5			2	T8
N9	4			4	T9

Fig. 4-14 shows that the groups' colour tone without penetrant treatment in construction year (N groups, Photos in the left column) is mainly greyish black and bright due to some coarse aggregate (stone) leakage. While, for the fewer coarse aggregates exposed, the colour tone of the treated groups (T groups, Photos in the right column) is grey of the mortar dominates. According to the visual rating, it can be seen that the anti-salt scaling performance of the concrete treated with the compound penetrants is better than that of the untreated groups.

In groups of N1, T2 and T4, salt solution leakage was found during the experiment. After several repairs, no results were obtained. Therefore, the concrete surface was placed upside down in the container, and the lower side was raised with two spacers. The salt solution was added to the container to make the liquid level exceed the concrete test surface about 6mm. The experimental results vary considerably since the solution supply method has changed from upper solution storage to lower solution absorption. These three test blocks will be discarded during data processing.

Visual evaluation still has a lot of subjective judgments and cannot be quantified. There are ambiguities among all levels, and it is difficult to determine the level of attribution. It mainly reflects the state of the results after certain conditions are met and cannot reflect the changes in the process. The following is an evaluation of the degradation rate from the perspective of the scaling amount.

4.2.5.2 Salt-frost resistance changes with service life

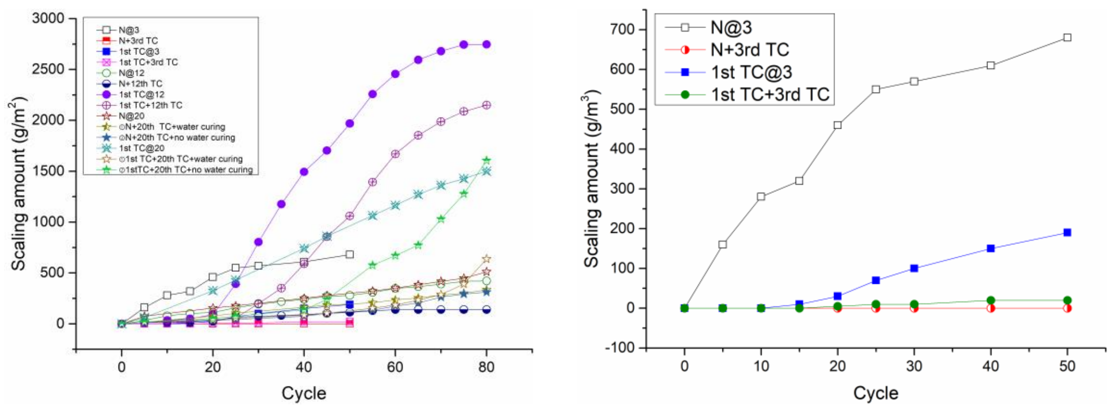

(a) All

(b) The 3rd year

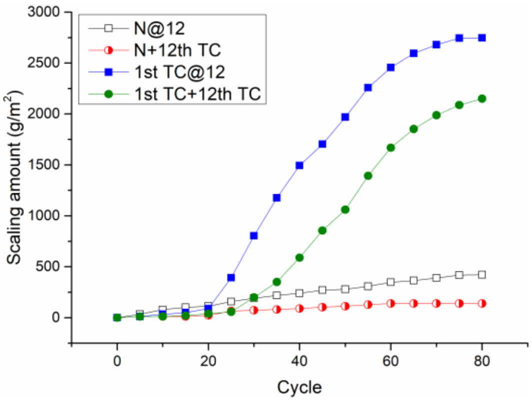

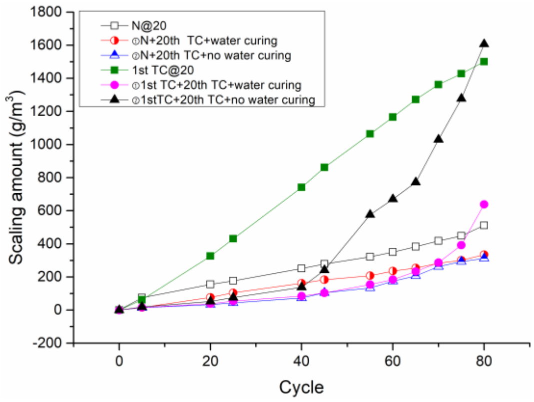

(b) The 12th year (d) The 20th year

Fig. 4-15 Scaling amount VS cycles groups by year

In Fig. 4-15, the approximate slope of each group can be regarded as the concrete scaling speed. Its unit is g/m²/cycle. The larger the slope, the more concrete mass is spalled in per cycle per unit area. The poorer the salt-freeze-thaw resistance of concrete is. From Fig. 4-15(a), the salt-freeze-thaw situation of concrete can be viewed as a whole after 3 years, 12 years, and 20 years. Among them, the scaling speed of the five groups is more prominent and faster than others. Their order is 1st TC @12 ＞ 1st TC + 12th TC ＞ 1st TC@20≈ N @3 ＞1st TC +20th TC + no water curing. The difference between the other groups is slight, so they have not been discussed in this figure.

The following apparent conclusions can be obtained: ① The treatment groups have the largest spalling in the 12th year. The reason may be that regardless of whether the concrete surface is treated or not, the salt-freeze-thaw spalling speed process of the concrete surface is slow → fast → slow. At first, the concrete surface was intact, and the freeze-thaw development was slow. Then, freeze-thaw cracks were formed under frost stress, and then the surface layer gradually appeared freeze-thaw pit corrosion. When the freeze-thaw pit corrosion gradually connects into pieces, the scaling speed increases rapidly. As the scaling depth increases, the aggregate slowly leaks out. Under the same frozen area, the aggregate leakage groups' frozen mortar area is less than those without the aggregate leakage groups. The frozen mortar area decreases, so the scaling amount decreases and the scaling speed decreases slowly. The application of the impregnating agents can delay the appearance of this process. The untreated groups had experienced this rapid freeze-thaw spalling process in nature by the 20^{th} year. They had entered a relatively stable slow spalling period. The scaling amount in the marine environment over the years is obviously more remarkable than the treated groups. Still, this scaling amount is hard to grasp. The concrete surface treated with impregnants has gradually weakened its anti-salt-freezing-thawing effect after 12 years of service in the marine environment. Duration of 20 freeze-thaw cycles in the laboratory, the surface layer began to peel off rapidly. Therefore, it shows that the treatment group's scaling speed (slopes) is greater than that of the untreated group. However, it can be seen from the visual evaluation of the concrete surface in Fig. 4-14 that the salt-freezing resistance of the treated groups is significantly better than that of the untreated group.

②In the same year, the scaling amount of the re-treated groups was less than that of the once treatment application groups; this affirmed the effect of re-treatment. As the upper impregnant silane is hydrophobic, it will prevent the entry of water. Therefore, we doubt whether the impregnating materials can enter the concrete surface already have been covered impregnants once. This experiment proved the effectiveness and necessity of re-treatment again after several years.

The reason may be that: firstly, with the extension of service life, the hydrophobic effect of silane gradually weakens, and there are weak spots on the concrete surface that is easy to enter the solution; secondly, according to the principle of chemical similarity, the impregnant repels water but not the impregnant.

③ From 1st TC@20≈N @3, It indicates that the application of impregnants makes the freeze-thaw state of the treated concrete in the 20th year approximately equal to the untreated group's anti-freeze state in the 3rd year. The treatment made the concrete "freeze age" for 17 years.

It can be seen from the N@3 group in **Fig. 4-15** (b) that the freeze-thaw scaling rate of the untreated group gradually scaling slowed down after three years of service in the marine environment + about 25 indoor freeze-thaw cycles. However, when it (equivalent to the natural year) began to enter the rapid freeze-thaw spalling period, it is necessary to know the relationship between the number of indoor freeze-thaw cycles and the natural annual freeze-thaw cycle of the marine environment to calculate it.

For the groups been applied or re-applied penetrants on the concrete surface (the other three groups in this figure)before the lab-freezing-thawing test, the development of scaling speed can be quickly inhibited. Even after 50 freeze-thaw cycles indoors, the rapid spalling stage has not been reached.

Fig. 4-15 (c) shows that after 12 years of concrete service in the marine environment, the concrete spalling speed of the untreated group has gradually become flat. Combined with **Fig. 4-15** (b), it can be qualitatively deduced that the year in the marine environment for 3 years +50 salt-freeze-thaw cycles in the lab is less than 12 years in the marine environment.

The groups treated in the construction year after service for 12 years in the marine environment (1st @12) experienced 20 freeze-thaw cycles in the lab and then entered the rapid freeze-thaw spalling period. The re-treatment groups at the 12th year (1st @12+12th TC group), after experiencing 25- 30 freeze-thaw cycles, also enter the rapid freeze-thaw spalling period. The spalling rate is about 45g/m^2/cycle. The re-application of penetrants in the 12th year can delay 5-10 freeze-thaw cycles of entering the rapid scaling period.

Therefore, it can be concluded that the time for re-maintenance of concrete should not be later than 12 years of natural marine environment + 20 indoor freeze-thaw cycles. How many years the 20 rapid indoor freeze-thaw cycles can be equivalent to the marine environment is a question that needs to be further resolved. But it also shows that the effect of re-applying in the 12th year is minimal, and it can only delay 5-10 freeze-thaw cycles. Combined with **Fig. 4-15** (b), it can be qualitatively inferred that the second maintenance time should preferably be between 3-12 years. After 70 freeze-thaw cycles in the lab, the freeze-thaw scaling rate gradually slowed down.

Fig. 4-15 (d) shows that the groups treated in the construction year have the fastest spalling speed. According to calculations, it is about 20g/m^2/cycle, much smaller than the rapid spalling stage in **Fig. 4-15** (c) 45g/m^2/cycle, indicating that the treated groups have entered a relatively slow scaling stage. However, it still has a more significant scaling amount and a faster scaling speed than other groups. The reason is the same as that explained in **Fig. 4-15** (a).

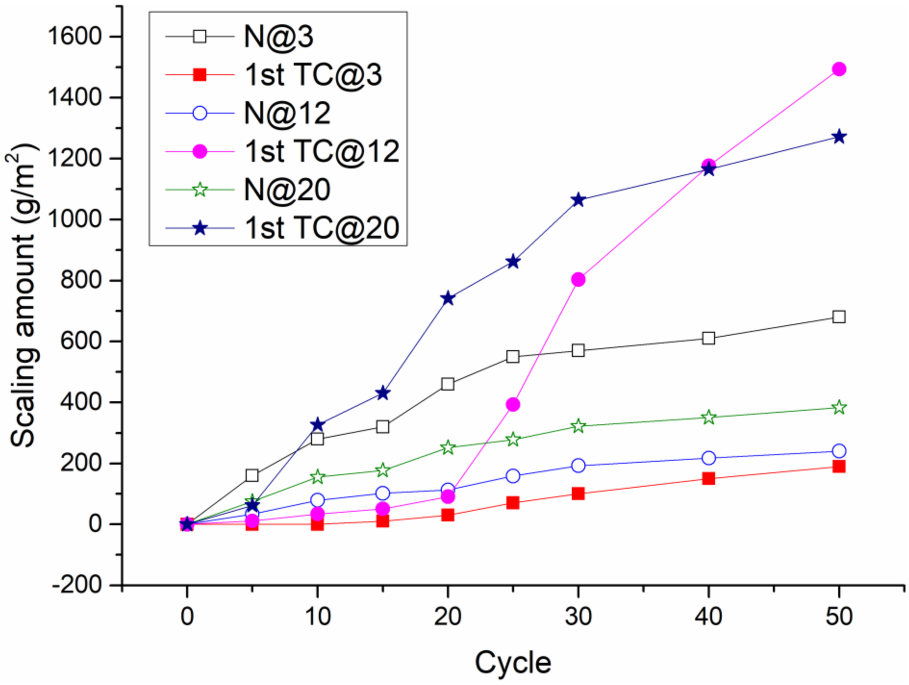

Fig. 4-16 Scaling amount in each year of the treatment groups and the untreated groups in the construction year VS Cycles

Fig. 4-16 shows that in the 12th year of untreated, the spalling rate and the amount of spalling in 20 years are less than that of the third year, indicating that the rapid spalling period of the untreated group is roughly in the 3+n cycle. The equivalent year of the 3+n cycle should be less than 12 years. The maximum spalling rate appeared in the treatment group after the 12th year +20 rapid indoor freeze-thaw cycles. In the experimental period, the treatment group showed that the scaling amount gradually increased with years. There was no inflexion point such as the fall of the spalling amount like the untreated group. This again indirectly confirms the decision that the impregnant can make the concrete "freeze age" for 17 years.

4.2.5.3 Influence of the number of treatments on the concrete surface on anti-freeze performance

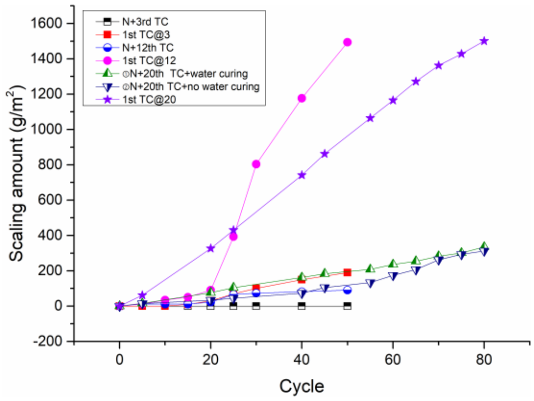

Fig. 4-17 One-time surface treatment

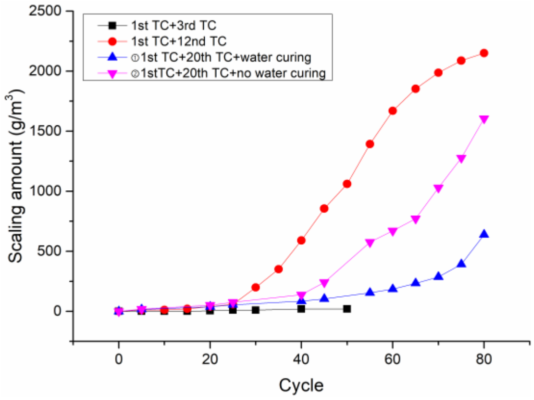

Fig. 4-18 Re-treatments on concrete surface

The maintenance effect of applying penetrants at different time notes is different. Fig. 4-17 shows the salt-freeze scaling after penetrants were used at different time nodes in this experiment. The spalling process was one step behind the untreated group treated with impregnant on the concrete surface during the construction year. The total spalling amount was always smaller than the other groups that were only maintained once. After three years + 25 freeze-thaw cycles for the untreated group, they all entered the relatively slow scaling stage. Although the years of application were different, the scaling stages were similar and more comparable. The figure shows that N+3rd TC < N+12th TC < N+20th TC. It can conclude that for existing concrete, even if it enters a slow spalling period, it is advisable to treat it with penetrants as soon as possible. The sooner the treatment, the more conducive it is.

4.2.5.4 The effect of curing method of penetrants on salt- freezing-thawing resistance

The concrete surface impregnants used in this project is a combination of two impregnants. The bottom layer is a sodium silicate solution, and the upper layer is a silane solution with hydrophobic properties. According to the maintenance principle, the chemical reaction process of sodium silicate solution with the concrete substrate requires water. Therefore, in theory, it is necessary to carry out 14 days of the watering shower curing to improve its maintenance effect. While silane with good hydrophobic properties is applied to the upper layer of sodium silicate, so there are doubts about whether the water shower can effectively cure the bottom layer. Therefore, in this experiment, a 14-day water shower maintenance group① and a non-water shower maintenance group② were carried out to clarify the doubts. Indeed, in the process of water shower for curing, it was found that after applying silane, water droplets on the surface of the concrete are like rainwater on the lotus leaf. Silane has a good lotus leaf effect. Unfortunately, due to the limited number of experimental groups, Fig. 4-19 shows contradictory conclusions in the two comparison groups. That is, no judgment is available. After analysis and consideration, it is believed that applying sodium silicate →water shower for curing for 14 days → using silane solution may have an excellent protective effect. This is an idea for this work in the future, and it needs practice to verify its authenticity.

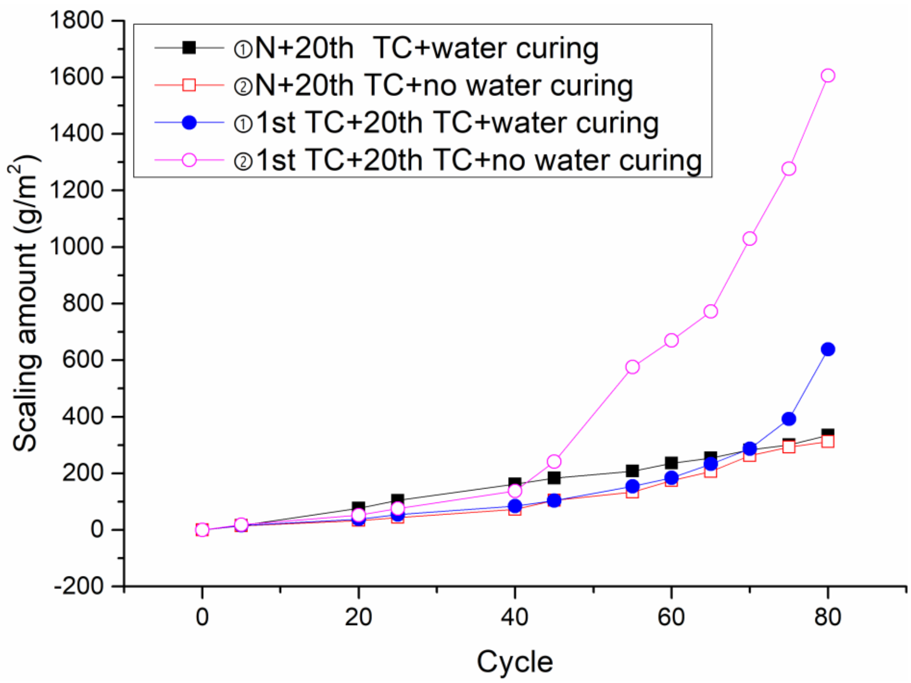

Fig. 4-19 The difference between water shower curing and non-water shower curing after the impregnant applied

4.3 Conclusions

The coating of impregnants can effectively slow down the penetration rate of chloride ions into the concrete with water. The chloride ion concentration of the treated groups was lower than the untreated groups. The chloride ion development frontier was roughly 35mm in the 12th year. Then it reached a depth of 45mm in the 20th year after construction. Because of the existence of the concrete surface convective zone[2, 3], the surface layer chloride ions concentration tends to deviate from Fick's second law [114], they are lower than the second layer in the 20th year after construction, the impact is not noticeable enough at the 12th year.

The penetrants have no advantage in delaying the carbonation of concrete in the marine environment. The carbonization depth of the untreated groups at the 20th year after construction need to be corrected because of the surface scaling. Due to the much higher humidity and small carbon dioxide intrusion of the untreated concrete than that of the treated concrete, the carbonization depth of the former is shallower than the latter. The pH of the concrete in the treatment groups is less than 12 within the range of 0-60mm, while for the untreated groups, except for the first layer, all the inner layers are greater than 12, which is consistent with the carbonization results. The [Cl-]/[OH-] ratio of the treated concrete are larger than the untreated one, while at a depth of 60mm, they were almost the same; they were about 1.8. According to the opinion of the scholar Syed, Ehtesham and Hussain [62, 115]et al., they may be both in the state of high risk of steel corrosion in the 20th year. It can be affirmed with a higher probability that the depth of the front edge that the steel bars will corrode in the concrete has reached about 50mm.

The impregnant has a good filling effect for pores larger than 400nm (at the 12th year). Regardless of whether it was the 12th year or the 20th year, the cumulative pore volume of the surface layer of the treated group was smaller than that of the untreated group. In the 20th year, both groups' macropores (greater than 1000nm) increased sharply due to the deterioration of freezing and thawing. However, the pore size of the treated group at the peak volume in large pore ranges was smaller than that of the untreated group. In the 20th year, the cumulative pore volume of the inner layer of the treated group and the untreated group were almost equal. For treated concrete, the volume of the pores with a diameter larger than 1000nm of the inner layer is more significant than that of the first layer. It means that when the freezing and thawing progress to an inner layer deep level, the deterioration of the internal pore structure of the treatment group may be more serious than that of the first layer. The reason may be that sodium silicate and silane can not completely prevent water penetration, it can slightly penetrate water. Still, they do not retain water. This is why that freeze-thaw scaling will increase dramatically after a certain depth of scaling on the surface of silane-coated concrete.

Whether the concrete surface is treated or not, the concrete surface's salt-freeze-thaw spalling speed process is slow and → slow.

The concrete surface treated with impregnants has gradually weakened its anti-salt-freezing-thawing effect after 12 years of service in the marine environment.

Compared with the concrete without penetrants, the reuse of the concrete surface impregnant can delay the rapid spalling period of the concrete surface by 20-45 cycles.

CHAPTER 5. LIFETIME DISTRIBUTIONS PREDICTION OF TOMAKOMAI DAM PROJECT

5.1 Life Prediction Based On Chloride Ion Attack

5.1.1 Overview

It can be seen from Section 2.3.3 shows that the life span of concrete is affected by the cover, the chloride ion diffusion coefficient, the chloride ion threshold of steel corrosion, and the chloride ion content on the surface of the concrete. The chloride diffusion coefficient and the chloride ion content on the concrete surface are time-variant and spatially variable. The method closest to the actual life should be an integral method that simultaneously considers continuous changes in time and space or the summation method in sections. The operability of the method is very low. Under normal circumstances, we assume that after the chloride ion has diffused in concrete for a certain number of years, the chloride ion content on the surface of the concrete and the apparent chloride ion diffusion coefficient will tend to stabilize, which can be considered as a fixed value. However, there are different opinions about how many years later it will reach a stable state. Based on the experimental data of Tomakomai Dam's field engineering experiments, this paper found that even after 12 years, the chloride ion content and apparent diffusion coefficient on the concrete surface have not stabilized because the measured data in the 20th year and the 12th year were significant differences.

According to Table 5-1 and Fig. 5-1, it can be seen that the coastal countermeasures of Tomakomai for flood dike are divided into S, which is greatly affected by salt damage. The influence of salt damage on the life of the Tomakomai flood dike cannot be ignored.

Table 5-1 Areas affected by salt damage [120, 121][2-29]

地域区分	地域	海岸線からの距離	塩害の影響度合いと対策区分	
			対策区分	影響度合い
B	北海道のうち，宗谷支庁の礼文町，利尻富士町・稚内市，猿払村・豊富町，留萌支庁，石狩支庁，後志支庁，渡島支庁の松前町	海上部及び海岸線から 100m まで	S	影響が激しい
		100m をこえて 300m まで	I	影響を受ける
		300m をこえて 500m まで	II	
		500m をこえて 700m まで	III	
C	上記以外の地域	海上部及び海岸線から 20m まで	S	影響が激しい
		20m をこえて 50m まで	I	影響を受ける
		50m をこえて 100m まで	II	
		100m をこえて 200m まで	III	

Fig. 5-1 Geographical distinction of the degree of influence of salt damage[120, 121][2-29]

Adhering to the principle of prevention first and maintenance second, we all hope to judge the future development trend of the project and the remaining life span through the early experimental data. Therefore, this paper analyses concrete life based on the experimental data of the 12th and 20th years, respectively, and establishes a time-varying relationship from it, which references similar projects in the future.

5.1.2 Basic calculation formula

This calculation uses the classic Fick's second law (Formula 5.1)

$$C(x,t)-C_i=C_{0s}\left\{1-\mathrm{erf}\left(\frac{x}{2\sqrt{D_{aps}\cdot t}}\right)\right\} \tag{5.1}$$

Where

C(x,t): the total initial chloride ion concentration at the distance x from the concrete surface, kg/m^3;

x: The distance between the test point of the total chloride ion concentration from the concrete surface, x=0.5, 1.5, 2.5, 3.5, 4.5, or 5.5 cm,

t: exposure time, t=12 or 20, years.

C_{0s}: surface total chloride ion concentration, kg/m^3;

C_i: the initial total chloride ion concentration in the concrete, kg/m^3;

D_{aps}: the apparent diffusion coefficient of perchloride ions, mm^2/year

erf: error function (Formula 5.2).

$$\mathrm{erf}(s)=\frac{2}{\sqrt{\pi}}\int_0^s e^{-\eta^2}d\eta \tag{5.2}$$

Deformation of formula 5.1 the concrete life calculation formula 5.3 can be obtained.

$$t=\frac{x_c^2}{4D_{aps}\left[erf^{-1}\left(1-\frac{c_{cr}-c_i}{c_{0s}}\right)\right]^2} \tag{5.3}$$

5.1.3 Calculation and determination of key parameters

5.1.3.1 Calculational total chloride ion concentration distribution

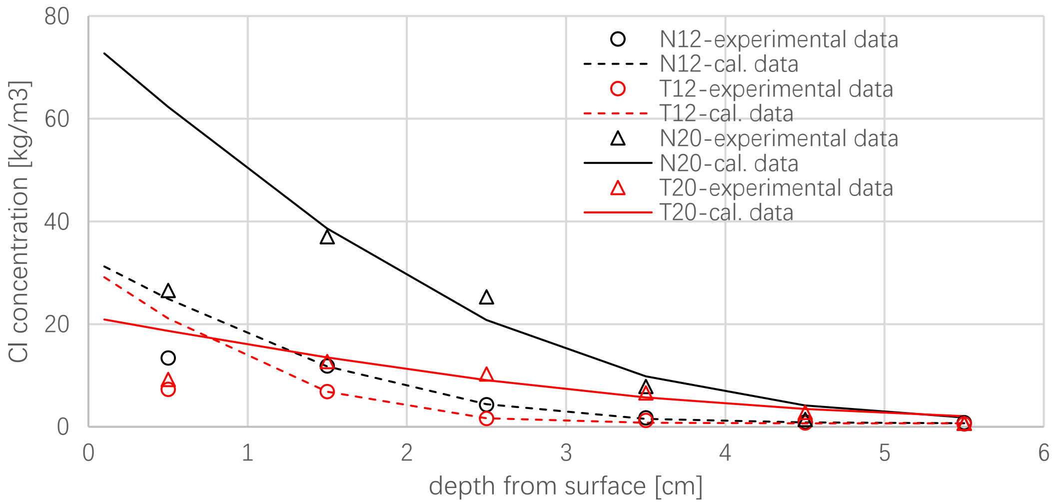

Fig. 5-2 The experimental and calculational total chloride ion distribution (kg/m^3)

The transmission behavior of chloride ions in concrete complies with Fick's second law. Therefore, the Fick's second law can be used to fit the chloride ion concentration of concrete obtained from the experiment from the surface to the inside. After fitting, the chloride ion diffusion coefficient D_{aps} and concrete surface chloride ion content C_{0s} are obtained simultaneously. Here, the initial chloride ion concentration is taken as the average value of the chloride ion concentration of the innermost layer (50-60mm), which is 0.68kg/m^3.

The fitting process is realized by the data solver tool in Excel software. The detailed steps are:

① Input the experimental data and the known parameters in an Excel sheet.

② Establish the calculation formula of each layer's calculational (theoretical) total chloride ion concentration according to Fick's 2nd law.

③ Establish the residual square calculation formula of each layer's experimental and calculational total chloride ion concentration, and sum the residual square

④ Use the "Solver" tool under the "Data" menu to calculate the fitting solution. Locate the cell of the sum of the residual squares as the target cell, and set it to be the smallest,

⑤ Set the cell where D_{aps} and C_{0s} are located as the variable cells.

⑥ The constraint parameter can be without setting the constraint parameter, check the non-constrained parameter as a non-negative value,

⑦ Use nonlinear Solve.

⑧ solve

Then the D_{aps} and C_{0s} can be obtained at the same time. The connecting line corresponding to each layer's calculated total chloride ion concentration is the fitting distribution curve of the total chloride ion concentration. In some cases of the calculation process, the fitting curve may deviate from the experimental data range, but the calculation is terminated. At this time, it is only necessary to manually adjust the C_{0s} to the approximate range of the fitting curve according to the experimental data and then execute the Solver process again.

The experimental data of chloride ion concentration and fitting curves are shown in **Fig. 5-2**.

Fig. 5-2 shows that at the same test depth: (a) In the same year, the chloride ion concentration of the treated part was lower than the untreated part. The penetrants can effectively resist the water and corrosive substances into the concrete. (b) For the same part, the concentration of the 12th year is lower than the 20th year's because the chloride ions were cumulated over time. Along the depth direction: (a) In the 12th year, chloride ion concentration decreases gradually from surface to inside. The chloride ion development frontier is roughly 35mm. (b) In the 20th year, the first layer chloride ion concentration is lower than the second layer; there is a gradual downward trend from the surface to the inside from the second layer. The chloride ion front reaches a depth of 45mm. The reason is that the concrete surface layer is a convective zone [112, 113]. The chloride ions concentration of this layer is affected by rain, tides and waves erosion and carbonization. When the surface chloride ions increase to a specific value, it is not easy to continue to grow. In this convective zone, the surface chloride ions concentration tends to deviate from Fick's second law [114]; therefore, it starts from the second layer in the fitting process. The calculations related to chloride ion concentration should also select the surface chloride ion concentration obtained by curve fitting regression. The concrete interior is dominated by diffusion, conforming to Fick's second law.

Fig. 5-2 also shows that the chloride ion concentration in each layer of the untreated concrete part increases synchronously with the year, showing no intersection of the fitting curves. For the untreated part, the chloride ion concentration of the inner layers (depth ≤ 10mm) have a changing trend consistent with the treated part. In contrast, in the first layer, there is an intersection. It is because, in the 12th year, the chloride ion concentration of the first layer and the sub-layer differed significantly. By the 20th year, the concentration difference between the first layer and the sub-layer became smaller. It indicates that the first layer's penetration barrier function gradually weakened along the service year.

5.1.3.2 Surface Total chloride ion concentration C_{0S}

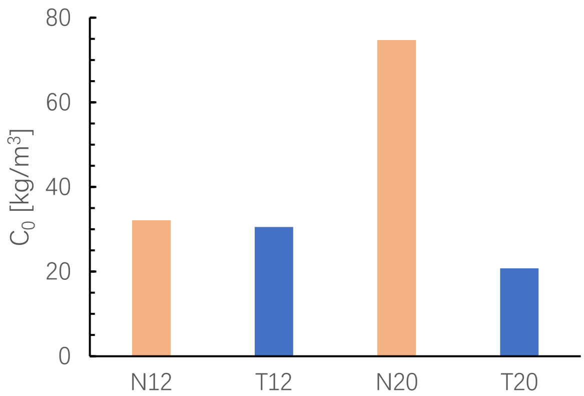

Fig. 5-3 The surface total chloride ion concentration (kg/m^3)

Fig. 5-3 shows that the chloride ion concentration on the concrete surface is time-varying and is affected by the surface treatment. In the 12th year, the chloride ion concentration on the concrete surface of the treated part and the untreated part was almost equal. Still, as the service life increased, by the 20th year, the untreated concrete surface had a faster accumulation of chloride ion concentration than the concrete treated with impregnating agents, increasing from 32.16kg/m^3 in the 12th year to 74.68kg/m^3 of the 20th. In contrast, the treatment group has decreased from 30.54kg/m^3 to 20.78kg/m^3. The 20th year's chloride ion concentration on the concrete surface of the untreated part is about 2.32 times that of the 12th year of itself and 3.59 times that of the treatment part of the 20th year. And the treatment part, compared with itself 12th year, even decreased by 31.97%. After coated with penetrants, the calculated surface chloride ion concentration were reduced by 5.04%/72.18% (the 12th year/the 20th year). The longer the time, the greater the difference between the surface chloride ions concentration of the two parts concrete .It is mainly because sodium silicate continuously reacts with the calcium hydroxide inside in water conditions during the concrete service. At the same time, the surface carbonization of the concrete is faster than that of the untreated group. All of these can make the concrete surface dense. So, the water and chloride ions are not easy to enter. The existing chloride ions in the inner part will diffuse deeper into the concrete under the difference of chloride ion concentration, thereby reducing the surface chloride ion concentration of the treatment part. It can be seen that the concrete surface penetrants can effectively reduce the growth rate of the chloride ion concentration on the concrete surface.

In the durability design, the chloride ion concentration on the concrete surface is generally set to 13 kg/m^3 proposed by the Civil Engineering Society [114].

For all the groups, the calculations show that the theoretical chloride ion concentration on the concrete surface have exceeded 13 kg/m^3 at the service of 12, let alone the nearly 80 of the 20th year of the untreated part. Suppose the target service year is 100 and the concrete surface is without additional treatment. In that case, the theoretical chloride ion concentration of the concrete surface is obviously far more than 13 during 90% of the service time. Further, the measured chloride ion concentration has far exceeded 13kg/m^3 in the 20th year.

In the concrete durability design, if the design value of 13 kg/m^3 is taken and the mix ratio are designed as this project, it is far from achieving the 100-year service goal. Other concrete durability maintenance measures, such as covering the concrete surface with effective penetrants used in this project, should be used. But it is not a one-time fix. The service process still needs to be maintained in stages.

Another suggestion is to increase the surface chloride ion concentration for concrete durability design depending on the concrete service environment.

5.1.3.3 The chloride diffusion coefficient D_{aps}

5.1.3.3.1 The calculation of chloride diffusion coefficient

Fig. 5-4 shows that the chloride ion diffusion coefficient of the treated part concrete has almost no change from the 12th year to the 20th year, indicating that the chloride ion diffusion rate in ordinary concrete tends to be stable after 12 years. However, the diffusion coefficient of the treated part has grown from about half of the untreated group's diffusion coefficient in the 12th year to twice that in the 20th year, which is a considerable change. It also means that, in the 20th year, the protective effect of the penetrants on the concrete surface was partially or wholly lost, leading to the chloride ion diffusion coefficient on the concrete surface increasing sharply. Although the chloride ion diffusion coefficient has become much larger, it can be known from section 2.2 that the chloride ion concentration on the surface of the treated group is about 27.82% of that of the untreated group, so the amount of chloride ions that can eventually be transmitted into the inner concrete is much smaller than that of the untreated group.

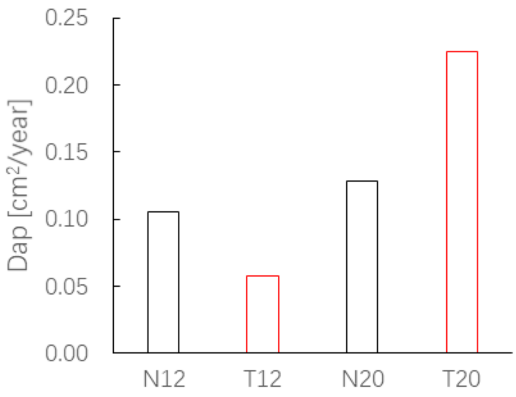

Fig. 5-4 Chloride diffusion coefficient D_{aps}

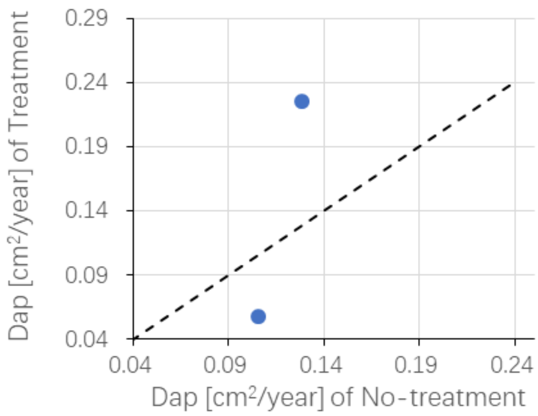

Fig. 5-5 The relationship of the Chloride diffusion coefficient D_{aps} between the treatment part and no-treatment part.

Fig. 5-5 shows the relationship between the treatment and the untreated groups' chloride ion diffusion coefficient. The treatment group's diffusion coefficient was lower than that of the untreated group in the

12th year, and a reversal occurred in the 20th year. The reversal time point can be regarded as the time when the protective effect of the impregnant on the concrete surface begins to lose. The reversal point is the intersection point of the two straight lines. This intersection's chloride ion diffusion coefficient can be obtained at 0.11 cm^2/year.

5.1.3.3.2 Diffusion coefficient attenuation index over the year

The change index m is calculated by Formula 5.4.

$$D(t) = D_{\text{ref}} \left(\frac{t_{\text{ref}}}{t} \right)^m \quad (5.4)$$

Table 5-2 lists the change index m of the Chloride diffusion coefficientD_{aps}. For the treatment group, D_{aps}-*12* is still used as Dref, and 0.11cm^2/year in Section 2.3.1 is used as D(t) into the above formula 2. The value of m is -2.90, and the tref is 12, then the t can be calculated. It is 15.11. The time for the protective effect of the impregnant on the concrete surface to significantly reduce the inflexion point is about 15 years. After this year, the chloride ion diffusion effect was greater than that of the untreated group. This conclusion suggests that the secondary maintenance of the concrete in the treatment group should be less than 15 years.

Table 5-2 The change index m

Groups	D_{aps}-*12*	D_{aps}-*20*	Decay index m
	(cm^2/year)		
No-treatment	0.11	0.13	-0.33
Treatment	0.06	0.23	-2.63

5.1.3.4 Determination of the critical chloride ion concentration for corrosion C_{cr}

In <Draft recommendation for repair strategies for concrete structures damaged by reinforcement corrosion >[56], as a recommendation, a chloride content in the range 0.3-0.5% and below by the weight of cement can be considered to lead to a low corrosion risk in most cases. Or 0.05% by the weight of concrete. The critical chloride ion concentration of concrete can be increased by 4 to 5 times when the alkalinity of concrete increases, or the rust inhibitors are added, or anticorrosive steel bars are used [55, 57]. Therefore, in European countries and North America, it has become common to limit the chloride content threshold to about 0.4% by weight of cement.

The Japanese Society of Civil Engineering recommends that C_{cr} is 1.2kg/m^3.

Scholar Kenichi Horiguchi [58] concluded that the threshold is related to cementitious materials and concrete mixing ratio. The chloride threshold value for corrosion initiation of concrete using ordinary cement was 1.6, 2.5, 3.0, and 3.0 kg/m^3, respectively, when the amount of unit binding material was 254, 291, 362, 446 kg/m^3. It was approximately 0.8 % binding material by weight and was a reasonable result within the range of 0.3 to 1.8 % of cement shown in the past research. It is about 2.2 kg/m^2 in this study, calculated from his experimental conclusion.

Takuro Matsumura(松村　卓郎) [59] https://criepi.denken.or.jp/jp/env/outline/2003/10.pdf had also shown that the chloride ion threshold for steel corrosion might be as high as 4-6 kg/m^3 in the marine dry-wet cycle environment.

Combined with the mix ratio data of the Tomakomai dam, the Chloride ion threshold calculation result is shown in Table 5-3 at the ratio mentioned above.

Table 5-3 Chloride ion threshold

item	Mass[kg/m^3]	Ratio:%	C_{cr}[kg/m^3]
cement	277	0.3	0.831
	277	0.4	1.108
	277	0.5	1.385
	277	0.8	2.216
concrete	2369	0.05	1.1845

In order to extensively verify and discuss the impact of the threshold on life and predict the existence of various possibilities, Here we take C_{cr} as 1.2 kg/m^2, 2.2 kg/m^2, and 4 kg/m^2 to estimate the life span of the Tomakomai dam.

5.1.3.5 Regulations on the thickness of the concrete cover *x*

Table 5-4 is from Table-6.2.2 of Road Bridge Specification III (6.2.3 道路橋示方書III6.2.3 の表-6.2.2).

Table 5-4 Requirements for the minimum cover of concrete

表−1 鋼材の腐食を生じさせないための最小かぶり（mm）

塩害の影響の度合い ＼ 部材・部位	対策区分	(1)工場で製作されるプレストレストコンクリート構造	(2)(1)以外のプレストレストコンクリート構造	(3)鉄筋コンクリート構造
影響が激しい	S	70※1		
影響を受ける	I	50	70	
	II	35	50	70
	III	25	30	50

※1） 塗装鉄筋又はコンクリート塗装等かぶりによる方法以外の方法を併用する

As can be seen from the above table, to prevent salt damage, the thickness of the concrete protective layer should be at least 25mm. In the case of cast-in-place PC structure (girder, floor slab), salt damage category II is "cover 50 mm"; salt damage category I is "cover 70 mm"; and salt damage category S is "cover 70 mm + use of painted reinforcing bars or concrete painting". In this paper, in order to examine the impact of different concrete protective layer thickness on the concrete life (remaining life), the development of chloride ions along with the depth of the protective layer, and the development of the failure of the protective layer of different thicknesses, the calculation process also takes into account the deviation of construction and design. The cover thickness is widely selected, took 10mm as interval, the value ranges from 10 to 120 mm, and the life of the protective layer between 50-70mm is focused in combination with this project.

5.1.4 Calculation methods and process

The calculation methods include the deterministic and Monte Carlo methods. Each calculation method includes the A method and B method (**Fig. 5-6**).

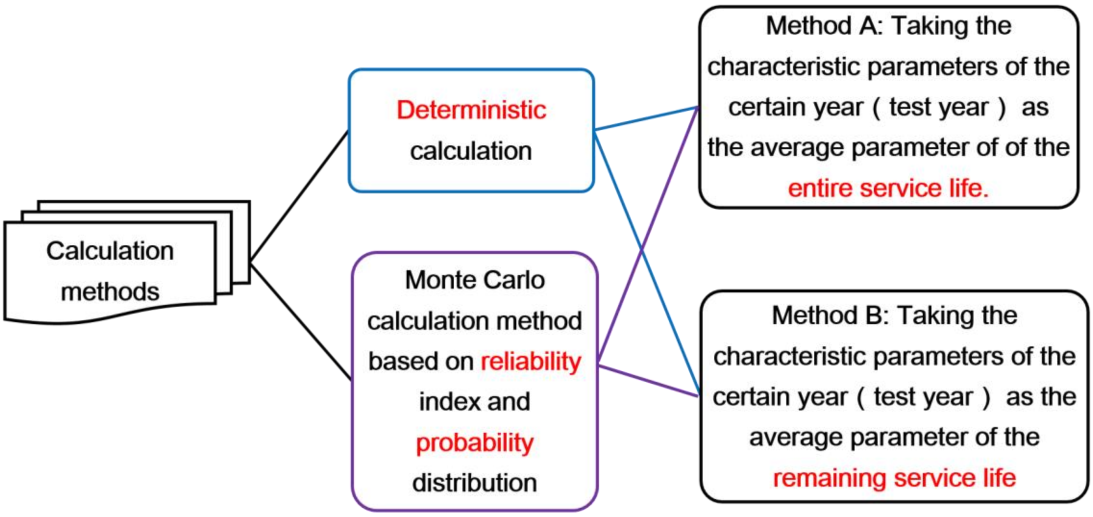

Fig. 5-6 map of Calculation methods

5.1.4.1 Deterministic method

Calculate the life of concrete according to formula 5.3 and regard each calculation parameter as the only determined value, regardless of its possible probability distribution, nor the reliability index of material life failure.

The main steps are as follows:

① Let $C(x,t) = C_{cr}$

② Putting the C_{cr}, C_i, C_{0S}, D_{aps} obtained from section 5.1.3 and the target value of cover (x=c) into the formula 5.3. The predicted total life T_{tot} based on the t_i-year data can be obtained.

5.1.4.2 Monte Carlo method

Monte Carlo calculation is a method based on probability distribution and reliability index (failure probability). Here, the normal distribution of the concrete cover thickness is mainly considered, and two situations corresponding to different construction quality levels are considered; at the same time, the reliability index of the material, that is, its failure probability, is considered.

The thickness and quality of the concrete cover are the most critical factors for the concrete structure to resist the corrosion of chloride ions. Chloride ions migrate into the concrete and accumulate year by year. When the chloride ion on the surface of the steel bar reaches a critical concentration(chloride threshold), the passive film of the steel bar will be destroyed, and the steel bars will begin to corrode. Once the corrosion of the steel bar begins, it develops quickly. Therefore, the initial corrosion of the steel bar is generally regarded as the end of the service life of the concrete structures in the chloride environment, and the corrosion development stage of the steel bar is used as a safety reserve.

If the diffusion depth of chloride ions is regarded as the generalized load effect S, then the thickness of the concrete cover can be regarded as the generalized structural resistance R, both of which change with time. The corresponding service life can be calculated according to the structure's service life definition when the structural reliability index is specified.

The failure probability P_f of the structure can be defined as the target probability P_t [122]:,

$$P_{\mathrm{f}} = P\{Z \leqslant 0\} \leqslant P_{\mathrm{t}} \tag{5.5}$$

The limit state equation can be described as

$$Z = R - S \tag{5.6}$$

Substituting formula 5.6 into 5.5, 5.7 can be get

$$P_f = P\{R - S \leqslant 0\} \leqslant P_{\mathrm{t}} \tag{5.7}$$

When R and S obey the normal distribution, Z also obeys the normal distribution. Then, the failure probability can be expressed as:

$$P_f = \Phi(-\mu_z / \sigma_z) = \Phi(-\beta) \quad 5.8$$

$$\beta = \frac{\mu_Z}{\sigma_Z} \quad 5.9$$

Where β is the reliability index, μ_Z and σ_Z are the expected value and variance of Z, respectively. If there is no significant statistical data, the average value and standard deviation can be used instead.

$$\mu_Z = \mu_R - \mu_S \quad 5.10$$

$$\sigma_Z = \sqrt{\sigma_R^2 + \sigma_S^2} \quad 5.11$$

$$R = C_{cr} \quad 5.12$$

$$S = C_x \quad 5.13$$

Where, C_{cr} is the chloride ion concentration when steel bars corrode, that is threshold value; C_x is the chloride ion concentration at the depth of *x*. Put 5.12 and 5.13 into formula 5.7 to obtain the failure probability of the structure under the chloride ion erosion environment

$$P_f = P\{C_{cr} - C_x \leqslant 0\} \leqslant P_t \quad 5.14$$

calculation steps:

Using the software Crystal Ball to calculate:

1. Open the excel with Crystal Ball and establish the concrete life calculation process in method A or method.
2. Define the hypothesis:

Inputting of concrete cover distribution. Due to the lack of statistical data, it is assumed that the allowable deviation of concrete cover construction is 10mm here[123]p103. As prescribed by JASS5 - 11.10 (Table 5-5), from the most unfavourable point of view, assuming that the measured concrete cover is about 15% less than the minimum cover, 10/1.036=9.65mm can be used as Standard deviation σ_C [123]p103. At the same time, it also estimated the life of the concrete under chloride ion erosion when the construction guarantee rate of a set of concrete cover reached 95% (allowable deviation 10mm). At this time, the standard deviation of the concrete cover σ_C is 10/1.645=6.079mm to discuss the impact of the variability of the cover caused by different construction quality levels on the life expectancy.

The thickness of the concrete cover μ_C is still progressively 10mm, ranging from 10mm to 90mm.

Table 5-5 Criteria for concrete cover (11.10 of JASS5)

表6　かぶり厚さの判定基準

項　目	判定基準
測定値と最小かぶり厚さとの関係	x ≧ Cmin-10
最小かぶり厚さに対する不良率	P（x＜Cmin）≦ 0.15
測定結果の平均値の範囲	Cmin≦X≦Cd＋20

注：　x　　：個々の測定値（mm）
　　　X　　：測定値の平均値（mm）
　　　Cmin：最小かぶり厚さ（mm）
　　　Cd　：設計かぶり厚さ（mm）
　　　P（X＜Cmin）：測定値がCminを下回る確率

3. Define the total life (A method)or the rest life (B method) of concrete as a decision variable;
4. Define $C_{cr} - C_x$ as the forecasts value;
5. Set running preferences: test times, here select the software default times 1000; Speed term: According to experience, if the denominator variable in the formula may become 0, consider choosing "normal Speed." If there is no such situation where the denominator becomes 0, we can choose "extreme Speed," and this option can significantly shorten the calculation time. In this article, we can choose the " normal Speed " mode;
6. Optquest setting, according to the life judgment criterion β≥1.5, corresponding to the failure probability of 6.681%, which can be set as the target probability of the predicted value of $C_{cr} - C_x \leqslant 0$.
7. Freeze non-calculated cells because the software can only calculate one decision value at a time. Of course, not freezing will not affect the smooth progress of the calculation, but it will significantly affect the calculation speed.
8. Set constraint items. Here, set constraints on the decision value based on the deterministic result, The life obtained after considering the probability distribution is smaller than that obtained by the deterministic calculation, so the life obtained by the deterministic calculation can be defined as the upper limit of the decision variable.
9. "Options" settings can be set according to personal requirements, or you can choose the default

options. The optimization type is selected to use random simulation; the decision variable cell is automatically set as the most extreme solution.

10. Click "Run";
11. At the end of "running," the total life or the rest life of concrete under this condition calculation can be obtained.

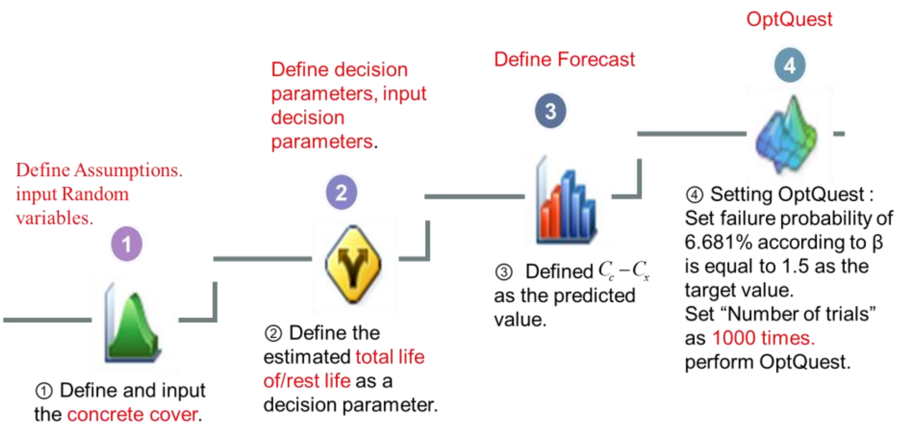

Fig. 5-7 The key steps of calculation in crystal-ball

The key calculation steps and corresponding operation icons in Crystal Ball are shown in the **Fig. 5-7**.

5.1.4.3 Method A and Method B

The calculation steps of them are almost the same except for the value of C_i. Furthermore, the meaning of T finally solved is also different.

In method A, C_i is the initial concentration of chloride ions 0.68 kg/m^3, and the calculated life T is the total life of the concrete.

In method B, Let C_i be equal to the measured value of the chloride ion concentration of each layer of concrete + 0.68 kg/m^3. Assuming that the calculation is based on the experimental data of the year t, it can be understood as starting from the year $t+1$, taking the characteristic parameters of the year t as the average parameter of the remaining life.

5.1.5 Life span summary based on the deterministic method

According to Method A and Method B, calculate the dam's total life and remaining life when the chloride ion content threshold is 1.2kg/m^3, 2.2 kg/m^3, and 4 kg/m^3, respectively. The total life span is listed in Table 5-6 and Table 5-7.

Table 5-6 Total service life-of A method

Group	depth [cm]	Critical chloride ion concentration Ccr[kg/m^3] 1.2	2.2	4
12-N	1.0	0.8	1.2	1.8
	2.0	3.4	5.0	7.4
	3.0	7.6	11.2	16.6
	4.0	13.6	19.9	29.4
	5.0	21.2	31.1	46.0
	6.0	30.6	44.8	66.2
	7.0	41.6	61.0	90.1
	8.0	54.3	79.7	117.7
	9.0	68.8	100.8	149.0
	10.0	84.9	124.5	183.9
	11.0	102.7	150.6	222.6
	12.0	122.2	179.2	264.9
12-T	1.0	1.5	2.3	3.4
	2.0	6.1	9.1	13.6
	3.0	13.8	20.4	30.5
	4.0	24.5	36.2	54.2
	5.0	38.3	56.6	84.7
	6.0	55.1	81.5	122.0
	7.0	75.0	111.0	166.0
	8.0	98.0	145.0	216.9
	9.0	124.0	183.5	274.5
	10.0	153.1	226.5	338.8
	11.0	185.3	274.1	410.0
	12.0	220.5	326.1	487.9
20-N	1.0	0.5	0.7	1.0
	2.0	2.2	2.9	3.9

	3.0	4.9	6.6	8.8
	4.0	8.6	11.7	15.6
	5.0	13.5	18.3	24.3
	6.0	**19.4**	26.3	35.0
	7.0	26.4	35.8	47.7
	8.0	34.5	46.7	62.3
	9.0	43.7	59.2	78.8
	10.0	54.0	73.0	97.3
	11.0	65.3	88.4	117.7
	12.0	77.7	105.2	140.1
20-T	1.0	0.5	0.7	1.2
	2.0	1.8	2.8	4.6
	3.0	4.1	6.4	10.4
	4.0	7.2	11.3	18.4
	5.0	11.3	**17.7**	28.8
	6.0	**16.3**	25.5	41.5
	7.0	22.2	34.7	56.4
	8.0	29.0	45.3	73.7
	9.0	36.7	57.4	93.3
	10.0	45.3	70.8	115.2
	11.0	54.8	85.7	139.4
	12.0	65.2	102.0	165.9

Table 5-7 Total service life-of B method

Group	depth	Critical chloride ion concentration Ccr[kg/m^3]		
	[cm]	1.2	2.2	4
12-N	1.0	-	-	-
	2.0	-	-	-
	3.0	-	-	-
	4.0	-	25.0	35.8
	5.0	29.9	41.0	56.1
	6.0	40.0	55.1	76.6
	7.0	50.2	70.7	100.0

	8.0	61.8	88.7	126.9
	9.0	75.1	109.0	157.4
	10.0	89.9	131.8	191.6
	11.0	106.2	156.9	229.3
	12.0	124.1	184.5	270.6
12-T	1.0			
	2.0			
	3.0		26.5	39.7
	4.0		42.0	64.5
	5.0	49.0	67.7	102.2
	6.0	70.4	95.9	145.5
	7.0	91.5	126.3	193.7
	8.0	115.8	161.2	249.3
	9.0	143.4	200.9	312.4
	10.0	174.2	245.2	382.8
	11.0	208.2	294.1	460.7
	12.0	245.5	329.1	546.0
20-N	1.0	-	-	-
	2.0	-	-	-
	3.0	-	-	-
	4.0	-	-	-
	5.0		34.7	41.7
	6.0	39.2	46.0	54.7
	7.0	46.1	55.4	67.2
	8.0	54.1	66.3	81.7
	9.0	63.2	78.6	98.1
	10.0	73.3	92.3	116.4
	11.0	84.5	107.5	136.6
	12.0	96.8	124.1	158.8
20-T	1.0			
	2.0			
	3.0			
	4.0			
	5.0	20.0	20.0	35.6
	6.0	36.3	45.2	60.8
	7.0	42.2	54.3	75.6

8.0	49.0	64.8	92.6
9.0	56.7	76.8	111.8
10.0	65.4	90.1	133.4
11.0	74.9	104.8	157.2
12.0	85.3	120.9	183.2

Notes: 12-N(T): 12 represents the calculation base as the experimental characteristic parameter of the 12th year, and T takes this group as the treated group, N is the untreated group.

The cells in Table 5-7 which are without data, means that

The meaning of the cells without data in Table 5-7 is: in the test year, the chloride ion concentration at this depth has exceeded the chloride ion threshold.

The thickness corresponding to the red data in the table is the necessary thickness required for the concrete surface to resist chloride ion erosion for more than 100 years.

The **black bold** data in the table means that the estimated concrete life is too small by judging from the current measured data. It can be seen that the small range is about 0-6 years. Similarly, the estimated life should also be larger than actual life. According to the fitting principle, it can be judged that the life error calculated by this method may be about ±6 years.

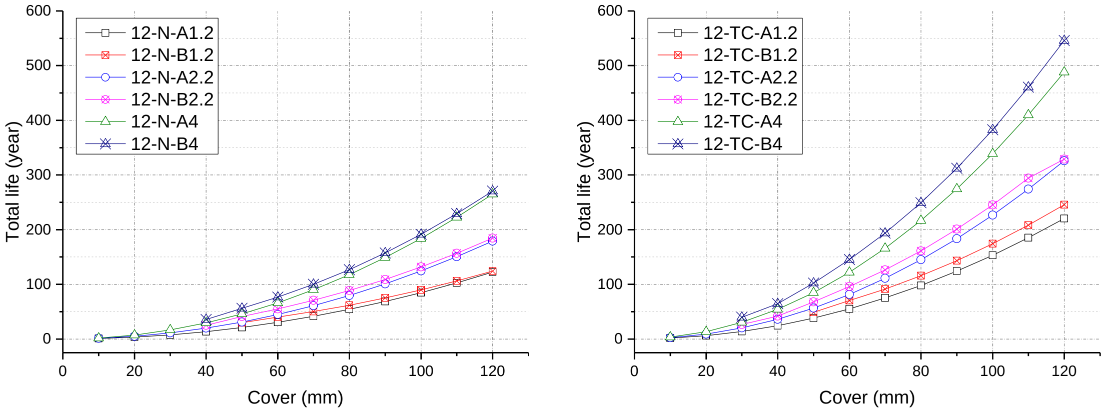

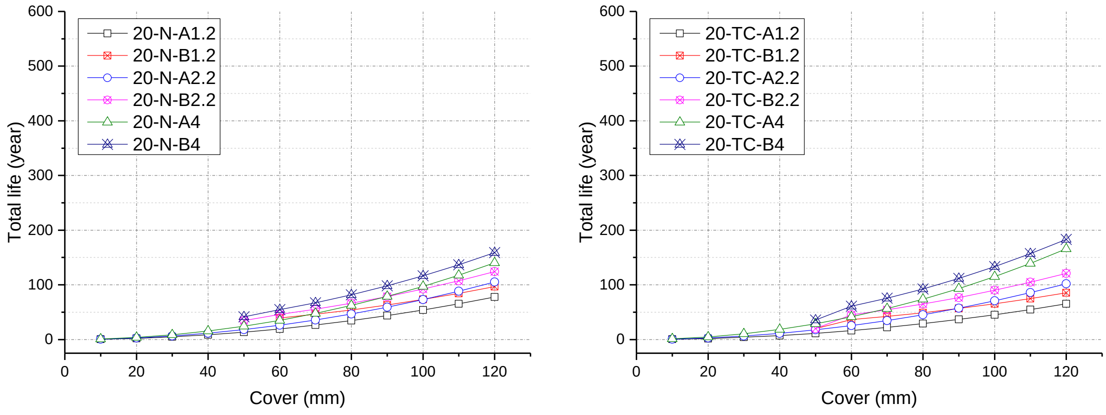

Fig. 5-8 Total life VS concrete cover by deterministic method (A method)

Notes:

Meaning of 12-N-A-1.2:

12: Based on data collected in the 12th year;

N: No concrete surface impregnant treatment, untreated groups;

TC: The concrete surface is treated with impregnant, treated groups;

1.2: chloride ion threshold 1.2kg/m^3;

A: A method;

Fig. 5-8 shows the longest concrete life is calculated from the data collected in 12th year of the treatment group. The concrete life based on the 20th year is less than that based on the 12th year.

5.1.6 Life span summary based on Monte Carlo calculation method

The results list in Table 5-8 and Table 5-9。

Table 5-8　Total concrete life calculated based on Monte Carlo-A method

Group	depth	cover 0.85 (0.9648 cm)	cover 0.95 (0.6079 cm)

		Critical chloride ion concentration Ccr[kg/m3]			Critical chloride ion concentration Ccr[kg/m3]		
	[cm]	1.2	2.2	4	1.2	2.2	4
12-N	1.0	-	-	-	-	-	-
	2.0	-	-	-	-	-	-
	3.0	2.1	3.3	4.6	3.7	5.4	8.1
	4.0	5.4	7.9	11.6	7.4	10.9	16.2
	5.0	10.1	14.9	22.0	13.5	19.8	29.3
	6.0	17.7	26.0	38.5	21.8	31.1	46.8
	7.0	25.0	36.8	54.5	31.2	45.8	67.9
	8.0	35.02	51.42	76.29	41.03	60.29	89.39
	9.0	46.2	67.9	100.7	54.0	79.3	117.6
	10.0	61.1	89.7	133.1	68.0	100.0	148.2
	11.0	74.2	109.0	161.6	82.6	121.3	179.9
	12.0	92.27	135.62	200.8	101.74	149.37	221.42
12-T	1.0	-	-	-	-	-	-
	2.0	-	-	-	-	-	-
	3.0	3.4	5.1	7.6	6.5	9.5	14.3
	4.0	9.49	14.03	21.01	14.23	21.05	31.5
	5.0	19.4	28.7	42.9	24.5	36.2	54.2
	6.0	30.8	45.5	68.1	39.8	58.8	88.0
	7.0	45.3	66.9	100.1	58.1	85.9	128.5
	8.0	65.17	96.41	144.21	75.23	111.29	166.48
	9.0	87.8	129.9	194.3	99.3	146.9	219.7
	10.0	109.4	161.8	242.1	126.2	186.7	279.3
	11.0	140.3	207.5	310.4	154.4	228.4	341.7
	12.0	169.96	251.31	376.06	186.49	275.85	412.68
20-N	1.0	-	-	-	-	-	-
	2.0	-	-	-	-	-	-
	3.0	1.21	1.63	2.18	2.42	3.26	4.34
	4.0	3.46	4.68	6.23	5.1	6.91	9.2
	5.0	6.6	9.0	11.9	9.0	12.2	16.2
	6.0	10.9	14.7	19.6	14.2	19.2	25.6
	7.0	16.5	22.3	29.7	19.7	26.7	35.5
	8.0	23.31	31.3	41.7	26.8	36.27	48.33
	9.0	30.06	40.68	54.2	34.75	47.02	62.53

	10.0	38.9	52.65	70.14	44.59	60.36	80.52
	11.0	48.81	66.06	88.01	54.17	73.31	97.69
	12.0	59.5	80.53	107.28	66.18	89.56	119.28
20-T	1.0	-	-	-	-	-	-
	2.0	-	-	-	-	-	-
	3.0	1	1.56	2.54	1.87	2.92	4.75
	4.0	2.85	4.46	7.26	4.2	6.56	10.66
	5.0	5.5	8.6	13.9	7.4	11.3	18.3
	6.0	9.0	14.1	22.8	11.3	17.7	28.7
	7.0	13.6	21.3	34.6	16.6	25.9	42.1
	8.0	19.11	29.88	48.57	21.88	34.21	55.58
	9.0	24.83	38.84	63.11	28.66	44.83	72.82
	10.0	32.13	50.26	81.66	36.43	56.98	92.57
	11.0	40.33	63.07	102.48	44.57	69.71	113.26
	12.0	49.15	76.88	124.91	53.83	84.2	136.8

Due to the existence of the error function, the calculation process is slightly complicated and prone to interruptions, and the calculation is time-consuming. Therefore, the life in the conditions of the chloride ion threshold being 1.2kg/m^3 and the construction guarantee degree of 95% was calculated only in this chapter.

Table 5-9 Total concrete life calculated based on Monte Carlo-B method

Group	depth [cm]	M-1.2-95%-B	Group	depth [cm]	M-1.2-95%-B
12-N	1.0	-	20-N	1.0	-
	2.0	-		2.0	-
	3.0	-		3.0	-
	4.0	-		4.0	-
	5.0	23.7		5.0	-
	6.0	31.8		6.0	33.6
	7.0	40.8		7.0	39.9
	8.0	51.23		8.0	46.65
	9.0	62.9		9.0	54.95
	10.0	76.9		10.0	63.73

	11.0	91.3		11.0	74.37
	12.0	108.19		12.0	85.71
12-T	1.0	-	20-T	1.0	-
	2.0	-		2.0	-
	3.0	-		3.0	-
	4.0	-		4.0	-
	5.0	37.4		·	-
	6.0	53.8		6.0	31.7
	7.0	72.2		7.0	37.0
	8.0	92.48		8.0	43.06
	9.0	116.3		9.0	49.43
	10.0	146.3		10.0	57.56
	11.0	176.8		11.0	66.56
	12.0	211.98		12.0	74.96

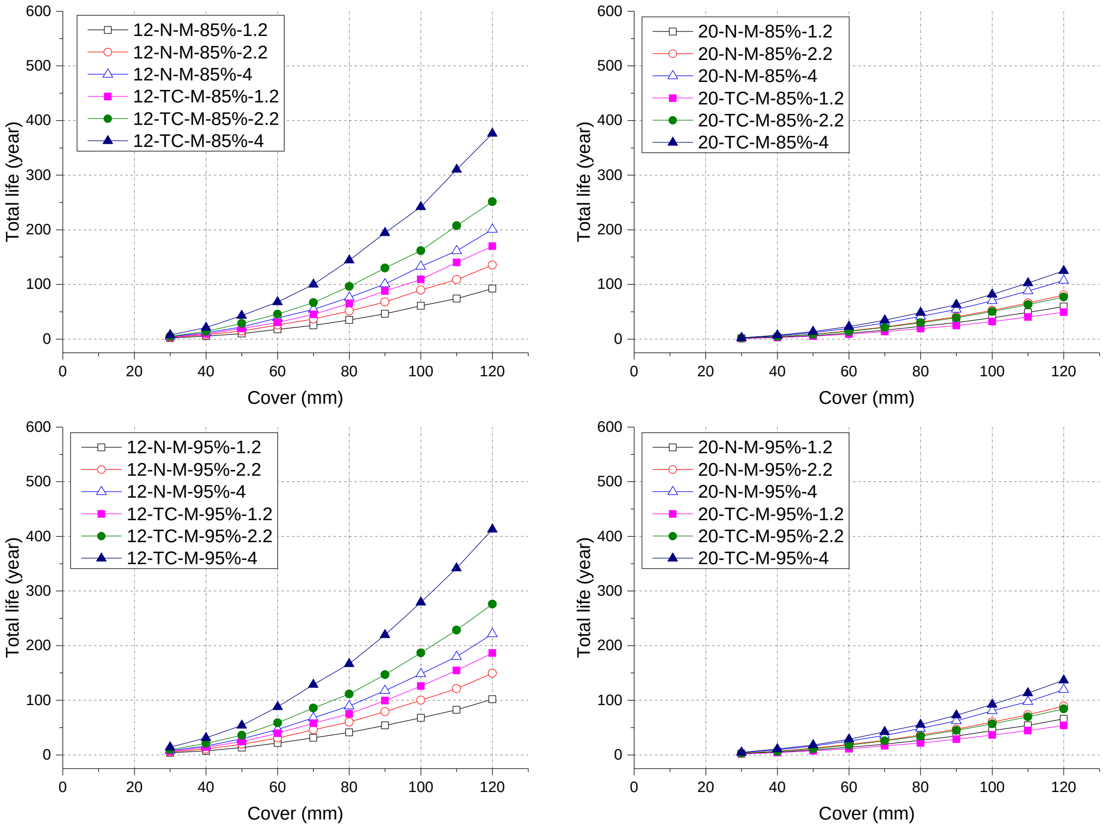

Fig. 5-9 Total life VS concrete cover (Monte Carlo-A method)

Notes:

Meaning of 12- N-M-85%-1.2 or 20-TC-95%-2.2;

M: Monte Carlo method;

85%/95% (9.648mm/6.079mm): The construction guarantee degree of the concrete cover thickness is 85%/95%, and the deviation of the cover thickness is 9.948mm/6.079mm;

1.2/4: chloride ion threshold 1.2kg/m^3 or 4 kg/m^3.

The rest of the abbreviations are the same as before.

5.1.7 Discussion the factors affecting on concrete life

It is well known that the thicker the cover, the higher the anti-corrosion threshold of the steel bar, the better the durability is, and the longer the concrete service life span. So it is not the focus of this article. The following discusses the factors affecting concrete life from the use of penetrant, sampling year of the primary data, and concrete life calculation method.

5.1.7.1 The effect of penetrants on concrete life extension

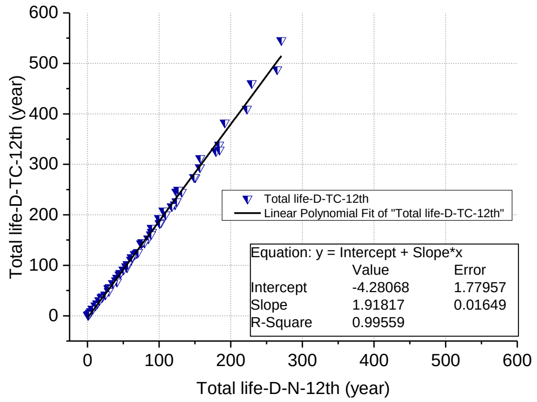

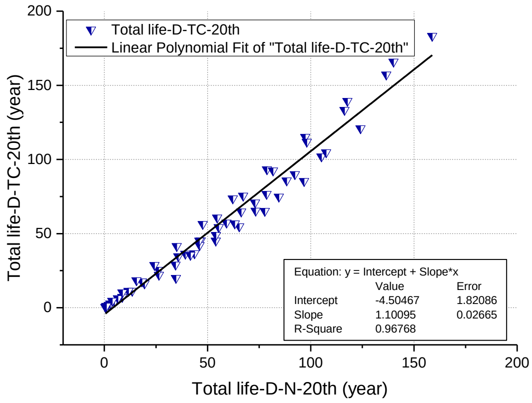

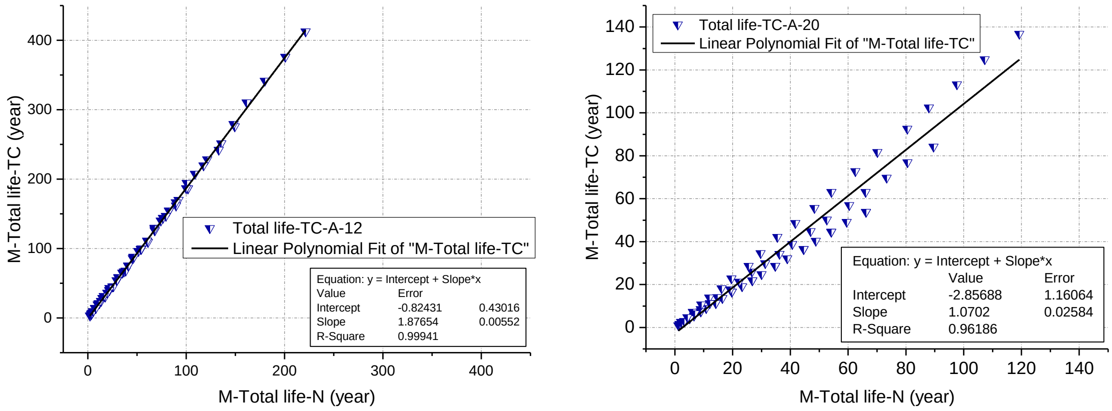

Fig. 5-10 The prolongation rate of concrete surface penetrants on concrete life

Notes:

D is deterministic calculation method; M is Monte Carlo method.

Fig. 5-10 shows: The total life of the concrete treated by the penetrants calculated by the Monte Carlo method has the following relationship with that of the untreated group. The total life of the treated groups is about 1.07-1.92 times that of the untreated group. Based on the data collected in the 12th year, the calculated value is about 1.9. Based on the 20th year, it is 1.1. The research results are consistent with the result of 1.5-4.8 times proposed by Hirotake ENDOH [124]

It can be seen that the multiple relationships have a lot to do with the primary data. In the 12th year, both the chloride ion content and chloride diffusion coefficient on the concrete surface of the treated groups were small.

In the 20th year, the chloride ion diffusion coefficient of the untreated groups tends to be stable. In the treated groups, due to the gradual loss of the impregnant's protective effect, the coefficient of chloride ion increases year by year, especially on the concrete surface so its calculated total life becomes small, and the multiple is reduced in the 20th year.

The magnifications calculated by the deterministic calculation method（D）Monte Carlo method (M) are very close.

5.1.7.2 Influence of chloride ion threshold for steel corrosion on concrete life

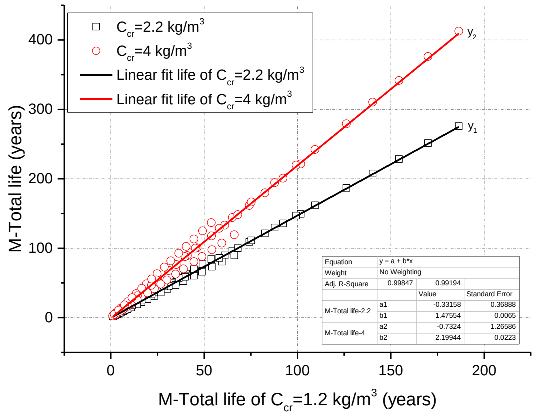

Fig. 5-11 Influence of chloride ion threshold for steel corrosion on concrete life

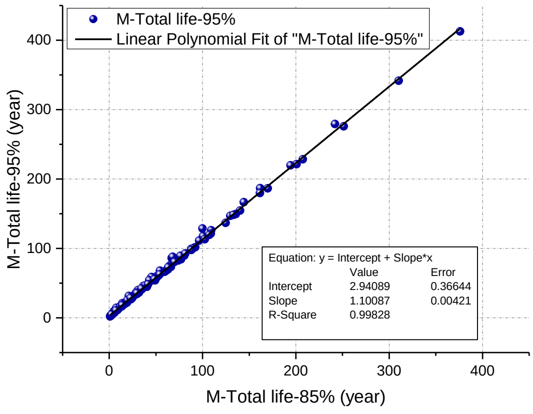

Fig. 5-12 Concrete cover thickness construction guarantee 95% VS 85%

Fig. 5-11 shows that improving the anti-rust ability of steel bars, when the chloride ions threshold is increased from 1.2kg/m^3 to 2.2 kg/m^3, the concrete life value can be extended by 1.48 times of the original life; when it is increased by 4 kg/m^3, it can even reach the original 2.20 times. It can be seen that if the technology is feasible and the economy is acceptable, improving the anti-rust ability of the steel surface can also significantly prolong the life of the concrete.

5.1.7.3 Influence of concrete cover thickness and construction quality on concrete life

Fig. 5-12 shows that the influence of the construction guarantee rate of concrete cover on its life. The concrete life with the cover guaranteed rate of 95% (allowable construction deviation is 10mm, and the construction standard deviation is 6.079mm) is longer than that of the groups with the guaranteed rate of 85% (construction standard deviation is 9.684mm). The relationship between the two is shown in Fig. 5-12. When the construction deviation of the cover is decreased from 9.648mm to 6.079mm, the concrete life can be increased to be about 1.1 times and three years of the original life.

For example, the design cover is 70mm; if the actual construction cover is 70-9.948=60.052mm, the concrete can last 100 years. When the construction quality is improved, the actual construction cover can reach 70- 6.079=63.921mm, and then, the service life can reach 113 years. If we guarantee 4mm more for a hundred-year project, we can extend the service life by eight years. It can be seen that ensuring the cover during construction by improving the construction quality can also effectively improve the durability of the concrete.

5.1.7.4 The impact of sampling year

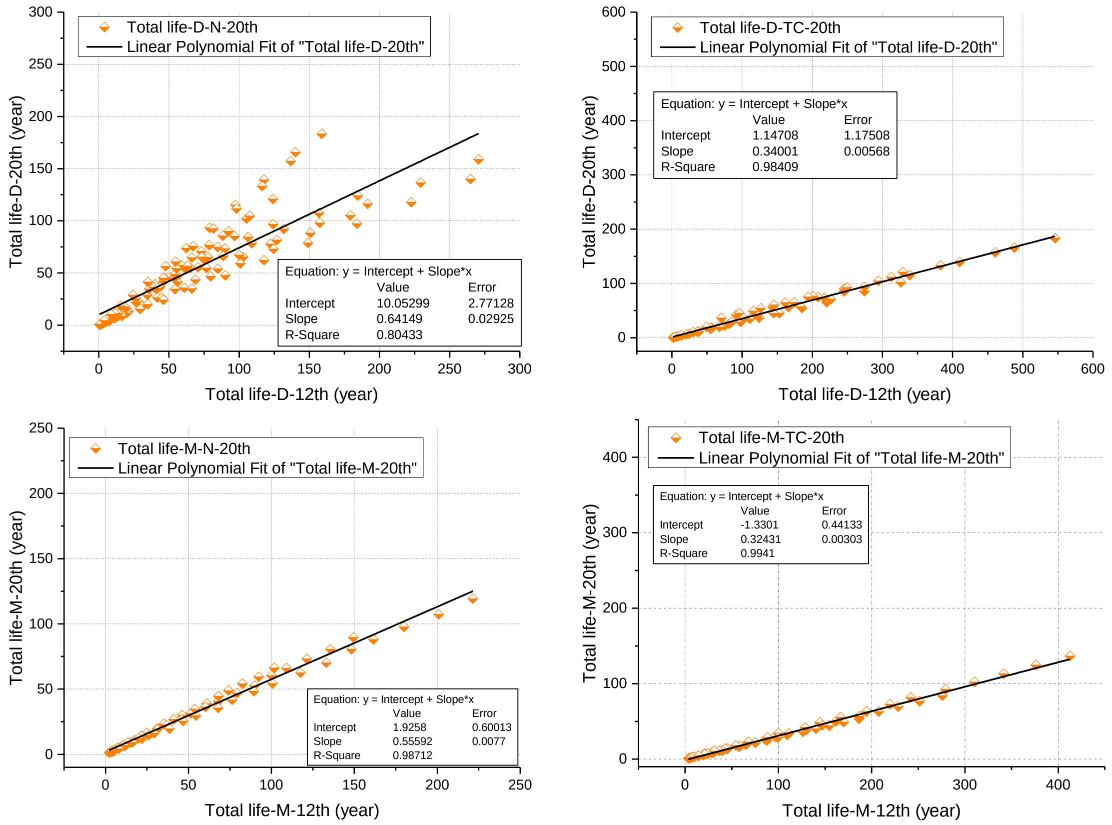

Fig. 5-13 The relationship between the T_{20tot} and T_{12tot}

Fig. 5-13 shows the relationship between the concrete life based on the experimental data collected in 20th year and in the 12th year data under the deterministic or Monte Carlo methods. Based on the experimental data in the 20th year, the lifespan obtained is less than that obtained in the 12th year. For the untreated part, the former is about 60% of the latter, while the value of the treated group is about 30%. The deterministic calculation method and the Monte Carlo calculation method have little impact on this relationship. However, for a given concrete structure, with stable environmental factors and no maintenance treatment during the service period, the durability life of the concrete should be relatively fixed, and should not vary with the test years.

The reason for this phenomenon may be due to: With the extension of the service life of concrete, the surface chloride ion content C_{OS} of the untreated increases greatly, while for treated part, the Daps increase sharply, all of them will reduce the life of the concrete. Therefore, the influence of Daps on the life of concrete is more significant than that of C_{OS}. As a result, the concrete life calculated based on the 20th year is less than the life calculated based on the data of the 12th year.

Based on the opinion that the longer the service time, the more stable the chloride ion diffusion is. For untreated part, the concrete life span obtained based on the data from the 20th year may be much closer to its actual life span.

However, compared with 20 years, the experimental data of a shorter year is easier to obtain (for example, about ten years). It is hoped that the life expectancy and operating early maintenance management of the structure can be estimated based on the data of the earlier year, thereby extending the service life of concrete more economically. Therefore, it needs to establish the relationship between concrete life based on the experimental data of the 12th and 20th years. The estimated life based on the early year can be indirectly closer to the real-life in the future.

According to the above fitting results, the approximate calculation formula can be expressed as follows formula 5.15 (just for untreated concrete).

$$T_{20} = 0.6T_{12} + 8 \tag{5.15}$$

When the experimental data of about ten years are obtained, the service life span calculated based on them can be revised using the above formula. The coefficient is not affected by whether the concrete surface is treated or not. That is, it may have universal significance. It has excellent reference significance for the calculation of the service life of similar projects in the future.

While, for the treated part, the experimental data showed that the chloride ion diffusion of the treated part of Tomakomai Dam did not reach a relatively stable state in the 20th year. Due to the presence of the penetrants, the microstructure of concrete surface has been changed, thereby the chloride ions diffusion process is also changing. It can be seen from the concrete surface core samples that the surface morphology of the treated group was significantly better than that of the untreated group in the 20th year with the naked eye. The life of the treated concrete is definitely longer than that of the untreated group. The reason of the instantaneous increment of the chloride ions diffusion coefficient in the 20th year may be because that it is in the initial stage of concrete surface deterioration. Affected by the weak layer mortar on the concrete surface, the chloride ion diffusion coefficient on the surface will increase in a short time (year), and after through this layer, the chloride ion diffusion coefficient will gradually decrease. Therefore, it is inappropriate to use the instantaneous chloride ion diffusion coefficient of the 20th year as the chloride ion diffusion coefficient of its entire life cycle or the rest of its life. It should be considered that the chloride ion diffusion coefficient will fall back and then tend to be stable. Briefly, when estimating the life of the treatment group, considering the penetrate depth of the impregnant and its failure process, it will be more accurate to use different chloride ion diffusion coefficients to estimate the life by years. However, in fact, this process is difficult to determine. After the increase of the chloride ion diffusion coefficient, it is necessary to measure the change process of the chloride ion diffusion coefficient with the years in the encrypted sampling period. Drilling core sampling is harmful to the actual project in use (the Tomakomai breakwater is a project in service), unless it is specially set up as an experimental sample. Judging from the experiment, the lifespan of the treatment group should be between the 12th and 20th year experimental data.

5.1.7.5 Influence of calculation method on concrete life

5.1.7.5.1 Comparison of deterministic calculation method and Monte Carlo calculation method

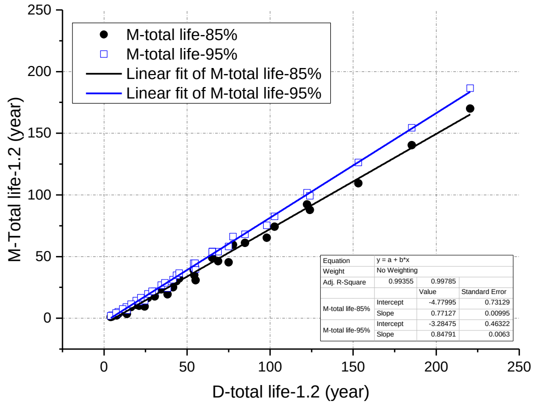

Fig. 5-14 Deterministic method VS Monte Carlo method

The concrete life obtained by the deterministic calculation method is longer than that based on the probability because the deterministic method neither considers the existence of the construction deviation of the concrete cover thickness nor introduces the failure probability. In essence, the deterministic method calculates the concrete life in an absolutely ideal state. Due to the deviation between actual engineering and theoretical design, it can be seen from the short board effect, the actual life of concrete will be shortened than the ideal life. Although the calculation accuracy of the deterministic method is insufficient, the calculation process of the method is simple and the calculation tools are easy to obtain. Fig. 5-14 gives the relationship between the deterministic method and the Monte Carlo method considering different construction quality levels:

$$M_{0.85} = 0.77D\text{-}4.78 \tag{5.16}$$

$$M_{0.95} = 0.85D\text{-}3.28 \tag{5.17}$$

With the above formulas, we can achieve further correction of the low-precision deterministic method.

The correction of the low-precision deterministic method can be achieved by the above formulas.

5.1.7.5.2 The influence of methods A and B on life span

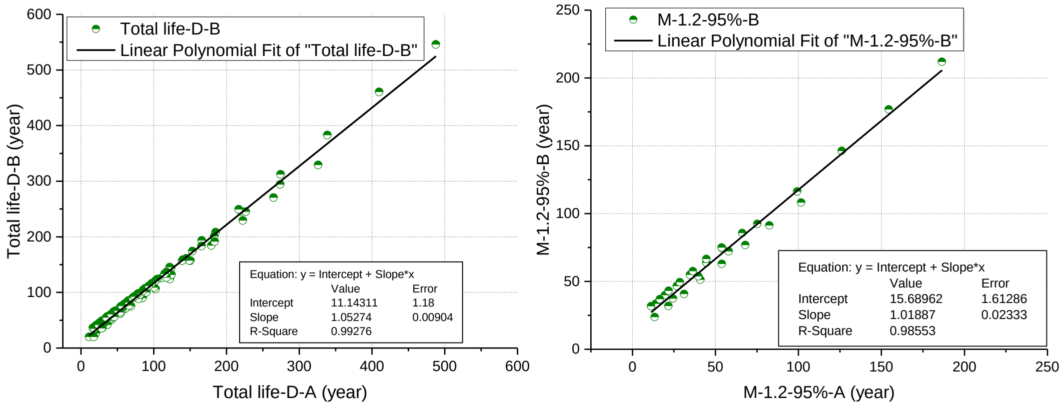

Fig. 5-15 Life relationship based on method A and B

Fig. 5-15 shows that the concrete life obtained by calculating method B is slightly longer than method A. Method A is equivalent to assuming that the characteristic parameters of the entire lifespan are equal to the test year, and Method B only assumes that the characteristic parameters after the test year to the end of the life are equal to the data of the test year. Obviously, the larger the test year, the closer the life calculated by the B method is to the real life of the concrete. However, Method A can reproduce the development state of chloride ion diffusion depth with the years before the test year and reproduce its history, which is of great reference for other projects.

In summary, for untreated concrete with the data of 20th year' as the calculation base, the estimated life of concrete calculated according to Method B should be closer to the actual life.

5.1.8 Conclusion

(a) The use of penetrants on the surface of concrete changes the diffusion law of chloride ions in ordinary concrete. To be precise, it postpones the enlightenment year that the chloride ion diffusion coefficient on the surface of concrete increases first and then decreases, thereby prolonging the service life of the concrete.

(b) The attenuation index of chloride ion diffusion coefficient cannot be unified into a numerical value, and it varies in space. For the concrete whose surface is impregnated, the attenuation index maybe is negative. It means that the chloride ion diffusion coefficient is increased, which should depend on which stage of service the treated concrete is in;

(c) Even if the dam has been serviced in the marine environment for 20 years, the diffusion of chloride ions of treated concrete may not have reached a stable state. Therefore, using the data at this time to estimate its life, The result is not exactly, and it is necessary to make corrections;

(d) During the service process of dams and other concretes, the chloride ion diffusion is constantly changing in time and space, and it takes a long time to reach a stable state. At the same time, it is not easy to estimate the life span by considering the time-space integral method. Therefore, when using the deterministic method to estimate life, the minimum assumptions should also be followed. The original data should be retained as much as possible to make data return to reality and close to nature—for example, method B in this article.

(e) In order to predict life more accurately, it needs to consider both Cos and Daps as variables in pairs when using Fick's second law. Field experimental data show that, in general, the Cos gradually increases and the Daps gradually decreases to a stable condition (In the typical case, without considering the concrete surface treatment measures).

(f) The life span between the treatment group and the treated groups should be in the established multiple relationships under the specified conditions and use environment. It is the numerical embodiment of the inherent properties of the resistance of these two groups to the external environment. The ideal calculation process should be to find the change function of each variable with time, and then establish the failure probability density function equation of t, and integrate the function equation. When the probability reaches the critical probability, the obtained t is the concrete life. However, It is challenging to establish the relationship between variables and time t through limited data. The simplified calculation process indicates that the instantaneous state of a particular year represents the state of change throughout the life cycle. Establishing the functional relationship between variables and time t is a breakthrough point in time engineering research.

5.2 Life Prediction Based On Carbonization

5.2.1 Overview

In the general atmospheric environment, the carbonization life of a concrete structure is one of the most direct manifestations of concrete durability. This section discusses the carbonization depth development model of reinforced concrete structures. It predicts the carbonization life of the Tomakomai flood dike under the ocean in severe cold areas through the impregnant treatment groups and the untreated groups.

5.2.2 Deterministic calculation method

5.2.2.1 calculation process

First, the deterministic calculation method is adopted. The idea is the same as the calculation of the life of concrete under chloride ion erosion. There is also the A method and B method.

Method A: Take the concrete carbonization coefficients obtained in the 12^{th} and 20^{th} years as their average carbonization coefficients for the entire life to calculate the total carbonization life of the concrete under different covers, minus the years of already service, and then the remaining life can get;

Method B: Take the carbonization coefficient of the test year as the carbonization coefficient of the subsequent remaining life years, and obtain the years in which the remaining protective layer thickness can be used continuously, then the remaining life plus the service life, and the total carbonization life can be obtained.

$$\text{From} \quad x = k\sqrt{t} \tag{5.18}$$

can derive into

$$t = \frac{x^2}{k^2} \tag{5.19}$$

Because carbonization is slower than chloride ion erosion, the cover here is only 10 ~ 90mm.

5.2.2.2 Result and discussion

5.2.2.2.1 Result

Calculate the total life and remaining life based on carbonization with A and B methods, respectively. The calculation results are summarized in Table 5-10.

Table 5-10 Service life based on carbonization

Group	Cover(mm)	Method A		Method B	
		T-total	T-Rest	T-total	T-Rest
Untreated-12 years: y_1 based on $k_{12\text{-}N\text{-}Mean}$ =0.986 mm/year$^{0.5}$	10	103	91	57	45
	20	411	399	295	283
	30	926	914	739	727
	40	1646	1634	1389	1377
	50	2571	2559	2244	2232
	60	3703	3691	3305	3293
	70	5040	5028	4572	4560
Treated-12 years: y_2 based on $K_{12\text{-}T\text{-}Mean}$ =1.746 mm/year$^{0.5}$	10	33	21	17	5
	20	131	119	76	64
	30	295	283	200	188
	40	525	513	390	378
	50	820	808	646	634
	60	1181	1169	967	955
	70	1607	1595	1354	1342
Untreated-12 years: y_3 based on $k_{12\text{-}N\text{-}Max}$ =1.732 mm/year$^{0.5}$	10	33	21	26	14
	20	133	121	104	92
	30	300	288	248	236
	40	533	521	458	446
	50	833	821	735	723
	60	1200	1188	1079	1067
	70	1633	1621	1490	1478
Treated-12 years: y_4 based on $k_{12\text{-}T\text{-}Max}$ =3.002 mm/year$^{0.5}$	10	11	-1	14	2
	20	44	32	34	22
	30	100	88	76	64
	40	178	166	140	128
	50	277	265	226	214
	60	399	387	335	323
	70	544	532	466	454

Untreated-20 years: y_5 based on $k_{20\text{-}N\text{-}Mean}$=1.118 mm/year$^{0.5}$	10	80	60	40	20
	20	320	300	200	180
	30	720	700	520	500
	40	1280	1260	1000	980
	50	2000	1980	1640	1620
	60	2880	2860	2440	2420
	70	3920	3900	3400	3380
Treated-20 years: y_6 based on $k_{20\text{-}T\text{-}Mean}$=1.859 mm/year$^{0.5}$	10	29	9	20	0
	20	116	96	55	35
	30	260	240	147	127
	40	463	443	298	278
	50	723	703	506	486
	60	1042	1022	772	752
	70	1418	1398	1096	1076
Untreated-20 years: y_7 based on $k_{20\text{-}N\text{-}Max}$ =2.012 mm/year$^{0.5}$	10	25	5	26	6
	20	99	79	76	56
	30	222	202	174	154
	40	395	375	323	303
	50	618	598	520	500
	60	889	869	767	747
	70	1210	1190	1064	1044
Treated-20 years: y_8 based on $k_{20\text{-}T\text{-}Max}$=3.030 mm/year$^{0.5}$	10	11	-9	20	0
	20	44	24	33	13
	30	98	78	68	48
	40	174	154	125	105
	50	272	252	203	183
	60	392	372	303	283
	70	534	514	425	405

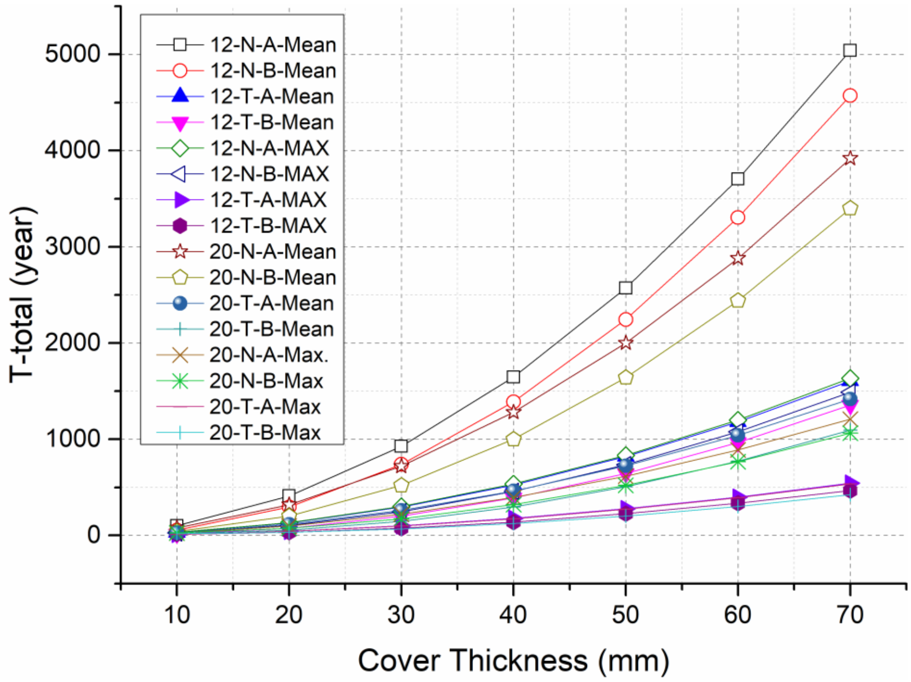

Fig. 5-16 Total service life VS cover based on carbonation action

It can be seen from Fig. 5-16 that the estimated life expectancy calculated based on the 12th year experimental data are much longer than that of other groups based on the 20th year for both treated groups and untreated groups. The largest one even reaches thousands of years. It is almost consistent with the conclusion that the complete carbonization process took a thousand-year proposed by previous scholars [125]. The reason may be that in the 12th year, the concrete surface has a depth of spalling. Due to the lack of carbonation-related data in previous years and the spalling depth of the 12th year, the carbonization coefficient has not been revised. The carbonization depth used in the calculation is smaller than the actual carbonization depth, which results in the obtained carbonization coefficient being too small so that the carbonization life becomes longer in further calculations. In addition, The carbonization life calculated by the B method is less than that obtained by the A method. In the calculation of the B method, the hypothetical data year is shorter. In theory, the B method is closer to the actual state. Therefore, it is more reliable to use the data based on the 20th year with the B method to calculate the carbonization life in a deterministic way.

5.2.2.2.2 Factors affecting carbonization life

The detailed discussion here is still only from whether the concrete surface penetrants are applied or not, the selection of the calculation based year, and the selection of the calculation methods.

① The influence of concrete surface penetrants on the concrete carbonization life

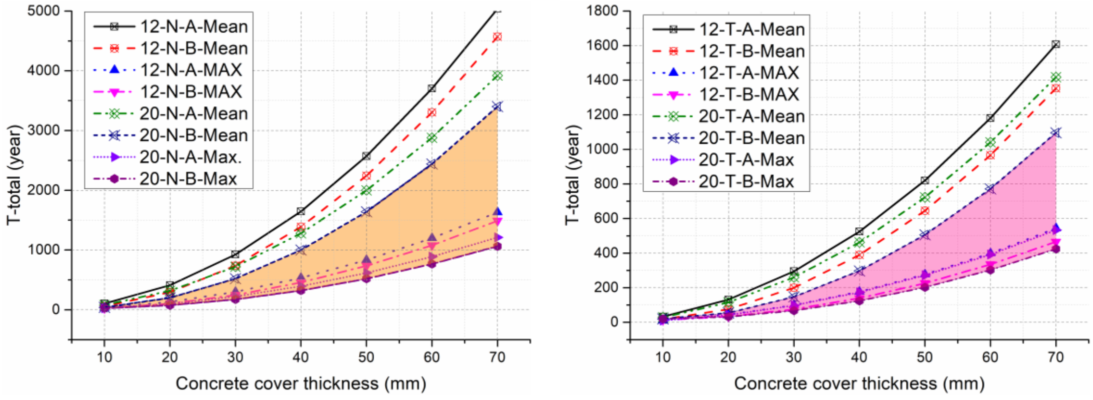

(a) Untreated group (b) Treated group

Fig. 5-17 carbonation life span

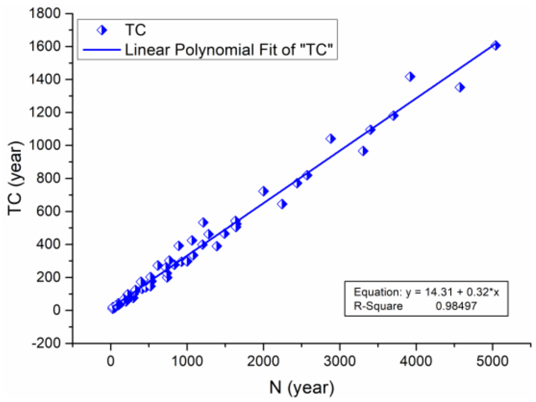

Fig. 5-18 The prolongation rate of concrete surface penetrants on concrete carbonation life

Fig. 5-17 (a) and (b) show the carbonation life of untreated and treated groups separately. Theoretically, the carbonization life of each group through different primary data and different calculation methods should be convergent near a specific value, which depends on the quality of the concrete and the service environment. However, the actual calculation results are pretty different.

According to the analysis in Fig. 5-16, it is determined in Fig. 5-17 that the minimum carbonization life obtained based on the *k-Mean* and *k-Max* under the B method is its life envelope of concrete (the colour-filled part in the figures). The minimum of *K-max* is the life when the front of carbonization depth reaches the surface of the steel bar, and the minimum of *k-Mean* is the life when most of the carbonization depth reaches the surface of the steel bar.

Fig. 5-18 indicates that after treatment, the carbonization life of concrete is only 0.32 times (32%) of the untreated groups. In the marine environment, the application of the compound penetrants will shorten concrete carbonization life. Still, even so, when the cover depth is about 50 mm, at the most unfavourable point (the carbonization coefficient is the largest ($k_{\text{-}T\text{-}20\text{-}Max}$=3.030 mm/year$^{0.5}$), and the carbonization develops the fastest), its carbonization life can be as long as a hundred years for treated groups. When the cover thickness reaches up to 70mm, it can reach about 425 years. Therefore, carbonization is not the key to determining its life. The corrosion of chloride ions is the shortboard of its life. In comparison, the use of impregnant can effectively prevent the intrusion of chloride ions and prolong its life in a salt-freeze corrosion environment to about 1.6 times the original life. Combining these two aspects, the use of impregnant ultimately prolongs the life of the concrete.

② Selection of calculation based year

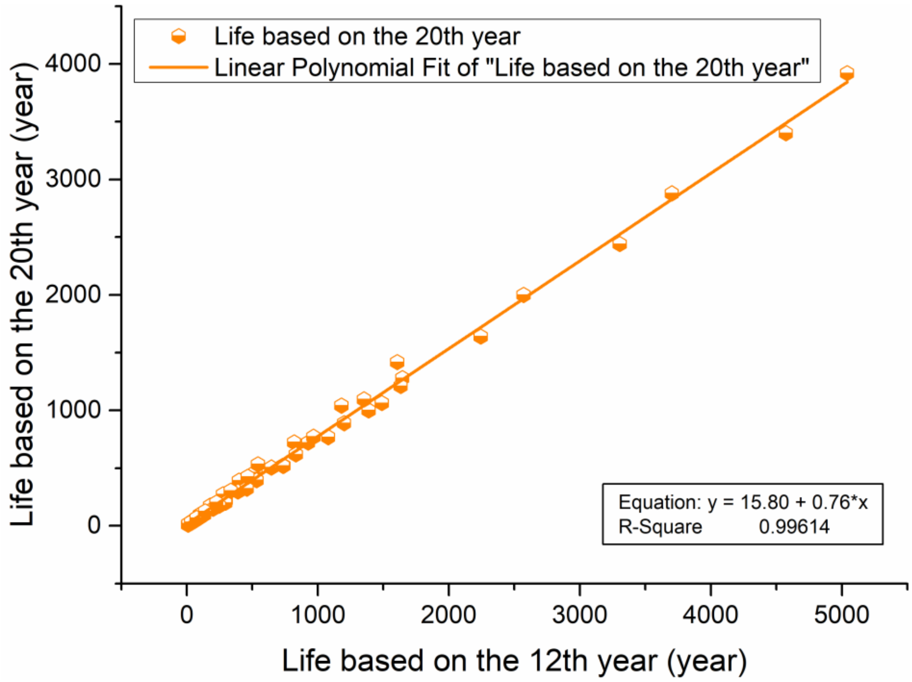

Fig. 5-19 The relationship between the T_{20tot} and T_{12tot} (carbonation action)

Fig. 5-19 shows that the estimated life of concrete carbonization based on the primary data of the 20th year is approximately 0.76 times that based on the primary data of the 12th year. Carbonation data collected about the 10th year can be used in the future to use this relationship (formula 5.20)for more accurate life prediction and correction.

$$T_{20} = 15.80 + 0.76 T_{12} \qquad 5.20$$

③ The influence of calculation method on carbonization life

The previous figures show that the estimated life calculated by method A is more significant than that obtained by method B. The relationship between them is shown in Fig. 5-20. The life span based on method B is about 0.89 times that of method A.

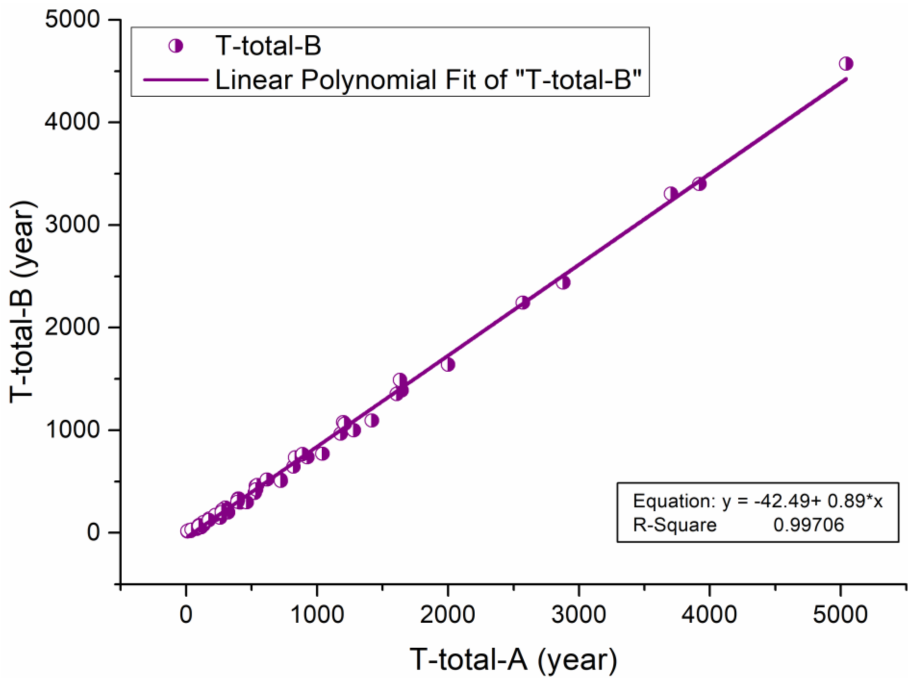

Fig. 5-20 The relationship between method A and method B (carbonation life)

5.2.3 Calculation method based on reliability

5.2.3.1 Calculation process

Thinking framework for calculation.

① Determine the failure criteria and evaluation criteria of concrete materials. The reliability index β corresponding to the carbonization depth exceeding the concrete cover is less than 1.5 as the criterion.

② Establish a model for the degradation of concrete materials' carbonization life——the degradation of effective protective layer thickness.

③ Calculate the statistical parameters of concrete resistance (cover) and corrosion factors (carbonization depth, carbonization coefficient).

④ Use the principle of stepwise search to determine a reasonable step length to calculate dynamic reliability

⑤ The reliability index limit β is 1.5. When the reliability is less than 1.5, the calculated T is the rest life of the structure.

The specific calculation process is as follows:

It is assumed that the depth of carbonization development $N(\mu_X, \sigma_X)$ and the cover $N(\mu_C, \sigma_C)$ obey the standard normal distribution.

$$f_x(x,t) = \frac{1}{\sqrt{2\pi}\sigma_x(t)} \exp\left\{-\frac{\left[x-\mu_x(t)\right]^2}{2\left[\sigma_x(t)\right]^2}\right\} \quad 5.21$$

$\mu_x(t)$ Expected value function of concrete carbonization depth;

$\sigma_x(t)$ Variance function of concrete carbonization depth;

Here, the means and standard deviations of experiments from test year are taken as their values, expressed by $\mu_0(t)$ and $\sigma_0(t)$

From $$\mu_0(t) = k\sqrt{t} \quad 5.22$$

can derive into $$k = \frac{\mu_0}{\sqrt{t}} \quad 5.23$$

Coefficient of Variation $$v = \frac{\sigma_0}{\mu_0} \quad 5.24$$

Then the carbonization depth in year t: $$\mu_x(t) = k\sqrt{t} \quad 5.25$$

Standard deviation in year t: $$\sigma_x(t) = v\mu_x = vk\sqrt{t} \quad 5.26$$

The probability that the carbonation depth exceeds the concrete cover (the steel bars may corrode) can be expressed as $$P_{f_c}(t) = P\left\{c - vk\sqrt{t} < 0\right\} \quad 5.27$$

The reliability index can be expressed as:

$$\beta = -\Phi^{-1}\left(P_{f_c}\right) \tag{5.28}$$

The concrete cover still considers the variances σ_C of 9.648mm (when the allowable construction deviation is less than 10mm, the construction guarantee rate is 85%) and 6.079mm (when the allowable construction deviation is less than 10mm, the construction guarantee rate is 95%).

The thickness of the concrete cover is still progressively 10mm, ranging from 10mm to 90mm.

The carbonation depth and concrete cover can be considered two independent normal distributions, so:

$$\beta = \frac{\mu_c - \mu_x}{\sqrt{\sigma_c^2 + \sigma_x^2}} \tag{5.29}$$

The untreated groups have been calculated based on the 12th year data, and the treated groups have been calculated based on the 20th year data. Calculate the downward trend of their reliability indicators β over the years.

Use the principle of step-by-step search to determine a reasonable step length and calculate the

Depending on the concrete cover, the increment step distance t_n (year) can be adjusted appropriately. For example, if the concrete cover is small, it can be increased by 20 years. When the concrete cover is large, it can be increased by 50 years or even 100 years. By this, the range interval of reliability 1.5 can be quickly reached. Then take $t_n/2$, $t_n/4$, $t_n/8$ ..., or even one year as steps in the interval range until the reliability index is lower than 1.5. The maximum value of the year when β is greater than or equal to 1.5 is the estimated carbonization life of concrete under this condition.

5.2.3.2 Result and discussion

5.2.3.2.1 Result

The decrease of reliability index β with the number of years under carbonization condition is shown in Fig. 5-21. It can be seen from the figure that the decay rate is first fast and then slow, which is consistent with the slowdown of the diffusion of carbon dioxide in the concrete year by year, and the carbonization effect has also been weakened year by year.

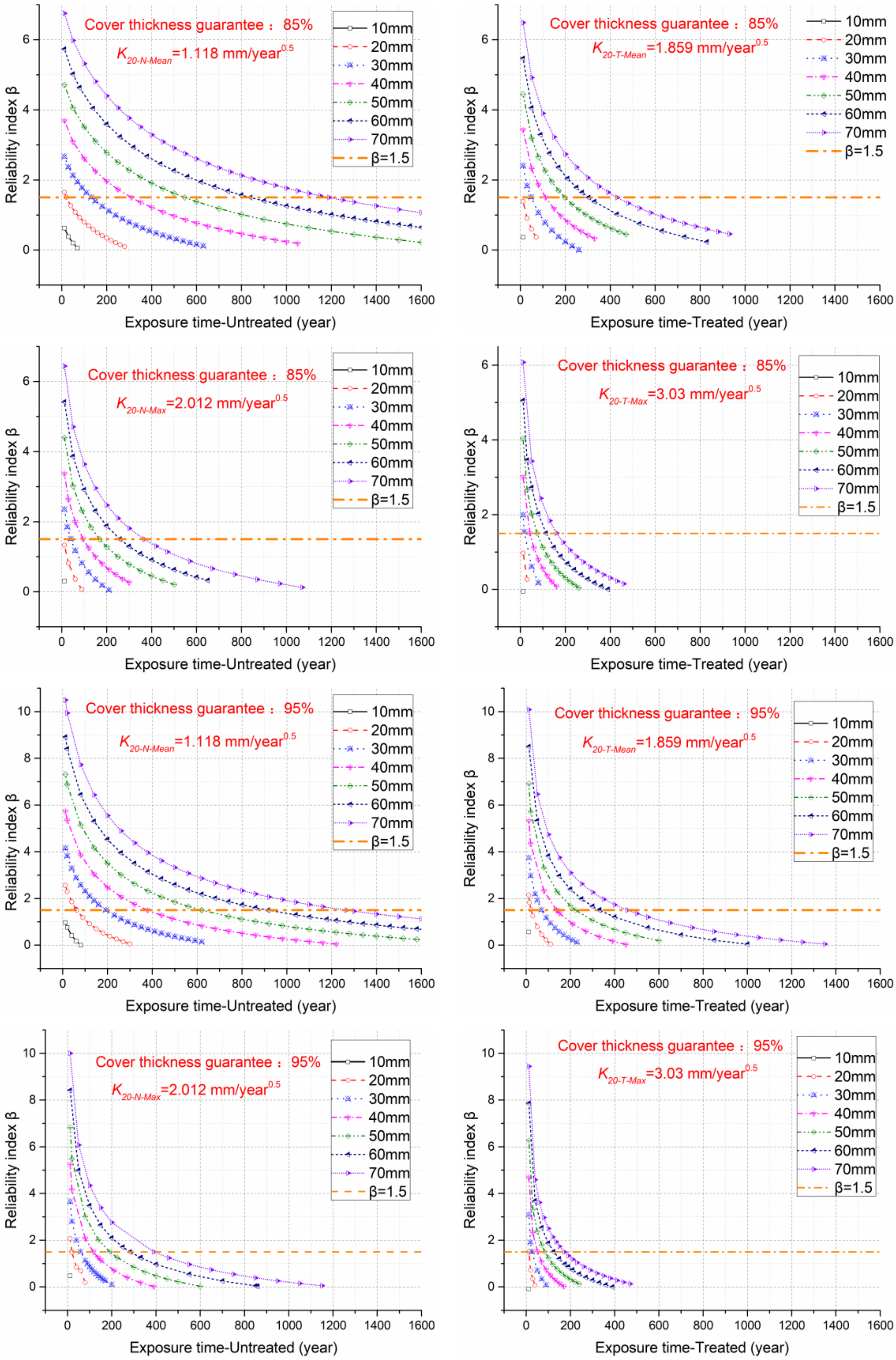

Fig. 5-21 Reliability decays over the years

Note: N means untreated group; TC means treated group.

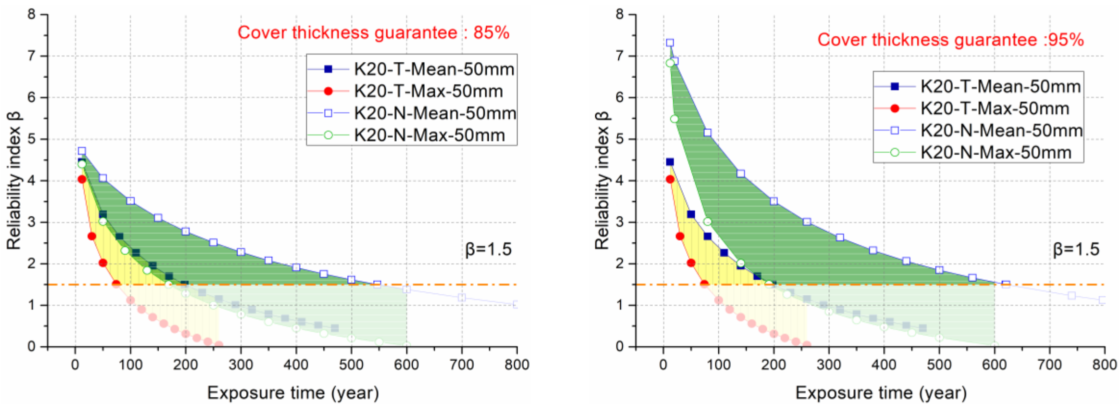

(a) 85%

(b) 95%

Fig. 5-22 Carbonization life range

Fig. 5-22 shows the carbonization life range of the concrete with 50mm cover depth under the condition of 85% and 95% of cover thickness guarantee, separately. It can be seen that the life span zone of the treatment group (yellow filled part above β=1.5) is the bottom left direction of the untreated group (green filled part above β=1.5). Being left means when the reliability index is the same, such as β=1.5, the life of the treatment group is shorter than that of the untreated group; down means that when the service life is the same, the reliability index of the treatment group is lower than that of the untreated group. Comparing figures (a) and (b), the 95% group is better than the 85% group.

The intersection of the reference line β=1.5 and each curve in the figures are the estimated total carbonization life of the concrete. The total life of concrete carbonization under various conditions is summarized in Table 5-11.

Table 5-11 Total carbonization life (year)

	Cover (mm)	$k_{20\text{-}N\text{-}Mean}$=1.118 mm/year$^{0.5}$	$k_{20\text{-}T\text{-}Mean}$=1.859 mm/year$^{0.5}$	$k_{20\text{-}N\text{-}Max}$ =2.012 mm/year$^{0.5}$	$k_{20\text{-}T\text{-}Max}$=3.030 mm/year$^{0.5}$
Cover thickness guarante : 85%	10	< 12 (0.63)	< 12 (0.36)	< 12 (0.31)	< 12 (-0.05)
	20	20	< 12 (1.39)	< 12 (1.33)	< 12 (0.97)
	30	131	47	40	17
	40	310	112	95	42

	50	547	198	169	74
	60	840	304	259	114
	70	1189	430	367	161
Cover thickness guarante : 95%	Cover (mm)	$k_{20\text{-}N\text{-}Mean}$=1.118 mm/year$^{0.5}$	$k_{20\text{-}T\text{-}Mean}$=1.859 mm/year$^{0.5}$	$k_{20\text{-}N\text{-}Max}$ =2.012 mm/year$^{0.5}$	$k_{20\text{-}T\text{-}Max}$=3.030 mm/year$^{0.5}$
	10	< 12 (0.97)	< 12 (0.57)	< 12 (0.48)	< 12 (-0.08)
	20	62	22	19	12
	30	192	69	59	26
	40	379	137	117	51
	50	620	224	191	84
	60	916	331	283	124
	70	1266	457	390	172

Note: < 12 (0.63) means the carbonization life is smaller than 12 years, and in the 12th year, the reliability index β is 0.63.

5.2.3.2.2 Factors affecting carbonization life

① The influence of concrete surface impregnant on the carbonization life of concrete

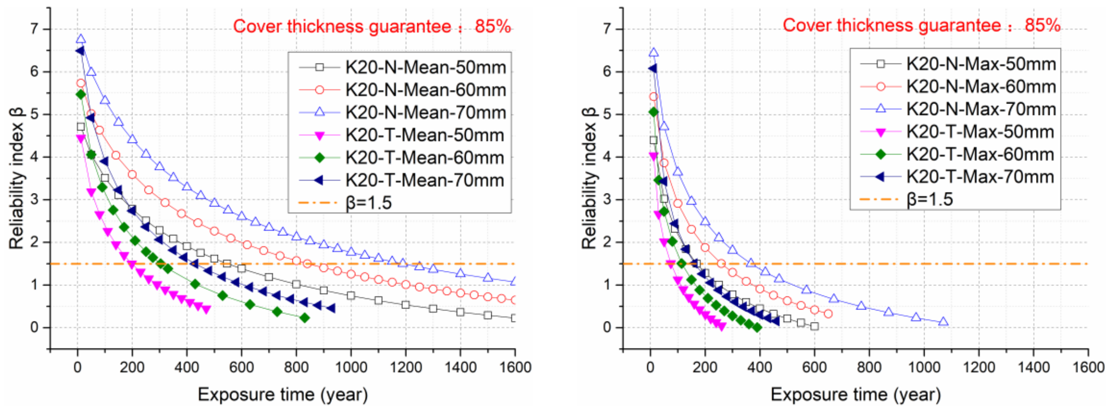

(a) $K_{\text{-}20\text{-}Mean}$ (b) $K_{\text{-}20\text{-}Max}$

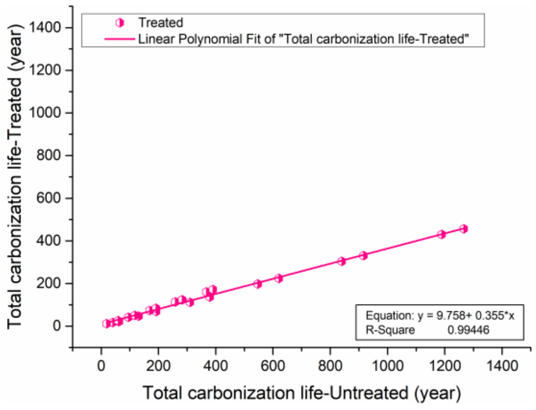

(c) Treated groups VS untreated groups

Fig. 5-23 Influence of impregnant on the carbonization life of concrete

Comparing the attenuation speed of the treated groups and the untreated groups with the concrete cover of 50mm-70mm, Fig. 5-23 (a) and (b) show that the treated groups have a faster carbonation attenuation (more significant absolute value of the slope) than the untreated groups. It is determined by the unique hydrophobic and air permeability characteristics of the impregnant materials brushed on the concrete surface.

Fig. 5-23 (c) shows that the total carbonization life of groups applied with penetrants is about 0.36 of the untreated groups with an intercept of 9.758. In the deterministic calculation method, It is 0.32 and with a more significant intercept of 14.31. Therefore, the relationship between them calculated by the two methods is almost consistent.

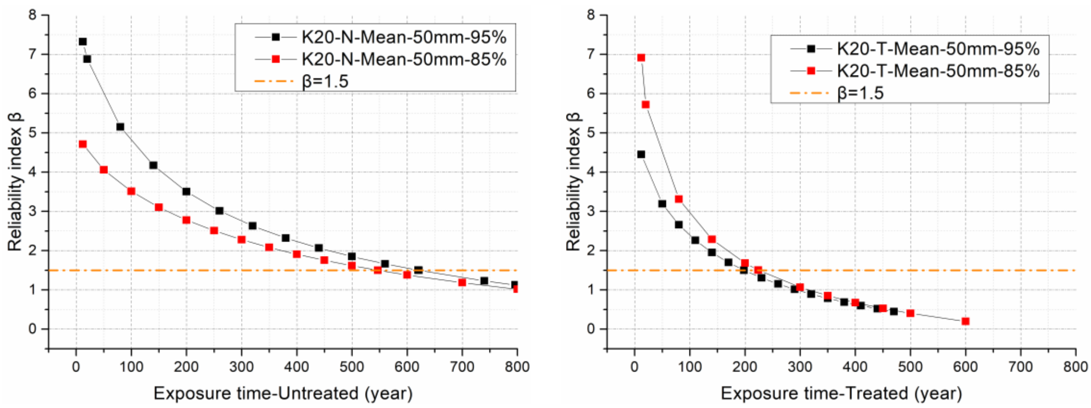

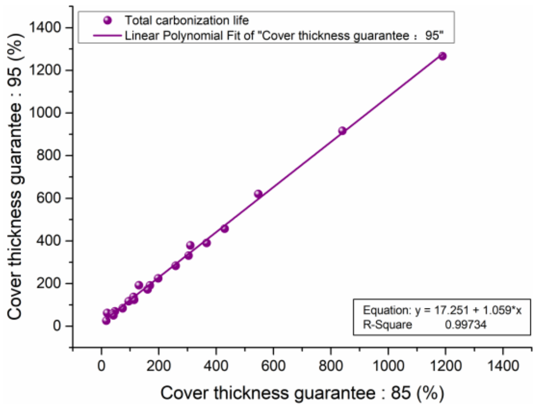

Fig. 5-24 The influence of concrete cover thickness guarantee rate on carbonization life

If the construction quality improves, the probability of the concrete cover construction deviation of 10mm is reduced from 15% to 5%; the guaranteed rate is increased from 85% to 95%. At this time, the concrete carbonization life will be significantly improved. The total carbonization life of the concrete can be prolonged at least 17.25 years and 1.1 times. It can be seen that improving the quality of construction is also one of the effective means to extend the life of concrete.

5.2.4 Monte Carlo Method

Based on section 5.2.3, this section considers the statistical distribution of each variable in life prediction as much as possible, using the Monte-Carlo calculation principle and crystal-ball software to calculate the life of the concrete.

Here, the untreated groups are also based on the 12th year of experimental data, and the treated groups are also based on the 20th year of experimental data.

The detailed calculation steps are described as follows:

① Determine the characteristic distribution parameters of each variable according to experimental data and historical experience data referring to sections 5.2.3 and 5.1.4. See the summary in Table 5-12.

② According to the life expectancy criterion (5.30), Establish a calculation sheet of the life prediction model in excel.

$$P_{f_c}(t)=P\left\{c-k\sqrt{t}<0\right\}=\Phi(-\beta)=\Phi(-1.5)=6.681\% \qquad 5.30$$

The next steps are completed under the crystal-ball plug-in in Excel:

③ Start crystal-ball and open the above Excel sheet. Click the crystal-ball plug-in button.

④  Define Assumptions. input Random variables. The carbonization depth and the concrete cover are defined as hypothetical variables. They conform to the normal distribution, which is consistent with the previous section.

⑤  Define decision parameters, input decision parameters. Set the estimated total life of concrete as a decision-making parameter, and limit the scope of decision-making parameters.

⑥ 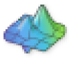 Perform the OptQuest operation. Set the β=1.5 as the target value, set the number of simulations 1000 times, and perform the first calculation. The calculation process finds that the "best solution" is generally around 300 calculations.

⑦ Summarize the total life of concrete in Table 5-13 and Fig. 5-25.

The most significant difference between this method and the reliability-based method in section 5.2.3 is:

a) The carbonation depth and the concrete cover are considered variables in the calculation process. The carbonation coefficient is also considered a variable; it is affected by the fluctuation range of the concrete carbonization depth in the test year, while Section 5.13 is considered a fixed value.
b) The calculation principle and formula are simple, dramatically reducing the calculation workload by computerizing the process instead of manually approaching the target and have more accurate results.
c) It is more consistent with the actual situation than the previous methods.

Table 5-12 List of critical parameters

<table>
<tr><td rowspan="3">Groups</td><td colspan="3">Random variables</td><td colspan="3">Decision parameters</td></tr>
<tr><td rowspan="2">Measured carbonization depth dc</td><td colspan="2">Cover thickness dc</td><td colspan="3">Total life</td></tr>
<tr><td>85%</td><td>95%</td><td>Lower limit</td><td colspan="2">Upper limit</td></tr>
<tr><td>Untreated</td><td>dc20 : N(8.316, 3.782)</td><td>N(10～90,9.65)</td><td>N(10～90,6.079)</td><td rowspan="2">0</td><td colspan="2" rowspan="2">$t=\left(\frac{d_c}{k}\right)^2$</td></tr>
<tr><td>Treated</td><td>dc20 : T(8.784, 4.162)</td><td>N(10～90,9.65)</td><td>N(10～90,6.079)</td></tr>
<tr><td rowspan="3">Groups</td><td colspan="2">Forecast value</td><td colspan="4">Other calculation parameters</td></tr>
<tr><td rowspan="2">Formula</td><td rowspan="2">OptQuest</td><td rowspan="2">k (mm/year$^{0.5}$)</td><td colspan="3">Characteristic value of carbonization depth in any year (t year)</td></tr>
<tr><td>$\boxed{\mu_x(t)}$</td><td>$\boxed{\sigma_x(t)}$</td><td>$\boxed{v}$</td></tr>
<tr><td>Untreated</td><td rowspan="2">$\beta=\frac{\mu_c-\mu_x}{\sqrt{\sigma_c^2+\sigma_x^2}}$</td><td rowspan="2">β=1.5</td><td>$k_{20\text{-N-Mean}}$=1.18</td><td rowspan="2">$\mu_x(t)=k\sqrt{t}$</td><td rowspan="2">$\sigma_x(t)=v\mu_x=vk\sqrt{t}$</td><td>0.455</td></tr>
<tr><td>Treated</td><td>$k_{20\text{-}T\text{-}Mean}$=1.859</td><td>0.474</td></tr>
</table>

Table 5-13 List of total service life based on Monte-Carlo

cover	Guarantee rate of cover thickness			
	85%		95%	
mm	Untreated (k=1.18)	Treated (k=1.859)	Untreated (k=1.18)	Treated (k=1.859)
10	0 (1.03)	0 (1.03)	0.23	0.18
20	7.72	6.89	25.52	22.70
30	52.25	45.39	88.44	79.08
40	134.88	118.39	193.84	171.10
50	254.89	232.29	338.81	313.86
60	431.40	376.99	549.58	486.15
70	621.18	560.40	767.90	700.20

Notes:

- 0(1.03) means if the concrete cover is only 10mm, due to uncertain factors such as construction deviation, as soon as the construction is over (0 year), the β is 1.03, which is smaller than 1.5.

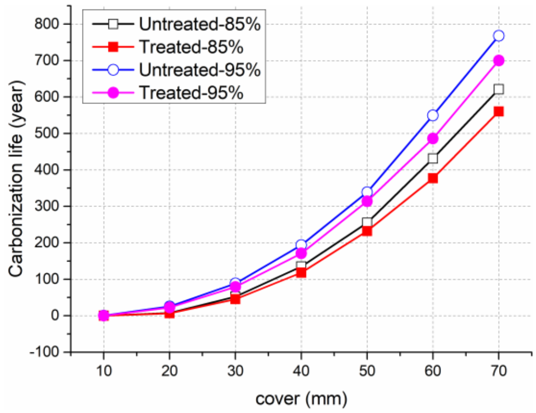

Fig. 5-25 Carbonization life VS concrete cover thickness calculated by Monte-Carlo method

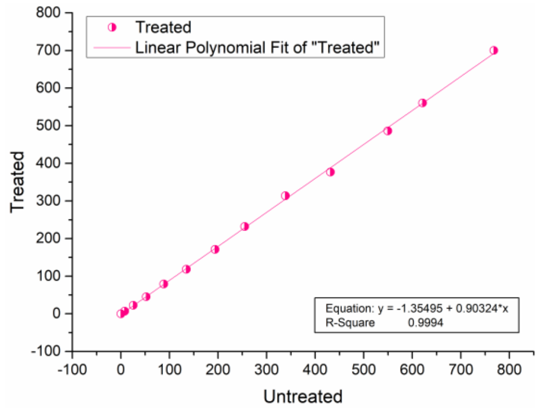

Fig. 5-26 Treated groups VS untreated groups by Monte-Carlo method

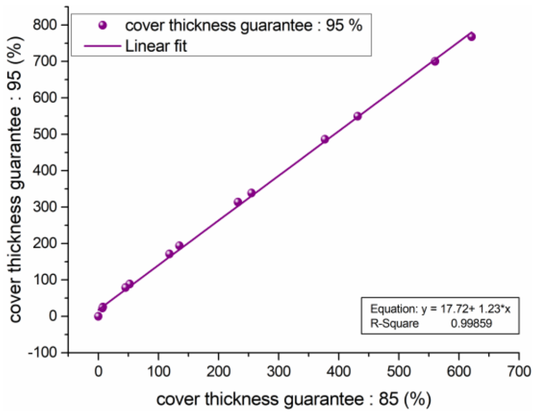

Fig. 5-27 The influence of concrete cover thickness guarantee rate on carbonization life by Monte-Carlo method

Fig. 5-25 shows that for ordinary concrete without surface treatment when the cover reaches 50 mm, its carbonization life can reach 254 years. For vital infrastructures such as dams, the designed target life is long, and the durability requires high, so the concrete cover is often more than 50mm.

After the impregnants are treated, the concrete life under freeze-thaw and chloride ion erosion is prolonged, and the carbonization life is shortened. Nevertheless, the carbonization life of the concrete can be at least 232 years when the concrete cover is 50mm, which is enough for the target year. The life of Tomakomai Dam is ultimately determined by the service life calculated based on chloride ion and freeze-thaw erosion. From the results, it is worth sacrificing part of the carbonization life to improve the resistance to salt-freeze-thaw erosion.

The life of the treated group is about 0.90 times that of the untreated group (Fig. 5-26), which is larger than the previous two methods. The other reason may be that the probability distribution of carbonization depth is not considered in the first two calculations. When *k-mean* and *k-max* are considered simultaneously in the calculation process, it is equivalent to thinking that the two appear with equal probability, which is somewhat different from the fact that the small probability of *k-max* appears. The distribution of the carbonization coefficient is indirectly defined by defining the normal distribution of the carbonization depth in the Monte Carlo method. It agrees with the actual situation.

5.2.5 Comparison of different methods and conclusions

Here is a comparison of the concrete carbonization life calculated under three different methods (see Fig. 5-28).

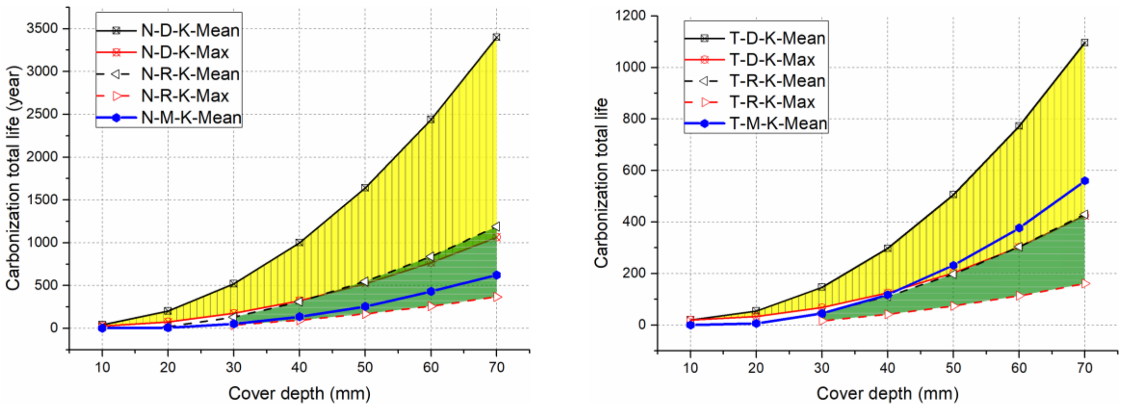

(a) Untreated groups (b) Treated groups

Fig. 5-28 Summary of predicted life of each method

Notes:

① D: Deterministic calculation method; R: Reliability index method; M: Monte Carlo method.

② In untreated groups : $k_{\text{-}Mean}$=1.118 mm/year$^{0.5}$， $k_{\text{-}Max}$ =2.012 mm/year$^{0.5}$;

③ In treated groups: $k_{\text{-}Mean}$=1.18 mm/year$^{0.5}$， $k_{\text{-}Max}$ =1.859 mm/year$^{0.5}$;

④ The Reliability index method and Monte Carlo method only consider the case where the guarantee of cover thickness is 85%, which is more unfavourable than the groups of 95%.

The length order of life calculated by the three methods is: Deterministic calculation method>Based on Monte-Carlo≈Based on reliability (Fig. 5-28). The total carbonization life obtained by the deterministic calculation method is several times that of the latter two methods. The reason is that the deterministic method actually is the carbonization life when the reliability β is 0, corresponding failure probability is 50%; while the other two methods which based on the reliability index β=1.5, corresponding to the failure probability is only 6.68%; the failure probabilities of them are far different.

In addition, in terms of the thickness of the concrete cover, the deterministic method did not consider the fluctuation of the cover thickness caused by the construction, and the calculation result was too ideal. Although the deviation was considered in the reliability calculation method, the calculation accuracy was insufficient. The Monte Carlo method can define the thickness distribution of the concrete cover and simulates thousands of calculations to obtain the high probability distribution life value of the concrete life.

- Comparison of the advantages and disadvantages of the three calculation methods

In the calculation method of certainty and reliability, in order to consider the most unfavourable situation (the shortest concrete life) and calculate the concrete carbonization life under the average carbonization coefficient, the situation when the carbonization coefficient is the largest is also calculated. The final result is a set of Carbonization life span. The Monte Carlo calculation method considers the distribution of carbonization depth in the calculation process, which is equivalent to considering the various possibilities of the carbonization coefficient. Therefore, it is only necessary to calculate the case of k_{Mean}. In addition, the calculation process is entirely computerized, which can simulate thousands of carbonization possibilities in a short time and finally get a more accurate concrete life, which significantly reduces the amount of calculation and the calculation process and calculation results are much more accurate. The result calculated by Monte Carlo is a specific value that is more instructive in the actual concrete maintenance and decision-making process.

The deterministic method: The amount of data collected is small, and the calculation idea is simple. At first glance, there are the fewest assumptions in the calculation process, and all the data are uniquely determined. It seems to be the closest to the truth, but it ignores the large discreteness of concrete materials. Moreover, During construction, the thickness of the concrete cover is difficult to control accurately, and the carbonization depth distribution is random. Therefore, it does not have the guiding significance of actual maintenance. It is not recommended to use in the carbonization life calculation process.

The calculation based on the reliability method is a little clumsy, but its advantage is that there is no need to learn and use professional analysis software Crystal Ball. If there is no professional Crystal Ball software, this method can be regarded as a reliable method.

Although the calculation method based on reliability considers the distributions of carbonization depth and concrete cover, it does not consider the time-varying properties of the carbonization diffusion coefficient. The Monte-Carlo method considers various variables' distribution and time-varying properties and has the highest calculation efficiency. It is recommended first.

After the concrete surface is applied with impregnant, the carbonization process is accelerated due to the water-repellent and breathable effect of the impregnant, and the total carbonization life of the concrete is shortened. The total carbonization life of concrete in the treatment group is shorter than that of the untreated group. However, the carbonization of the untreated group develops very slowly. Their carbonization life is hundreds of thousands. Therefore, even the carbonization life is reduced after applying the impregnant, but it can still meet the long carbonization life. This adverse effect is negligible. Its advantage is that after application, it can significantly improve the salt-freezing-thawing corrosion resistance of concrete. Under a severe cold ocean environment, chloride ion erosion, freezing, and thawing are the shortcomings of concrete life.

The study in literature [126] also shows that silanes will accelerate the progress of neutralization under certain circumstances. However, at the same time, it should also be considered that the water repellency of silane can inhibit the corrosion current and play a positive role in protecting the corrosion of steel bars.

5.3 Life Prediction Based On Salt-Freeze-Thaw Damage

5.3.1 Climatic characteristics of frost damage in Tomakomai

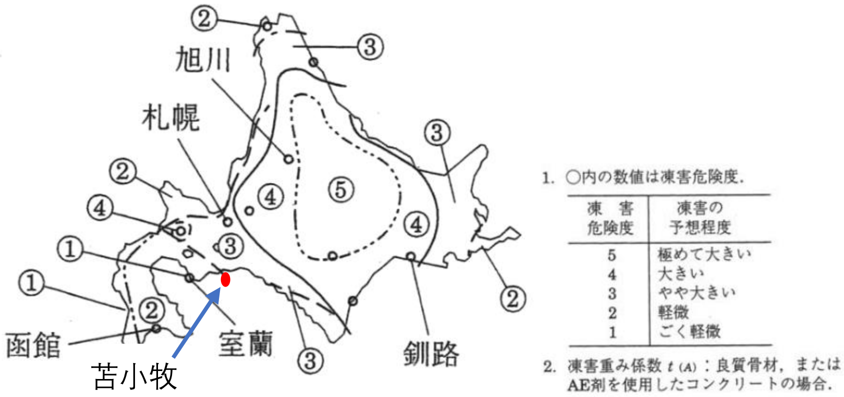

Fig. 5-29 Frost damage risk distribution map Hasegawa version [127]

Fig. 5-29 shows the exposure experiment location of Tomakomai. Scholar Hasegawa proposes the frost damage risk value shown in Eq. 5.31 [127]as an index showing the risk of frost damage calculated from temperature, solar radiation, etc. Precipitation based on five years (1965-1970) [128]of meteorological statistics in 1975.

$$V_F = \{(FT + F \times u) \times t + I\} \times c \qquad 5.31$$

Where

VF: Freezing damage risk value

FT: Freezing and thawing days at outside temperature

F: Number of days frozen at outside temperature

u: Melting rate due to solar radiation on days when the temperature remains frozen due to outside temperature

t: Freezing damage weighting coefficient due to temperature change

I: Correction value of frost damage temperature considering the lowest temperature of the day as statistical on the outside temperature

c: Frozen damage reduction coefficient depending on the degree of wetness

Then, as shown in Table 5-14, the frost damage risk values are divided into six stages and graded as frost damage risk levels 0 to 5.

Table 5-14 Frost damage values and frost damage risk degree [127]

Frost damage value	Frost damage risk	Anticipated degree of frost damage
~ 200	0	—
201 ~ 500	1	Very slight
501 ~ 800	2	slight
801 ~ 1100	3	a bit severe
1104 ~ 1400	4	Severe
1401 ~	5	Very severe

The Frost damage risk of Tomakomai is three, it is a bit severe.

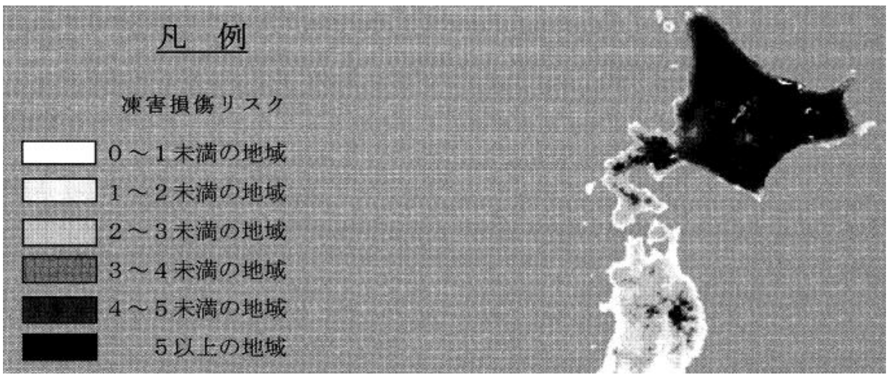

Fig. 5-30 Frost damage risk distribution map Saito vesion（a pat of ） [129]

Based on the calculation method proposed by scholar Hasegawa，in 2008, scholars Ken Narita et al.

carried out further calculations on the national freezing damage degree based on the meteorological data for 30 years from 1971 to 2000 accuracy of 1 square kilometer. The freezing damage degree is shown in Fig. 5-30. According to this version of the definition, Tomakomai's frost damage degree is between 4-5. However, scholars still used to cite the scholar Hasegawa version when researching.

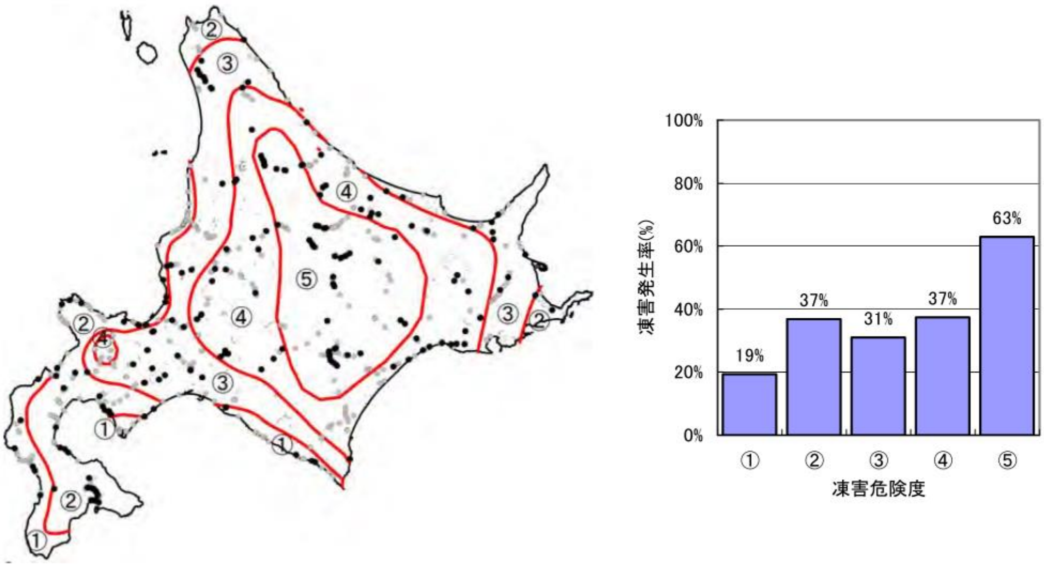

図 2.3.6　凍害危険度と凍害発生率

Fig. 5-31 The degree of frost damage and the probability of frost damage

Hokkaido Civil Engineering Society Concrete Research Committee conducted a frost damage survey on 800 bridges in the Hokkaido area and obtained the relationship between the degree of frost damage and the probability of frost damage as shown in Fig. 5-31 [121][2-47]. According to this, the probability of frost damage in Tomakomai Dam is 31%.

According to the meteorological statistics for ten years in literature[130], 99 times of freezing and thawing in Tomakomai per year.

5.3.2 Scaling and life prediction

5.3.2.1 Scaling prediction based on rapid salt-freeze-thaw experiments of ASTM C672 in the laboratory for untreated groups

Using formula 5.32 and the corresponding prediction program Fig. 2-7, predict and analyze the rapid indoor freezing and thawing experiments of Tomakomai dam at the 3rd, 12th, and 20th years.

$$D_m = ae^{b\log\frac{t}{A}} \tag{5.32}$$

Here n_{cycle} is used instead of t, where D_m is expressed as the scaling amount, in g/cm^2, recorded as D_{msc}.

The forecast formulas corresponding to the data of each year are shown in Table 5-15.

Table 5-15 Prediction of Freeze-thaw Scaling of the Untreated Groups in lab

Groups	N@3	N@12	N@20
Prediction formula	$D_{msc} = 48.2e^{1.48\log\frac{n_{cycle}}{25}}$	$D_{msc} = 23.8e^{2.05\log\frac{n_{cycle}}{40}}$	$D_{msc} = 0.03e^{1.57\log\frac{n_{cycle}}{40}}$
a	48.2	23.8	0.03
b	1.48	2.05	1.57

Notes: N means Untreated groups.

Since the service environment of Tomakomai Dam is relatively stable year by year, the scaling of the concrete from the first year can be predicted by these formulas. The number of indoor freeze-thaw cycles that it can withstand can be calculated according to the given limit D_{msc} and year. The relationship between the number of indoor freeze-thaw cycles and the annual freeze-thaw cycles of the natural environment is the key to predicting the life span of freeze-thaw scaling.

Here, the unit D_{msc} is g/cm^2. In order to establish an equivalent relationship between the laboratory and the natural environment salt-freeze-thaw cycles, it needs to be unified into the degree of freezing and thawing D_{mdep} in mm following the on-site prediction formula.

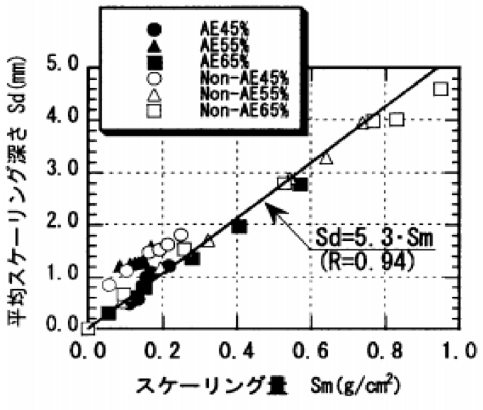

Fig. 5-32 Average scaling depth VS scaling amount [131]

It can be seen from Fig. 5-32 that the relationship between the average scaling depth scaling amount has nothing to do with the concrete mix ratio. Therefore, it shows that the conclusion obtained in this literature is universal. Here it is quoted to perform the above-mentioned required transformations.

Replace the mean scaling depth sd in Fig. 5-32 with D_{mdep} and D_{msc} instead Sm in this thesis. (Assuming when it is the average scaling degree, the scaling area ratio is 100%, so the scaling depth equals the scaling degree. It may lead to being a slightly larger situation than the actual one.):

$$D_{mdep} = 5.3 D_{msc} \quad 5.33$$

Substitute formula 5.33 into the three formulas in Table 5-15, the following three prediction formulas get:

N@3 $\quad D_{mdep} = 255.46 e^{1.48 \log \frac{n_{cycle}}{25}} \quad$ (a)

N@12 $\quad D_{mdep} = 126.14 e^{2.05 \log \frac{n_{cycle}}{40}} \quad$ (b)

N@20 $D_{mdep} = 0.159e^{1.57\log\frac{n_{cycle}}{40}}$ (c) 5.34

5.3.2.2 Scaling and prediction in Tomakomai marine environment for untreated groups

First of all, determining the cumulative scaling depth of a specific year is the key to predicting the on-site concrete freeze-thaw. Since this project did not collect the scaling depth in the field, we refer to the studies of predecessors in similar conditions: such as the Tomakomai Project or other similar projects with close freezing-thawing cycles per year, Similar material composition such as close water-to-binder ratio, close air content, or extensive samples statistics with universal significance, and combined with photos collected in the 12th and 20th year of this project, and carbonization calculation data, to determine the scaling depth in a specific year.

Table 5-16 Reference list of scaling depth in the natural environment

Location/Reason for Selection	Year of construction	Test year	Year past	Scaling degree mm	Cement type	w/c or Cement weight/ m^3	Air content	Literature source
苫小牧防波提 岸壁/同环境	昭和 53 年	昭和 54 年 7-8 月	1	0.1-0.4 取 0.1	-	-	-	[132]
北海道地区文献图 2 及图 7 中 Q 桥/冻结溶解次数接近（97）	2016	2018	2	≈0.25	NP	55%/264	4.6	[133]
E 中 参考表 2/同环境	-	-	12	Mean 0.5				[69]

钏路港北防波堤	昭和 62 年	2005	18	4.3	BB	-	-	[134]
苫小牧东港区中防波堤F部 胸壁/本工程	2000	2020	20	4.067+0.4=4.47	N	-	-	This thesis formula 4.4

It can be seen from the collected photos that the entire area (100%) has been peeled off at the 20^{th} year, so the scaling degree is equal to the scaling depth.

Enter the above year and the corresponding scaling degree into the forecasting program, and the forecast formula is as follows:

$$D_{mdep} = 1.31e^{2.62\log\frac{t}{10}} \qquad 5.35$$

Formula 5.35 is only applicable to the estimation of the life of untreated concrete.

5.3.2.3 Life Estimated for untreated groups

It is still assumed that the scaling area accounts for 100% of the test area, and the scaling degree is equal to the scaling depth. Substitute the four levels of allowable scaling into the formula 5.35, The relationship between the maximum allowable scaling and service life can be obtained as shown in the following Table 5-17.

Table 5-17 Service life at allowable scaling degree

Allowable scaling degree（mm）	2.50	5.00	10.00	20.00
service life	17.65	32.45	59.67	109.73

5.3.2.4 Scaling and life prediction for all the groups

Calculate the scaling depth in the marine environment of the treated groups.

Fig. 5-33 Calculation diagram of aggregate exposure rate

Fig. 5-33 uses the software Image-Pro Plus to calculate the aggregate exposure rate of the treated group concrete in the 20th year, and the aggregate exposure rate is 2.03%<10%.

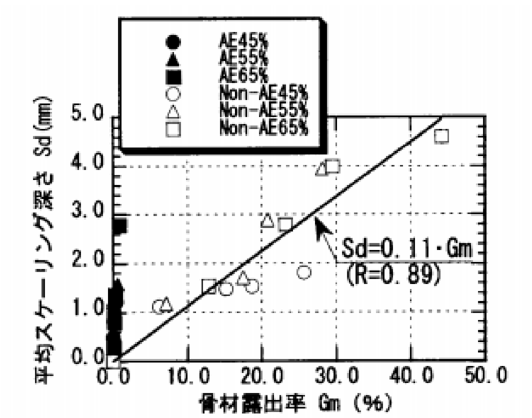

Fig. 5-34 Average scaling depth VS aggregate exposure rate[131]

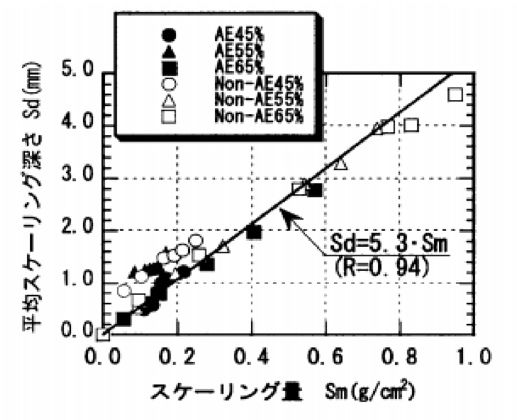

Fig. 5-35 Average scaling depth VS scaling amount[131]

Pond, Osamuet et al. established the relationship between the average scaling depth and the exposure rate of aggregate (Fig. 5-34) and the relationship between the average scaling depth of concrete and the scaling amount (Fig. 5-35) through the rapid freeze-thaw experiment based on ASTM C672 in the lab.

Fig. 5-34 and Fig. 5-35show relationships between aggregate exposure rate and scaling depth, and the relationship between scaling amount and scaling depth have nothing to do with concrete mix ratio. Therefore, the fitting formula of the above figure is universal. When the exposure rate of aggregate is 10%, the average scaling depth is 1.1mm. The scaling degree is less than 1.1mm (when the average scaling degree is small, the ratio of the scaling area to the test area is generally less than 100%). Still, to be conservative, the scaling depth of the concrete surface of the 20th year treatment group is taken here as 1mm. In the 3rd and 12th years, according to the photos (Fig. 4-3) taken in the 12th year, the surface is entirely intact. Therefore, the scaling degree is considered to be 0mm in the 3rd and 12th years. After analysis, the aggregate exposure rate has an upper limit. The scaling depth can continue to develop without limit with the service year on-site or the freeze-thaw cycles in the lab after the aggregate is completely exposed. Therefore, this formula is only applicable to the aggregate exposure rate range from 0% to the aggregate's complete (100%) leakage, so this method is not used to calculate the scaling depth for the untreated group in this article.

The relationship between the scaling amount and the average scaling depth in Fig. 5-35 is used to calculate the scaling depth of the Tomakomai Project in the lab and considered the scaling depth already happened in the marine environment. The results are shown in Appended Table 1 to Appended Table 3.

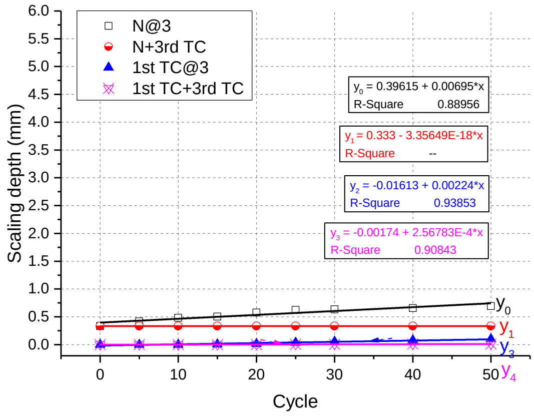

(a) The 3rd year

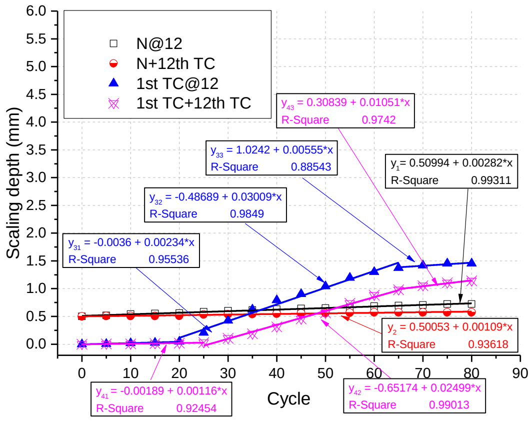

(b) The 12th year

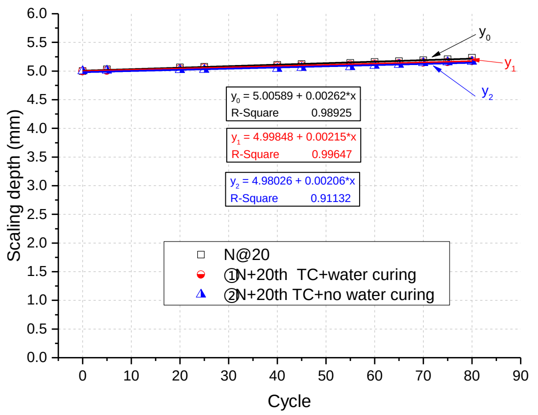

(c) The 20th year — initial without treatment groups

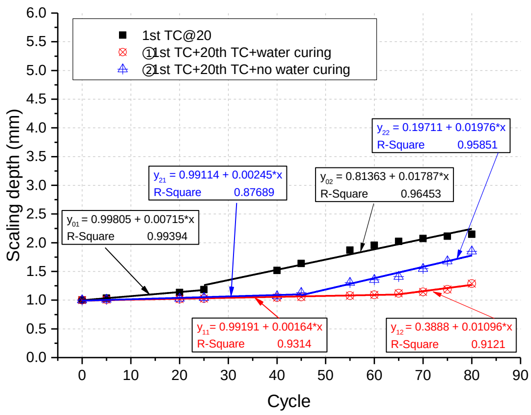

(d) The 20th year —initially treated groups

Fig. 5-36 Scaling depth VS cycles

Notes:

1st, 12th, and 20th represent the first year, the 12th year, and the 20th year respectively.

N: No treatment.

TC: Treatment。

N/1st TC@12/20: The untreated group or Treated group was tested as it was in the 12th or 20th year.

N+12th TC: The untreated groups applied penetrants at the 12th year.

N+20th TC+no water curing: The untreated groups applied penetrants at the 20th year and after treatment without water curing.

1st TC+20th TC+ water curing: Penetrants were applied in the first year and re-applied in the 20th year, after treatment with water curing.

The rest of the labels have similar meanings.

According to Appended Table 1 to Appended Table 3, draw the relationship diagram of scaling depth and cycles for each group, perform the fitting, and Fig. 5-36 get.

Calculation ideas:

Under normal circumstances, after obtaining the above-mentioned fitting formulas for each group, take the scaling depth limit (mm) as y value and enter the fitting formulas to obtain the number of freeze-thaw cycles that the concrete can withstand under this condition in the lab. Then the number of freeze-thaw cycles is calculated into equivalent years, and the corresponding life can be obtained. However, there are contradictions with the actual situation, such as for the same scaling depth: The life calculated based on the 1st TC+12th TC group fitting formula will be <based on the N@20 group. The reason is that the scaling speed changes with the depth and the year. If the data of a specific year is used to represent its entire life, it would be a partial generality, and it would be untrue. Similar situations exist in other groups.

Therefore, after a comparative analysis of the fitting data between the same set of different years in Fig. 5-36, and combining the two key factors of the surface structure of the concrete and the penetration depth of the penetrants in concrete, along the depth direction, the method of different peeling speeds in different peeling depth ranges is used for life prediction.

- Concrete surface structure: There is a 5mm [135]weak layer of mortar on the surface of the concrete, and the scaling speed in this range will be greater than the part below 5mm.

- The penetrating depth of impregnants: It can be seen from Fig. 5-36 that after the penetrants were applied or re-applied, the continuous freeze-thaw cycle period of concrete scaling inhibition varies from 20 cycles to 65 cycles. According to the literature[72][P152], the duration of the effect is roughly the same; the depth at which the B-type (Silane) impregnant can act varies from 1.8 to 3.1 mm, and the mean is about 2.5 mm. The A-type (Sodium silicate) is not considered because of without relevant supporting data of penetrating depth. The calculation result should be conservative and safe.

The scaling speed and the corresponding depth of action are summarized in the following Table 5-18 and

Table 5-19 (individual values obtain the average value of multiple fitting slopes. Here, the two cases ① and ② in the 20th years are considered together):

Table 5-18 Scaling speed and the corresponding depth of action ①

Groups	Scaling depth limit (mm)	scaling speed ki (mm/cycles)	ki: Range of action
N	1.5	0.00695	1.5
	2.5	0.00695	1
	5	0.00695	2.5
	10	0.00272	5
	20	0.00272	10
1st TC	1.5	0.00229	1.5
	2.5	0.00229	1
	5	0.00229	2.5
	10	0.00272	5
	20	0.00272	10

1st TC+3rd TC	2.5	0.000256783	1
	5	0.012935	2.5
	10	0.00272	5
	20	0.00272	10
1st TC+12th TC	2.5	0.00229	1.5
	2.5	0.00116	1
	5	0.00116	2.5
	10	0.00272	5
	20	0.00272	10
1st TC+20th TC	2.5	0.00229	1.5
	2.5	0.002045	1
	5	0.01536	2.5
	10	0.00272	5
	20	0.00272	10

Table 5-19 Scaling speed and the speed range ②

Groups	2.5mm for treated	~ 5mm	> 5mm
N+12th TC	0.00109	0.03009	0.00272
N+20th TC	0.00215	0.03009	0.00272

Note: The scaling depth before treatment is determined according to the formula 5.35.

The number of laboratory freeze-thaw cycles equivalent to that of Tomakomai's marine environment in one year (named the equivalent cycles): Here, the untreated group's (control group) scaling depth (Chapter 4.3 for 20 years is 4.475mm as the control point for the calculation. The scaling speed is 0.00695mm/cycle, and the equivalent cycle times are 4.475/0.00695/20=32.19424cycle/year.

Obviously, the same scaling depth and different scaling speeds will result in different equivalent cycles. The dynamic nature of the freeze-thaw scaling speed determines the non-uniqueness of the equivalent cycle number, which is why it is difficult to find an exact equivalent cycle number in the literature.

Calculation steps:

1) Input the above scaling depth limitations and scaling speed ki into the following general fitting formula:

$$y = a + b*x$$

where:

Y: Scaling depth limit, mm

a: Scaling depth, mm

b: Scaling speed, mm/cycle

x: Freeze-thaw cycles in lab, cycles

then x get.

2) The corresponding life is obtained by the equivalent freeze-thaw cycles—the summary of estimated life in Table 5-20.

Table 5-20 Summary of estimated life

Groups	Scaling depth limit (mm)	lifetime (year)
N	2.5	11.17
	5	22.35
	10	79.44

	20	193.64
1st TC	2.5	33.91
	5	67.82
	10	124.92
	20	239.11
N+3rd TC	2.5	
	5	
	10	
	20	
1st TC+3rd TC	2.5	260.05
	5	266.05
	10	323.15
	20	437.35
N+12th TC	2.5	83.24
	5	85.31
	10	170.95
	20	285.15
1st TC+12th TC	2.5	38.78
	5	105.72
	10	162.82
	20	277.01
N+20th TC	2.5	11.17
	5	22.35
	10	141.77
	20	170.31

1st TC+20th TC	2.5	42.78
	5	47.84
	10	104.94
	20	219.13

Note: In the N+3rd TC group, because there was no peeling during the 50 cycles in the lab experiment, the peeling speed was not obtained, so the life expectancy could not be carried out. Theoretically, the life expectancy can be approximately equal to the 1st TC group.

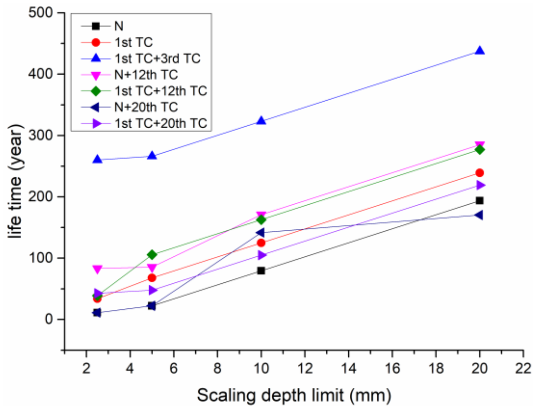

Fig. 5-37 Lifetimes and scaling depth limit

Fig. 5-37 shows that the order of life from long to short is 1st TC+3rd TC>N+12th TC ≈1st TC+12th TC>1st TC+20th TC>N+20th TC>N. It can be seen that the sooner the penetrant was applied, the better, and multiple treatments are better than once.

5.4 Summary

The magnification calculated by the A method is slightly larger than that by the B method. The B method has fewer assumptions and is closer to actual life. The calculation of the B method is more safe and conservative, which is also beneficial to the maintenance of the actual project.

The Monte Carlo method that considers the statistical distribution of the calculated parameters and the probability of failure is better than the deterministic calculation method. The Monte Carlo calculation method is recommended.

After the impregnants are treated, the concrete life under freeze-thaw and chloride ion erosion are prolonged, and the carbonization life is shortened. Nevertheless, the carbonization life of the concrete can be at least 170 years when the concrete cover is 50mm, which is enough for the target year. The life of Tomakomai Dam is ultimately determined by the service life calculated based on chloride ion and freeze-thaw erosion. From the results, it is worth sacrificing part of the carbonization life to improve the resistance to salt-freeze-thaw corrosion.

The use of composite impregnant will shorten the carbonization life of concrete to 0.3 times the carbonization life of the untreated group. Still, it can extend the concrete's salt and freeze corrosion resistance life to 1.2-3.5 times the original lifespan. The life of concrete in a marine environment in a cold area is mainly determined by salt and freezing corrosion.

Penetrants can improve the resistance of concrete to chloride corrosion and freeze-thaw deterioration. Still, it is not conducive to the resistance to carbonization. Therefore, they are not suitable for the dry and warm environment that is easily eroded by carbon dioxide

If the construction quality improves, the probability of the concrete cover construction deviation of 10mm is reduced from 15% to 5%; the guaranteed rate is increased from 85% to 95%. At this time, the concrete carbonization life will be significantly improved. When the concrete cover is more than 20mm (30mm in the treatment groups), when the guaranteed rate is increased by 10%, the total carbonization life of the concrete can be prolonged by an average of 37 years. The untreated groups are slightly longer than the treatment groups.

CHAPTER 6. EVALUATION OF THE ECONOMIC EFFECT OF THE MAINTENANCE PLAN

6.1 Overview

This chapter introduces the calculation method of maintenance and repair cost of Tomakomai dam based on chloride ion diffusion factors and freeze-thaw scaling depth. It provides a theoretical basis for maintenance and repair, determining the time nodes for maintenance and repair and selecting maintenance measures. Under the premise of considering the discount rate, the specific maintenance and repair programs for different status index levels are discussed, and the cost calculations and pros and cons of various programs are analyzed.

6.2 Repair Method, The Unit Price, And Maintenance Time Point

1) Repair method

If the chloride ion does not reach the threshold on the surface of the steel bars and the scaling of the concrete surface is slight, the impregnant method A and the surface coating method B can be used. When the chloride ion on the surface of the steel bars (at a depth of concrete cover) reaches the threshold, the large section repair method C is required. Alternatively, salt discharge method D can also be combined with impregnant method A or surface coating method B at the same time.

- Untreated groups:

According to Chapter 5, it can be known that for the untreated group, after 20 years of service, the concrete cover of 50mm was basically within the chloride ion threshold range, and the coarse aggregate leaked (the peeling depth is about 4.47mm). The repair methods that can be used are:

A: Impregnant method

B: Surface coating method

C: Salt discharge method

D: Large section repair method

I: Large section repair + impregnating agent method D+A

II: Large section repair + impregnating agent method D+B

III: Salt discharge method + impregnant method C+A

While, at the 12th year, the untreated group was slightly peeled off (Fig. 4-3). If the repair is carried out once every ten years, just the impregnant method A or the surface coating method B is enough.

- Treated groups

There was almost no peeling on the concrete surface in the third year and the 12th year of the treatment groups, and the peeling was not apparent in the 20th year. The method of re-apply impregnant (method A) can be used within the range of 20 years. Considering the unknown chemical reaction that may exist, using the same penetrants for re-maintenance is recommended.

2) The unit price

The unit price of each maintenance method is detailed in Table 6-1.

Table 6-1 Unit price of each maintenance method (Yen/m^2)

Methods	Main construction procedure	Price
T&C method——A	Base adjustment: Removal of dirt and deposits, cleaning of the construction surface.	448
	Application of liquid A: 0.2 kg/m^2, roller, brush coating,	1683

	spraying	
	Application of liquid B: 0.2 kg/m^2, roller, brush coating, spraying	2769
	Total price	4900
Traditional surface coating method ——B	Base material adjustment	448
	Primer	1683
	Undercoat	2123
	Middle coat	2123
	Topcoat	2123
	Total price	8500
Salt discharge method——C	Total price	70000
Large section repair method——D	Total price	100000

Note: Excluding tax, maintenance costs are included.

Unit price comes from:

https://www.hirato-co.jp/wp-content/themes/wp_hirato/assets_hrt/pdf/liquidglass/concrete.pdf

https://st-techno.net/pdf/st-techno.pdf [136][p20]。

3) Determining the maintenance time node

The maintenance time should meet T≤min (T of chloride ion life, T of carbonization life, T of salt-scaling life).

Summary of Chapter 5 shows that among the lifespans calculated based on chloride ion corrosion, neutralization, and freeze-thaw damage, the neutralization life is the longest, usually longer than the concrete design life. The chloride ion corrosion and freeze-thaw damage are the key factors determining Tomakomai dam' life. Therefore, the following sections discuss the main effects of chloride ion erosion and freeze-thaw scaling (actually a coupling effect), the concrete reaches its design service life (assuming 100 years), and the economic effects of different maintenance programs.

4) Calculation formula

See the formulas in Chapter 2.4 for details.

6.3 The Influence Of The Concrete Cover On The Maintenance Plans

The following maintenance plans correspond to the two concrete scenarios with different concrete covers without any maintenance at the initial stage and with penetrants maintenance at the initial stage.

The initial protection time (for untreated groups: N groups) and the re-protection time (for the treatment group: TC groups) start when the chloride ion reaches the concrete covers -10mm. Plan B (Case B) was used to repair untreated groups; plan A (Case A) was still used to repair the treatment group. Now take the concrete cover of 50mm (the maintenance time node refers to the life of concrete cover thickness of 40mm) as an example.

Based on the experimental data of the 12th year, the chloride ion threshold value of 2.2, and the construction guarantee rate of the concrete cover thickness of 95% as the basic data for calculation, the concrete life results calculated by the Monte Carlo method are used as the basis, combined with the concrete surface condition, the maintenance time nodes are selected as follows: For the maintenance group where the impregnating agent was applied in the initial year of construction, the re-repair start time was 15 years after construction; for the group without maintenance in the initial year, the repair start time was 12 years after construction, and the duration of continuous maintenance is 15 years per application of the penetrants.

The calculation process and results are shown in Table 6-2 and Table 6-3. The calculation processes and results of the 60-90mm concrete cover are detailed in the Appended Table 4.

Table 6-2 LCC of the initial treated group maintained with penetrants ——Case A

Group (Case A)					TC-Based 12th Cl-
Cover (mm)					50
The life span of A1.2					21
Life span of B1.2					23
Min（A1.2,B1.2）					21
Repair start time: after construction					15
Maintenance hold time					15
Construction time					2000
Maintenance Details	Maintenance year	One-time maintenance cost(yen/m^2)	t from 2020	Discount Rate of t year	Present value of one-time maintenance(yen/m^2)
	2015	4900	-5	1.217	5961.60
	2030	4900	10	0.676	3310.26
	2045	4900	25	0.375	1838.07
	2060	4900	40	0.208	1020.62
	2075	4900	55	0.116	566.71
	2090	4900	70	0.064	314.68
Total (PV) ① (yen/m^2)					13011.94
Durable year-end	2105				
T_P	10				
T_D	15				
Survival value (PV)(yen/m^2)					65.33
LCC (①-②) (yen/m^2)					12946.61

Table 6-3 LCC of the initial untreated group maintained with traditional surface coating method —— Case B

Group (Case B)					N-Based 12th Cl-
Cover (mm)					50
The life span of A1.2					17
The life span of B1.2					-
Min（A1.2,B1.2）					17
Repair start time: after construction					12
Maintenance hold time					15
Construction time					2000
Maintenance Details	Maintenance year	One-time maintenance cost(yen/m^2)	t from 2020	Discount Rate of t year	Present value of one-time maintenance(yen/m^2)
	2012	8500	-8	1.369	11632.84
	2027	8500	7	0.760	6459.30
	2042	8500	22	0.422	3586.62
	2057	8500	37	0.234	1991.52
	2072	8500	52	0.130	1105.82
	2087	8500	67	0.072	614.02
	2102	8500	82	0.040	340.95
Total (PV) ① (yen/m^2)					25731.07
Durable year-end	2102				
T_P	13				
T_D	15				
Survival value (PV)(yen/m^2)					45.33
LCC (①-②) (yen/m^2)					25685.74

Notes: PV is present value. Columns "t from 2020" of Table 6-2 and Table 6-3 can see negative years, indicating that the current (the year 2020) had missed the maintenance and repair time node for several years; this phenomenon can be widespread in existing projects. For this, we change the maintenance and repair plan as described in the following section 6.4.

From the data in Chapter 4, it also can be seen that for the concrete cover of 50mm, since in the 20th year, chloride ions had reached the depth of 50mm, then it is of little significance to re-applied compound penetrants and other protective treatments need to be combined.

Table 6-4 Maintenance cost comparison

Cover (mm)	N (Yen/m^2)	TC (Yen/m^2)	δ=(N-TC)(Yen/m^2)	δ/N (%)
50	25682.34	12901.57	12780.77	49.76%
60	20978.50	8014.38	12964.13	61.80%
70	20140.71	6524.38	13616.32	67.61%
80	15517.47	3992.56	11524.91	74.27%
90	7881.94	2719.62	5162.32	65.50%

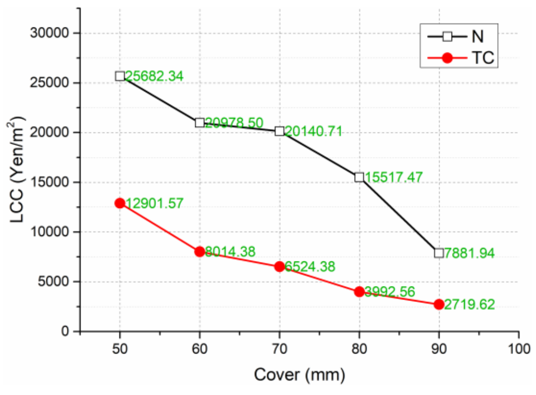

Fig. 6-1 LCC VS concrete cover (Case A and case B)

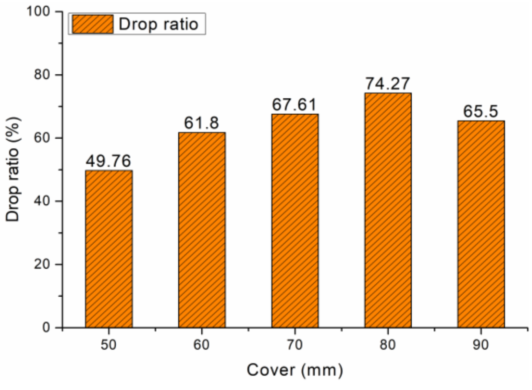

Fig. 6-2 Drop ration of cost

Fig. 6-2 is the percentage reduction in maintenance costs during the lifetime of initial maintenance compared with no initial maintenance in the construction year. It can be seen from Fig. 6-1 and Fig. 6-2 that once the concrete is constructed, maintenance of the composite impregnants on the concrete surface has an excellent economic effect. Under the goal of one hundred years of service, the subsequent maintenance cost can be reduced by 50-75%.

6.4 Evaluation Of The Economic Effects Of Different Maintenance Plans

Still taking the Tomakomai project as an example, the goal is to serve in the marine salt-freeze environment within 100 years. Case1-case6 are listed below, corresponding to six different maintenance time nodes and corresponding maintenance plans and their maintenance costs.

Table 6-5 LCC of kinds of maintenance plans

Year	Years of service	Case1			Case2		
		Plan	Cost (yen/m²)	Cost –PV (yen/m²)	Plan	Cost (yen/m²)	Cost –PV (yen/m²)
2000	0	A	4900	10737	B	8500	18625
2015	15	A	4900	5962	B	8500	10342
2029	29	A	4900	3443	B	8500	5972
2044	44	A	4900	1912	B	8500	3316
2059	59	A	4900	1061	B	8500	1841
2074	74	A	4900	589	B	8500	1022
2089	89	A	4900	327	B	8500	568
Total (PV) (yen/m²) ①				24030			41685
Durable year-end				2110			2104
Planned service year-end				2100			2100
Planned service year-end discount rate				0.0434			0.0434

T_P	11			11
T_D	21			15
Survival value(PV) (yen/m²) ②	101			57
LCC(①-②) (yen/m²)	23929			41629

Continue to the table

Year	Years of service	Case3			Case4		
		Plan	Cost (yen/m²)	Cost –PV (yen/m²)	Plan	Cost (yen/m²)	Cost –PV (yen/m²)
2000	0	A	4900	10737	A	4900	10737
2020	20	I (D+A)	104900	104900	III (C+A)	74900	74900
2035	35	A	4900	2721	A	4900	2721
2050	50	A	4900	1511	A	4900	1511
2065	65	A	4900	839	A	4900	839
2080	80	A	4900	466	A	4900	466
Total (PV) (yen/m²) ①				121173			91173
Durable year-end				2101			2101
Planned service year-end				2100			2100
Planned service year-end discount rate				0.0434			0.0434
T_P				20			20
T_D				21			21
Survival value(PV) (yen/m²) ②				10			10
LCC(①-②) (yen/m²)				121163			91163

Continue to the table

Year	Years of service	Case5			Case6		
		Plan	Cost (yen/m^2)	Cost –PV (yen/m^2)	Plan	Cost (yen/m^2)	Cost –PV (yen/m^2)
2000	0						
2020	20	I (D+A)	104900	104900	II (D+B)	108500	108500
2035	35	A	4900	2721	B	8500	4720
2050	50	A	4900	1511	B	8500	2621
2065	65	A	4900	839	B	8500	1455
2080	80	A	4900	466	B	8500	808
2095	95				B	8500	449
Total (PV) (yen/m^2) ①				110436			118552
Durable year-end				2101			2110
Planned service year-end				2100			2100
Planned service year-end discount rate				0			0
T_P				20			5
T_D				21			15
Survival value(PV) (yen/m^2) ②				10			142
LCC(①-②) (yen/m^2)				110426			118411

Notes:

A	Impregnant method	I (D+A)	Large section repair + impregnating agent method
B	Surface coating method	III (C+A)	Salt discharge method + impregnant method
C	Salt discharge method	II (D+B)	Large section repair + surface coating method
D	Large section repair method		

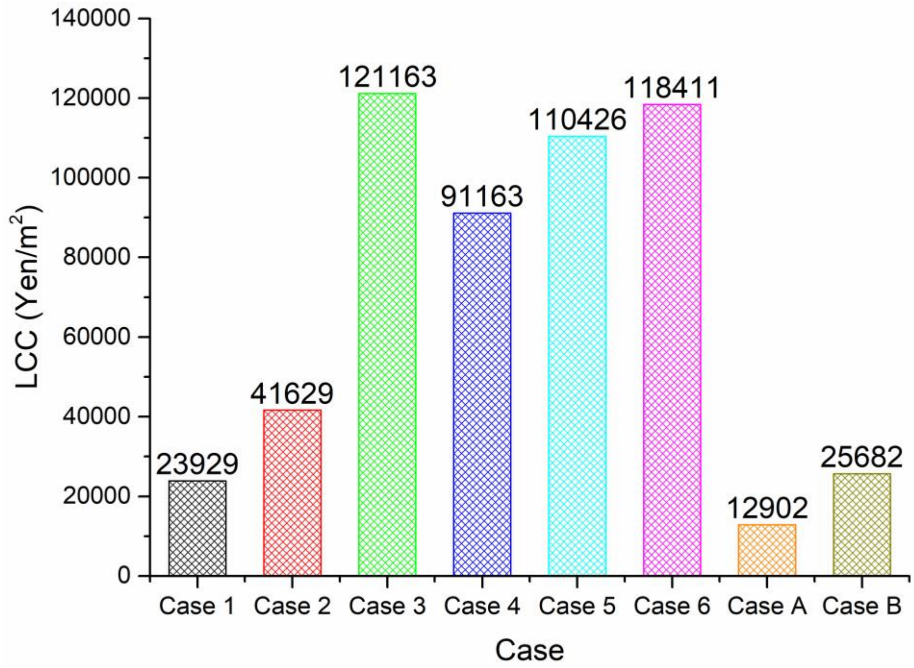

Fig. 6-3 LCC of all cases

Table 6-6 LCC comparison table

Case	Cost (Yen)	Mean (Yen)	δ=Cost-Mean (Yen)	δ/Mean
Case 1	23929	68163	-44234	-64.89%
Case 2	41629		-26534	-38.93%
Case 3	121163		53000	77.75%
Case 4	91163		23000	33.74%
Case 5	110426		42263	62.00%
Case 6	118411		50248	73.72%
Case A	12902		-55261	-81.07%
Case B	25682		-42481	-62.32%

Table 6 shows that Case 1 and Case A have good economic benefits. They are recommended.

6.5 The Impact Of The Allowable Peeling Depth On The Maintenance Plan—Based On Freeze-Thaw Damage

This section mainly discusses the re-treated schemes for LCC based on salt freeze-thaw damage. Although it combines salt and freeze-thaw damage, the surface layer was missing after some freeze-thaw cycles, and the specimen became thin. It was inconvenient and inaccurate to sample and test its chloride ion content by layering. At the same time, considering the experimental process, the sealing tape around the test piece was leaking somewhere. There will be seepage chloride ions on the surface of the lower concrete, so the change of chloride ion concentration test after retreated was not conducted. So when analyzing here, it can correspond to the following scenarios: by layering. At the same time, considering the experimental process, the sealing tape around the test piece was leaking somewhere. There will be seepage chloride ions on the surface of the lower concrete, so the change of chloride ion concentration after retreated was not conducted. So when analyzing here, it can correspond to the following scenarios:

① Repair of plain concrete in the salt freeze-thaw environment;

② Suppose the reinforced concrete water conservancy projects are used in the cold areas of freshwater lakes such as rivers and lakes. In that case, chloride erosion is not the main factor, and the impact of freeze-thaw spalling on its lifespan should be considered. Since this data is obtained under the couple presence of salt and freezing-thawing, it is well known that compound degradation is faster than the degradation of a single factor. Therefore, the application of this experimental data to this scenario is biased towards safety; that is, it may be repaired in advance.

For the untreated groups, the concrete life corresponding to the allowable spalling depth takes the smaller value in Table 5-17 and Table 5-20， it is Table 6-7.

Table 6-7 Lifetimes of scaling depth limits (all)

Groups	Scaling depth limit (mm)	lifetime (year)

N	2.5	Min(17.65, 11.17)
	5	Min(32.45, 22.35)
	10	Min(59.67, 79.44)
	20	Min(109.73, 193.64)
1st TC	2.5	33.91
	5	67.82
	10	124.92
	20	239.11
N+3rd TC	2.5	
	5	No data.
	10	
	20	
1st TC+3rd TC	2.5	260.05
	5	266.05
	10	323.15
	20	437.35
N+12th TC	2.5	83.24
	5	85.31
	10	170.95
	20	285.15
1st TC+12th TC	2.5	38.78
	5	105.72
	10	162.82
	20	277.01
N+20th TC	2.5	11.17

	5	22.35
	10	141.77
	20	170.31
1st TC+20th TC	2.5	42.78
	5	47.84
	10	104.94
	20	219.13

Table 6-8 lists each group's maintenance plans and corresponding LCC at an allowable scaling depth of 2.5mm. Under other allowable scaling depths, the results list in Appended Table 5. See the notes at the end of the table for the meaning of each abbreviation.

Table 6-8 LCC of Allowable scaling depth is 2.5mm

Group		N			1st TC		
Scaling depth limit (mm)		2.5			2.5		
Lifetime (Take an integer*) (year)		11.17 (10)			33.91（30）		
Year	Service year	Plan	Cost (yen/m^2)	Cost –PV (yen/m^2)	Plan	Cost (yen/m^2)	Cost –PV (yen/m^2)
2000	0				A	4900	10737
2003	3						
2005	5						
2010	10	A	4900	7253			
2012	12						
2015	15						
2020	20						

2025	25						
2030	30				A	4900	3310
2035	35						
2040	40	A	4900	2236			
2045	45						
2050	50						
2055	55						
2060	60				A	4900	1021
2065	65						
2070	70	A	4900	689			
2075	75						
2080	80						
2085	85						
2090	90				A	4900	315
2095	95						
2100	100						
Total (PV) (yen/m2) ①				10179			15382
T_P				30			10
T_D				30			30
Survival value(PV) (yen/m^2) ②				0			142
LCC(① - ②) (yen/m^2)				10179			15240
Group		N+3rd TC			1st TC+3rd TC		
Scaling depth limit (mm)		2.5			2.5		

Lifetime (Take an integer*) (year)		33.91 (30)			260.05 (260)		
Year	Service year	Plan	Cost (yen/m^2)	Cost –PV (yen/m^2)	Plan	Cost (yen/m^2)	Cost –PV (yen/m^2)
2000	0				A	4900	10737
2003	3	A	4900	9545	A	4900	9545
2005	5						
2010	10						
2012	12						
2015	15						
2020	20						
2025	25						
2030	30	A	4900	3310			
2035	35						
2040	40						
2045	45						
2050	50						
2055	55						
2060	60	A	4900	1021			
2065	65						
2070	70						
2075	75						
2080	80						
2085	85						
2090	90	A	4900	315			
2095	95						
2100	100						

Total (PV) (yen/m2) ①			14190			20281
T_P			10			97
T_D			30			260
Survival value(PV) (yen/m^2) ②			142			133
LCC(① - ②) (yen/m^2)			14049			20148

Group		N+12th TC			1st TC+12th TC		
Scaling depth limit (mm)		2.5			2.5		
Lifetime (Take an integer*) (year)		83.24（80）			38.78（35）		
Year	Service year	Plan	Cost (yen/m^2)	Cost –PV (yen/m^2)	Plan	Cost (yen/m^2)	Cost –PV (yen/m^2)
2000	0				A	4900	10737
2003	3						
2005	5						
2010	10						
2012	12	A	4900	6706	A	4900	6706
2015	15						
2020	20						
2025	25						
2030	30						
2035	35						
2040	40						

2045	45				A	4900	1838
2050	50						
2055	55						
2060	60						
2065	65						
2070	70						
2075	75				A	4900	567
2080	80						
2085	85						
2090	90	A	4900	315			
2095	95						
2100	100						
Total (PV) (yen/m2) ①				7021			19847
T_P				10			25
T_D				30			30
Survival value(PV) (yen/m^2) ②				142			35
LCC(① - ②) (yen/m^2)				6879			19812

Group		N+20th TC			N+20th TC		
Scaling depth limit (mm)		2.5-①			2.5-②		
Lifetime (Take an integer*) (year)		11.17 (10)			11.17 (10)		
Year	Service	Plan	Cost	Cost –PV	Plan	Cost	Cost –PV

	year		(yen/m^2)	(yen/m^2)		(yen/m^2)	(yen/m^2)
2000	0						
2003	3						
2005	5						
2010	10						
2012	12						
2015	15						
2020	20	A	4900	4900	A	4900	4900
2025	25						
2030	30	A	4900	3310	I (D+A)	104900	70867
2035	35						
2040	40	A	4900	2236			
2045	45						
2050	50	A	4900	1511			
2055	55						
2060	60	A	4900	1021	A	4900	1021
2065	65						
2070	70	A	4900	689			
2075	75						
2080	80	A	4900	466			
2085	85						
2090	90	A	4900	315	A	4900	315
2095	95						
2100	100						
Total (PV) (yen/m2) ①				14448			77102

T_P	10		10			10
T_D	10		10			30
Survival value(PV) (yen/m²) ②			0			142
LCC(① - ②) (yen/m²)			14448			76960

Group		1st TC+20th TC				
Scaling depth limit (mm)		2.5				
Lifetime (Take an integer*) (year)		42.78（40）				
Year	Service year	Plan	Cost (yen/m²)	Cost –PV (yen/m²)		
2000	0	A	4900	10737		
2003	3					
2005	5					
2010	10					
2012	12					
2015	15					
2020	20	A	4900	4900		
2025	25					
2030	30					
2035	35					
2040	40					
2045	45					
2050	50					

2055	55						
2060	60	A	4900	1021			
2065	65						
2070	70						
2075	75						
2080	80						
2085	85						
2090	90	A	4900	315			
2095	95						
2100	100						
Total (PV) (yen/m2) ①				16972			
T_P				10			
T_D				30			
Survival value(PV) (yen/m^2) ②				142			
LCC(① - ②) (yen/m^2)				16830			

Notes：

A	Impregnant method	I (D+A)	Large section repair + impregnating agent method
B	Surface coating method	III (C+A)	Salt discharge method + impregnant method
C	Salt discharge method	II (D+B)	Large section repair + surface coating method
D	Large section repair method		

Take an integer*: Take an integer that is a multiple of 5 for a Lifetime and is less than the lifetime

T_D: The (allowable) durability of the last treatment method is different from the previous section. It is not equal to the durability of the concrete surface reinforcement method but is also related to the allowable spalling depth.

N+3rd TC: without treatment for the first and treated in the third year, refer to the maintenance group for the first year.

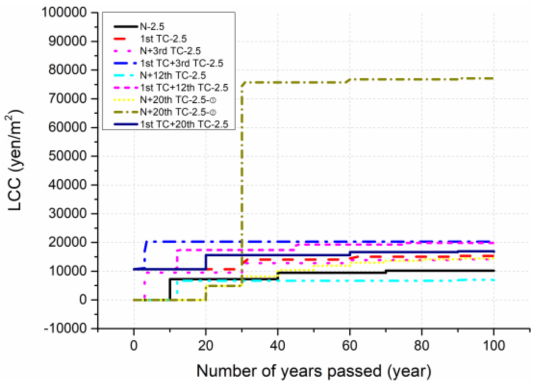

(a1) 2.5mm

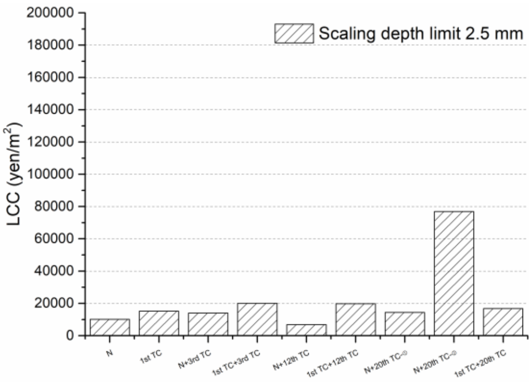

(a2) 2.5mm

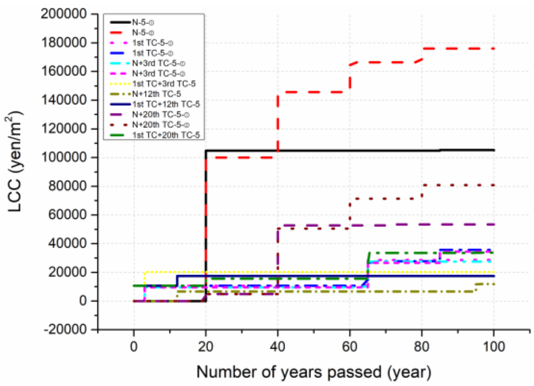

(b1) 5mm

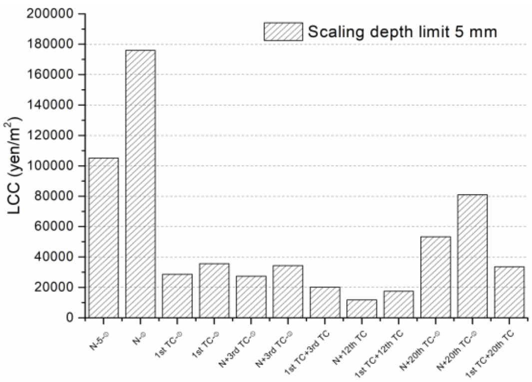

(b2) 5mm

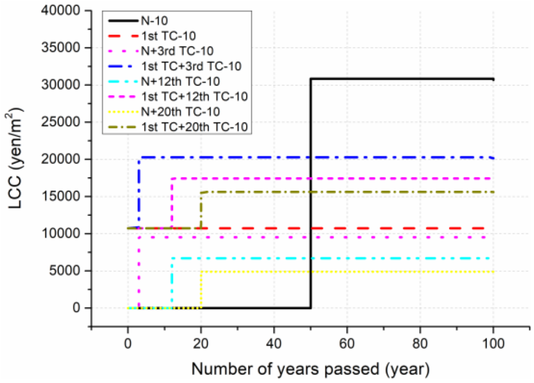

(c1) 10mm

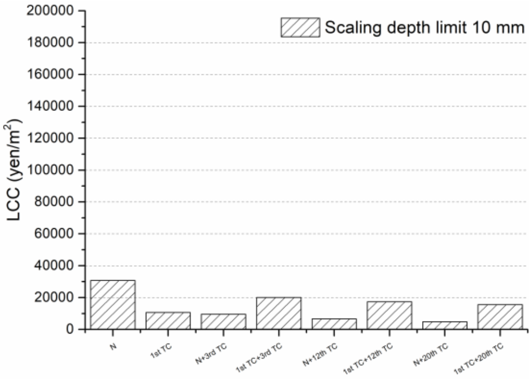

(c2) 10mm

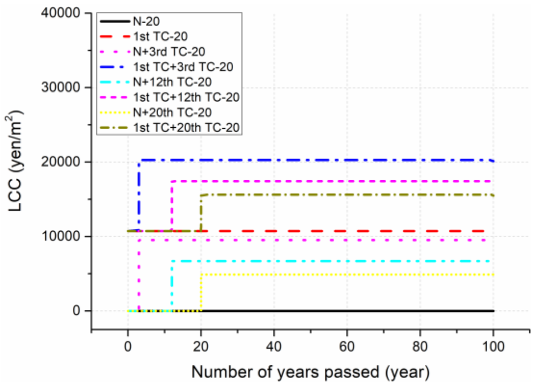

(d1) 20mm

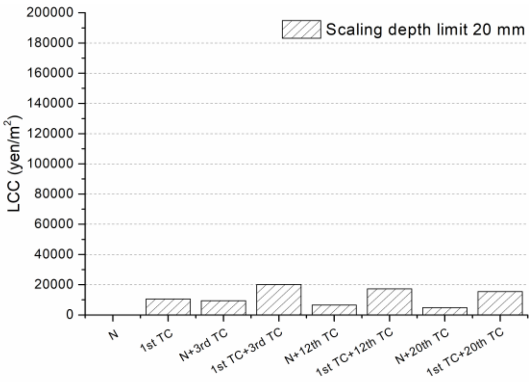

(d2) 20mm

Fig. 6-4 LCC of each group under different allowable scaling depths

(*1) The cumulative growth of LCC over the years of service

（*2） LCC of each maintenance plan at the end of 100 years of service

Overview Fig. 6-4 Shows that if the goal is 100 years, the maintenance cost will increase first and then decrease as the allowable spalling depth increases. When the allowable spalling depth is 5mm, the maintenance cost is the largest. The acceptable peeling depth is large to a certain extent. If the concrete mixture ratio is good, the expected service life can be reached within 100 years without any repairs or only a small number of repairs. This point is easy to understand by comparison. The smaller the limit, the higher the requirement for the maintenance of the concrete surface quality, and the higher the maintenance frequency, but it is not the smaller, the higher the cost. When the concrete surface spalling depth is less than 2.5mm, due to the coarse aggregate is not leaked, simply repair is enough. Although the repair frequency may be higher than that of the 5mm groups (not absolute, depending on the repair method), the overall cost is lower. When the spalling depth reaches 5mm, the coarse concrete aggregates are severely exposed, and large cross-section repairs are needed. At this time, the repair cost will increase sharply, which is most apparent for the untreated group (see Fig. 6-4 -(b1), (b2)). Although the number of repairs may be reduced, the unit price of repairs has increased a lot. It can be seen that a good grasp of the repair time node can reduce the repair cost of the concrete life cycle. It is the most economical to repair the concrete surface before the spalling depth reaches 2.5mm.

Fig. 6-4 (a1) (a2) and Fig. 6-4 (b1) (b2) show that when the concrete is first treated after 12 years of service, the LCC is the lowest. The cost of the groups with the initial treatment conducted in the 20th year is the largest. The reason is that there was almost no peeling on the concrete surface in 12 years. From the laboratory data, applying the compound penetrants at this time is almost equivalent to the maintenance measures taken in the construction year. Since money will generate time value, under the influence of a 4% social growth rate, post-investment (the year 2012) is always more economical than pre-investment (the year 2000). Compare the groups with concrete surface impregnant treatment in the construction year and the initial maintenance taken in the 12th year, equivalent to using the quality of a part of the concrete cover in advance to generate time value for money. Still, for the initial maintenance in the 20th year, it is quite different because the concrete cover falls off deeply, reaching 4.75mm, far more than 2.5mm. At least at this time, it is necessary to carry out an expensive large-section repair. Then the relatively cheap and long-lasting compound impregnants treatment can be used for maintenance in subsequent years. The economic value reduction produced by the time is not as high as the increment of the unit price of the treatment method, so finally, the maintenance costs increase.

All in all, there is a principle to be mastered when performing maintenance and repairs. The concrete surface should not be peeled off to the degree of aggregate severely exposed to avoid the use of expensive large-section repair solutions.

There is an unexplained point here: because this section is the LCC calculation based on the concrete surface scaling state and the scaling depth, in some groups, the concrete was just initial treated in the 3rd and 12th year, before treating, they had experienced freezing and thawing for some years. Although the concrete surface seemed to be basically intact, there should be an existing freeze-thaw "internal injury". The impact of this internal injury on lifespan is difficult to quantify.

6.6 Summary

It can conclude that for existing concrete, even if it enters a slow spalling period, it is advisable to treat it with penetrants as soon as possible. The sooner the treatment, the more conducive it is.

The principle of performing maintenance and repairs with cost-effectiveness is to avoid expensive large-section repair solutions. Using or re-using composite penetrant maintenance before the scaling depth reaches 2.5 mm can effectively reduce the life cycle cost by at least 50%. Fortheinfrastructures treated with composite penetrant in the construction year, the secondary maintenance time should be ≤33 years. For the infrastructures without maintenance in the construction year, the maintenance interval should be ≤17 years. The impregnant can make the concrete "freeze age" about 17 years.

CHAPTER 7. CONCLUSIONS AND OUTLOOK

7.1 Conclusions

This thesis studies the application of a set of impregnants on the concrete surface. After applying the penetrants, the concrete surface's air permeability, surface water absorption, surface pore structure, pH, and salt-freezing-thawing resistance have been studied through laboratory research. In addition, a 20-year durability tracking study, life prediction, maintenance decision-making and economic analysis of the service concrete in the severe cold marine environment (Tomakomai Breakwater) have been carried out. The main conclusions are as follows:

Concrete surface water absorption, air permeability, pH, surface micro-pore size distributions, and the anti-salt freezing-thawing properties of concrete after applying the impregnating agents were conducted indoor experiments. The results show that: Compared with the untreated groups after using the impregnants, the concrete surface: The surface water absorption is significantly reduced by 60.97%.

The air permeability is almost unaffected. When the concrete surface water content decreases slightly, there is even a slight tendency to increase.

pH increases by testing time (390 days after the test block is formed, about 330 days after the impregnant is applied).

The dosage of impregnant can be adjusted according to the surface quality of the concrete to be repaired. When the air permeability is good(≤ 0.12 (ml/m2/s)), the dosage of the penetrants can be considered to be half of the recommended dosage.

The concrete surface compound penetrants can effectively reduce the pore diameter of 400 nm (12 years), especially above 1000 nm (390 d), in the concrete surface (0-10 nm). It shows that over time (1 year to

12 years), the impregnant can fill smaller pores. However, from the 12th year to the 20th year, the pore structure deteriorated, indicating that the impregnant protective effect was weakened during this period. Therefore, the maintenance interval should not exceed 20 years.

Penetrants have a significant effect on improving the resistance of concrete to chloride corrosion and freeze-thaw deterioration. Still, it is not conducive to the resistance to carbonization. Therefore, they are not suitable for the dry and warm environment that is easily eroded by carbon dioxide

The magnification calculated by the B method is slightly larger than that by the A method. The B method has fewer assumptions and is closer to actual life.

The Monte Carlo method that considers the statistical distribution of the calculated parameters and the probability of failure is better than the deterministic calculation method. The Monte Carlo calculation method is recommended on the premise of distribution statistics. When the construction guarantee of the thickness of the concrete cover is 85%-95% (the construction error is 9-6mm), the concrete chloride life calculated by the Monte Carlo method is about 0.77-0.8 times the concrete life under the deterministic method.

Increasing the chloride ion concentration threshold of corrosion on the steel surface can also significantly improve the concrete life. When the chloride ion threshold is increased from 1.2kg/m^3 to 2.2 kg/m^3, the concrete life can be extended by 1.48 times of the original life; when it is increased by 4 kg/m^3, it can even reach the original 2.20 times.

After using the penetrants, the concrete life under freeze-thaw and chloride ion erosion is prolonged, and the carbonization life is shortened. Nevertheless, the carbonization life of the concrete can be at least 170 years when the concrete cover is 50mm, which is enough for the target year. The life of Tomakomai Dam is ultimately determined by the service life calculated based on chloride ion and freeze-thaw erosion. From the results, it is worth sacrificing part of the carbonization life to improve the resistance to salt-freeze-thaw corrosion.

The use of composite impregnant will shorten the carbonization life of concrete to 0.3 times the carbonization life of the untreated group. Still, it can extend the concrete's salt and freeze corrosion resistance life to 1.1-3.5 times the original lifespan. The life of concrete in a marine environment in a cold area is mainly determined by salt-freezing-thawing corrosion.

Compared with the concrete without penetrants, the reuse of the concrete surface impregnant can delay the rapid spalling period of the concrete surface by 20-65 cycles (ASTM-C 672).

If the construction quality improves, the probability of the concrete cover construction deviation of 10mm is reduced from 15% to 5%; the guaranteed rate is increased from 85% to 95%. The life under chloride ion attack can be extended by 10%. The concrete carbonization life is also significantly improved. When the concrete cover is more than 20mm (30mm in the treatment groups), the total carbonization life of the concrete can be prolonged by an average of 37 years. The untreated groups are slightly longer than the treatment groups.

It can conclude that for existing concrete, even if it enters a slow spalling period, it is advisable to treat it with penetrants as soon as possible. The sooner the treatment, the more conducive it is.

The use of composite penetrant maintenance before the scaling depth reaches 2.5 mm can effectively reduce the life cycle cost by at least 50%. Fortheinfrastructures treated with composite penetrant in the construction year, and the secondary maintenance time should be ≤33 years. For the infrastructures without maintenance in the construction year, the maintenance interval should be ≤17 years. The impregnant can make the concrete "freeze age" for 17 years.

7.2 Outlook

It is challenging to establish the relationship between variables and time t through limited data. The simplified calculation process indicates that the instantaneous state of a particular year represents the state of change throughout the life cycle. Establishing the functional relationship between variables and time *t* is a breakthrough point in time engineering research. The effect of penetrants on the long-term (greater than or equal to 20 years) chloride ion diffusion properties of concrete surfaces needs to be continually studied and clarified.

It is believed that applying sodium silicate →water shower for curing for 14 days → using silane Solution may have an excellent protective effect. It is an idea for this work in the future, and it needs practice to verify its authenticity.

To determine the equivalent relationship between the number of freeze-thaw cycles of concrete treated with penetrants in the lab (based on ASTM-C 672) and that in the natural environment is a difficult problem to be solved in the future. It may not be a definite value.

REFERENCE

1. Yao, Y., et al., *Ｒesearch and Progress on Durability of Concrete underCombined Mechanical Load and Environment Actions.* MATEＲIALS CHINA, 2018. **37**(11): p. 855-865+879.

2. Gagg, C.R., *Cement and concrete as an engineering material: An historic appraisal and case study analysis.* Engineering Failure Analysis, 2014. **40**: p. 114-140.

3. Schlangen, E., *Foreword*, in *Eco-Efficient Repair and Rehabilitation of Concrete Infrastructures*. 2018.

4. Zhao, J., et al., *Ｒesearch Status of Electrochemical Ｒepair Effect of ＲeinforcedConcrete Structure under Chloride Environment.* Bulletin of the Chinese Ceramic Society, 2019. **38**(12): p. 3868-3872+3877.

5. Ministry of Land, I., Transport and Tourism, *Summary Of The White Paper On Land Infrastructure Transport And Tourism In Japan*. 2020.

6. Lindsey, R. *Climate Change: Atmospheric Carbon Dioxide*. 2020; Available from: https://www.climate.gov/news-features/understanding-climate/climate-change-atmospheric-carbon-dioxide.

7. グリーンピース・ジャパン. *日本、中国、韓国がCO2「ネットゼロ宣言」温暖化対策への影響は？*. 2020.12.16; Available from: https://www.greenpeace.org/japan/nature/story/2020/12/16/46308/.

8. Web, W.W. *US media: Biden signed a series of executive orders after taking office to rejoin the WHO (translated)*. 2021; Available from: https://finance.sina.com.cn/world/gjcj/2021-01-21/doc-ikftssan9016938.shtml.

9. Transpot, T.C.C.P.P.S.o.t.M.o., *Study on Cement Con-crete Pavement*. 1997, Bei jing: China Com-munications Press.

10. Gao, H., *Cement Concrete Pavement Repair Technology*. 1997, Bei jing: China Com-munications Press.

11. Mehta, P.K.J.S.P., *Durability of concrete--fifty years of progress?* 1991. **126**: p. 1-32.

12. Mehta, P.K. and P.J. Monteiro, *Concrete: microstructure, properties, and materials*. 2014: McGraw-Hill Education.

13. Yan, Y., et al., *Research and Progress on Durability of Concrete under Combined Mechanical Load and Environment Actions.* 2018. **37**(11): p. 855-865+879.

14. *The fib Model Code for Concrete Structures*. Available from: https://www.fib-international.org/publications/model-codes.html.

15. 国土交通省. *ダムの定期検査の結果について*. 令和元年; Available from: https://www.mlit.go.jp/river/shishin_guideline/kenzensei/index.html.

16. china.com.cn. *What is the content of the "Ping An Centennial Quality Project" construction research and promotion plan? (translated).* Available from: http://guoqing.china.com.cn/zhuanti/201903/02/content_74523284.htm.

17. 佐伯, 昇., 耕. 鮎田, and 静. 前川, *北海道における海岸および港湾コンクリート構造物の凍害による表面剥離損傷.* 土木学会論文報告集, 1982. **1982**(327): p. 151-162.

18. Guo, D., *Study on Performance Degradation and Remaining Useful Life Prediction for R.C. Bridge near Coastal Areas*. 2014, Zhejiang University.

19. Zhong, Y. and G. Li, *Review of research on concrete for marine works durability* Sichuan Building Science Research, 2007(01): p. 90-95.

20. Neville, A., *Chloride attack of reinforced concrete: an overview.* Materials and Structures, 1995. **28**(2): p. 63.

21. Mansfeld, F.J.C., *Recording and analysis of AC impedance data for corrosion studies.* 1981. **37**(5): p. 301-307.

22. Bremner, T., et al., *Protection of metals in concrete against corrosion*, in *Technical Report for ACI Committee 222: Farmington Hills, MI, USA*. 2001.

23. Czarnecki, L. and P.J.B.o.t.P.A.o.S.T.S. Woyciechowski, *Modelling of concrete carbonation; is it a process unlimited in time and restricted in space?* 2015. **63**(1).

24. 片平博, et al., *土木研究所 「コンクリート構造物の補修対策施工マニュアル (案)」.* 2016. **54**(12): p. 1162-1168.

25. Powers, T.C. *A working hypothesis for further studies of frost resistance of concrete*. in *Journal Proceedings*. 1945.

26. Powers, T.C. and R. Helmuth. *Theory of volume changes in hardened portland-cement paste during freezing*. in *Highway research board proceedings*. 1953.

27. 庄谷征美 and 月.J. コンクリート工学, *東北地方のコンクリート構造物の凍害について.* 2004. **42**(12): p. 3-8.

28. Valenza, J.J. and G.W. Scherer, *Mechanism for salt scaling of a cementitious surface.* Materials and Structures, 2007. **40**(3): p. 259-268.

29. Tsukinaga, Z.M.S.A., *Effect of initial curing conditions on air permeability and deicing salt scaling resistance of surface concrete.* Journal of Asian Concrete Federation, 2019. **5(1)**.

30. Zhao, J.f., et al., *Research Status of Electrochemical Repair Effect of Reinforced Concrete Structure under Chloride Environment.* BULLETIN OF THE CHINESE CEＲAMIC SOCIETY, 2019. **38**(12): p. 3868-3872,3877.

31. Shiba, X.J., Ding, and F. Hsing, *Research s tatus of elect rochemical chloride ext ract ion(ECE) on s teel reinforced concrete.* 2008(09): p. 22-24.

32. Shen, E.B., et al. *A Study on Factors influencing the efficiency of electrochemical desalination in reinforced concrete*. in *Applied Mechanics and Materials*. 2014. Trans Tech Publ.

33. Gao, X.j., X.m. Zheng, and Y.z. Yang, *Influence of electrochemical parameters on chloride extraction efficiency.* Journal of Shenyang University of Technology, 2010. **32**(05): p. 579-584.

34. Ihekwaba, N.M., et al., *Structural shape effect on rehabilitation of vertical concrete structures by ECE technique.* 1996. **26**(1): p. 165-175.

35. Garcés, P., M.S. De Rojas, and M.J.C.S. Climent, *Effect of the reinforcement bar arrangement on the efficiency of electrochemical chloride removal technique applied to reinforced concrete structures.* 2006. **48**(3): p. 531-545.

36. Fajardo, G., G. Escadeillas, and G.J.C.s. Arliguie, *Electrochemical chloride extraction (ECE) from steel-reinforced concrete specimens contaminated by "artificial" sea-water.* 2006. **48**(1): p. 110-125.

37. GB50068, M.J.M.o.H. and H.D. Urban-Rural Construction of the People's Republic of China, Beijing, China, *Unified standard for reliability design of building structures.* 2018.

38. Guo, D.J.Z.U., Hangzhou, China, *Study on Performance Degradation and Remaining Useful Life Prediction for RC Bridge near Coastal Areas.* 2013.

39. Cusson, D., et al., *Benefits of internal curing on service life and life-cycle cost of high-performance concrete bridge decks–A case study.* 2010. **32**(5): p. 339-350.

40. Di-tao ., N., *Durability andLife Forecast of Ｒeinforced Concrete Structure* 2003: Bei-jing: Science Press. p. 164 － 167.

41. Somerville, G., *The design life of structures*. 1991: CRC Press.

42. Jin, W., Q. Lu, and W.J.J.J.X.J.o.B.S. Gan, *Research progress on the durability design and life prediction of concrete structures.* 2007. **28**(1): p. 7-13.

43. Funahashi, M.J.A.M.J., *Predicting corrosion-free service life of a concrete structure.* 1990. **87**: p. M62.

44. Liang, M., et al., *Service life prediction of reinforced concrete structures.* 1999. **29**(9): p. 1411-1418.

45. Yu, H., et al., *Study on prediction of concrete service life I-theoretical model.* 2002. **30**: p. 686-690.

46. Ahmad, S.J.C. and c. composites, *Reinforcement corrosion in concrete structures, its monitoring and service life prediction—a review.* 2003. **25**(4-5): p. 459-471.

47. Berke, N.S., M.C.J.C. Hicks, and C. Composites, *Predicting long-term durability of steel reinforced concrete with calcium nitrite corrosion inhibitor.* 2004. **26**(3): p. 191-198.

48. Liu, H., J. Yao, and D.J.J.o.B.S. Niu, *Durability evaluation and prediction of residual life for existing concrete structures under common atmosphere environment.* 2006. **30**: p. 143-148.

49. Stewart, M.G. and D.V.J.S.s. Rosowsky, *Time-dependent reliability of deteriorating reinforced concrete bridge decks.* 1998. **20**(1): p. 91-109.

50. Xianming, W. and Z.J.J.o.B.S. Hongyan, *Residual Life Prediction of RC Members under Ordinary Atmospheric Environment [J]*. 1996. **3**.

51. Prezzi, M., P. Geyskens, and P.J.J.M.J. Monteiro, *Reliability approach to service life prediction of concrete exposed to marine environments.* 1996. **93**(6): p. 544-552.

52. Du, P., et al., *Research Progress on the Prediction of Concrete's Service Life Based on Freeze-thaw Damage*. Journal of Yangtze River Scientific Research Institute, 2014. **31**(04): p. 77-84.

53. Song, H.-W., et al., *Service life prediction of concrete structures under marine environment considering coupled deterioration.* 2006. **12**(4): p. 265-284.

54. Poulsen, E. and L. Mejlbro, *Diffusion of Chloride in Concrete_ Theory and Application*. 2006: Taylor & Francis.

55. Hongfa, Y., et al., *Study on Prediction OF Concrete Service Life Ⅲ——Evaluation OF Influencing Factors and Service Life*. Journal of the Chinese Ceramic Society, 2002(06): p. 696-701.

56. Recommendation, R.D.J.M. and Structures, *Draft recommendation for repair strategies for concrete structures damaged by reinforcement corrosion.* 1994. **27**(171): p. 415-436.

57. Dinghai, H., *Corrosion and protection of reinforcement in concrete*. China Railway Press.

58. Horiguchi, K., *Evaluation of Initiation Period and Propagation Period of Reinforced Concrete under Chloride Environment by using Proposed Quantitative Methods of Threshold Chloride Ion Content and Corrosion Rate of Steel Bars* in *東北大学.* 2019, 東北大学. p. 1.

59. 卓郎，松.; Available from: https://criepi.denken.or.jp/jp/env/outline/2003/10.pdf.

60. Hirotake, E., K. Yoshimori, and S. Akinori, *The frost and salt damage protective effect of existing concrete by surface penetrants in cold regions*. 2016, 寒地土木研究所月報.

61. Glass, G.K. and N.R.J.C.s. Buenfeld, *The presentation of the chloride threshold level for corrosion of steel in concrete.* 1997. **39**(5): p. 1001-1013.

62. 北後征雄, et al., *電気化学的手法によるコンクリートの改質と補修効果に関する実証的研究.* 2000(641): p. 101-115.

63. Sarja, A. and E. Vesikari, *Durability design of concrete structures*. 2004: CRC Press.

64. 権代，由., et al., *塩化物環境下におけるスケーリング抵抗性の評価試験法に関する基礎的研究.* コンクリート工学論文集, 2009. **20**(1): p. 1_59-1_70.

65. Testing, A.S.f., M.C.C.-o. Concrete, and C. Aggregates, *Standard test method for scaling resistance of concrete surfaces exposed to deicing chemicals*. 2003: ASTM International.

66. Setzer, M.J., et al., *CDF test—Test method for the freeze-thaw resistance of concrete-tests with sodium chloride solution (CDF).* 1996. **29**(9): p. 523-528.

67. Setzer, M.J., R.J.M. Auberg, and Structures, *Freeze-thaw and deicing salt resistance of concrete testing by the CDF method CDF resistance limit and evaluation of precision.* 1995. **28**(1): p. 16-31.

68. 北海道開発局港湾部港湾建設課, *海洋環境下におけるコンクリートの耐 久性向上技術検討業務報告書.* 2003.03, 北海道開発局港湾部港湾建設課-寒地港湾技術研究センター.

69. 遠藤裕丈, et al., *10 数年および約 40 年経過した北海道の港湾コンクリート構造物のスケーリング進行性評価.* 2008. **64**(3): p. 484-499.

70. コンクリートライブラリー，土.J., *自己充てん型高強度高耐久コンクリート構造物 設*

計 施工指針 (案)-新世代交通システム用構造物への試み. 2001. **105**.

71. 洪悦郎, *コンクリートの凍害.* コンクリート工学 1975.03. **13 No.3**: p. 33-44.

72. Hirotake）, 遠.裕.E., et al., *凍結融解と塩化物による複合作用に対するコンクリートの耐久性設計法および表面含浸材を活用した耐久性向上に関する研究*. 2011.03, 寒地土木研究所.

73. 遠藤裕丈, 島多昭典, and 高木典彦, *地域特性を考慮したスケーリング抑制のための適切な水セメント比の設定方法の提案*, in *コンクリート工学年次論文集、Vol.43、No.1、pp.586-591*. 2021.

74. 土木学会, *コンクリート標準示方書［維持管理編］改訂資料*. 2018.10. p. 39.

75. Frangopol, D.M., K.-Y. Lin, and A.C.J.J.o.s.e. Estes, *Life-cycle cost design of deteriorating structures.* 1997. **123**(10): p. 1390-1401.

76. 食料・農業・農村政策審議会 and 農. 技術小委員会, *農業水利施設の機能保全の手引き.* 平成２７年５月.

77. 国土交通省, *公共事業評価の費用便益分析に関する技術指針 (共通編)」 p5*. 2009.

78. の策定について, 農.J.パ., *農業水利施設の機能保全の手引き*. 2015.

79. Sun, W., et al., *Effect of chloride salt, freeze–thaw cycling and externally applied load on the performance of the concrete.* Cement and Concrete Research, 2002. **32**(12): p. 1859-1864.

80. Li, J., et al., *Durability of ultra-high performance concrete – A review.* Construction and Building Materials, 2020. **255**: p. 119296.

81. Frangopol, D.M.J.S. and i. Engineering, *Life-cycle performance, management, and optimisation of structural systems under uncertainty: accomplishments and challenges 1*. 2011. **7**(6): p. 389-413.

82. Habibnejad Korayem, A., et al., *Graphene oxide for surface treatment of concrete: A novel method to protect concrete.* Construction and Building Materials, 2020. **243**: p. 118229.

83. Phoo-ngernkham, T., et al., *Low cost and sustainable repair material made from alkali-activated high-calcium fly ash with calcium carbide residue.* Construction and Building Materials, 2020. **247**: p. 118543.

84. Chakraborty, A.K. and S.J.I.C.J. Mondal, *Bacterial concrete: A way to enhance the durability of concrete structures.* 2017. **91**: p. 30-36.

85. Kim, H., et al., *Recent advances in microbial viability and self-healing performance in bacterial-based cementitious materials: A review.* Construction and Building Materials, 2021. **274**: p. 122094.

86. Pan, X., et al., *A review on concrete surface treatment Part I: Types and mechanisms.* Construction and Building Materials, 2017. **132**: p. 578-590.

87. Sørensen, P.A., et al., *Anticorrosive coatings: a review.* Journal of Coatings Technology and Research, 2009. **6**(2): p. 135-176.

88. Yang, X.F., et al., *Blistering and degradation of polyurethane coatings under different accelerated weathering tests.* Polymer Degradation and Stability, 2002. **77**(1): p. 103-109.

89. Vipulanandan, C. and J. Liu, *Performance of polyurethane-coated concrete in sewer environment.* Cement and Concrete Research, 2005. **35**(9): p. 1754-1763.

90. Hinder, S.J., et al., *Intercoat adhesion failure in a multilayer organic coating system: An X-ray photoelectron spectroscopy study.* Progress in Organic Coatings, 2005. **54**(1): p. 20-27.

91. Perrin, F.X., et al., *Degradation study of polymer coating: Improvement in coating weatherability testing and coating failure prediction.* Progress in Organic Coatings, 2009. **64**(4): p. 466-473.

92. Guo, T. and X. Weng, *Evaluation of the freeze-thaw durability of surface-treated airport pavement concrete under adverse conditions.* Construction and Building Materials, 2019. **206**: p. 519-530.

93. Zhang, P., et al., *Steel reinforcement corrosion in concrete under combined actions: The role of freeze-thaw cycles, chloride ingress, and surface impregnation.* Construction and Building Materials, 2017. **148**: p. 113-121.

94. Liu, Z. and W. Hansen, *Effect of hydrophobic surface treatment on freeze-thaw durability of concrete.* Cement and Concrete Composites, 2016. **69**: p. 49-60.

95. Carneiro, A., et al., *Effectiveness of surface coatings in concrete: chloride penetration and carbonation.* 2021. **6**(1): p. 1-8.

96. 綾野克紀, *けい酸塩系表面含浸材の現状における課題と解決策.* 防水ジャーナル, 2018. **49**(2): p. 21-25.

97. Herb, H., A. Gerdes, and G. Brenner-Weiß, *Characterization of silane-based hydrophobic admixtures in concrete using TOF-MS.* Cement and Concrete Research, 2015. **70**: p. 77-82.

98. 卓見, 荒., et al. *シラン系表面含浸材の表面保護効果に及ぼす温湿度の影響に関する*. in *Proceedings of the Japan Concrete Institue*. 2013. Japan.

99. *JSCE Standards: TEST METHODS OF SILICATE- TYPE SURFACE PENETRANT FOR CONCRETE STRICTURES*. 2012.

100. Torrent, R., et al., *Specification and site control of the permeability of the cover concrete: The Swiss approach.* Materials and Corrosion, 2012. **63**(12): p. 1127-1133.

101. Basheer, P.A.M., et al., *Surface treatments for concrete: assessmentmethods and reported performance.* Construction and Building Materials, 1997. **11**(7): p. 413-429.

102. Coutinho, A. and A.J.L. Gonçalves, Lisbon, Portugal, *Production and properties of concrete (in Portuguese), vol III.* 1993.

103. C, A., et al., *The suitability of the 'TPT' to measure the air-permeability of the covercrete*, in *5th CANMET/ACI international conference on durability of concrete*. 2000: Barcelona, Spain.

104. Neves, R., F. Branco, and J. de Brito, *About the statistical interpretation of air permeability assessment results.* Materials and Structures, 2011. **45**(4): p. 529-539.

105. Kumar, R. and B. Bhattacharjee, *Porosity, pore size distribution and in situ strength of concrete.* Cement and Concrete Research, 2003. **33**(1): p. 155-164.

106. Pan, X., et al., *Effect of Inorganic Surface Treatment on Air Permeability of Cement-Based Materials.* Journal of Materials in Civil Engineering, 2016. **28**(3).

107. Y, Sakoi., A.B.A. M, and T. Y. *Influence of re-application of surface penetrant on progression of carbonation of concrete with surface penetrant*. in *Sixth International Symposium on Life-Cycle Civil Engineering, Life- Cycle Analysis and Assessment in Civil Engineering*. 2018.

108. Y. H, K., Y, Sakoi., et al. *INFLUENCE OF PENETRANT PAINTING AMOUNT AND CURING METHOD ON THE COCRETE SURFACE QURITY*. in *Sixth International Conference on Construction Materials: Performance, Innovations, and Structural Implications*. 2020.

109. *太田晃博 表面含浸材を施行したコンクリートの塩化物環境下におけるスケーリング抵抗性 修士学位論文 平成 23 年度, 八戸工業大学, 日本.*

110. *遠藤裕丈, et al. "4 年の暴露実験に基づく寒冷地の凍結防止剤散布環境下でのコンクリートのスケーリング進行予測に関する研究." 寒地土木技術研究: 国立研究開発法人土木研究所寒地土木研究所月報: monthly report 811 (2020): 11-20.*

111. *遠藤裕丈, 久保善司, and 島多昭典. "寒冷地における表面含浸材による既設コンクリ*

ートの凍・塩害抑制効果." 寒地土木研究所月報 752 (2016): 2-10.

112. Meira, G.R., et al., *Durability of concrete structures in marine atmosphere zones – The use of chloride deposition rate on the wet candle as an environmental indicator.* Cement and Concrete Composites, 2010. **32**(6): p. 427-435.

113. Zuquan, J., et al., *Chloride ions transportation behavior and binding capacity of concrete exposed to different marine corrosion zones.* Construction and Building Materials, 2018. **177**: p. 170-183.

114. Mao, J., et al., *Durability Improvement and service Life Prediction of Reinforced Concrete Under Chloride Attac.* China Jornal of Highway and Transport, 2016. **29**(01): p. 61-66.

115. Hussain, S.E. and A.S.J.M.J. Al-Gahtani, *Chloride threshold for corrosion of reinforcement in concrete.* 1996. **93**(6): p. 534-538.

116. Pettersson, K., *Concrete 2000 (eds. R.K. Dhir and M.R. Jones), Vol. 1, p. 461, E and FN Spon, London.* 1993.

117. Lambert, P., et al., *Investigations of reinforcement corrosion. 2. Electrochemical monitoring of steel in chloride-contaminated concrete.* 1991. **24**(5): p. 351-358.

118. 丈，遠.藤.裕., *シラン系表面含浸材について— 寒冷地での適用の留意点 —.* 2017/09/20.

119. Obla, K.H., H. Kim, and C.L.J.A.i.C.E.M. Lobo, *Criteria for freeze-thaw resistant concrete mixtures.* 2016. **5**(2): p. 119-141.

120. コンクリート橋編, 日., *道路橋示方書・同解説 III*. 2002.03.

121. 北海道土木技術会コンクリート研究委員会 and コンクリート維持管理小委員会, *北海道におけるコンクリート構造物維持管理の手引き（案）*. 平成 18 年 3 月 北海道土木技術会コンクリート研究委員会.

122. Zhao, G., *Reliability Theory and Application of Engineering Structure （translation）*. 1996: Dalian University of Technology Press.

123. Gjørv, O.E., *Durability design of concrete structures in severe environments*. 2009: CRC Press.

124. ENDOH, H., et al., *Effect of surface penetrance （silane type） improving the durability of concrete structure in cold regions* Journal of the Japan Society of Civil Engineers（translated）, 2010. **67**: p. 69-88.

125. Liu, Z. and W. Sun, *Modeling carbonation for corrosion risk service life prediction of concrete under combined action o fdurability factors.* 2003(12): p. 3-7.

126. 林大介, 守屋進, and 杉田好春, *各種浸透性コンクリート保護材の性能に関する実験的検討.* 土木学会コンクリートの表面被覆および表面改質に関するシンポジウム論文集, 2004.2: p. 45-54.

127. 長谷川, 寿., *コンクリートの凍害に対する外的要因の研究.* 1975, 北海道大学.

128. 成田, 健., 慎. 小山, and 博. 三橋, *実構造物群の調査結果に基づく凍害損傷リスクマップの作成に関する研究.* コンクリート工学論文集, 2008. **19**(1): p. 29-38.

129. 成田, 健., 慎. 小山, and 博. 三橋, *実構造物群の調査結果に基づく凍害損傷リスクマップの作成に関する研究.* コンクリート工学論文集 = Concrete research and technology, 2008. **19**(1): p. 29-38.

130. 寒地港湾技術研究センター, 北., *海洋環境下におけるコンクリートの耐久性向上技術検討業務報告書.* 北海道開発局港湾部港湾建設課、 寒地港湾技術研究センター, 2000.3.

131. 池, 翰., et al., *凍結融解作用を受けるコンクリートの凍害深さに関する一考察.* コンクリート工学年次論文集, 2006. **28**(1): p. 725-730.

132. 佐伯昇, 鮎田耕一, and 前.J. 土木学会論文報告集, *北海道における海岸および港湾コンクリート構造物の凍害による表面剥離損傷.* 1982. **1982**(327): p. 151-162.

133. 遠藤裕丈, 安中新太郎, and 高木典彦, *北海道の凍結防止剤散布環境下での凍害暴露実験 2 冬までの評価.* コンクリート工学年次論文集, 2019. **41-1**: p. 4.

134. 遠藤裕丈, et al., *建設から 10 数年経過したコンクリート防波堤での表面剥離調査.* 2005(622): p. 14-22.

135. 温品達也, et al., *表層透気試験で得られたコンクリート表層品質の判定結果に関する一考察*, in *コンクリート工学年次論文集(CD-ROM)*. 2012. p. ROMBUNNO.1282.

136. 上東泰, *橋梁構造物の耐久性向上に関する実践的研究.* 2015.

APPENDED TABLES AND GRAPHS

I Appended Tables For Chapter 5

Appended Table 1 Cumulative scaling depth of the 3rd year（mm)

Cycle	N@3	N+3rd TC	1st TC@3	1st TC+3rd TC
0	0.333	0.333	0.000	0.000
5	0.418	0.333	0.000	0.000
10	0.481	0.333	0.000	0.000
15	0.503	0.333	0.005	0.000
20	0.577	0.333	0.016	0.003
25	0.625	0.333	0.037	0.005
30	0.635	0.333	0.053	0.005
40	0.656	0.333	0.080	0.011
50	0.693	0.333	0.101	0.011

Appended Table 2 Cumulative scaling depth of the 12th year (mm)

Group	Cycle	N①	N②	Mean	Standard deviation
N@12	0	0.500	0.500	0.500	0.000
	5	0.524	0.512	0.518	0.008
	10	0.557	0.527	0.542	0.021
	15	0.575	0.533	0.554	0.030
	20	0.575	0.545	0.560	0.021
	25	0.614	0.554	0.584	0.042
	30	0.638	0.566	0.602	0.051
	35	0.665	0.566	0.615	0.070

	40	0.683	0.572	0.627	0.078	
	45	0.704	0.584	0.644	0.085	
	50	0.713	0.584	0.648	0.091	
	55	0.725	0.602	0.663	0.087	
	60	0.758	0.611	0.684	0.104	
	65	0.773	0.614	0.693	0.112	
	70	0.791	0.623	0.707	0.119	
	75	0.806	0.638	0.722	0.119	
	80	0.809	0.638	0.723	0.121	

Group	Cycle	N①	N②	N③	Mean	Standard deviation
N+12th TC	0	0.500	0.500	0.500	0.500	0.000
	5	0.503	0.506	0.509	0.506	0.003
	10	0.503	0.506	0.509	0.506	0.003
	15	0.503	0.506	0.509	0.506	0.003
	20	0.509	0.512	0.515	0.512	0.003
	25	0.518	0.524	0.563	0.535	0.024
	30	0.524	0.524	0.569	0.539	0.026
	35	0.530	0.530	0.569	0.543	0.023
	40	0.536	0.533	0.575	0.548	0.023
	45	0.542	0.539	0.584	0.555	0.025
	50	0.548	0.542	0.590	0.560	0.026
	55	0.551	0.545	0.608	0.568	0.035
	60	0.557	0.548	0.617	0.574	0.037
	65	0.557	0.548	0.617	0.574	0.037

	70	0.557	0.548	0.617	0.574	0.037
	75	0.557	0.548	0.617	0.574	0.037
	80	0.557	0.548	0.617	0.574	0.037

Group	Cycle	TC①	TC②	Mean	Standard deviation
1st TC @12	0	0.000	0.000	0.000	0.000
	5	0.003	0.009	0.006	0.007
	10	0.015	0.021	0.018	0.007
	15	0.018	0.036	0.027	0.022
	20	0.042	0.054	0.048	0.014
	25	0.210	0.207	0.208	0.004
	30	0.510	0.342	0.426	0.203
	35	0.777	0.471	0.624	0.369
	40	0.930	0.654	0.792	0.333
	45	1.023	0.783	0.903	0.290
	50	1.128	0.960	1.044	0.203
	55	1.248	1.146	1.197	0.123
	60	1.362	1.242	1.302	0.145
	65	1.431	1.320	1.375	0.134
	70	1.506	1.335	1.420	0.206
	75	1.542	1.368	1.455	0.210
	80	1.545	1.368	1.456	0.214

Group	Cycle	TC①	TC②	TC③	TC④	Mean	Standard deviation
1stTC + 12th	0	0.000	0.000	0.000	0.000	0.000	0.000
	5	0.009	0.003	0.006	0.006	0.006	0.005

TC	10	0.009	0.003	0.006	0.009	0.007	0.005
	15	0.009	0.003	0.009	0.024	0.011	0.017
	20	0.018	0.009	0.018	0.039	0.021	0.024
	25	0.027	0.021	0.021	0.054	0.031	0.029
	30	0.030	0.021	0.309	0.063	0.106	0.255
	35	0.045	0.042	0.588	0.069	0.186	0.500
	40	0.069	0.117	0.603	0.462	0.313	0.487
	45	0.090	0.198	0.861	0.666	0.454	0.688
	50	0.282	0.357	0.921	0.690	0.562	0.555
	55	0.609	0.498	1.074	0.774	0.739	0.468
	60	0.798	0.744	1.197	0.801	0.885	0.391
	65	0.936	0.906	1.263	0.825	0.982	0.360
	70	1.041	1.032	1.299	0.843	1.053	0.349
	75	1.116	1.137	1.326	0.849	1.107	0.366
	80	1.158	1.203	1.344	0.855	1.140	0.384

Appended Table 3 Cumulative scaling depth of the 20th year 20th year（mm)

Group	Cycle	N1	N2	N3	Mean	Standard deviation
N@20	0	5.000	5.000	5.000	5.000	0.000
	5	5.009	5.005	5.075	5.030	0.039
	20	5.026	5.017	5.148	5.064	0.073
	25	5.034	5.021	5.167	5.074	0.081
	40	5.053	5.047	5.220	5.106	0.098

---------	45	5.063	5.057	5.238	5.119	0.103
	55	5.081	5.085	5.256	5.141	0.100
	60	5.098	5.100	5.271	5.156	0.099
	65	5.111	5.121	5.285	5.172	0.098
	70	5.124	5.146	5.297	5.189	0.094
	75	5.142	5.167	5.308	5.206	0.089
	80	5.150	5.226	5.316	5.231	0.083

Group	Cycle	N4	N5	N6	Mean	Standard deviation
① N+20th TC+water curing	0	5.000	5.000	5.000	5.000	0.000
	5	5.004	5.007	5.013	5.008	0.005
	20	5.012	5.026	5.084	5.041	0.038
	25	5.014	5.049	5.103	5.055	0.045
	40	5.028	5.061	5.169	5.086	0.074
	45	5.033	5.067	5.192	5.097	0.084
	55	5.040	5.072	5.219	5.110	0.095
	60	5.047	5.077	5.251	5.125	0.110
	65	5.050	5.079	5.274	5.135	0.122
	70	5.056	5.082	5.312	5.150	0.141
	75	5.061	5.085	5.333	5.160	0.150
	80	5.064	5.088	5.381	5.178	0.176

Group	Cycle	N7	N8	N9	Mean	Standard deviation
② N+20th TC+no water	0	5.000	5.000	5.000	5.000	0.000
	5	5.006	5.008	5.010	5.008	0.002
	20	5.018	5.012	5.023	5.018	0.006

curing	25	5.022	5.018	5.030	5.023	0.006
	40	5.043	5.026	5.048	5.039	0.012
---------	45	5.059	5.039	5.069	5.056	0.015
	55	5.064	5.054	5.094	5.071	0.021
	60	5.108	5.062	5.108	5.092	0.027
	65	5.140	5.070	5.118	5.109	0.036
	70	5.207	5.074	5.136	5.139	0.067
	75	5.227	5.082	5.157	5.155	0.073
	80	5.234	5.088	5.174	5.165	0.074

Group	Cycle	TC1	TC2	TC3	Mean	Standard deviation
1st TC@20	0	1.000	1.000	1.000	1.000	0.000
	5	1.021	1.035	1.044	1.034	0.011
	20	1.057	1.051	1.289	1.132	0.136
	25	1.089	1.096	1.367	1.184	0.159
	40	1.122	1.767	1.664	1.517	0.347
	45	1.166	2.004	1.748	1.639	0.430
	55	1.226	2.488	1.903	1.872	0.632
	60	1.254	2.632	1.981	1.956	0.689
	65	1.284	2.719	2.065	2.022	0.718
	70	1.338	2.771	2.106	2.072	0.717
	75	1.368	2.830	2.146	2.115	0.732
	80	1.387	2.852	2.204	2.147	0.734

Group	Cycle	TC4	TC5	TC6	Mean	Standard deviation
① 1st	0	1.000	1.000	1.000	1.000	0.000

Group	Cycle	TC7	TC8	TC9	Mean	Standard deviation
TC+20th TC+water curing	5	1.008	1.008	1.009	1.008	0.000
	20	1.018	1.024	1.017	1.020	0.004
	25	1.022	1.035	1.023	1.027	0.007
	40	1.045	1.049	1.041	1.045	0.004
	45	1.055	1.057	1.053	1.055	0.002
	55	1.070	1.077	1.087	1.078	0.008
	60	1.079	1.090	1.106	1.092	0.013
	65	1.108	1.100	1.148	1.118	0.026
	70	1.123	1.110	1.194	1.143	0.045
	75	1.146	1.130	1.286	1.187	0.086
	80	1.181	1.172	1.505	1.286	0.189

Group	Cycle	TC7	TC8	TC9	Mean	Standard deviation
② 1stTC+20th TC+no water curing	0	1.000	1.000	1.000	1.000	0.000
	5	1.007	1.007	1.015	1.010	0.004
	20	1.026	1.021	1.036	1.028	0.008
	25	1.044	1.028	1.047	1.040	0.010
	40	1.102	1.043	1.074	1.073	0.029
	45	1.231	1.054	1.098	1.128	0.092
	55	1.675	1.066	1.175	1.305	0.325
	60	1.766	1.071	1.228	1.355	0.365
	65	1.838	1.073	1.317	1.409	0.391
	70	1.975	1.076	1.586	1.546	0.451
	75	2.076	1.080	1.876	1.677	0.527
	80	2.185	1.083	2.285	1.851	0.667

Notes:

1^{st}, $12^{th,}$ and 20^{th} represent the first year, the 12th year, and the 20th year respectively.

N: No treatment.

TC: Treatment。

N/1st TC@12/20: The untreated group or Treated group was tested as it was in the 12^{th} or 20^{th} year.

N+12^{th} TC: The untreated groups applied penetrants at the 12^{th} year.

N+20^{th} TC+no water curing: The untreated groups applied penetrants at the 20^{th} year and after treatment without water curing.

1^{st} TC+20^{th} TC + water curing: Penetrants were applied in the first year and re-applied in the 20^{th} year after treatment with water curing.

The rest of the labels have similar meanings.

II Appended Tables For Chapter 6

Appended Table 4 LCC of all the groups (cover 50-90mm)—Case A and Case B

Group				**N-Based 12th Cl-**	
Cover (mm)				**50**	
The life span of A1.2				17	
The life span of B1.2				-	
Min（A1.2,B1.2）				17	
Repair start time: after construction				12	
Maintenance hold time				15	
Construction time				2000	
Maintenance Details	Maintenance year	One-time maintenance cost(yen/m^2)	t from 2020	Discount Rate of t year	Present value of one-time maintenance(yen/m^2)

	2012	8500	-8	1.369	11632.84
	2027	8500	7	0.760	6459.30
	2042	8500	22	0.422	3586.62
	2057	8500	37	0.234	1991.52
	2072	8500	52	0.130	1105.82
	2087	8500	67	0.072	614.02
	2102	8500	82	0.040	340.95
Total (present value) ① (yen/m^2)					**25731.07**
Durable year-end	2102				
T_P	13				
T_D	15				
Survival value (present value)(yen/m^2)					**48.73**
LCC (①-②) (yen/m^2)					**25682.34**

Group					**N-Based 12th Cl-**
Cover (mm)					**60**
The life span of A1.2					18
Life span of B1.2					21
Min（A1.2,B1.2）					18
Repair start time: after construction					17
Maintenance hold time					15
Construction time					2000
Maintenance Details	Maintenance year	One-time maintenance cost(yen/m^2)	t from 2020	Discount Rate of t year	Present value of one-time maintenance(yen/m^2)
	2017	8500	-3	1.125	9561.34
	2032	8500	12	0.625	5309.07
	2047	8500	27	0.347	2947.94
	2062	8500	42	0.193	1636.89
	2077	8500	57	0.107	908.91
	2092	8500	72	0.059	504.68
	2107	8500	87	0.033	280.23
Total (present value) ① (yen/m^2)					**21149.07**
Durable year-end	2107				
T_P	8				
T_D	15				
Survival value (present value)(yen/m^2)					**170.57**

LCC (①-②) (yen/m²)	**20978.50**

Group					**N-Based 12th Cl-**
Cover (mm)					**70**
The life span of A1.2					24
Life span of B1.2					24
Min（A1.2,B1.2）					24
Repair start time: after construction					18
Maintenance hold time					15
Construction time					2000
Maintenance Details	Maintenance year	One-time maintenance cost(yen/m²)	t from 2020	Discount Rate of t year	Present value of one-time maintenance(yen/m²)
	2018	8500	-2	1.082	9193.60
	2033	8500	13	0.601	5104.88
	2048	8500	28	0.333	2834.56
	2063	8500	43	0.185	1573.93
	2078	8500	58	0.103	873.95
	2093	8500	73	0.057	485.27
	2108	8500	88	0.032	269.45
Total (present value) ① (yen/m²)					**20335.64**
Durable year-end	2108				
T_P	7				
T_D	15				
Survival value (present value)(yen/m²)					**194.93**
LCC (①-②) (yen/m²)					**20140.71**

Group					**N-Based 12th Cl-**
Cover (mm)					**80**
The life span of A1.2					32
Life span of B1.2					27
Min（A1.2,B1.2）					27
Repair start time: after construction					24
Maintenance hold time					15
Construction time					2000
Maintenance Details	Maintenance year	One-time maintenance cost(yen/m²)	t from 2020	Discount Rate of t year	Present value of one-time maintenance(yen/m²)

	2024	8500	4	0.855	7265.84
	2039	8500	19	0.475	4034.46
	2054	8500	34	0.264	2240.19
	2069	8500	49	0.146	1243.90
	2084	8500	64	0.081	690.69
	2099	8500	79	0.045	383.52
Total (present value) ① (yen/m^2)					**15858.60**
Durable year-end	2114				
T_P	1				
T_D	15				
Survival value (present value)(yen/m^2)					**341.13**
LCC (①-②) (yen/m^2)					**15517.47**

Group					**N-Based 12th Cl-**
Cover (mm)					**90**
The life span of A1.2					40
Life span of B1.2					31
Min（A1.2,B1.2）					31
Repair start time: after construction					27
Maintenance hold time					15
Construction time					2000
Maintenance Details	Maintenance year	One-time maintenance cost(yen/m^2)	t from 2020	Discount Rate of t year	Present value of one-time maintenance(yen/m^2)
	2027	4900	7	0.760	3723.60
	2042	4900	22	0.422	2067.58
	2057	4900	37	0.234	1148.05
	2072	4900	52	0.130	637.47
	2087	4900	67	0.072	353.97
Total (present value) ① (yen/m^2)					**7930.67**
Durable year-end	2102				
T_P	13				
T_D	15				
Survival value (present value)(yen/m^2)					**48.73**
LCC (①-②) (yen/m^2)					**7881.94**

Group	**TC-Based 12th Cl-**

Cover (mm)					**50**
The life span of A1.2					21
Life span of B1.2					23
Min（A1.2,B1.2）					21
Repair start time: after construction					15
Maintenance hold time					15
Construction time					2000
Maintenance Details	Maintenance year	One-time maintenance cost(yen/m^2)	t from 2020	Discount Rate of t year	Present value of one-time maintenance(yen/m^2)
	2015	4900	-5	1.217	5961.60
	2030	4900	10	0.676	3310.26
	2045	4900	25	0.375	1838.07
	2060	4900	40	0.208	1020.62
	2075	4900	55	0.116	566.71
	2090	4900	70	0.064	314.68
Total (present value) ① (yen/m^2)					**13011.94**
Durable year-end	2105				
T_P	10				
T_D	21				
Survival value (present value)(yen/m^2)					**110.37**
LCC (①-②) (yen/m^2)					**12946.61**

Group					**TC-Based 12th Cl-**
Cover (mm)					**60**
The life span of A1.2					24
Life span of B1.2					27
Min（A1.2,B1.2）					24
Repair start time: after construction					21
Maintenance hold time					21
Construction time					2000
Maintenance Details	Maintenance year	One-time maintenance cost(yen/m^2)	t from 2020	Discount Rate of t year	Present value of one-time maintenance(yen/m^2)
	2021	4900	1	0.962	4711.54
	2042	4900	22	0.422	2067.58
	2063	4900	43	0.185	907.32
	2084	4900	64	0.081	398.16

Total (present value) ① (yen/m²)					**8084.61**
Durable year-end	2105				
T_P	16				
T_D	24				
Survival value (present value)(yen/m²)					**70.23**
LCC (①-②) (yen/m²)					**8037.94**

Group					**TC-Based 12th Cl-**
Cover (mm)					**70**
The life span of A1.2					32
Life span of B1.2					33
Min（A1.2,B1.2）					32
Repair start time: after construction					24
Maintenance hold time					24
Construction time					2000
Maintenance Details	Maintenance year	One-time maintenance cost(yen/m²)	t from 2020	Discount Rate of t year	Present value of one-time maintenance(yen/m²)
	2024	4900	4	0.855	4188.54
	2048	4900	28	0.333	1634.04
	2072	4900	52	0.130	637.47
	2096	4900	76	0.051	248.69
Total (present value) ① (yen/m²)					**6708.75**
Durable year-end	2120				
T_P	4				
T_D	32				
Survival value (present value)(yen/m²)					**184.36**
LCC (①-②) (yen/m²)					**6545.41**

Group	**TC-Based 12th Cl-**
Cover (mm)	**80**
The life span of A1.2	42
Life span of B1.2	39
Min（A1.2,B1.2）	39
Repair start time: after construction	32
Maintenance hold time	32
Construction time	2000

Maintenance Details	Maintenance year	One-time maintenance cost(yen/m^2)	t from 2020	Discount Rate of t year	Present value of one-time maintenance(yen/m^2)
	2032	4900	12	0.625	3060.53
	2064	4900	44	0.178	872.43
	2096	4900	76	0.051	248.69
Total (present value) ① (yen/m^2)					**4181.64**
Durable year-end	2128				
T_P	4				
T_D	39				
Survival value (present value)(yen/m^2)					**189.09**
LCC (①-②) (yen/m^2)					**4010.14**

Group	**TC-Based 12th Cl-**
Cover (mm)	**90**
The life span of A1.2	54
Life span of B1.2	46
Min（A1.2,B1.2）	46
Repair start time: after construction	39
Maintenance hold time	39
Construction time	2000

Maintenance Details	Maintenance year	One-time maintenance cost(yen/m^2)	t from 2020	Discount Rate of t year	Present value of one-time maintenance(yen/m^2)
	2039	4900	19	0.475	2325.75
	2078	4900	58	0.103	503.80
Total (present value) ① (yen/m^2)					**2829.55**
Durable year-end	2117				
T_P	22				
T_D	46				
Survival value (present value)(yen/m^2)					**109.93**
LCC (①-②) (yen/m^2)					**2744.12**

Notes:

① Plan B (Case B) was used to repair untreated groups (N- groups);

② Plan A (Case A) was still used to repair the treatment (TC- groups).

Appended Table 5 LCC of all the allowable scaling depth

Group		N			N		
Scaling depth limit (mm)		2.5			5-①		
Lifetime (Take an integer*) (year)		11.17 (10)			22.35（20）		
Year	Service year	Plan	Cost (yen/m^2)	Cost –PV (yen/m^2)	Plan	Cost (yen/m^2)	Cost –PV (yen/m^2)
2000	0						
2003	3						
2005	5						
2010	10	A	4900	7253			
2012	12						
2015	15						
2020	20				I (D+A)	104900	104900
2025	25						
2030	30						
2035	35						
2040	40	A	4900	2236			
2045	45						
2050	50						
2055	55						
2060	60						
2065	65						
2070	70	A	4900	689			
2075	75						
2080	80						
2085	85				A	4900	383
2090	90						
2095	95						
2100	100						
Total (PV) (yen/m2) ①				**10179**			**105283**
T_P				30			15
T_D				30			65
Survival value(PV) (yen/m^2) ②				**0**			**164**
LCC(①-②) (yen/m^2)				**10179**			**105119**

Group		N			N		
Scaling depth limit (mm)		5-②			10		
Lifetime (Take an integer*) (year)		22.35（20）			59.67（55）		
Year	Service year	Plan	Cost (yen/m²)	Cost –PV (yen/m²)	Plan	Cost (yen/m²)	Cost –PV (yen/m²)
2000	0						
2003	3						
2005	5						
2010	10						
2012	12						
2015	15						
2020	20	D	100000	100000			
2025	25						
2030	30						
2035	35						
2040	40	D	100000	45639			
2045	45						
2050	50				D	100000	30832
2055	55						
2060	60	D	100000	20829			
2065	65						
2070	70						
2075	75						
2080	80	D	100000	9506			
2085	85						
2090	90						
2095	95						
2100	100						
Total (PV) (yen/m2) ①				**175974**			**30832**
T_P				20			20
T_D				20			55
Survival value(PV) (yen/m²) ②				**0**			**135**
LCC(①-②) (yen/m²)				**175974**			**30697**

Group	N	1st TC

Scaling depth limit (mm)		20			2.5		
Lifetime (Take an integer*) (year)		109.73（105）			33.91（30）		
Year	Service year	Plan	Cost (yen/m^2)	Cost –PV (yen/m^2)	Plan	Cost (yen/m^2)	Cost –PV (yen/m^2)
2000	0				A	4900	10737
2003	3						
2005	5						
2010	10						
2012	12						
2015	15						
2020	20						
2025	25						
2030	30				A	4900	3310
2035	35						
2040	40						
2045	45						
2050	50						
2055	55						
2060	60				A	4900	1021
2065	65						
2070	70						
2075	75						
2080	80						
2085	85						
2090	90				A	4900	315
2095	95						
2100	100						
Total (PV) (yen/m2) ①				**0**			**15382**
T_P							10
T_D							30
Survival value(PV) (yen/m^2) ②				**0**			**142**
LCC(①-②) (yen/m^2)				**0**			**15240**

Group	**1st TC**	**1st TC**
Scaling depth limit (mm)	5-①	5-②

Lifetime (Take an integer*) (year)		67.82（65）			67.82（65）		
Year	Service year	65	Cost (yen/m^2)	Cost –PV (yen/m^2)	Plan	Cost (yen/m^2)	Cost –PV (yen/m^2)
2000	0	A	4900	10737	A	4900	10737
2003	3						
2005	5						
2010	10						
2012	12						
2015	15						
2020	20						
2025	25						
2030	30						
2035	35						
2040	40						
2045	45						
2050	50						
2055	55						
2060	60						
2065	65	I (D+A)	104900	17959	D	100000	17120
2070	70						
2075	75						
2080	80						
2085	85				D	100000	7813
2090	90						
2095	95						
2100	100						
Total (PV) (yen/m2) ①				**28695**			**35670**
T_P				35			15
T_D				65			20
Survival value(PV) (yen/m^2) ②				**98**			**53**
LCC(①-②) (yen/m^2)				**28597**			**35616**

Group	**1st TC**	**1st TC**
Scaling depth limit (mm)	10	20

Lifetime (Take an integer*) (year)		124.92（120）			239.11（235）		
Year	Service year	Plan	Cost (yen/m^2)	Cost –PV (yen/m^2)	Plan	Cost (yen/m^2)	Cost –PV (yen/m^2)
2000	0	A	4900	10737	A	4900	10737
2003	3						
2005	5						
2010	10						
2012	12						
2015	15						
2020	20						
2025	25						
2030	30						
2035	35						
2040	40						
2045	45						
2050	50						
2055	55						
2060	60						
2065	65						
2070	70						
2075	75						
2080	80						
2085	85						
2090	90						
2095	95						
2100	100						
Total (PV) (yen/m2) ①				**10737**			**10737**
T_P				100			100
T_D				120			235
Survival value(PV) (yen/m^2) ②				**35**			**122**
LCC(①-②) (yen/m^2)				**10701**			**10614**

Group	**N+3rd TC**	**N+3rd TC**
Scaling depth limit (mm)	2.5	5-①
Lifetime (Take an integer*) (year)	33.91（30）	67.82（65）

Year	Service year	Plan	Cost (yen/m²)	Cost –PV (yen/m²)	65	Cost (yen/m²)	Cost –PV (yen/m²)
2000	0						
2003	3	A	4900	9545	A	4900	9545
2005	5						
2010	10						
2012	12						
2015	15						
2020	20						
2025	25						
2030	30	A	4900	3310			
2035	35						
2040	40						
2045	45						
2050	50						
2055	55						
2060	60	A	4900	1021			
2065	65				I (D+A)	104900	17959
2070	70						
2075	75						
2080	80						
2085	85						
2090	90	A	4900	315			
2095	95						
2100	100						
Total (PV) (yen/m2) ①				**14190**			**27503**
T_P				10			35
T_D				30			65
Survival value(PV) (yen/m²) ②				**142**			**98**
LCC(①-②) (yen/m²)				**14049**			**27405**

Group	**N+3rd TC**	**N+3rd TC**
Scaling depth limit (mm)	5-②	10
Lifetime (Take an integer*) (year)	67.82（65）	124.92（120）

Year	Service year	Plan	Cost (yen/m^2)	Cost –PV (yen/m^2)	Plan	Cost (yen/m^2)	Cost –PV (yen/m^2)
2000	0						
2003	3	A	4900	9545	A	4900	9545
2005	5						
2010	10						
2012	12						
2015	15						
2020	20						
2025	25						
2030	30						
2035	35						
2040	40						
2045	45						
2050	50						
2055	55						
2060	60						
2065	65	D	100000	17120			
2070	70						
2075	75						
2080	80						
2085	85	D	100000	7813			
2090	90						
2095	95						
2100	100						
Total (PV) (yen/m2) ①				**34478**			**9545**
T_P				15			100
T_D				20			120
Survival value(PV) (yen/m^2) ②				**53**			**35**
LCC(①-②) (yen/m^2)				**34425**			**9509**

Group	**N+3rd TC**			**1st TC+3rd TC**		
Scaling depth limit (mm)	20			2.5		
Lifetime (Take an integer*) (year)	239.11（235）			260.05（260）		

Year	Service year	Plan	Cost (yen/m^2)	Cost –PV (yen/m^2)	Plan	Cost (yen/m^2)	Cost –PV (yen/m^2)

2000	0				A	4900	10737
2003	3	A	4900	9545	A	4900	9545
2005	5						
2010	10						
2012	12						
2015	15						
2020	20						
2025	25						
2030	30						
2035	35						
2040	40						
2045	45						
2050	50						
2055	55						
2060	60						
2065	65						
2070	70						
2075	75						
2080	80						
2085	85						
2090	90						
2095	95						
2100	100						
Total (PV) (yen/m2) ①				**9545**			**20281**
T_P				100			97
T_D				235			260
Survival value(PV) (yen/m^2) ②				**122**			**133**
LCC(①-②) (yen/m^2)				**9423**			**20148**

Group		**1st TC+3rd TC**			**1st TC+3rd TC**		
Scaling depth limit (mm)		5			10		
Lifetime (Take an integer*) (year)		266.05（265）			323.15（320）		
Year	Service year	Plan	Cost (yen/m^2)	Cost –PV (yen/m^2)	Plan	Cost (yen/m^2)	Cost –PV (yen/m^2)
2000	0	A	4900	10737	A	4900	10737
2003	3	A	4900	9545	A	4900	9545

2005	5						
2010	10						
2012	12						
2015	15						
2020	20						
2025	25						
2030	30						
2035	35						
2040	40						
2045	45						
2050	50						
2055	55						
2060	60						
2065	65						
2070	70						
2075	75						
2080	80						
2085	85						
2090	90						
2095	95						
2100	100						
Total (PV) (yen/m2) ①				**20281**			**20281**
T_P				97			97
T_D				265			320
Survival value(PV) (yen/m^2) ②				**135**			**148**
LCC(①-②) (yen/m^2)				**20146**			**20133**

Group		**1st TC+3rd TC**			**N+12th TC**		
Scaling depth limit (mm)		20			2.5		
Lifetime (Take an integer*) (year)		437.35（435）			83.24（80）		
Year	Service year	Plan	Cost (yen/m^2)	Cost –PV (yen/m^2)	Plan	Cost (yen/m^2)	Cost –PV (yen/m^2)
2000	0	A	4900	10737			
2003	3	A	4900	9545			
2005	5						
2010	10						

2012	12				A	4900	6706
2015	15						
2020	20						
2025	25						
2030	30						
2035	35						
2040	40						
2045	45						
2050	50						
2055	55						
2060	60						
2065	65						
2070	70						
2075	75						
2080	80						
2085	85						
2090	90				A	4900	315
2095	95						
2100	100						
Total (PV) (yen/m2) ①				**20281**			**7021**
T_P				97			10
T_D				435			30
Survival value(PV) (yen/m^2) ②				**165**			**142**
LCC(①-②) (yen/m^2)				**20116**			**6879**

Group		**N+12th TC**			**N+12th TC**		
Scaling depth limit (mm)		5			10		
Lifetime (Take an integer*) (year)		85.31（85）			170.95（170）		
Year	Service year	Plan	Cost (yen/m^2)	Cost –PV (yen/m^2)	Plan	Cost (yen/m^2)	Cost –PV (yen/m^2)
2000	0						
2003	3						
2005	5						
2010	10						
2012	12	A	4900	6706	A	4900	6706
2015	15						

2020	20						
2025	25						
2030	30						
2035	35						
2040	40						
2045	45						
2050	50						
2055	55						
2060	60						
2065	65						
2070	70						
2075	75						
2080	80						
2085	85						
2090	90						
2095	95	D	100000	5278			
2100	100						
Total (PV) (yen/m2) ①				**11984**			**6706**
T_P				5			80
T_D				20			170
Survival value(PV) (yen/m²) ②				**159**			**113**
LCC(①-②) (yen/m²)				**11825**			**6593**

Group		**N+12th TC**			**1st TC+12th TC**		
Scaling depth limit (mm)		20			2.5		
Lifetime (Take an integer*) (year)		285.15（285）			38.78（35）		
Year	Service year	Plan	Cost (yen/m²)	Cost –PV (yen/m²)	Plan	Cost (yen/m²)	Cost –PV (yen/m²)
2000	0				A	4900	10737
2003	3						
2005	5						
2010	10						
2012	12	A	4900	6706	A	4900	6706
2015	15						
2020	20						
2025	25						
2030	30						

2035	35						
2040	40						
2045	45				A	4900	1838
2050	50						
2055	55						
2060	60						
2065	65						
2070	70						
2075	75				A	4900	567
2080	80						
2085	85						
2090	90						
2095	95						
2100	100						
Total (PV) (yen/m2) ①				**6706**			**19847**
T_P				80			25
T_D				285			30
Survival value(PV) (yen/m²) ②				**153**			**35**
LCC(①-②) (yen/m²)				**6553**			**19812**

Group		**1st TC+12th TC**			**1st TC+12th TC**		
Scaling depth limit (mm)		5			10		
Lifetime (Take an integer*) (year)		105.72（105）			162.82（160）		
Year	Service year	Plan	Cost (yen/m²)	Cost –PV (yen/m²)	Plan	Cost (yen/m²)	Cost –PV (yen/m²)
2000	0	A	4900	10737	A	4900	10737
2003	3						
2005	5						
2010	10						
2012	12	A	4900	6706	A	4900	6706
2015	15						
2020	20						
2025	25						
2030	30						
2035	35						
2040	40						

2045	45						
2050	50						
2055	55						
2060	60						
2065	65						
2070	70						
2075	75						
2080	80						
2085	85						
2090	90						
2095	95						
2100	100						
Total (PV) (yen/m2) ①				**17442**			**17442**
T_P				88			88
T_D				105			160
Survival value(PV) (yen/m²) ②				**34**			**96**
LCC(①-②) (yen/m²)				**17408**			**17347**

Group		**1st TC+12th TC**			**N+20th TC**		
Scaling depth limit (mm)		20			2.5-①		
Lifetime (Take an integer*) (year)		277.01（275）			11.17（10）		
Year	Service year	Plan	Cost (yen/m²)	Cost –PV (yen/m²)	Plan	Cost (yen/m²)	Cost –PV (yen/m²)
2000	0	A	4900	10737			
2003	3						
2005	5						
2010	10						
2012	12	A	4900	6706			
2015	15						
2020	20				A	4900	4900
2025	25						
2030	30				A	4900	3310
2035	35						
2040	40				A	4900	2236
2045	45						
2050	50				A	4900	1511

2055	55						
2060	60				A	4900	1021
2065	65						
2070	70				A	4900	689
2075	75						
2080	80				A	4900	466
2085	85						
2090	90				A	4900	315
2095	95						
2100	100						
Total (PV) (yen/m2) ①				**17442**			**14448**
T_P				88	10		10
T_D				275	10		10
Survival value(PV) (yen/m²) ②				**145**			**0**
LCC(①-②) (yen/m²)				**17298**			**14448**

Group		**N+20th TC**			**N+20th TC**		
Scaling depth limit (mm)		2.5-②			5-①		
Lifetime (Take an integer*) (year)		11.17（10）			22.35（20）		
Year	Service year	Plan	Cost (yen/m²)	Cost –PV (yen/m²)	Plan	Cost (yen/m²)	Cost –PV (yen/m²)
2000	0						
2003	3						
2005	5						
2010	10						
2012	12						
2015	15						
2020	20	A	4900	4900	A	4900	4900
2025	25						
2030	30	I (D+A)	104900	70867			
2035	35						
2040	40				I (D+A)	104900	47875
2045	45						
2050	50						

2055	55						
2060	60	A	4900	1021			
2065	65						
2070	70				A	4900	689
2075	75						
2080	80						
2085	85						
2090	90	A	4900	315			
2095	95						
2100	100						
Total (PV) (yen/m2) ①				**77102**			**53464**
T_P				10			30
T_D				30			65
Survival value(PV) (yen/m²) ②				**142**			**114**
LCC(①-②) (yen/m²)				**76960**			**53350**

Group		**N+20th TC**			**N+20th TC**		
Scaling depth limit (mm)		5-②			10		
Lifetime (Take an integer*) (year)		22.35（20）			141.77（140）		
Year	Service year	Plan	Cost (yen/m²)	Cost –PV (yen/m²)	Plan	Cost (yen/m²)	Cost –PV (yen/m²)
2000	0						
2003	3						
2005	5						
2010	10						
2012	12						
2015	15						
2020	20	A	4900	4900	A	4900	4900
2025	25						
2030	30						
2035	35						
2040	40	D	100000	45639			
2045	45						
2050	50						
2055	55						
2060	60	D	100000	20829			

2065	65						
2070	70						
2075	75						
2080	80	D	100000	9506			
2085	85						
2090	90						
2095	95						
2100	100						
Total (PV) (yen/m2) ①				**80874**			**4900**
T_P				20			80
T_D				20			140
Survival value(PV) (yen/m^2) ②				**0**			**91**
LCC(①-②) (yen/m^2)				**80874**			**4809**

Group		**N+20th TC**			**1st TC+20th TC**		
Scaling depth limit (mm)		20			2.5		
Lifetime (Take an integer*) (year)		170.31（170）			42.78（40）		
Year	Service year	Plan	Cost (yen/m^2)	Cost –PV (yen/m^2)	Plan	Cost (yen/m^2)	Cost –PV (yen/m^2)
2000	0				A	4900	10737
2003	3						
2005	5						
2010	10						
2012	12						
2015	15						
2020	20	A	4900	4900	A	4900	4900
2025	25						
2030	30						
2035	35						
2040	40						
2045	45						
2050	50						
2055	55						
2060	60				A	4900	1021
2065	65						
2070	70						

2075	75						
2080	80						
2085	85						
2090	90				A	4900	315
2095	95						
2100	100						
Total (PV) (yen/m2) ①				**4900**			**16972**
T_P				80			10
T_D				170			30
Survival value(PV) (yen/m^2) ②				**113**			**142**
LCC(①-②) (yen/m^2)				**4787**			**16830**

Group		**1st TC+20th TC**			**1st TC+20th TC**		
Scaling depth limit (mm)		5			10		
Lifetime (Take an integer*) (year)		47.84（40）			104.94（100）		
Year	Service year	Plan	Cost (yen/m^2)	Cost –PV (yen/m^2)	Plan	Cost (yen/m^2)	Cost –PV (yen/m^2)
2000	0	A	4900	10737	A	4900	10737
2003	3						
2005	5						
2010	10						
2012	12						
2015	15						
2020	20	A	4900	4900	A	4900	4900
2025	25						
2030	30						
2035	35						
2040	40						
2045	45						
2050	50						
2055	55						
2060	60						
2065	65	I (D+A)	104900	17959			
2070	70						
2075	75						

2080	80						
2085	85						
2090	90						
2095	95	A	4900	259			
2100	100						
Total (PV) (yen/m2) ①				**33854**			**15637**
T_P				5			80
T_D				65			100
Survival value(PV) (yen/m²) ②				**196**			**43**
LCC(①-②) (yen/m²)				**33658**			**15594**

Group		**1st TC+20th TC**					
Scaling depth limit (mm)		20					
Lifetime (Take an integer*) (year)		219.13（215）					
Year	Service year	Plan	Cost (yen/m²)	Cost –PV (yen/m²)			
2000	0	A	4900	10737			
2003	3						
2005	5						
2010	10						
2012	12						
2015	15						
2020	20	A	4900	4900			
2025	25						
2030	30						
2035	35						
2040	40						
2045	45						
2050	50						
2055	55						
2060	60						
2065	65						
2070	70						
2075	75						
2080	80						
2085	85						

2090	90						
2095	95						
2100	100						
Total (PV) (yen/m2) ①				**15637**			
T_P				80			
T_D				215			
Survival value(PV) (yen/m²) ②				**133**			
LCC(①-②) (yen/m²)				**15503**			

Group		**N**			**N**		
Scaling depth limit (mm)		2.5			5-①		
Lifetime (Take an integer*) (year)		11.17 (10)			22.35（20）		
Year	Service year	Plan	Cost (yen/m²)	Cost –PV (yen/m²)	Plan	Cost (yen/m²)	Cost –PV (yen/m²)
2000	0						
2003	3						
2005	5						
2010	10	A	4900	7253			
2012	12						
2015	15						
2020	20				I (D+A)	104900	104900
2025	25						
2030	30						
2035	35						
2040	40	A	4900	2236			
2045	45						
2050	50						
2055	55						
2060	60						

2065	65						
2070	70	A	4900	689			
2075	75						
2080	80						
2085	85				A	4900	383
2090	90						
2095	95						
2100	100						
Total (PV) (yen/m2) ①				**10179**			**105283**
T_P				30			15
T_D				30			65
Survival value(PV) (yen/m^2) ②				**0**			**164**
LCC(①-②) (yen/m^2)				**10179**			**105119**

Group			**N**			**N**	
Scaling depth limit (mm)			5-②			10	
Lifetime (Take an integer*) (year)			22.35（20）			59.67（55）	
Year	Service year	Plan	Cost (yen/m^2)	Cost –PV (yen/m^2)	Plan	Cost (yen/m^2)	Cost –PV (yen/m^2)
2000	0						
2003	3						
2005	5						
2010	10						
2012	12						
2015	15						
2020	20	D	100000	100000			
2025	25						
2030	30						
2035	35						

2040	40	D	100000	45639			
2045	45						
2050	50				D	100000	30832
2055	55						
2060	60	D	100000	20829			
2065	65						
2070	70						
2075	75						
2080	80	D	100000	9506			
2085	85						
2090	90						
2095	95						
2100	100						
Total (PV) (yen/m2) ①				**175974**			**30832**
T_P				20			20
T_D				20			55
Survival value(PV) (yen/m²) ②				**0**			**135**
LCC(①-②) (yen/m²)				**175974**			**30697**

Group		**N**			**1st TC**		
Scaling depth limit (mm)		20			2.5		
Lifetime (Take an integer*) (year)		109.73（105）			33.91（30）		
Year	Service year	Plan	Cost (yen/m²)	Cost –PV (yen/m²)	Plan	Cost (yen/m²)	Cost –PV (yen/m²)
2000	0				A	4900	10737
2003	3						
2005	5						
2010	10						
2012	12						

2015	15						
2020	20						
2025	25						
2030	30				A	4900	3310
2035	35						
2040	40						
2045	45						
2050	50						
2055	55						
2060	60				A	4900	1021
2065	65						
2070	70						
2075	75						
2080	80						
2085	85						
2090	90				A	4900	315
2095	95						
2100	100						
Total (PV) (yen/m2) ①				**0**			**15382**
T_P							10
T_D							30
Survival value(PV) (yen/m^2) ②				**0**			**142**
LCC(①-②) (yen/m^2)				**0**			**15240**

Group		**1st TC**			**1st TC**		
Scaling depth limit (mm)		5-①			5-②		
Lifetime (Take an integer*) (year)		67.82（65）			67.82（65）		
Year	Service year	65	Cost (yen/m^2)	Cost –PV (yen/m^2)	Plan	Cost (yen/m^2)	Cost –PV (yen/m^2)

2000	0	A	4900	10737	A	4900	10737
2003	3						
2005	5						
2010	10						
2012	12						
2015	15						
2020	20						
2025	25						
2030	30						
2035	35						
2040	40						
2045	45						
2050	50						
2055	55						
2060	60						
2065	65	I (D+A)	104900	17959	D	100000	17120
2070	70						
2075	75						
2080	80						
2085	85				D	100000	7813
2090	90						
2095	95						
2100	100						
Total (PV) (yen/m2) ①				**28695**			**35670**
T_P				35			15
T_D				65			20
Survival value(PV) (yen/m^2) ②				**98**			**53**
LCC(①-②) (yen/m^2)				**28597**			**35616**

Group		1st TC			1st TC		
Scaling depth limit (mm)		10			20		
Lifetime (Take an integer*) (year)		124.92（120）			239.11（235）		
Year	Service year	Plan	Cost (yen/m^2)	Cost –PV (yen/m^2)	Plan	Cost (yen/m^2)	Cost –PV (yen/m^2)
2000	0	A	4900	10737	A	4900	10737
2003	3						
2005	5						
2010	10						
2012	12						
2015	15						
2020	20						
2025	25						
2030	30						
2035	35						
2040	40						
2045	45						
2050	50						
2055	55						
2060	60						
2065	65						
2070	70						
2075	75						
2080	80						
2085	85						
2090	90						
2095	95						
2100	100						
Total (PV) (yen/m2) ①				**10737**			**10737**
T_P				100			100

T_D			120			235
Survival value(PV) (yen/m^2) ②			**35**			**122**
LCC(①-②) (yen/m^2)			**10701**			**10614**

Group		**N+3rd TC**			**N+3rd TC**		
Scaling depth limit (mm)		2.5			5-①		
Lifetime (Take an integer*) (year)		33.91（30）			67.82（65）		
Year	Service year	Plan	Cost (yen/m^2)	Cost –PV (yen/m^2)	65	Cost (yen/m^2)	Cost –PV (yen/m^2)
2000	0						
2003	3	A	4900	9545	A	4900	9545
2005	5						
2010	10						
2012	12						
2015	15						
2020	20						
2025	25						
2030	30	A	4900	3310			
2035	35						
2040	40						
2045	45						
2050	50						
2055	55						
2060	60	A	4900	1021			
2065	65				I (D+A)	104900	17959
2070	70						
2075	75						
2080	80						
2085	85						

2090	90	A	4900	315			
2095	95						
2100	100						
Total (PV) (yen/m2) ①				**14190**			**27503**
T_P				10			35
T_D				30			65
Survival value(PV) (yen/m^2) ②				**142**			**98**
LCC(①-②) (yen/m^2)				**14049**			**27405**

Group		**N+3rd TC**			**N+3rd TC**		
Scaling depth limit (mm)		5-②			10		
Lifetime (Take an integer*) (year)		67.82（65）			124.92（120）		
Year	Service year	Plan	Cost (yen/m^2)	Cost –PV (yen/m^2)	Plan	Cost (yen/m^2)	Cost –PV (yen/m^2)
2000	0						
2003	3	A	4900	9545	A	4900	9545
2005	5						
2010	10						
2012	12						
2015	15						
2020	20						
2025	25						
2030	30						
2035	35						
2040	40						
2045	45						
2050	50						
2055	55						
2060	60						

2065	65	D	100000	17120			
2070	70						
2075	75						
2080	80						
2085	85	D	100000	7813			
2090	90						
2095	95						
2100	100						
Total (PV) (yen/m2) ①				**34478**			**9545**
T_P				15			100
T_D				20			120
Survival value(PV) (yen/m^2) ②				**53**			**35**
LCC(①-②) (yen/m^2)				**34425**			**9509**

Group		**N+3rd TC**			**1st TC+3rd TC**		
Scaling depth limit (mm)		20			2.5		
Lifetime (Take an integer*) (year)		239.11（235）			260.05（260）		
Year	Service year	Plan	Cost (yen/m^2)	Cost –PV (yen/m^2)	Plan	Cost (yen/m^2)	Cost –PV (yen/m^2)
2000	0				A	4900	10737
2003	3	A	4900	9545	A	4900	9545
2005	5						
2010	10						
2012	12						
2015	15						
2020	20						
2025	25						
2030	30						
2035	35						

2040	40						
2045	45						
2050	50						
2055	55						
2060	60						
2065	65						
2070	70						
2075	75						
2080	80						
2085	85						
2090	90						
2095	95						
2100	100						
Total (PV) (yen/m2) ①				**9545**			**20281**
T_P				100			97
T_D				235			260
Survival value(PV) (yen/m^2) ②				**122**			**133**
LCC(①-②) (yen/m^2)				**9423**			**20148**

Group		**1st TC+3rd TC**			**1st TC+3rd TC**		
Scaling depth limit (mm)		5			10		
Lifetime (Take an integer*) (year)		266.05（265）			323.15（320）		
Year	Service year	Plan	Cost (yen/m^2)	Cost –PV (yen/m^2)	Plan	Cost (yen/m^2)	Cost –PV (yen/m^2)
2000	0	A	4900	10737	A	4900	10737
2003	3	A	4900	9545	A	4900	9545
2005	5						
2010	10						
2012	12						

2015	15						
2020	20						
2025	25						
2030	30						
2035	35						
2040	40						
2045	45						
2050	50						
2055	55						
2060	60						
2065	65						
2070	70						
2075	75						
2080	80						
2085	85						
2090	90						
2095	95						
2100	100						
Total (PV) (yen/m2) ①				**20281**			**20281**
T_P				97			97
T_D				265			320
Survival value(PV) (yen/m^2) ②				**135**			**148**
LCC(①-②) (yen/m^2)				**20146**			**20133**

Group		**1st TC+3rd TC**			**N+12th TC**		
Scaling depth limit (mm)		20			2.5		
Lifetime (Take an integer*) (year)		437.35（435）			83.24（80）		
Year	Service year	Plan	Cost (yen/m^2)	Cost –PV (yen/m^2)	Plan	Cost (yen/m^2)	Cost –PV (yen/m^2)

2000	0	A	4900	10737			
2003	3	A	4900	9545			
2005	5						
2010	10						
2012	12				A	4900	6706
2015	15						
2020	20						
2025	25						
2030	30						
2035	35						
2040	40						
2045	45						
2050	50						
2055	55						
2060	60						
2065	65						
2070	70						
2075	75						
2080	80						
2085	85						
2090	90				A	4900	315
2095	95						
2100	100						
Total (PV) (yen/m2) ①				**20281**			**7021**
T_P				97			10
T_D				435			30
Survival value(PV) (yen/m^2) ②				**165**			**142**
LCC(①-②) (yen/m^2)				**20116**			**6879**

Group	**N+12th TC**	**N+12th TC**

Scaling depth limit (mm)		5			10		
Lifetime (Take an integer*) (year)		85.31（85）			170.95（170）		
Year	Service year	Plan	Cost (yen/m^2)	Cost –PV (yen/m^2)	Plan	Cost (yen/m^2)	Cost –PV (yen/m^2)
2000	0						
2003	3						
2005	5						
2010	10						
2012	12	A	4900	6706	A	4900	6706
2015	15						
2020	20						
2025	25						
2030	30						
2035	35						
2040	40						
2045	45						
2050	50						
2055	55						
2060	60						
2065	65						
2070	70						
2075	75						
2080	80						
2085	85						
2090	90						
2095	95	D	100000	5278			
2100	100						
Total (PV) (yen/m2) ①				**11984**			**6706**
T_P				5			80
T_D				20			170

Survival value(PV) (yen/m²) ②			**159**			**113**
LCC(①-②) (yen/m²)			**11825**			**6593**

Group		**N+20th TC**			**N+20th TC**		
Scaling depth limit (mm)		2.5-②			5-①		
Lifetime (Take an integer*) (year)		11.17（10）			22.35（20）		
Year	Service year	Plan	Cost (yen/m²)	Cost –PV (yen/m²)	Plan	Cost (yen/m²)	Cost –PV (yen/m²)
2000	0						
2003	3						
2005	5						
2010	10						
2012	12						
2015	15						
2020	20	A	4900	4900	A	4900	4900
2025	25						
2030	30	I (D+A)	104900	70867			
2035	35						
2040	40				I (D+A)	104900	47875
2045	45						
2050	50						
2055	55						
2060	60	A	4900	1021			
2065	65						
2070	70				A	4900	689
2075	75						
2080	80						
2085	85						

2090	90	A	4900	315			
2095	95						
2100	100						
Total (PV) (yen/m2) ①				**77102**			**53464**
T_P				10			30
T_D				30			65
Survival value(PV) (yen/m^2) ②				**142**			**114**
LCC(①-②) (yen/m^2)				**76960**			**53350**

Group		**N+20th TC**			**N+20th TC**		
Scaling depth limit (mm)		5-②			10		
Lifetime (Take an integer*) (year)		22.35（20）			141.77（140）		
Year	Service year	Plan	Cost (yen/m^2)	Cost –PV (yen/m^2)	Plan	Cost (yen/m^2)	Cost –PV (yen/m^2)
2000	0						
2003	3						
2005	5						
2010	10						
2012	12						
2015	15						
2020	20	A	4900	4900	A	4900	4900
2025	25						
2030	30						
2035	35						
2040	40	D	100000	45639			
2045	45						
2050	50						
2055	55						
2060	60	D	100000	20829			

2065	65						
2070	70						
2075	75						
2080	80	D	100000	9506			
2085	85						
2090	90						
2095	95						
2100	100						
Total (PV) (yen/m2) ①				**80874**			**4900**
T_P				20			80
T_D				20			140
Survival value(PV) (yen/m^2) ②				**0**			**91**
LCC(①-②) (yen/m^2)				**80874**			**4809**

Group		**N+20th TC**			**1st TC+20th TC**		
Scaling depth limit (mm)		20			2.5		
Lifetime (Take an integer*) (year)		170.31（170）			42.78（40）		
Year	Service year	Plan	Cost (yen/m^2)	Cost –PV (yen/m^2)	Plan	Cost (yen/m^2)	Cost –PV (yen/m^2)
2000	0				A	4900	10737
2003	3						
2005	5						
2010	10						
2012	12						
2015	15						
2020	20	A	4900	4900	A	4900	4900
2025	25						
2030	30						
2035	35						

2040	40						
2045	45						
2050	50						
2055	55						
2060	60				A	4900	1021
2065	65						
2070	70						
2075	75						
2080	80						
2085	85						
2090	90				A	4900	315
2095	95						
2100	100						
Total (PV) (yen/m2) ①				**4900**			**16972**
T_P				80			10
T_D				170			30
Survival value(PV) (yen/m^2) ②				**113**			**142**
LCC(①-②) (yen/m^2)				**4787**			**16830**

Group		**1st TC+20th TC**			**1st TC+20th TC**		
Scaling depth limit (mm)		5			10		
Lifetime (Take an integer*) (year)		47.84（40）			104.94（100）		
Year	Service year	Plan	Cost (yen/m^2)	Cost –PV (yen/m^2)	Plan	Cost (yen/m^2)	Cost –PV (yen/m^2)
2000	0	A	4900	10737	A	4900	10737
2003	3						
2005	5						
2010	10						
2012	12						

2015	15						
2020	20	A	4900	4900	A	4900	4900
2025	25						
2030	30						
2035	35						
2040	40						
2045	45						
2050	50						
2055	55						
2060	60						
2065	65	I (D+A)	104900	17959			
2070	70						
2075	75						
2080	80						
2085	85						
2090	90						
2095	95	A	4900	259			
2100	100						
Total (PV) (yen/m2) ①				**33854**			**15637**
T_P				5			80
T_D				65			100
Survival value(PV) (yen/m^2) ②				**196**			**43**
LCC(①-②) (yen/m^2)				**33658**			**15594**

Group	**1st TC+20th TC**	
Scaling depth limit (mm)	20	
Lifetime (Take an integer*) (year)	219.13（215）	

Year	Service year	Plan	Cost (yen/m²)	Cost –PV (yen/m²)			
2000	0	A	4900	10737			
2003	3						
2005	5						
2010	10						
2012	12						
2015	15						
2020	20	A	4900	4900			
2025	25						
2030	30						
2035	35						
2040	40						
2045	45						
2050	50						
2055	55						
2060	60						
2065	65						
2070	70						
2075	75						
2080	80						
2085	85						
2090	90						
2095	95						
2100	100						
Total (PV) (yen/m2) ①				**15637**			
T_P				80			
T_D				215			
Survival value(PV) (yen/m²) ②				**133**			
LCC(①-②) (yen/m²)				**15503**			

Notes:

A	Impregnant method	I (D+A)	Large section repair + impregnating agent method
B	Surface coating method	III (C+A)	Salt discharge method + impregnant method
C	Salt discharge method	II (D+B)	Large section repair + surface coating method
D	Large section repair method		

Take an integer*: Take an integer that is a multiple of 5 for a Lifetime and is less than the lifetime

T_D: The (allowable) durability of the last treatment method is different from the previous section. It is not equal to the durability of the concrete surface reinforcement method but is also related to the allowable spalling depth.

N+3rd TC: without treatment for the first and treated in the third year, refer to the maintenance group for the first year.